Biochemical Characterization of Lipid A Modification Enzymes From *Rhizobium leguminosarum* and *Rhizobium etli*

by

Brian O'Neal Ingram

Department of Biochemistry
Duke University

Date:_____

Approved:

_____
Christian R. H. Raetz, Supervisor

_____
Margarethe Kuehn

_____
Kenneth Kreuzer

_____
K. V. Rajagopalan

_____
James N. Siedow

Dissertation submitted in partial
fulfillment of the requirements for the degree
of Doctor of Philosophy in the Department of
Biochemistry in the Graduate School
of Duke University

2010

ABSTRACT

Biochemical Characterization of Lipid A Modification Enzymes From *Rhizobium leguminosarum* and *Rhizobium etli*

by

Brian O'Neal Ingram

Department of Biochemistry
Duke University

Date:_____
Approved:

_____
Christian R. H. Raetz, Supervisor

_____
Margarethe Kuehn

_____
Kenneth Kreuzer

_____
K.V. Rajagopalan

_____
James N. Siedow

An abstract of a dissertation submitted in partial fulfillment of the requirements for the degree of Doctor of Philosophy in the Department of Biochemistry in the Graduate School of Duke University

2010

Abstract

The lipid A component of lipopolysaccharide (LPS) in the nitrogen-fixing plant endosymbionts *Rhizobium leguminosarum* and *Rhizobium. etli* is strikingly different when compared to that of enteric bacteria such as *Escherichia coli*. The *Rhizobium* species produce several unique enzymes that process the lipid A biosynthetic intermediate Kdo_2-lipid IV_A. These enzymes include a 1-phosphatase (LpxE), a 4′-phosphatase (LpxF), a 3-*O*-deacylase (PagL), and a lipid A oxidase (LpxQ). The biological functions and enzymological properties of many of the modification enzymes have remained unconfirmed and/or unknown. The purpose of these studies was to confirm the activities of these enzymes and to explore the functional significance of the resulting lipid A modifications.

To confirm the proposed biological functions of the enzymes *in vivo*, homologs of the lipid A phosphatases, LpxE and LpxF, from *Francisella novicida* and the lipid A oxidase LpxQ, were expressed heterologously in combination in *E. coli*. The resulting novel lipid A hybrids were analyzed by thin-layer chromatography (TLC) and electrospray ionization-mass spectrometry (ESI-MS).

The lipid A oxidase LpxQ, was characterized further biochemically. Two new purification procedures and a new *in vitro* assay were developed to analyze the properties of the enzyme. Purified LpxQ was shown to be dependent on oxygen and

divalent cations for activity. Hydrogen peroxide was found to be a by-product of lipid A oxidation. A new fluorescence-based assay based on the detection of hydrogen peroxide was developed to monitor oxidation. LpxQ did not co-purifiy with any discernable cofactors, suggesting that it may employ a unique mechanism for the oxidation of lipid A.

The biological roles of LpxE and LpxF in plant nodulation were analyzed. Deletion mutants of the two phosphatases were generated in *R. etli*. The mutant strains accumulated the expected structures, confirming the specificity of the enzymes. Single and double phosphatase mutants were able to fix nitrogen *in planta*. Antimicrobial susceptibility testing indicated that dephosphorylation of lipid A increases resistance to cationic antimicrobials.

The biological role of the 3-*O*-deacylase, PagL, was also investigated. The *pagL* gene was identified using systematic homology searches. PagL was shown to be stimulated by calcium. A deletion mutant of the enzyme in *R. etli* was constructed and analyzed. A *pagL* deletion mutant in *R. etli* was found to be viable and unaltered in its ability to fix nitrogen. In conclusion, these studies have confirmed the roles of LpxE, LpxF, PagL, and LpxQ in *Rhizobium* lipid A biosynthesis and contributed new knowledge regarding the biochemical properties of LpxQ.

Dedication

For Mom and Dad.

Contents

List of Tables

List of Figures

List of Abbreviations

ACP	acyl carrier-protein
BCA	bicinchoninic acid
BSA	bovine serum albumin
CL	cardiolipin
DEAE	diethylaminoethyl
DMPE	dimethyl PE
EDTA	ethylenediaminetetraacetic acid
ESI	electrospray ionization
HR	horseradish peroxidase
IPTG	isopropyl β-$_{D}$-1-thiogalactopyranoside
Kdo	3-deoxy-D-*manno*-oct-2-ulosonic acid
l-Ara4N	4-amino-4-deoxy-l-arabinose
LC	liquid chromatography
LPS	lipopolysaccharide
MES	2-(N-morpholino)-ethanesulfonic acid
MIC	minimal inhibitory concentration
MPL	monophosphoryl lipid A
MS	mass spectrometry

OL	ornithine containing lipids
PBS	phosphate-buffered saline
PC	phosphatidylcholine
PE	phosphatidylethanolamine
PG	phosphatidylglycerol
PCR	polymerase chain reaction
pEtN	phosphoethanolamine
SDS-PAGE	sodium dodecylsulfate polyacrylamide electrophoresis
SL	sulfolipid
TLC	thin layer chromatography
TLR-4	toll-like receptor-4

Acknowledgements

I would like to thank Chris Raetz for his mentorship. He has provided a great training environment and has always been supportive. His persistence and dedication to his graduate students and post-docs has been remarkable. I would also like to thank members of my committee for their support, time, and encouragement.

I would like to thank members of the Raetz laboratory, both former and present. I have always enjoyed working with everyone in the lab. In particular, I would like to thank Mike Reynolds, Steve Breazeale, David Six, Allison Williams, and Suparna Kanjilal who played a big part in helping me adjust to the lab. I would also like to thank Hak Suk Chung, Craig Bartling, Adam Barb, Louis Metzer, and Ziquang Guan for their helpful discussions and support.

I would like to thank my friends out of the Raetz lab. Thanks to all who have been supportive. Lastly, I would like to thank Susanne for everything she has done for me. I am truly thankful for her support and encouragement.

Chapter 1: Introduction

1.1 Introduction

Lipopolysaccharide (LPS), a component of the Gram-negative bacterial cell wall, is a potent stimulator of mammalian innate and acquired immunity (Ulevitch & Tobias, 1999, Raetz, 2002, Rietschel *et al.*, 1994). In animal cells, immunorecognition of LPS leads to the production of pro-inflammatory cytokines and co-stimulatory-molecules that aid in bacterial clearance (Beutler & Cerami, 1988, Medzhitov & Janeway, 2000a). Overproduction of these factors, however, can result in severe sepsis and septic shock (Parrillo, 1993, Russell, 2006). In the United States, there are approximately 750,000 cases of sepsis reported annually. The mortality rate associated with severe sepsis ranges from 25-30% (Russell, 2006). There is, of course, considerable interest in the development of novel therapies for the treatment of severe sepsis. A greater understanding of LPS and its interactions with host cells should aid in the development of new drugs and vaccines.

Recently, it has been shown that subtle changes in the structure of LPS can have significant effects on bacterial survival and virulence. Modifications to LPS, particularly in its lipid A region, can significantly affect host responses (Rietschel et al., 1994). This dissertation describes the biochemical characterization of enzymes that catalyze modifications to the lipid A component of LPS in two plant endosymbionts: *R. leguminosarum* and *R. etli*. An understanding of the lipid A modifications found in these

non-pathogenic bacteria could aid in the understanding of LPS-host interactions and in the development of future therapeutics.

1.2 Bacterial membranes

Bacteria are protected from their extracellular environments by their cell walls and membranes. Bacterial cell walls are composed of peptidoglycan, a highly cross-linked polymer of *N*-acetyl-glucosamine and *N*-acetyl-muramic acid (Vollmer *et al.*, 2008). Peptidoglycan is responsible for maintaining the rigidity of cells and also plays a part in determining cell shape. All bacterial cells walls contain peptidoglycan, but not all bacteria have the same overall structure. There are two main types of bacteria cells: Gram-positive and Gram-negative (Fig. 1). The two types of cells can be differentiated by staining with the dye, crystal violet (Coico, 2005).

Gram-positive cells are characterized by the presence of a thick peptidoglycan layer above their cytoplasmic membrane, which is composed of a bilayer of phospholipids (Swoboda et al. *2010,* Vollmer *et al*., 2008). The peptidoglycan layer in Gram-positive cells is embedded with teichoic acids and teichuronic acids, which may be linked to lipids in the cytoplasmic membrane (Fig. 1). These components play a role in stabilizing the cytoplasmic membrane and in mediating extracellular interactions (Swoboda et al., 2010).

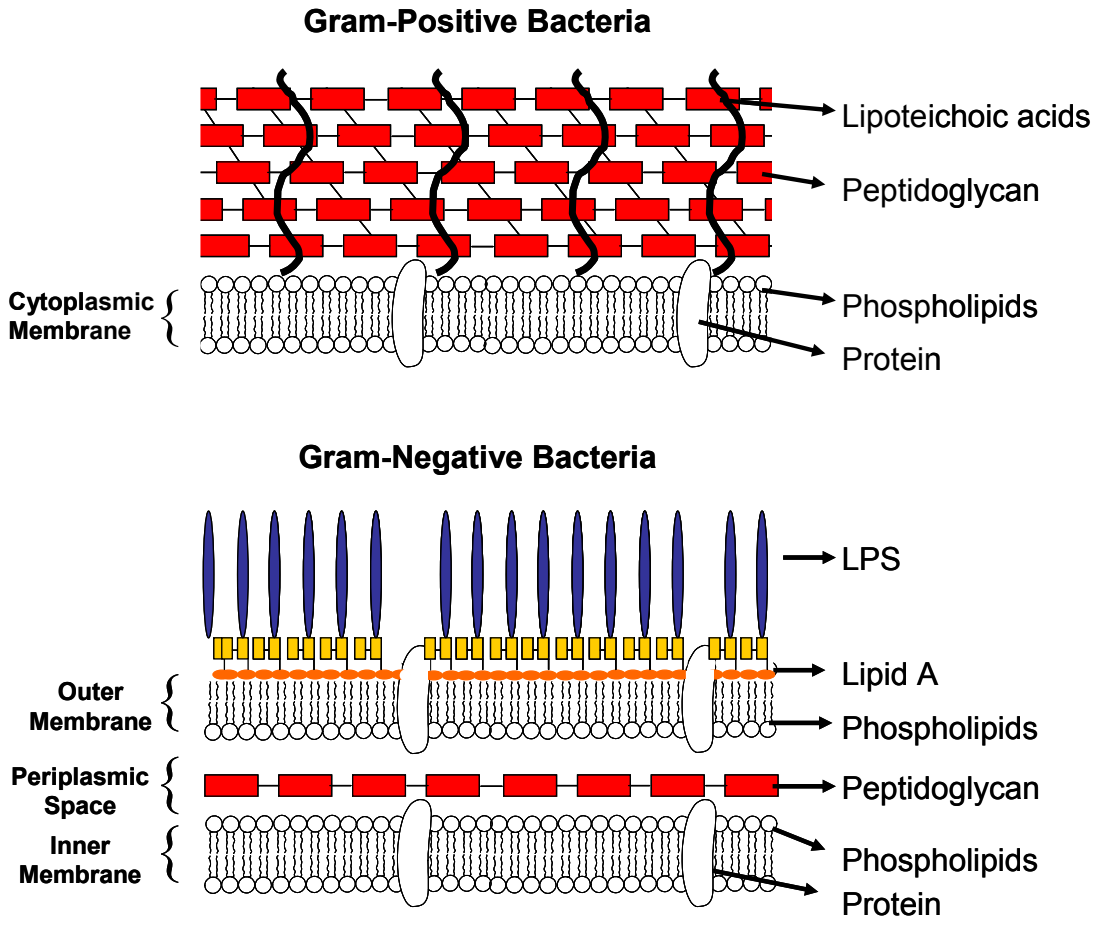

Figure 1: Structures of Gram-positive and Gram-negative cells envelopes.

The Gram-positive cell envelope consists of a cytoplamic membrane and a very thick layer of peptidoglycan. The cytoplasmic membrane is made up from phospholipids. Teichoic acids are imbedded in the cell wall. The Gram-negative cell envelope consists two membranes separated by a periplasmic space. A thin layer of peptidoglycan is present in the periplasmic space. The inner membrane is composd of phospholipids, but the outer membrane is asymmetric in composition. The inner leaflet of this membrane is composed of phospholipids and the outer leaflet is composed of the molecule lipopolysaccharide (LPS). Adapted from (Swoboda et al., 2010)

Gram-negative cells differ from Gram-positive cells in their membrane composition and peptidoglycan content (Vollmer et al., 2008). Gram-negative bacteria contain both an inner cytoplasmic membrane and an outer membrane. A thin layer of peptidoglycan is contained between the two membranes in an area known as the periplasmic space (Fig. 1). The inner membrane is similar to the cytoplasmic membrane of Gram-positive bacteria in that it is composed of phospholipids. The outer membrane, however, is unique in that it is an asymmetric bilayer. The inner leaflet of the outer membrane is composed of phospholipids and the outer leaflet, which faces the extracellular environment, contains the molecule lipopolysaccharide (LPS) (Raetz & Whitfield, 2002). Like the teichoic and teichuronic acids in Gram-positive bacteria, LPS provides structural integrity and acts as a permeability barrier to hydrophobic substances and large hydrophilic compounds (Nikaido, 1996, Nikaido, 2003).

1.3 Structure of LPS

LPS is a large, unique glycolipid composed of three covalently linked domains: 1) the lipid A moiety, 2) a non-repeating core domain, and 3) a distal O-antigen domain (Fig. 2) (Raetz & Whitfield, 2002). LPS frequently differs in composition among strains. The schematic structure shown in Fig. 2 is that of *E. coli* K-12 (Raetz & Whitfield, 2002).

Lipid A is the hydrophobic moiety that anchors LPS to the outer leaflet of the outer membrane. The structure of lipid A is relatively conserved among Gram-negative

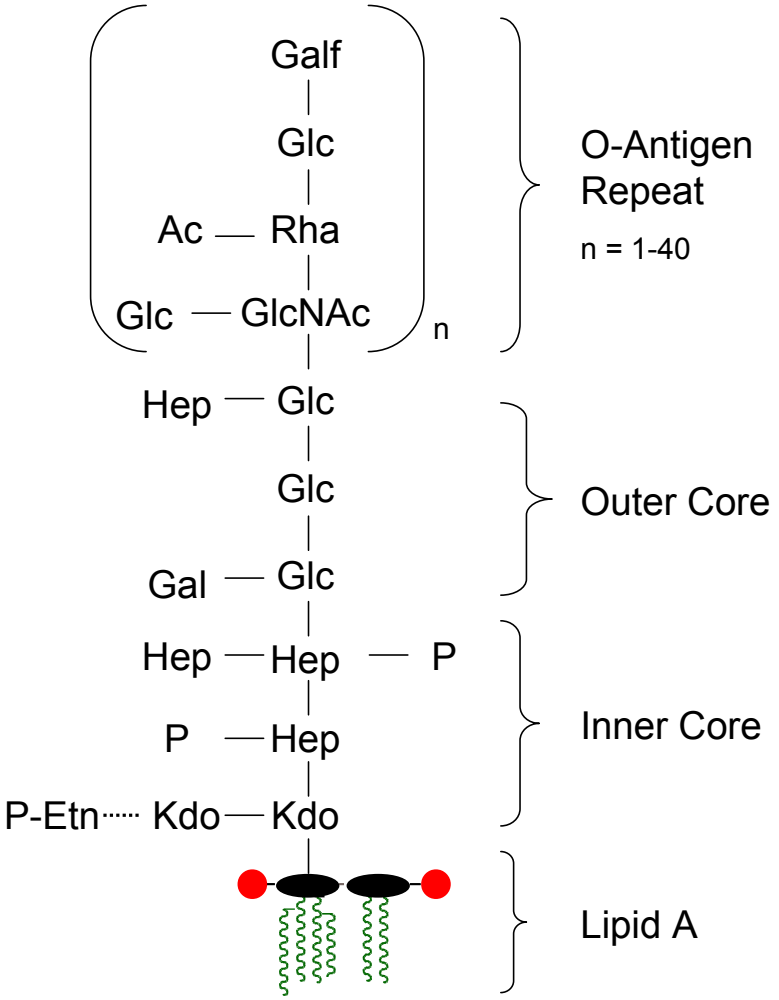

Figure 2: Schematic illustration of LPS from *E. coli*.

LPS is composed of 3 domains: 1) lipid A, 2) the non-repeating core domain, and 3) the O-antigen polymer. Abbreviations: Kdo, 3-deoxy-D-*manno*-octulosonic acid; Hep, L-glycero-D-*manno*-heptose; Glc, D-glucose; Gal, D-galactose; GlcNAc, N-acetyl-D-glucosamine; Rha, L-rhammose; Galf, D-galactofuranose; P, phosphate; P-Etn, phospho-ethanolamine; Ac, acetate. Adapted from (Raetz, 1996).

bacteria (Fig. 3). In *E. coli* and *Salmonella typhimurium*, lipid A is a β-1′,6-linked disaccharide of glucosamine, phosphorylated at positions 1 and 4′, and acylated with R-3 hydroxymyristate groups at positions 2, 3, 2′, and 3′. Two additional fatty acid groups, a laurate residue, and a myristate residue, are present as acyloxyacyl moieties at the 2′and 3′-positions (Raetz & Whitfield, 2002). The number of acyl chains and chain lengths vary among Gram-negative bacteria (Raetz & Whitfield, 2002).

The non-repeating core domain of LPS is composed of a non-repeating oligosaccharide of sugars (Raetz & Whitfield, 2002). The sugar composition and chain length of the core domain varies from strain to strain. The core domain in most Gram-negative bacteria including *E. coli* is linked to the lipid A domain via two 3-deoxy-D-*manno*-octulosonic (Kdo) sugars (Raetz & Whitfield, 2002). In some organisms, the linkage occurs through one Kdo sugar, or through an oxidized derivative of Kdo, D-glycero-alpha-D-talo-oct-2-ulosonic acid (Ko) (White *et al.*, 1997, Gronow *et al.*, 2010). The sugars of the core domain are commonly modified with chemical substituents such as phosphate and phosphoethanolamine (Raetz, 2002). The composition of the core and level of modifications can affect antimicrobial resistance (Raetz, 2002). The outermost domain of LPS, the O-antigen polymer, is made up from repeating sugars (Raetz, 2002). It is covalently attached to the inner core domain of LPS and is variable in composition

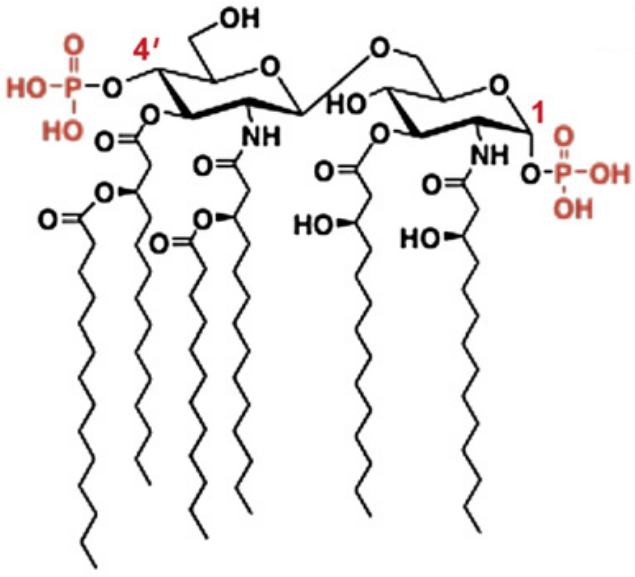

Figure 3: Covalent structure of *E. coli* Lipid A

Lipid A is a hexaacylated, β,(1′-6)-linked disaccharide of glucosamine with phosphate groups at positions 1 and 4′. Laurate and myristoyl chains are present on the distal end as acyloxyacyl-linked fatty acids (Raetz, 2002).

and in chain length. It is not essential for growth, but it is thought to be important in resistance to antibiotics and in the complement system of animals (Raetz, 2002). Strains lacking the O-antigen domain are considered to have a "rough" phenotype whereas strains with intact O-antigens are considered "smooth." Most laboratory strains of *E. coli* K-12 lack the O-antigen component (Stevenson *et al.*, 1994). Bacteria lacking O-antigen and part of the inner core are known as "deep rough" mutants. These bacteria display strong sensitivities to antibiotics and detergents (Vaara, 1992, Nikaido, 2003, Raetz & Whitfield, 2002).

1.4 Roles of LPS in pathogenic infections and in plant symbiosis

LPS is known as "endotoxin." The lipid A component of LPS is the "endotoxin" component of LPS and is associated with some of the complications of severe Gram-negative sepsis (Brade, 1999). The lipid A of pathogenic bacteria triggers an immune response in mammalian hosts by activating receptors located on the surface of mammalian macrophage cells. Detection of lipid A results in a complex signaling cascade which can result in septic shock. (Ulevitch & Tobias, 1999, Janeway & Medzhitov, 2002). Septic shock is characterized by severe hypotension, multiple organ failure, and death (Parrillo, 1993).

LPS is also important in biological processes carried out by non-pathogenic bacteria. The *Rhizobiaceae* family consists of bacteria that form a symbiotic relationship

with leguminous plants. These bacteria fix nitrogen within the root cells of plants when nitrogen is limited in the soil (Triplett, 2000). *Rhizobial* LPS is thought to be important in establishing this relationship, possibly by mediating recognition between the plant host and the symbiont (Kannenberg *et al.*, 1992, Triplett, 2000). Symbiotic bacteria lacking O-antigens are defective in generating nitrogen-fixing nodules (Kannenberg & Brewin, 1994).

1.5 Activation of innate immunity by lipid A and development of lipid A mimetics

The innate immune systems of mammals, insects, and plants has evolved to detect conserved features of pathogenic bacteria (Medzhitov & Janeway, 2000a). Receptors known as "pattern recognition receptors" recognize microbial features such as peptidoglycan, pilin, lipoteichoic acid, LPS, flagellin, and lipopeptides, (Janeway & Medzhitov, 2002). These bacterial components are sometimes referred to as PAMPs (pathogen-associated molecular patterns) and MAMPs (microbial-associated molecular patterns). Many of the conserved bacterial features, including lipid A, can be detected at picomolar levels (Aderem & Ulevitch, 2000, Miller *et al.*, 2005, Janeway & Medzhitov, 2002, Heine & Ulmer, 2005).

The "pattern-recognition receptors" in animals are members of the Toll-like receptor (TLR) family. These receptors are similar to Toll, a *Drosophila* receptor that is essential in fly development and in the production of antimicrobial peptides in response

to fungal pathogens (Anderson *et al.*, 1985, Hashimoto *et al.*, 1988, Lemaitre *et al.*, 1997). The Toll-Like-Receptors (TLRs) are a family of type I transmembrane receptors characterized by extracellular domains of leucine-rich repeats (LRRs) and intracellular Toll/Interleukin-1 receptor domains (TIR) (Rock *et al.*, 1998) (Aderem & Ulevitch, 2000, Janeway & Medzhitov, 2002, Beutler *et al.*, 2006). The leucine rich repeats give the receptors a horse-shoe like shape (Kim *et al.*, 2007, Jin *et al.*, 2007). At the present time, 10 members of the TLR family have been identified in humans (Matsushima *et al.*, 2007).

In mammals, Toll-like receptor-4 (TLR-4) is the primary toll receptor involved in detecting lipid A (Hoshino *et al.*, 1999, Aderem & Ulevitch, 2000, Poltorak *et al.*, 2000, Miller et al., 2005, Park *et al.*, 2009). The importance of the receptor in detecting LPS was demonstrated with mice harboring a point mutation in the TIR domain of TLR-4. These mice were found to be unresponsive to LPS (Poltorak *et al.*, 1998, Qureshi, 1999). LPS is recognized by TLR-4 in complex with a co-receptor protein named myeloid differentiation factor 2 (MD2). The TLR-4/MD-2 complex exists as heterodimers on the surface of many different cell types (Gangloff & Gay, 2004, Park et al., 2009, Bryant *et al.* 2010). During infections, LPS is extracted or secreted from the membranes of bacteria and is recognized by two accessory proteins, LPS-binding protein and CD14 which facilitate binding of LPS to the TLR-4/MD-2 complex (Fig. 4) (Ulevitch & Tobias, 1999, Aderem & Ulevitch, 2000, Janeway & Medzhitov, 2002, Miyake, 2006). The 3-

dimensional crystal structure of the TLR-4/MD-2 complex associated with lipid A was recently determined (Park et al., 2009). From this work and other studies, it is proposed that immunorecognition of lipid A leads to a dimerization event in which two TLR-4/MD-2 heterodimers dimerize to form a multimeric complex (Jin et al., 2007, Park et al., 2009). The multimer is held together by the hydrophobic interactions of lipid A with MD2 (Park et al., 2009). The phosphate groups of lipid A also contribute to the formation of the complex by forming ionic interactions with both TLR-4 and MD2 (Park et al., 2009). Formation of the multimeric complex leads to conformational changes of the TLR-4 receptor. These changes result in homodimerization of the cytoplasmic TIR domains of TLR-4 (Gay *et al*., 2006, Bryant *et al*., 2010). The homodimer formed by the TIR domains provides a scaffold for the recruitment of adaptor proteins that function in the formation of a complex signaling cascade. Adaptor proteins such as TRAM, TRIF, MAL, MyD88, and IRAK activate transcription factors such as nuclear factor-κB (NF-κB) and interferon regulatory factor 3 (IRF3) (O'Neill & Bowie, 2007, Bryant *et al*., 2010). These events lead to the production of pro-inflammatory cytokines such as tumor necrosis factor-α (TNF-α) that play a role in bacterial clearance (Janeway & Medzhitov, 2002, Bryant *et al*., 2010). The cytokines activate natural killer cells and initiate a cascade of signals that are recognized by the cells of the adaptive immune response (Perera *et al*., 1992, Janeway & Medzhitov, 2002). These signaling events are desirable for the clearance of localized

Figure 4: Detection of lipid A by the TLR-4 receptor of animal cells.

LPS is recognized in animal cells by the signal-transducing receptor, TLR-4 (Medzhitov & Janeway, 2000b). The lipid A component of LPS is recognized by several accessory molecules including LBP (LPS-binding protein), CD-14, and MD-2. Activation of the TLR4/MD2 complex leads to the recruitment of adaptor proteins which are involved in the activation of proinflammatory genes. These events lead to a complex signaling cascade that is recognized by the cells of the adaptive immune response. (Medzhitov & Janeway, 2000b) (Park et al., 2009, Bryant *et al.*, 2010). Structural representations of CD14 and the TLR4-MD-2 complex were created in PyMOL from the PDB files 1WWL and 3FXI.

Figure 4: Detection of lipid A by the TLR-4 receptor of animal cells.

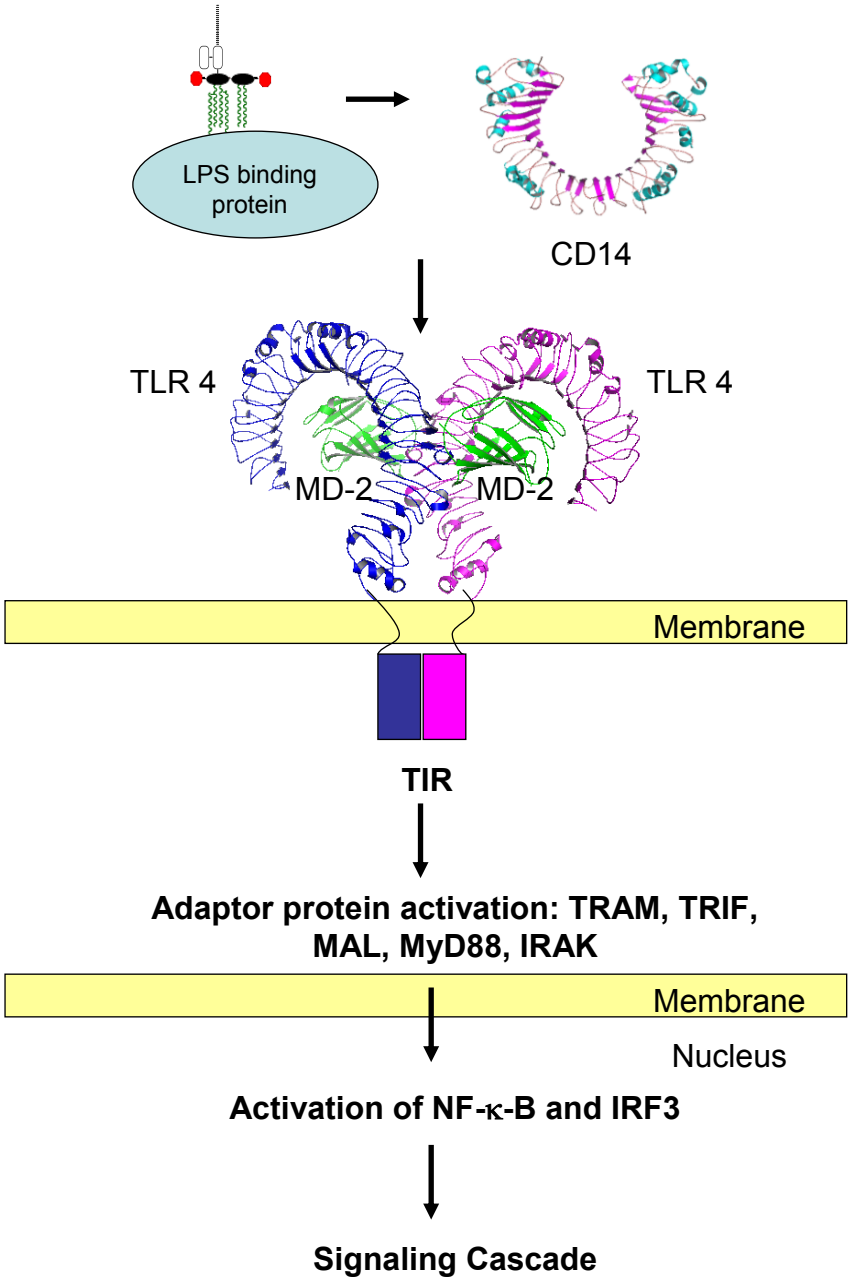

infections, but overproduction of these factors can lead to some of the complications of septic shock (Parrillo, 1993, Raetz & Whitfield, 2002).

There is a great interest in the development of agonist and antagonists of the TLR4-MD2 complex because pharmacological manipulation could lead to the development of new vaccines or anti-inflammatory therapies. Pharmacological studies have shown that the two phosphate groups as well as the acyl chains of lipid A are required for full activation of the endotoxin response in human cells (Golenbock *et al.*, 1991, Rietschel et al., 1994). This supports the model of ligand binding elucidated by structural studies of the TLR4-MD2 complex (Park et al., 2009). Partial agonists bind to the TLR4-MD2 complex and induce some conformation changes, but are incapable of fully activating the complex (Bryant *et al.*, 2010). Monophosphorylated lipid A, a derivative of lipid A, obtained by the hydrolysis of *Salmonella Minnesota*, has received considerable attention as a partial agonist (Fig 5A) (Qureshi *et al.*, 1982b, Persing *et al.*, 2002, Baldridge *et al.*, 2004). This compound has been proven to be a potent vaccine adjuvant when administered with heterologous antigens (Persing et al., 2002). It has been used extensively in human vaccine trials (Persing et al., 2002). Antagonists of the TLR4-MD2 complex bind to the receptor but are incapable of inducing any conformational changes (Bryant *et al.*, 2010). The most promising antagonist of the TLR4-MD2 receptor is eritoran, E5564 (Fig. 5B) (Mullarkey *et al.*, 2003).

1.6 Lipid A biosynthesis

Kdo_2-lipid A is synthesized by a constitutive pathway of nine enzymes (Fig. 6) (Raetz & Whitfield, 2002). The genes encoding the biosynthetic enzymes have all been identified in *E. coli*. The first seven enzymes of the pathway are well conserved in the genomes of Gram-negative bacteria. The early steps of the pathway are attractive antimicrobial targets (Raetz *et al.*, 2007).

Lipid A biosynthesis begins in the cytosol with the acylation of the sugar nucleotide UDP-N-acetylglucosamine (Anderson & Raetz, 1987, Coleman & Raetz, 1988, Anderson *et al.*, 1993). The acyltransferase that catalyzes the reaction, LpxA, transfers a R-3-hydroxyacylchain from R-3-hydroxylacyl acyl carrier protein (ACP) to the glucosamine 3-OH group of UDP-N-acetylglucosamine (Anderson & Raetz, 1987, Anderson et al., 1993, Odegaard *et al.*, 1997). The enzyme only functions with ACP thioesters; it does not recognize R-3-hydroxymyritoyl-coenzyme A (Anderson & Raetz, 1987, Anderson et al., 1993).

Several three dimensional structures of LpxA have been solved (Raetz & Roderick, 1995, Lee & Suh, 2003, Williams *et al.*, 2006, Robins *et al.*, 2009, Williams & Raetz, 2007). LpxA contains a unique, left-handed, parallel β-helix fold (Raetz & Roderick, 1995). The enzyme exists as a homotrimer, and the active sites are located between subunits (Williams et al., 2006). In *E. coli*, LpxA is specific for R-3-

hydroxymyristate. The acyl chain length specificity arises from a "hydrocarbon ruler" located in the fatty acid binding groove of LpxA (Williams & Raetz, 2007).

The equilibrium constant for the acylation of UDP-N-acetylglucosamine is unfavorable (Anderson et al., 1993, Williams et al., 2006). Thus, the second step of the lipid A biosynthetic pathway, the deacetylation of UDP-3-O-(R-3-hydroxyacyl)-N-acetylglucosamine, is the committed step of lipid A biosynthesis (Anderson *et al.*, 1988, Anderson et al., 1993, Young *et al.*, 1995). The enzyme responsible for this activity, LpxC, is a metal-dependent deacetylase (Jackman *et al.*, 1999, Jackman *et al.*, 2001). The enzyme can use zinc or iron (Jackman et al., 1999, Hernick *et al.* 2010).

The deacetylase is an attractive target for the design of novel inhibitors because it shows no sequence homology to known mammalian deacetylases or amidases. Several potent inhibitors have been described (Onishi *et al.*, 1996, Jackman *et al.*, 2000, Clements *et al.*, 2002, Kline *et al.*, 2002, Pirrung *et al.*, 2003, McClerren *et al.*, 2005a, Cuny, 2009, Barb *et al.*, 2009). Recent X-ray and NMR structures of LpxC with and without bound inhibitors have been determined (Coggins *et al.*, 2003, Coggins *et al.*, 2005, Mochalkin *et al.*, 2008, Barb *et al.*, 2007).

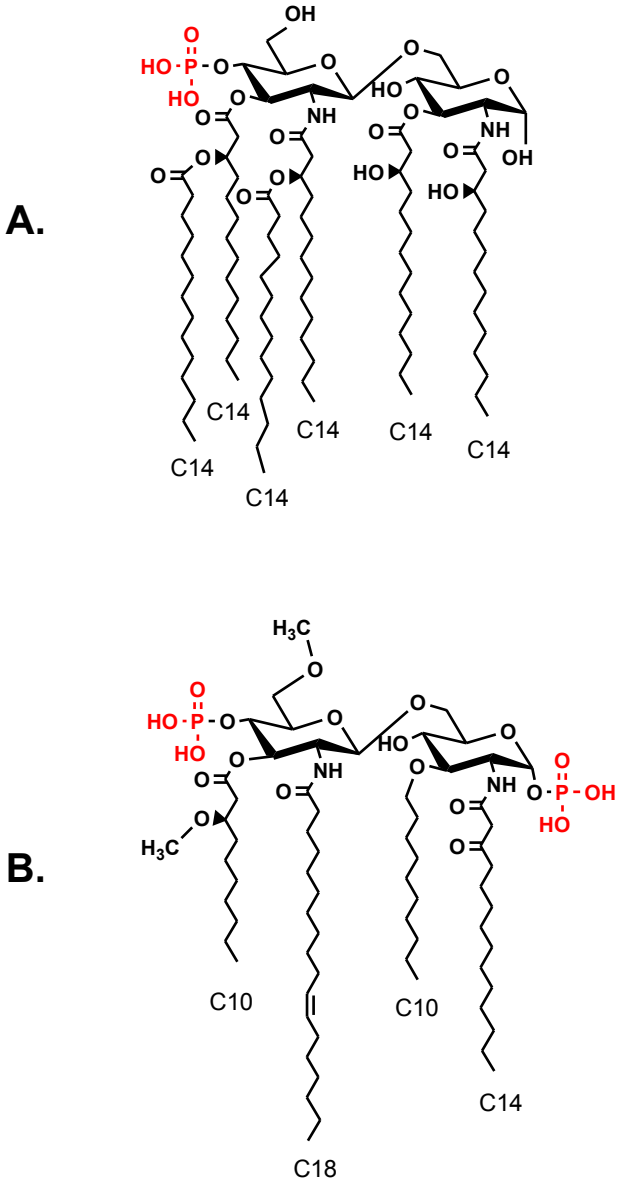

Figure 5: Lipid A mimetic structures.

A. Monophosphorylated lipid A derived from *Salmonela enterica* subsp *enterica* serovar Minnesota is a potent partial agonist of the human TLR4-MD2 complex (Baldridge et al., 2004). B. The synthetic lipid A analogue eritoran (E5564) is a potent antagonist of the TLR4-MD2 complex (Mullarkey et al., 2003).

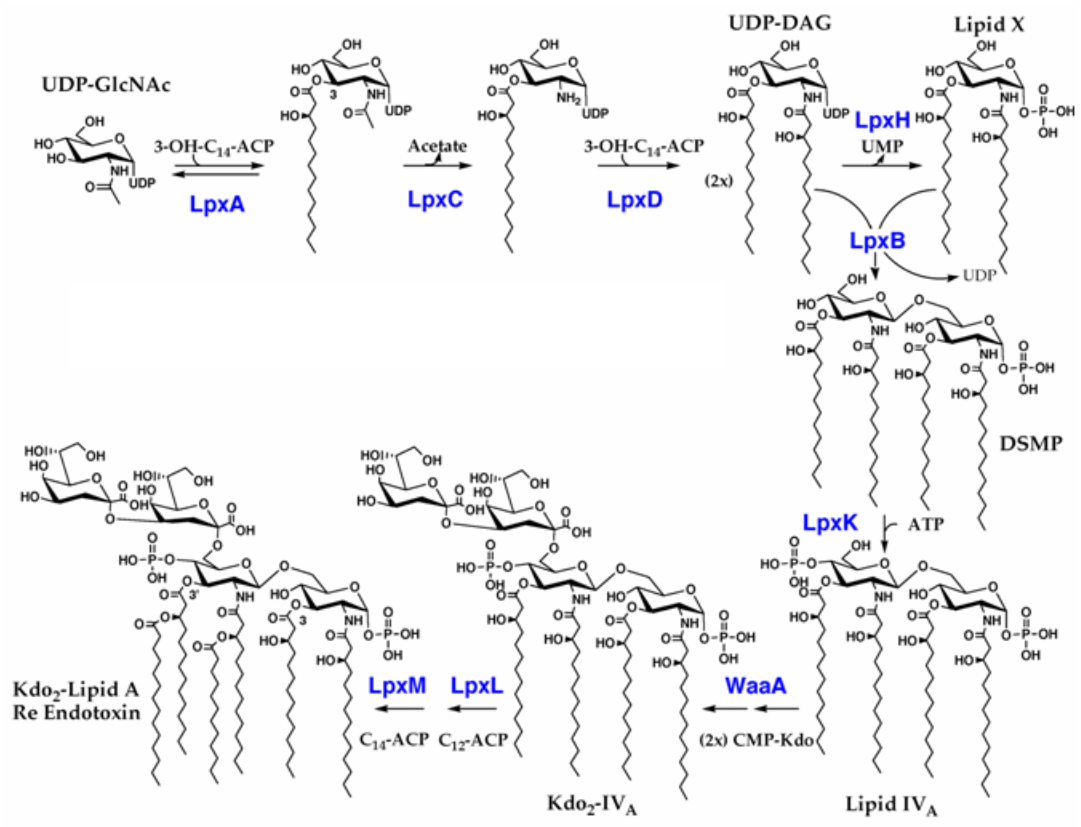

Figure 6: Kdo_2-lipid A biosynthesis in *E. coli*.

Kdo_2-lipid A is synthesized by nine constitutive enzymes (blue typeface). The biosynthetic pathway is highly conserved in Gram-negative bacteria. Kdo_2-lipid A is the minimal structure of LPS required for growth under most laboratory growth conditions. Adapted from (Raetz & Whitfield, 2002).

After the deacetylation step catalyzed by LpxC, an N-linked R-3-hydroxyacyl chain is incorporated to generate UDP-2,3-diacylglucosamine (Kelly *et al.*, 1993). The enzyme, LpxD, is the acyltransferase that catalyzes the reaction. Like LpxA, LpxD catalyzes the transfer of hydroxyl-acyl chains from R-3-hydroxyacyl-ACP (Kelly et al., 1993). The three dimensional structures of LpxD from *Chlamydia trachomatis* and *E. coli* were recently reported (Buetow *et al.*, 2007, Bartling & Raetz, 2009). Like LpxA, LpxD contains a left-handed, parallel β-helix fold. The two enzymes most likely share a similar mechanism.

The fourth step of the lipid A biosynthetic pathway is catalyzed by the enzyme LpxH, which catalyzes the hydrolysis of the pyrophosphate bond of UDP-2,3-diacylglucosamine. The products of the reaction are UMP and 2,3-diacylglucosamine-1-phosphate, also known as lipid X (Babinski *et al.*, 2002a, Babinski *et al.*, 2002b).

Hydrolysis of the pyrophosphate bond of UDP-2,3-diacylglucosamine is essential for growth. The *lpxH* gene, however, is only found in 70% of available sequenced genomes (Babinski et al., 2002b). A transformational analog of LpxH which encodes a similar pyrophosphatase activity is found in many other organisms including members of the *Rhizobiaceae* family. This enzyme, designated LpxI, has been identified in the organism *Caulobacter crescentus* (Metger and Raetz, in preparation).

In the next step of lipid A biosynthesis, the lipid A intermediate lipid X is condensed with a molecule of UDP-2,3-diacylglucosamine yielding the molecule disaccharide-mono-phosphate (DSMP) (Ray *et al.*, 1984, Radika & Raetz, 1988, Metzger & Raetz, 2009). Condensation of the two reactants yields the classical β-1′6-linked disaccharide of glucosamine that is common to all lipid A molecules (Raetz & Whitfield, 2002).

In the next step of the lipid A biosynthetic pathway, DSMP is phosphorylated at the 4′-position by the membrane bound kinase, LpxK, yielding the intermediate, lipid IV_A (Ray & Raetz, 1987, Garrett *et al.*, 1997, Garrett *et al.*, 1998). LpxK is essential for growth (Garrett et al., 1998). The enzyme is routinely used in the preparation of radiolabled lipid A substrates (Garrett et al., 1998, Raetz et al., 2007).

Next, the lipid A intermediate, lipid IV_A, is glycosylated by the enzyme KdtA. This bifunctional enzyme transfers two Kdo sugars from the activated donor CMP-Kdo to lipid IV_A to form the intermediate known as Kdo_2-lipid IV_A (Brozek *et al.*, 1989, Clementz & Raetz, 1991). The KdtA protein from *E. coli*, is bi-functional, but in some organisms, including *Haemophilus influenzae*, the glycosyltransferase is monofunctional (White et al., 1997). Organisms such as *Chlamydia trachomatis* are able to transfer three or more Kdo residues to lipid IV_A (Belunis *et al.*, 1992).

The lipid A intermediate, Kdo_2-lipid IV_A is further processed by two "late" acyltransferases, LpxL and LpxM. In *E. coli*, these enzymes transfer laurate and myristate residues to the 2′-hydroxy and 3′-hydroxy fatty acids on the distal glucosamine unit of Kdo_2-lipid IV_A, generating acyloxyacyl linkages (Brozek & Raetz, 1990, Clementz *et al.*, 1996, Clementz *et al.*, 1997). The two late acyl transferases show significant sequence similarity to each other, but not to LpxA or LpxD (Brozek & Raetz, 1990, Clementz et al., 1996, Clementz et al., 1997). The two acyltransferases are stimulated by the presence of the Kdo disaccharide moiety in their substrates and utilize ACP thioesters as acyl donors (Brozek & Raetz, 1990, Clementz et al., 1996). LpxL, however, shares distant homology with members of the lysophosphatidic acyltransferase (LPAT) family. Purified LpxL can utilize acyl-CoA as an alternative acyl donor at a slow rate *in vitro* (Six *et al.*, 2008).The number and length of the acyloxyacyl chains varies among Gram-negative bacteria (Raetz et al., 2007). The late acyltransferases are not required for growth at slow growth rates (Vorachek-Warren *et al.*, 2002) .

1.7 LPS synthesis and transport

The lipid A synthesized by the constitutive pathway in the cytosol must be transported to the outer surface of the outer membrane. The proposed pathway for lipid A transport is shown in Fig. 7. Newly synthesized lipid A made by the constitutive pathway is glycosylated with its core sugars on the cytoplasmic side of the inner

membrane before translocation across the inner membrane. The O-antigen component of LPS is not attached until the nascent LPS if flipped across the inner membrane (Raetz & Whitfield, 2002). Many questions remain regarding how lipid A is transported across the inner membrane and the perisplasmic space to its final location in the outer leaflet of the outer membrane. Recent studies have provided insights into this process. Newly synthesized lipid A on the cytoplasmic side of the inner membrane is proposed to be flipped to the periplasmic side of the inner membrane by the essential ATP-Binding Cassette (ABC) transporter, MsbA. Transport of lipid A occurs in an ATP-dependent manner (Polissi & Georgopoulos, 1996, Zhou *et al.*, 1998, Doerrler *et al.*, 2001). After transport to the periplasmic side of the inner membrane, the O-antigen domain is added (Raetz & Whitfield, 2002, Brade, 1999, Nikaido, 2003). The O-antigen is synthesized independently of lipid A in the cytoplasm and like lipid A it must be transported to the periplasm for proper assembly (Raetz & Whitfield, 2002). The intact, mature LPS is then translocated from the outer surface of the inner membrane to the outer surface of the outer membrane by a mechanism that is still poorly understood. The protein complex LptA/LptC/LptB/LptF/LptG is thought to be important in the flipping of LPS after MsbA has functioned (Sperandeo *et al.*, 2007, Ma *et al.*, 2008). The outer membrane protein Imp and its partner RlpB are thought to be involved in flipping LPS to the outer surface of the outer membrane (Bos *et al.*, 2004, Braun & Silhavy, 2002, Wu et al., 2006). Direct *in*

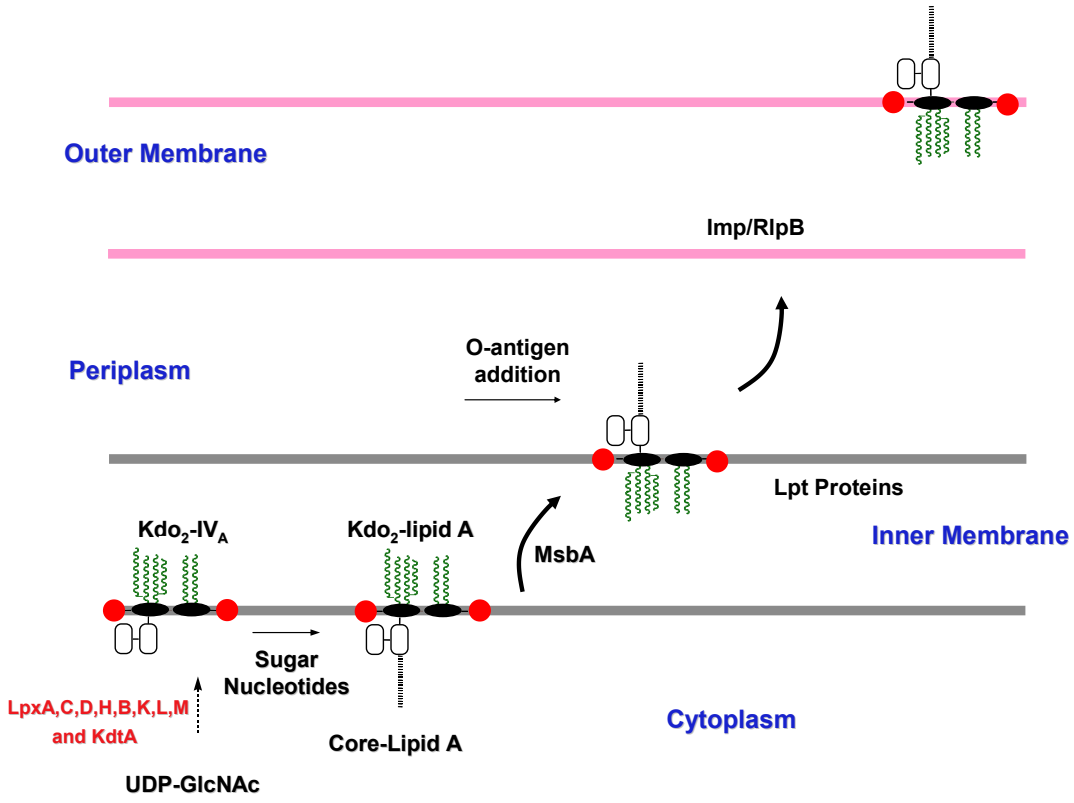

Figure 7: Transport of LPS.

Lipid A is synthesized on the cytoplasmic face of the inner membrane. After synthesis of the core region, the essential transporter, MsbA, is proposed to flip the nascent LPS molecule to the outer leaflet of the inner membrane (Raetz & Whitfield, 2002, Raetz et al., 2007). The O-antigen component is transferred to the nascent LPS on this surface. The Lpt proteins are thought to be involved in the transport of LPS from the outer surface of the inner membrane to the outer membrane. The proteins Imp and RlpB are thought to be responsible for orienting LPS in the correct orientation in the outer membrane (Sperandeo et al., 2007, Sperandeo *et al.*, 2006, Wu *et al.*, 2006, Ruiz *et al.*, 2008, Sperandeo *et al.*, 2008, Ma et al., 2008).

vitro transport assays have not been developed with any of the transport proteins (Raetz & Whitfield, 2002). The role of the proposed transport proteins has been supported by studies demonstrating that they can compensate for the loss of the Kdo transferase gene,*kdtA*. MsbA was identified as a multicopy suppressor of *E. coli* mutants deficient in KdtA (Meredith *et al.*, 2006, Reynolds & Raetz, 2009). The *kdtA* gene can also be deleted in cells overexpressing the LptA, LptB, and LptC proteins (Reynolds & Raetz, 2009).

1.8 Rhizobia and nodulation of legumes

The biosynthesis of lipid A in other Gram-negative bacteria besides *E. coli* is of general interest because some Gram-negative bacteria produce novel lipid A structures. Lipid A biosynthesis has been studied in *Rhizobium leguminosarum* and *R. etli* for the last 15 years. These bacteria are of interest because they can elicit nodule formation on leguminous plants and provide them with reduced nitrogen. They are part of a large family known as Rhizobia. This family of bacteria reduces nitrogen in symbiotic processes with important agricultural crops such as soybean, peanut, lentil, bean, pea, clover, and alfalfa (Buchanan *et al.*, 2000).

Rhizobia are classified into four categories within the α-proteobacteria class of bacteria: *Rhizobium*, *Mesorhizobium*, *Bradyrhizobium*, *Azorhizobium*, and *Sinorhizobium* (Segovia *et al.*, 1993). There are more than 15,000 species of leguminous plants, and most can be nodulated by rhizobia. The specificity between plant host and particular bacterial

symbionts is determined in large part by the structures of bacterial signaling molecules. Different rhizobia species producing similar signaling molecules can nodulate a single type of host plant. Some species can nodulate a broad range of hosts (Perret *et al.*, 2000, Buchanan et al., 2000).

The host-symbiont recognition event occurs in the rhizosphere and involves chemical recognition events (Fig. 8) (Denarie *et al.*, 1996, D'Haeze & Holsters, 2002). The process begins with the release of signaling molecules known as flavonoids by the root cells of plants when nitrogen is limiting in the soil. Rhizobia in the surrounding soil recognize the chemoattractants and move closer to the root hair cells. The flavonoids induce bacterial gene expression, which leads the rhizobia to secrete signaling molecules known as Nod factors (Cullimore *et al.*, 2001, D'Haeze & Holsters, 2002). The Nod factors are usually oligomers of N-acetyl-glucosamine. The degree of acylation in the oliomers differs among species (Perret et al., 2000). The root hair cells of legumes respond by altering their growth patterns. The root hairs often form a structure known as a "shepard's crook" to trap symbionts (Denarie et al., 1996, Triplett, 2000, Broughton *et al.*, 2000) An invasion structure known as the infection thread is formed at the curl of the crook by the plant and is composed of new plant cell wall material. The direction of

Figure 8: Stages of biological nitrogen fixation.

The cartoon depicts the various stages associated with endosymbiont-plant symbiosis and the formation of nodules. Step 1 involves chemical recognition between the plant and endosymbiont. The root cells of the plant, represented by ovals, release signaling components known as flavonoids. The bacteria, represented by the yellow diamonds, releases signaling molecules known as Nod factors (Denarie et al., 1996, D'Haeze & Holsters, 2002, Cullimore et al., 2001, Perret et al., 2000). In the second stage of this process, the root hairs of the plant deform into a structure known as a Shepard's crook. This structure traps the bacteria (Denarie et al., 1996, Triplett, 2000, Broughton et al., 2000). In stage 3, an invasive structure is formed at the curl of the crook. The endosymbionts use this structure as a point of entry and penetrate into the underlying cortical cells (Geiger *et al.*, 1991, Denarie et al., 1996, Spaink *et al.*, 1998). In the next stage of the infection, the bacteria are released from the walled infection thread in membrane-bound vacuoles derived from the plant host called symbiosomes. The bacteria undergo morphological changes and differentiate into a form known as a bacteroid . The plant synthesizes nodule tissue around the bacteria to provide an ideal environment for nitrogen fixation (Vandenbosch *et al.*, 1989, Denarie et al., 1996, Spaink, 2002). After the infection has been established, the bacteroids supply the plant with reduced nitrogen in the form of NH_4^+, and the plant supplies the bacteria carbon sources in the form of dicarboxylic acids. This process occurs inside the nodules on the root surface (depicted) by the red circles) (Buchanan et al., 2000).

Figure 8: Stages of biological nitrogen fixation.

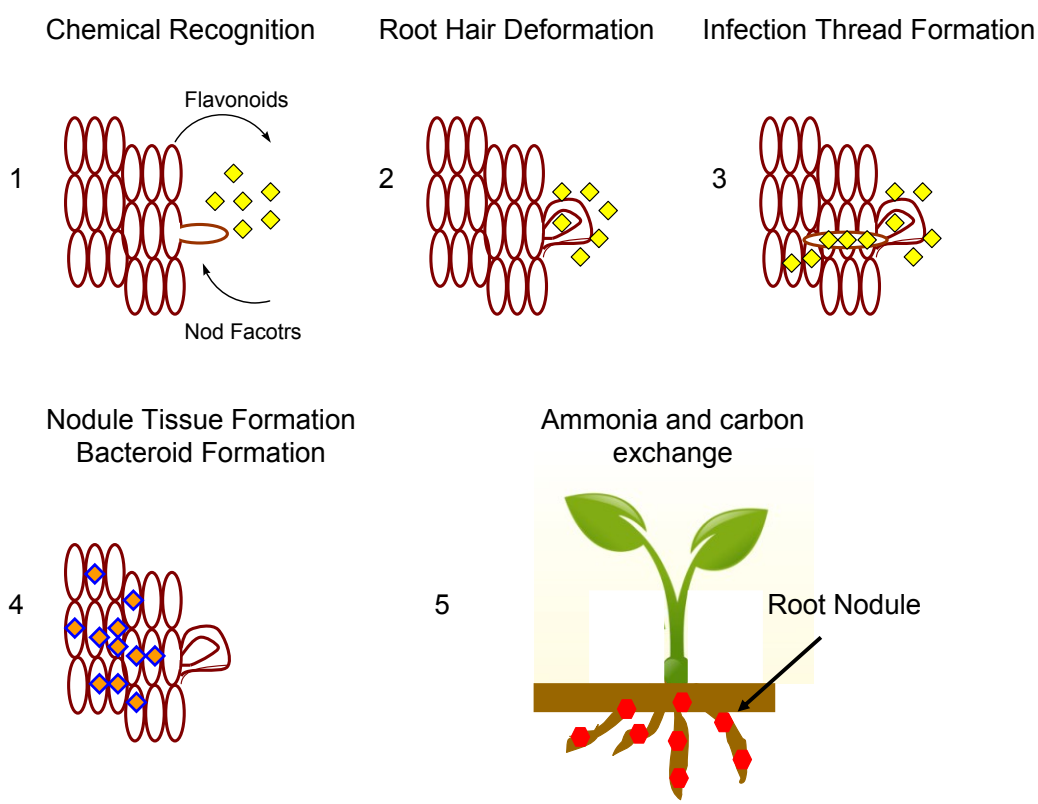

growth is inward, and its growth orientation is from the outside in. The infection thread is used by the bacteria for transport into the underlying cortical cells (Geiger et al., 1991, Denarie et al., 1996, Spaink et al., 1998). The bacteria then are released from the walled infection thread in membrane-bound vacuoles derived from the plant host called symbiosomes. The symbiosomes may contain one or more bacteria. Concomitant with this process, the cortical cells divide and eventually form nodule tissue (Noel *et al.*, 1986, Geiger et al., 1991, Denarie et al., 1996, Spaink et al., 1998, Triplett, 2000, Spaink, 2002). The nodules develop in either a determinate or indeterminate manner depending on the plant host involved. Cells in indeterminate nodules develop at different stages within the nodule. In determinate nodules, the cells all exist at the same stage of differentiation (Buchanan et al., 2000).

The bacteria undergo cell division and differentiate inside symbiosomes into a form known as bacteroids. In some species, there are significant morphological changes accompanying bacteriod formation. In some species, the bacteria and their symbiosomes divide extensively (Vandenbosch et al., 1989, Denarie et al., 1996, Spaink, 2002). The symbiosome membrane, which is also known as the peribacteroid membrane, undergoes extensive differentiation at this time. The symbiosome membrane is responsible for regulating the flow of nutrients and energy between the symbionts. The plant synthesizes nodule specific proteins known as nodulins that will be involved in

metabolic exchange processes and leghemoglobin, which is responsible for sequestering oxygen. Inside the nodules, the bacteroids produce the oxygen-sensitive nitrogenase enzyme, which is responsible for nitrogen fixation. The plants provide the bacteria carbon sources in the form of dicarboxylic acids, and the bacteria supplies nitrogen to the plant in the form of ammonia (Buchanan et al., 2000)

The invasive nature of the symbiotic process appears in many ways to be pathogenic. It may be derived evolutionarily from a pathogenic process (Triplett, 2000). Like the LPS of pathogenic bacteria, the LPS of Rhizobia has been proposed to play roles in the establishment of symbiosis. Given its location on the bacterial surface, LPS is thought to be involved in the recognition between rhizobia and plants, in the formation of infection threads, and in the formation of nodules. Genetic studies have shown that the exopolysaccharides and LPS components of many symbionts are required for successful plant invasion (Buchanan et al., 2000). *R. leguminosarum* LPS core mutants are able to stimulate root hair curling, but accumulate in infection threads (Poole *et al.*, 1994). Similar phenotypes have been observed in *R. leguminosarum* mutants lacking O-antigen (Noel et al., 1986, Priefer, 1989, Kannenberg et al., 1992).

1.9 Lipid A structures and biosynthesis in R. leguminosarum and R. etli

The lipid A from *R. eguminosarum* and *R. etli* is structurally very different from that found in most enteric bacteria (Fig. 9). The lipid A from these species is

heterogeneous and exists as a mixture of species (components B, C, D, and E) (Que *et al.*, 2000a, Que *et al.*, 2000b). The lipid A species all lack the 1 and 4′-position phosphates that are found in most other Gram-negative bacteria. The 4′-position phosphate is replaced with a galacturonic acid moiety and the proximal glucosamine residue can exist in the hemiacetal form (components B and C) or as an aminogluconate moiety (components D and E). *R. leguminosarum* and *R etli* both synthesize pentaacylated molecules with a peculiar 28 carbon fatty acid at the 2′-position. A portion of the lipid A molecules are deacylated at the 3-position (components C and E) (Bhat *et al.*, 1994, Forsberg & Carlson, 1998, Que et al., 2000a, Que et al., 2000b). There is also considerable heterogeneity with regards to acyl chain lengths. The composition of the core sugars of the LPS region are also different from that of *E. coli*. The heptose units of the core are replaced with mannose, galactose , and Kdo units (Carlson *et al.*, 1995, Brozek *et al.*, 1996b).

1.10 Lipid A modification enzymes of R. leguminosarum and R. etli

Despite its structural differences, the unique lipid A species found in *R. leguminosarum* and *R. etli* are initially synthesized in a manner that is similar to that of *E. coli*. The endosymbiont bacteria contain orthologues of the first seven *lpx* genes of the constitutive lipid A biosynthetic pathway except for LpxH. LpxH activity in the two *Rhizobium* species is catalyzed by a transformational analog termed LpxI (Metgzer and

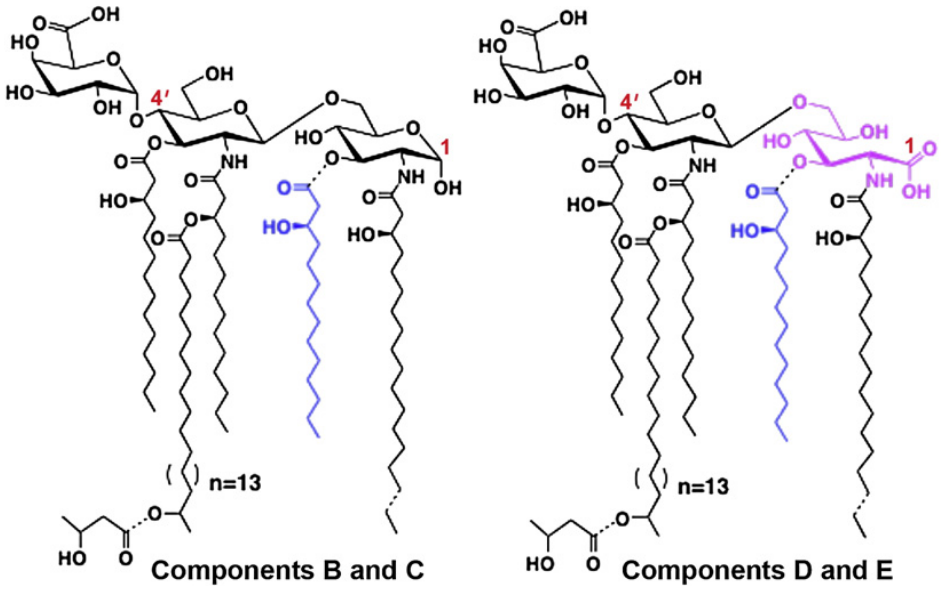

Figure 9: Lipid A structures present in *R. leguminosarum* and *R. etli* CE3.

The major lipid A species in *R. etli* and *R. leguminosarum* lack phosphate substituents and are more heterogeneous with respect to fatty acyl chain length (Que et al., 2000a, Que et al., 2000b). Components B and C are constructed around the typical glucosamine disaccharide found in the lipid A of other Gram-negative organisms. Components D and E feature an aminogluconate unit in place of the proximal glucosamine residue, derived by LpxQ-catalyzed oxidation of B and C respectively (Que-Gewirth *et al.*, 2003a, Que-Gewirth *et al.*, 2003b). All *R. etli* lipid A species contain a galacturonic acid moiety at position-4′ in place of the more typical monophosphate group, and they also contain an unusual C28 secondary acyl chain that may be further derivatized at the 27-OH moiety with a β-hydroxybutyrate group (Bhat et al., 1994). Components C and E differ from B and D by the absence of a hydroxyacyl chain at position 3, which is removed by the deacylase PagL (Basu *et al.*, 1999a). Dashed bonds highlight the most prominent micro-heterogeneity of *R. etli* lipid A with respect to its acyl chains and the presence of the β-hydroxybutyrate substituent.

Raetz, in preparation). The activities of LpxA, LpxC, LpxD, LpxI, LpxB, LpxK, and KdtA have been confirmed with *in vitro* biochemical assays (Price *et al.*, 1994). *Rhizobium* spp. therefore, initially synthesize the tetraacylated, bis-phosphorylated intermediate, Kdo_2-lipid IV_A. The Kdo_2-lipid IV_A intermediate is then processed by enzymes that are absent in *E. coli* (Fig. 10). The lipid A modification enzymes include a 4′-phosphatase (Price *et al.*, 1995), a 1-phosphatase (Karbarz *et al.*, 2003), a C28-specific long-chain acyltransferase (Brozek *et al.*, 1996a, Brozek et al., 1996b), a 3-*O*-deacylase (Basu et al., 1999a), and a lipid A oxidase (Que-Gewirth et al., 2003a, Que-Gewirth et al., 2003b). Additional novel enzymes that process LPS differently than that of *E. coli* include a mannosyl transferase (Brozek et al., 1996b, Kadrmas *et al.*, 1996) and a family of galacturonosyl transferases (Kanjilal-Kolar *et al.*, 2006, Kanjilal-Kolar & Raetz, 2006) that modify the core domain of *Rhizobium* LPS. Most of these modification enzymes can be assayed *in vitro* using the lipid A biosynthetic intermediate, Kdo_2-lipid IV_A.

Over the last several years, considerable progress has been made in the genetics, enzymology, and topography of *Rhizobium* lipid A modifications. The genes for almost all of the lipid A processing activities have been found. The genes for the relevant enzymes have been found using *in vitro* biochemical assays and expression cloning techniques (Karbarz et al., 2003, Brozek et al., 1996a, Basu *et al.*, 2002, Brozek et al., 1996b, Que-Gewirth et al., 2003a, Wang *et al.*, 2006a, Kanjilal-Kolar et al., 2006). It is now clear

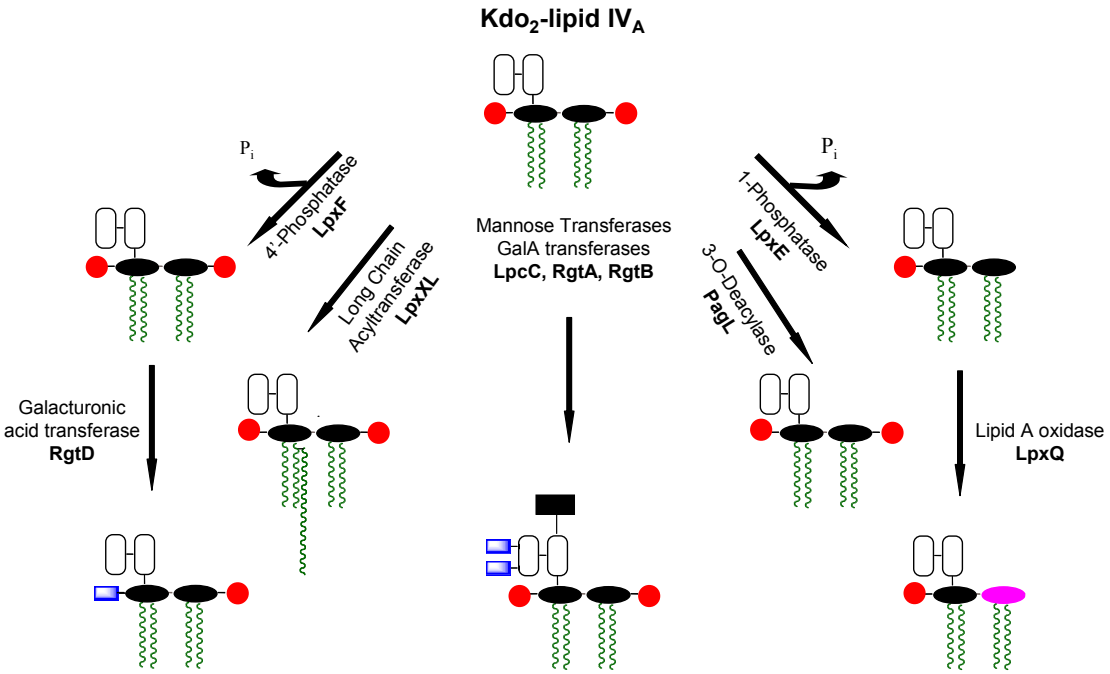

Figure 10: Novel Kdo_2-lipid IV_A processing enzymes found in *R. leguminosarum* and *R. etli*

Enzymes that process Kdo_2-lipid IV_A are shown. All of these activities have been identified in *R. leguminosarum* and *R. etli* (Raetz et al., 2007). The enzymes for most of the modifications have been identified and their names appear in bold typeface.

that most of the modifications work in the late stages of lipid A assembly. The proposed topography of the lipid A modifications is shown in Fig. 11.

Lipid A biosynthesis begins in the cytosol via the constitutive lipid A biosynthetic pathway. After Kdo_2-lipid IV_A formation, the enzyme LpxXL, a distant orthologue of LpxL, incorporates the 27-hydroxyoctacosanoate acyl chain at the 2′ position. It requires a special acyl carrier protein named ACP-XL as a cosubstrate (Basu et al., 2002, Brozek et al., 1996a). The long acyl chain is a characteristic structural feature of lipid A from many *Rhizobiaciae* (Bhat *et al.*, 1991b). Homologues of LpxXL are found in *Agrobacterium tumefaciens*, *Sinorhizobium meliloti*, *Mesorhizobium lot*, *Brucella melitensis*, and *Legionella pneumophila*. In *Rhizobium leguminosarum* and *R. etli*, the ω-1-hydroxy moiety of the hydroxyoctacosanoate acyl chain is modified with a β-hydroxy butyrate substituent (Que et al., 2000a, Que et al., 2000b). The acyltransferase responsible for this modification has not been identified.

After incorporation of the acyloxyacyl chain, the Kdo units of the nascent LPS are glycosylated by the enzymes LpcC, LpcA, and LpcB. These glycosyltransferases work sequentially and transfer mannose, galactose, and Kdo units from sugar nucleotides to Kdo_2- hydroxyoctacosanoate-lipid IV_A (Kadrmas & Raetz, 1998). After the

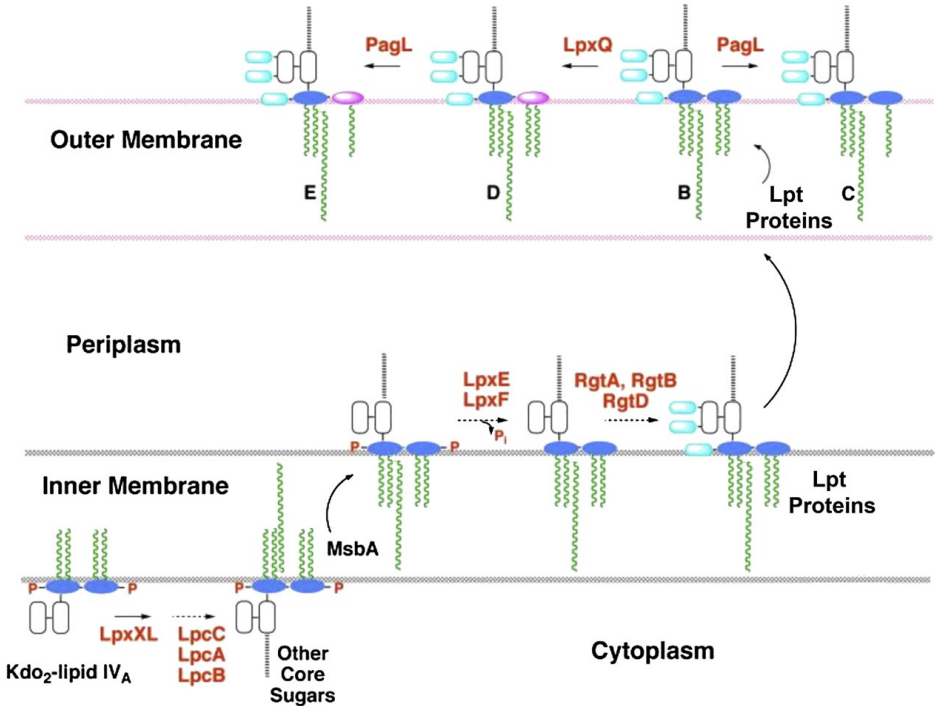

Figure 11: Topography of lipid A modification enzymes in *Rhizobium etli* and *Rhizobium leguminosarum*

The lipid A modifications found in *R. leguminosarum* and *R. etli* lipid A arise from modifications to the lipid A intermediate Kdo_2-lipid IV_A, which is made using the first seven enzymes of the constitutive lipid A biosynthetic pathway (Price et al., 1994). After Kdo_2-lipid IV_A formation, *R. leguminosarum* and *R. etli* lipid transfer a 27-hydroxyoctacosanoate chain to its 2′-position (Basu et al., 2002). After completion of core glycosylation and transport to the outer membrane by MsbA, the phosphatases LpxE and LpxF remove the phosphate moieties at the 1 and 4′-positions, respectively (Karbarz et al., 2003, Wang *et al.*, 2004, Wang et al., 2006a). Next, a set of galacturonosyltransferases glycosylate the Kdo and lipid A regions of LPS. The glycosyltransferases, RgtA and RgtB incorporate galacturonic acids to the outer Kdo units, and the galacturonsyltransferase RgtD, is proposed to incorporate a galacturonic acid at the 4′-position of lipid A (Kanjilal-Kolar et al., 2006, Kanjilal-Kolar & Raetz, 2006). After completion of O-antigen assembly and transport to the outer membrane by the Lpt proteins (Ruiz *et al.*, 2009), the 3-O-acyl chain may be removed by the deacylase PagL (Basu et al., 1999a) and the proximal glucosamine can be oxidized to an aminogluconate residue by the oxidase, LpxQ (Que-Gewirth et al., 2003a, Que-Gewirth et al., 2003b). Adapted from (Ingram *et al.* 2010).

incorporation of the sugars, the lipid A is flipped to the outer surface of the inner membrane by the flippase, MsbA (Polissi & Georgopoulos, 1996, Zhou et al., 1998, Doerrler et al., 2001).

Two phosphatases, LpxE and LpxF, catalyze the removal of the 1 and 4′-positionphosphates (Karbarz et al., 2003, Wang et al., 2006a). The phosphatases are inner membrane proteins with six predicted transmembrane helices (Karbarz et al., 2003, Wang et al., 2006a, Karbarz *et al.*, 2009). Both phosphatases display strict specificity for their respective substrates and display a preference for Kdosylated substrates. The topography and selectivity of the two phosphatases has been confirmed by heterologous expression of the two enzymes in *E. coli*. Expression of LpxE and LpxF orthologues from *F. novicida* in a *msbA* temperature-sensitive mutant results in robust dephosphorylation at the permissive temperature and no dephosphorylation at the non-permissive temperature (Wang et al., 2004, Wang *et al.*, 2006b). *Leptospira integrrogans*, *Helicobacter pylori*, and P*orphyromonas gingivalis* all possess 4′-phosphatase activity, but do not contain a LpxF orthologue. Orthologues of LpxE can be found in *H. pylori*, *S. meliloti*, and *Mesorhizobium huakuii*. LpxE and LpxF both contain variations of the lipid phosphate phosphatase sequence motif (Stukey & Carman, 1997).

After removal of the 4′-phosphate, the enzyme RgtD is proposed to incorporate the galacturonic acid moiety at the 4′-position using dodecaprenyl phosphate

galacturonic acid as a cosubstrate. The same donor is utilized by the enzymes RgtA, RgtB, and RgtC to incorporate galacturonic acid moieties into the Kdo region of *Rhizobium* LPS (Kanjilal-Kolar et al., 2006, Kanjilal-Kolar & Raetz, 2006).

After export to the outer membrane, the outer membrane enzyme PagL catalyzes the removal of the 3-O-acyl chain, and the lipid A oxidase, LpxQ, catalyzes oxidation of the proximal glucosamine (Basu et al., 1999a, Que-Gewirth et al., 2003a, Que-Gewirth et al., 2003b). Both outer membrane enzymes process a portion of the lipid A molecules of free-living bacteria. The partial activity of these enzymes gives rise to the heterogeneity associated with *R. leguminosarum* and *R etli* lipid A. The activity of the two enzymes might be regulated under some conditions. Other outer membrane enzymes that remodel lipid A are often activated by extracellular stimuli (Bishop, 2008).

The deacylase is highly specific for the 3-O-linked β-hydroxyacyl chain of lipid A. The gene for the activity has not been found previously. The activity is similar to that of PagL, an enzyme that is found in *Pseudomonas aeruginosa*, *Salmonella typhimurium*, and *Bordetella bronchiseptica*. The *pagL* gene product from *S. typhimurium* has been well characterized (Trent *et al.*, 2001b). In chapter 6, the *Rhizobium* 3-*O*-deacylase is shown to be a PagL homolog. It is unique among the group of PagL homologs in that it displays a dependency on calcium (Basu et al., 1999a).

LpxQ generates the aminogluconate residue of *R. leguminosarum* and *R. etli* lipid A in an oxygen-dependent manner. It is a unique outer membrane enzyme that displays no significant homology to other oxidases. LpxQ activity can be inhibited *in vitro* by the addition of EDTA, but it can be restored upon the addition of excess divalent cations. The enzyme requires substrates dephosphorylated at the 1-position (Que-Gewirth et al., 2003a, Que-Gewirth et al., 2003b).

1.11 Biological function of the lipid A modifications found in Rhizobium

The role LPS plays in bacterial-plant symbiosis is unclear. Genetic studies have shown that an intact O-antigen is necessary for completion of the late stages of plant infection by *R. leguminosarum* (Kannenberg et al., 1992, Noel et al., 1986, Priefer, 1989, de Maagd *et al.*, 1989, Perotto, 1994). In addition, covalent modifications to LPS have been shown to occur during the development of nitrogen fixing bacteroids (Bhat & Carlson, 1992, Duelli *et al.*, 2001, Kannenberg & Brewin, 1989, Kannenberg & Carlson, 2001). A direct role for lipid A in bacterial-plant symbiosis has not been established. It has been hypothesized that the lipid A modifications found in organisms such as *R. leguminosarum* and *R. etli* could play important roles in the process. The lipid A isolated from *R. leguminosarum* bacteroids is not drastically different to that of free-living bacteria. The major difference between the free-living bacteria and bacteroids in terms of lipid A composition is acyl chain composition. *R. leguminosarum* bacteroids are reported

to be uniformly tetraacylated (D'Haeze *et al.*, 2007). The results of this analysis suggest that deacylation is important in nodulation. The PagL gene has not been reported to date, thus, it has not been possible to make the relevant strains to test the importance of this modification.

AcpXL mutants have been reported in *R. leguminosarum* and in *S. meliloti* (Sharypova *et al.*, 2003, Vedam *et al.*, 2004) These mutants display a sensitivity to detergents, acidic conditions, changes in osmolarity, and display slower nodulation kinetics compared to wild type cells. The nodules from these mutant strains, however, display a normal morphology and fix nitrogen, but differ slightly in bacteroid development (Vedam et al., 2004). A recent report claims that *R. leguminosarum* AcpXL bacteroid mutants can be acylated with the 27-hydroxyoctacosanoic acid moiety in the nodule environment. The details of the mechanism by which this could occur remain unexplained (Vedam *et al.*, 2006). To date, only mutants deficient in AcpXL and/or LpxXL have been described in the literature. The effects of the phosphatases, aminogluconate residue, and the galacturonic acid have not been tested.

As mentioned previously, the function of the lipid A modifications in *R. leguminosarum* and *R. etli* are unknown. The lipid A modifications may play a role in protecting the bacteria from immune responses of their host. This appears to be one of the primary functions of lipid A modifications in pathogenic bacteria (Raetz et al., 2007).

Recent findings suggests that the lipid A moiety of LPS may be partially responsible for LPS perception in the plant *Arabidopsis thaliana* (Zeidler *et al.*, 2004). Suspension-cultured cells and leaves of *A. thaliana* produce a rapid burst of NO when treated with the LPS and lipid A moiety of Gram-negative pathogens. Treatment of these cells with LPS also leads to the activation of defense genes. This analysis suggests that some aspects of plant innate immunity are similar to that of innate immune responses in various vertebrate and invertebrate organisms. The role of lipid A modifications in bacterial endosymbionts therefore could be in evading such responses.

1.12 Contributions of this work to existing knowledge

As described in the preceding sections, *R. leguminosarum* and *R. etli* contain several lipid A modification enzymes that modify Kdo_2-lipid IV_A. Orthologues of some of the modification enzymes exist in animal and plant pathogens such as *F. novicida, H. pylori*, *Brucella. melitensis*, and *A. tumefaciens*. The lipid A modification enzymes, therefore, are of great interest. The aims of this work are to determine the enzymatic mechanism for some of the modification enzymes and to elucidate the biological roles of the modifications.

Chapter II describes the heterologous expression of LpxE, LpxF, and LpxQ in various strains of *E. coli.* Co-expression of these enzymes in the selected backgrounds yields novel lipid A structures that resemble those found in *R. leguminosarum* and *R. etli.*

The lipid A species accumulating in the *E. coli* strains confirms the proposed topography and selectivity of LpxE, LpxF, and LpxQ. The strains expressing the phosphatases are shown to be highly resistant to polymyxin, supporting a role for the modifications in avoiding cationic antimicrobials. The 4′-phosphatase is shown to be particularly important for this effect. *E. coli* strains lacking a complete core expressing LpxE and LpxF show slow growth phenotypes supporting a role for the phosphates of lipid A in stabilizing the outer membrane. This approach of re-engineering lipid A demonstrated in chapter II could have applications in vaccine development or in the development of novel lipid A adjuvants.

Chapter III describes the purification and characterization of the lipid A oxidase, LpxQ. Although the *lpxQ* gene was previously discovered and the enzymatic activity had been previously described (Que-Gewirth et al., 2003a, Que-Gewirth et al., 2003b), several questions remained about the mechanism of LpxQ. Purification of the enzyme facilitated further enzymatic characterization. In this work, the role of oxygen in the LpxQ catalyzed oxidation of lipid A is confirmed as that of an electron acceptor. The expected product of the reaction, H_2O_2, is shown to be produced in stoichiometric amounts concomitant with oxidized lipid A. In this work, two new assays are described for monitoring lipid A oxidation. The substrate, 1-dephospho Kdo_2-lipid IV_A, is shown to be a good alternative substrate to the ^{14}C substrates previously used in assaying the

oxidase. A coupled assay for monitoring lipid A oxidation based on the production of H_2O_2 is also introduced. LpxQ, like many other outer membrane proteins is shown to be very stable. The protein does not appear to co-purify with any particular cofactor.

Chapter IV describes the refolding of LpxQ from inclusion bodies. LpxQ refolding is demonstrated in the presence of non-ionic detergents. LpxQ is shown to be catalytically active upon refolding in the absence of any exogenously added cofactors. These results have implications regarding the route of electron transfer in the LpxQ-catalyzed oxidation of lipid A.

Chapter V describes deletion mutants of LpxE and LpxF in *R. etli*. These mutants are shown to accumulate the expected phosphorylated precursor molecules. The mutants are shown to be symbiotically active but normal in nitrogen fixation activities. *R. etli* mutants deficient in the phosphatases display a sensitivity to polymyxin, supporting a role for the phosphatases in aiding the bacteria to avoid cationic antimicrobials.

Lastly, Chapter VI describes the identification and characterization of the PagL gene from *R. etli* and *R. leguminosarum*. The gene was discovered by searching the recently completed *R. etli* genome with the distant PagL homologue from *S. typhimurium*. A homologue of the *R. etli* gene is show to exist in *S. meliloti*. The role of the PagL-catalyzed modification is also investigated in a nodulation study.

Chapter 2: Re-engineering *Escherichia coli* Lipid A Through Heterologous Expression of the *Francisella novicida* 1- and 4′-Phosphatases and the *Rhizobium leguminosarum* Lipid A Oxidase

2.1 Introduction

LPS (lipopolysaccharide) is the major surface molecule on the outer membrane of Gram-negative bacteria (Raetz & Whitfield, 2002). LPS contributes to the structural integrity of cells by acting as a protective barrier (Nikaido, 2003). It consists of three domains: a distal O-antigen polysaccharide, a non-repeating core oligosaccharide, and a lipid A moiety (Raetz & Whitfield, 2002). The lipid A moiety is relatively conserved and is responsible for anchoring LPS into the membrane (Raetz & Whitfield, 2002). This unique glucosamine-based saccharolipid is required for growth in almost all Gram-negative bacteria (Raetz & Whitfield, 2002) and acts as a potent stimulator of innate immunity in animals via the Toll-like receptor-4-MD-2 (TLR4/MD-2) complex (Park et al., 2009). Immune-recognition of lipid A leads to the production of several inflammatory cytokines, such as TNF-α, which play a role in bacterial clearance (Beutler & Cerami, 1988). Overproduction of these inflammatory mediators during sepsis, however, can result in Gram-negative shock (Parrillo, 1993, Russell, 2006).

In *E. coli*, the most abundant lipid A species is a β,1′-6-linked disaccharide of glucosamine that is hexaacylated and phosphorylated at the 1- and 4′-positions (Fig. 12

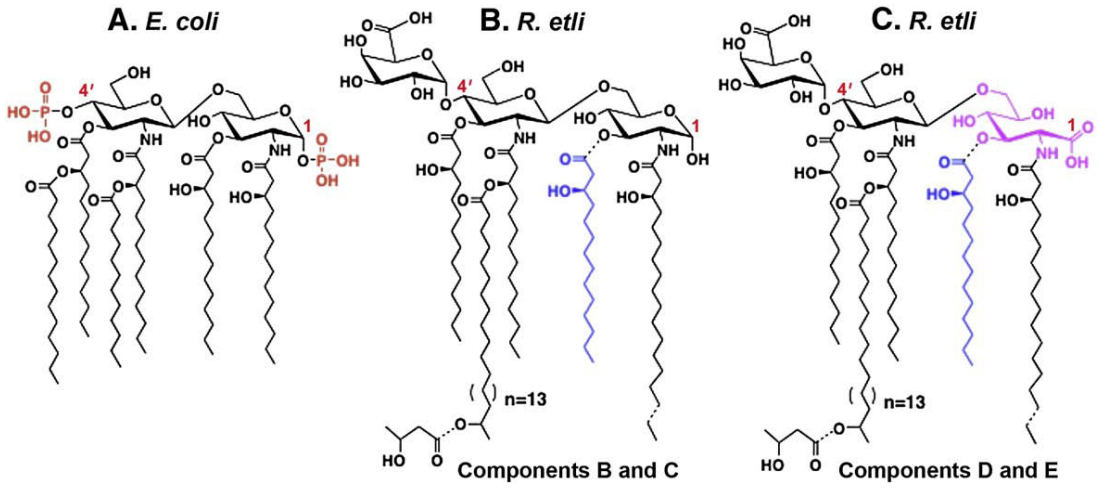

Figure 12: Structural variation of lipid A molecules.

Panel A. The most prevalent lipid A species found in wild-type *E. coli* consists of a hexaacylated disaccharide of glucosamine, substituted with monophosphate groups at the 1 and 4′ positions (Raetz & Whitfield, 2002). **Panels B and C.** The lipid A from *R. leguminosarum* is heterogeneous. The major forms are void of phosphate and differ from each other in their sugar composition and acylation status (Que et al., 2000a, Que et al., 2000b). Components B and C contain the typical glucosamine disaccharide found in the lipid A of other Gram-negative organisms. Components D and E feature an aminogluconate unit in place of the proximal glucosamine residue, and are derived from the LpxQ-catalyzed oxidation of B and C respectively (Que-Gewirth et al., 2003a, Que-Gewirth et al., 2003b). Components C and E differ from B and D by the absence of a hydroxyacyl chain at position 3, which is removed by the deacylase PagL (Basu et al., 1999a, Rutten *et al.*, 2006). Other unique structural features include the presence of a very long secondary acyl chain at position 2′ (Bhat et al., 1991b), and a galacturonic acid in place of phosphate at position-4′ (Que et al., 2000a, Que et al., 2000b). Dashed bonds highlight the most prominent micro-heterogeneity of *R. etli* lipid A with respect to acyl chains.

A)(Raetz & Whitfield, 2002). The disaccharide backbone is acylated at the 2-, 3-, 2′-, and 3′- positions with R-3-hydroxymyristate (Raetz & Whitfield, 2002). Secondary lauroyl and myristoyl chains forms the acyloxyacyl moieties at the 2′- and 3′-positions (Brozek & Raetz, 1990). These structural features are required for full activation of the TLR4/MD2 complex (Rietschel et al., 1994). Synthetic lipid A analogs lacking some of these features such as "Monophosphoryl-lipid A" (MPL), which lacks the phosphate at the 1-position, have been developed as adjuvants for use in human vaccines (Baldridge et al., 2004, Kundi, 2007). These modified lipids A analogs have been shown to be potent TLR4/MD-2 agonists, but they induce altered cytokine profiles that are much less toxic (Baldridge et al., 2004).

Lipid A is assembled on the cytosolic surface of the inner membrane by a conserved pathway of nine constitutive enzymes that process UDP-N-acetyl-glucosamine (Raetz & Whitfield, 2002). After assembly, the lipid A is glycosylated with core sugars and flipped by the ABC transporter, MsbA, (Zhou et al., 1998, Doerrler et al., 2001, Reyes & Chang, 2005) to the outer surface of the inner membrane where the O-antigen oligosaccharide is incorporated (Raetz & Whitfield, 2002). The nascent LPS molecule is then transported across the periplasm to the outer surface of the outer membrane (Sperandeo et al., 2007, Sperandeo et al., 2006, Wu et al., 2006, Sperandeo et al., 2008, Raetz et al., 2007). In various species, modification enzymes alter lipid A as it is

trafficked to the outer membrane (Raetz et al., 2007). These modifications are typically not required for growth (Raetz et al., 2007), but they often confer growth advantages under stressful environmental conditions. *E. coli* and *Salmonella*, for example, are capable of modifying their lipid A to evade cationic antimicrobials, such as polymyxin (Helander *et al.*, 1994). They modify their lipid A by covalently attaching 4-amino-4-deoxy-L-arabinose (L-Ara4N) (Gunn *et al.*, 1998) and phosphoethanolamine (pEtN) moieties (Lee *et al.*, 2004) to their phosphate groups These modifications mask the negative charges of the phosphate moieties rendering them polymyxin resistant (Raetz et al., 2007).

Modifications to lipid A in pathogenic bacteria are thought to be important for virulence. *F. novicida* and *F. tularensis*, the causative agents of tularemia in mice and humans, possess two inner membrane phosphatases, LpxE (Wang et al., 2004) and LpxF (Wang et al., 2006a), which are specific for the 1- and 4′-phosphates of lipid A. The dephosphorylation of lipid A in these pathogens is thought to be beneficial because dephosphorylated lipid A is attenuated in its ability to act as an activator of innate immunity and is resistant to cationic antimicrobial peptides (Baldridge & Crane, 1999). A recently characterized *F. novicida* 4′-phosphatase mutant was shown to be sensitive to polymyxin and highly attenuated in a mouse infection model (Wang *et al.*, 2007).

Modifications to lipid A, however, are not exclusive to pathogenic bacteria. The lipid A from *R. leguminosarum*, a bacterial endosymbiont that forms a nitrogen-fixing

symbiosis with leguminous plants, is strikingly different compared to that of *E. coli.* The lipid A in *R. leguminosarum* exists as a mixture of related components that are extensively modified (Figs. 12B and 12C) (Bhat et al., 1994, Raetz et al., 2007). Homologs of the *Francisella* LpxE and LpxF phosphatases are present in *R. leguminosarum* and are constitutively active (Karbarz et al., 2003) (Wang et al., 2006a). In these organisms, the 4′-position phosphate is replaced with a galacturonosyl residue, and the proximal dephosphorylated glucosamine is present either in the hemiacetal form (Fig. 12B) or as an oxidized 2-amino-2-deoxy-gluconate unit (Fig. 12C) (Bhat et al., 1994, Que et al., 2000a, Que et al., 2000b). Oxidation of the dephosphorylated glucosamine moiety is catalyzed by an outer membrane oxidase, LpxQ, in an oxygen-dependent manner (Que-Gewirth et al., 2003a, Que-Gewirth et al., 2003b). *R. leguminosarum* lipid A also differs from *E. coli* with respect to its acylation status (Fig. 12). *R. etli* lipid A lacks the secondary laurate and myristate chains found in *E. coli*, and is instead acylated with a secondary 27-hydroxyoctacosanoate chain (27OHC28:0) at the 2′-position (Bhat et al., 1991b, Bhat et al., 1994, Que et al., 2000a, Que et al., 2000b). This residue may be esterified further with a β-hydroxybutyrate moiety (Figs. 12B and 12C) (Bhat et al., 1994, Que et al., 2000a, Que et al., 2000b).

The biological role of the lipid A modifications in *Rhizobium leguminosarum* remains to be elucidated. It is unclear whether lipid A stimulates innate immunity in

plants; however, the innate immune response to *Rhizobium* lipid A has been studied in human cells. In human monocytes, the lipid A from *Rhizobium* Sin-1, which is structurally similar to that of *R. leguminosarum (Jeyaretnam et al., 2002)*, does not stimulate the production of pro-inflammatory cytokines and may be an antagonist of enteric LPS (Vandenplas *et al.*, 2002). Synthetic analogs of *Rhizobium* Sin-1 lipid A have been developed as lead compounds for the development of therapeutic agents for treating Gram-negative sepsis (Demchenko *et al.*, 2003, Santhanam *et al.*, 2004, Lee *et al.*, 2006).

In the present chapter we demonstrate the heterologous expression of the *F. novicida* phosphatases, LpxE and LpxF, and the *R. leguminosarum* lipid A oxidase, LpxQ, in *E. coli*. We show that the expression of these modification enzymes facilitates the dramatic re-engineering of lipid A structures. The novel lipid A species accumulating in these strains are structurally similar to those found in *R. leguminosarum* and *R.* Sin-1. The approach of re-engineering lipid A demonstrated here could be applicable to the development of novel lipid A-based adjuvants and can be applied in the development of new live bacterial vaccines.

2.2 Materials and Methods

2.2.1 Materials

[γ-^{32}P] ATP and [U-^{14}C]-acetate were obtained from PerkinElmer Life and Analytical Sciences, Inc. (Waltham, MA). Acetic acid, chloroform, sodium acetate, and

glass-backed 0.25-mm Silica Gel-60 thin layer chromatography (TLC) plates were from EMD Chemicals, Inc. (Gibbstown, NJ). Formic acid, pyridine, and methanol were from Mallinckrodt Baker, Inc. (Phillipsburg, NJ). Yeast extract, agar, and tryptone were from Becton, Dickinson, and Company (Franklin Lakes, NJ). Sodium chloride was from VWR International (West Chester, PA). Bicinchoninic (BCA) protein assay reagents and Triton X-100 were from Thermo Fisher Scientific (Waltham, MA). PCR reagents were purchased from EMD and Stratagene (La Jolla, CA). IPTG was from Invitrogen (Carlsbad, CA). All other chemicals were reagent grade and were purchased from either Sigma-Aldrich (St. Louis, MO) or VWR International (West Chester, PA).

2.2.2 Bacterial strains and growth conditions

The bacterial strains and plasmids used and their relevant characteristics are shown in Table 1. *E. coli* strains were grown at 37 °C in LB broth (1% tryptone, 0.5% yeast extract, and 1% sodium chloride) and supplemented with the following antibiotics, as appropriate: ampicillin (100 μg/mL), kanamycin (50 μg/mL), tetracycline (12.5 μg/ml) or chloramphenicol (30 μg/mL).

2.2.3 Recombinant DNA techniques

Protocols for handling DNA and preparing *E. coli* for electroporation were performed using standard protocols (Sambrook & Russell, 2001). Transformation-competent cells of *E. coli* were prepared by the method of Inoue *et al* (Inoue *et al.*, 1990).

Plasmids were isolated from cell cultures and purified using the QiAprep and QIAquick gel extraction kits from Qiagen (Valencia, CA). KOD hot start DNA polymerase (EMD), Pfu Turbo DNA polymerase (Stratagene), T4 DNA ligase (Invitrogen), restriction endonucleases (New England Biolabs, Ipswich, MA) and shrimp alkaline phosphatase from Affymetrix (Santa Clara, CA) were used according to the manufacturers' instructions. Double stranded DNA sequencing was performed with an ABI Prism 377 instrument at the Duke University DNA Analysis Facility. Primers were purchased from MWG Biotech (Huntsville, AL) and IDT Biosciences (Coralville, IA).

2.2.4 Construction of plasmids expressing the R. leguminosarum lpxQ, F. novicida lpxE, and F. novicida lpxF genes

Plasmids expressing combinations of LpxQ, LpxE, and LpxF were created in the lactose-inducible, low-copy expression vector, pWSK29. The combination plasmids were designed so that the coding region of each gene would be preceded by a ribosome binding site. The oligonucleotide primers are shown in Table 2. The oligonucleotide primers RlegQfor and RlegQrev were used to amplify the *R. leguminosarum lpxQ* gene from plasmid pQN233, resulting in PCR product 1. The PCR product contained the coding region of LpxQ. The oligonucleotide primers FnovEfor and FnovEHind were used to amplify the *F. novicida lpxE* gene from pWSK29-LpxE, resulting in PCR product 2. PCR product 2 contained the coding region of *lpxE*. The sequence upstream of the *lpxE*-coding region in the primer FnovEfor was complementary to the sequence

downstream of the *lpxQ*-coding region in the primer RlegQrev. PCR product 3, which contained the coding regions of *lpxQ* and *lpxE*, each with their own ribosome binding sites, was created by amplifying PCR products 1 and 2 with the primers RlegQfor and FnovEHind. PCR reaction product 3 was digested using *XbaI* and *HindIII* and analyzed on a 1% agarose gel. The desired band was excised and gel-purified. The purified PCR product was ligated into pWSK29 which had been similarly digested and treated with shrimp alkaline phosphatase. The ligation mixture was transformed into XL1-Blue cells, and several ampicillin resistant colonies were selected on LB plates. The plasmid pWSK29-LpxQE was isolated from this pool and transformed into W3110A and WBB06 cells.

Plasmid pWSK29-LpxQEF, encoding the *RllpxQ*, *FnlpxE*, and *FnlpxF* genes, was created in a second series of PCR reactions. The oligonucleotide primers RlegQfor and FnovErev were used to amplify the *lpxQ* and *lpxE* genes from plasmid pWSK29-LpxQE, resulting in PCR product 4. Primers FnovFfor and FnovFrev were used to amplify the *lpxF* gene from pWSK29-LpxF to create PCR product 5. The sequence upstream of the *lpxF*-coding region in the primer FnovFfor also coded for a ribosome binding site and was complementary to the sequence downstream of the *lpxE*-coding region in the primer FnovErev. PCR product 6, containing the coding regions of *RllpxQ*, *FnlpxE*, and *FnlpxF* each with their own ribosome binding sites, was created by amplifying the genes

from PCR products 4 and 5 using the RlegQfor and FnovFrev primers. PCR product 6 was digested using *XbaI* and *KpnI*, analyzed on a 1% agarose gel, and gel-purified. The purified PCR product was ligated into pWSK29 which had been similarly digested and treated with shrimp alkaline phosphatase. The ligation mixture was transformed into XL1-Blue cells, and several ampicillin resistant colonies were selected on LB plates. The plasmid pWSK29-LpxQEF was isolated from this pool and transformed into *E. coli* strains MLK1067 and SR8209.

Plasmid pWSK29-LpxEF which encodes both *lpxE* and *lpxF*, was constructed in another set of PCR reactions. The oligonucleotide primers FnovEXbaI and FnovFrev were used to amplify the *lpxE* and *lpxF* genes from plasmid pWSK29-LpxQEF to create PCR product 7. PCR product 7 was digested with *XbaI* and *KpnI*, and analyzed on a 1% agarose gel. The desired band was excised and gel-purified. The purified PCR product was ligated into pWSK29 which had been similarly digested and treated with shrimp alkaline phosphatase. The ligation mixture was transformed into XL1-Blue cells, and several ampicillin resistant colonies were selected on LB plates. The plasmid pWSK29-LpxEF was isolated from this pool and transformed into *E. coli* strains MLK1067and SR8209.

2.2.5 Preparation of washed membranes

All enzyme preparations were carried out at 0-4 °C. Cell-free extracts and washed membranes were prepared as described previously (Basu et al., 2002). Typically 200-mL cultures were grown to A_{600} = 1.0. The cells were harvested by centrifugation at 4000 x g for 20 min. The cell pellets were washed with 40 mL of 50 mM HEPES, pH 7.5 and stored at -80 ℃. The frozen pellets were later thawed and resuspended in 10 ml of 50 mM HEPES, pH 7.5. The cells were disrupted by passage through a French pressure cell at 18,000 p.s.i., and unbroken cells were removed by centrifugation at 10,000 X g for 20 min. The membranes were collected by centrifugation at 100,000 X g for 1 h and washed by suspension in 10 mL of 50 mM HEPES, pH 7.5. The membranes were resuspended in the same buffer at a concentration of 5-10 mg/ml and stored in aliquots at -80 °C. The bicinchoninic acid method (Smith *et al.*, 1985) was used to determined protein concentrations using bovine serum albumin as a standard.

2.2.6 Preparation of substrates

Preparation of the Kdo_2-lipid IV_A substrate was described previously (Six et al., 2008). Radiolabeled Kdo_2-[4′-^{32}P]-lipid IV_A was synthesized as described previously (Reynolds *et al.*, 2005). The substrates were stored frozen in 25 mM Tris-HCl, pH 7.8, 1 mM EDTA, 1mM EGTA, and 0.1% Triton X-100. Prior to use, the lipid substrates were dispersed by sonic irradiation for 1 min in a bath sonicator.

2.2.7 In vitro assay of LpxE and LpxQ

LpxE and LpxQ activity was assayed in 10-30 μL reactions mixtures at 30 °C. Standard assay conditions were as follows: the reaction mixture contained 50 mM MES, pH 6.5, 0.1% Triton X-100, 1 mM MgCl, and 10 μM Kdo_2-[4′-^{32}P]lipid IV_A (1,000 cpm/nmol). Reactions were initiated with the enzyme source. The reaction mixtures were incubated for the time indicated. Reactions were terminated by spotting 3-μl samples onto a TLC plate, which was developed in the solvent chloroform/methanol/acetic acid/water (25:15:4:4; v/v). After drying and overnight exposure of the plate to a PhosphorImager screen (GE Healthcare), product formation was detected and quantified with a Storm 840 PhosphorImager equipped with ImageQuant software (GE Healthcare).

2.2.8 Lipid A extraction

Single colonies of cells expressing pWSK29, pWSK29-LpxE, pWSK29-FnLpxF, pWSK29lpxQE, pWSK29-lpxEF, or pWSK29-lpxQEF were used to inoculate 5 mL of LB medium supplemented with 100 μg/ml ampicillin and grown overnight with shaking at 37 °C. The overnight cultures were used to inoculate 200 ml cultures of LB supplemented with 100 μg/ml ampicillin and 1mM IPTG, starting at A_{600} = 0.01. The cells were shaken (220 rpm) at 37 °C and grown to A_{600} = 1.0 .Cells were then harvested by centrifugation at 4000 x g for 20 min at 4 °C. The cells were washed once with

phosphate-buffered saline (PBS) and stored at -80 °C. The washed W3110A and MLK1067 cells were later thawed and extracted for 1 h at room temperature with a single phase Bligh-Dyer mixture consisting of chloroform/methanol/water (1:2:0.8, v/v). The cells were then centrifuged at 4000 x g for 20 min and the insoluble material was recovered and washed once more with a single-phase Bligh-Dyer mixture. The insoluble material was again recovered by centrifugation. The washed pellets were then resuspended in 12.5 mM sodium acetate and subjected to probe sonic irradiation. The suspensions were then placed in a boiling water bath for 30 min. The suspensions were then allowed to cool to room temperature. The cooled suspensions were then converted to two-phase Bligh Dyer mixtures (chloroform:methanol:water, 2:2:1.8, v/v) by adding chloroform and methanol. The phases were mixed and separated by centrifugation at 4000 x g for 20 min. The lower phases were removed and the upper water-methanol phases were extracted a second time by the addition of pre-equilibrated lower phase. The lower phases were pooled and dried with a rotary evaporator. The lipids were stored at -80 °C.

The lipid A extraction procedure for the WBB06 and SR8209 cells differed slightly because these strains harbor deletions that remove portions of both the *waaC* and *waaF* genes, which are involved in heptose incorporation. These strains accumulate a truncated "Re" LPS which is soluble in a single-phase Bligh Dyer mixture. The

extraction procedure was the same as that used for the other strains except the hydrolysis step was omitted. The supernatants from the single-phase Bligh Dyer extractions of the WBB06 and SR8209 cells were directly converted to two-phase Bligh Dyer solutions and further extracted as described above.

2.2.9 Isolation of lipid A species from ^{14}C-labeled MLK1067 strains

LB broth (10 mL) supplemented with 100 μg/ml ampicillin, 1mM IPTG, and 100 μCi/ml [U-14C] acetate were inoculated with the appropriate strains, starting at A600 = 0.01. The 14C-labeled cells were grown to A600 = 1.0, harvested, and washed with 5 ml of PBS. The washed cells were stored at -20 °C. The cell pellets were thawed at room temperature, resuspended in 1.6 ml PBS, and vortexed. Two ml of chloroform and 4 ml of methanol were added to form single-phase Bligh-Dyer mixtures which were incubated at room temperature for 60 min to delipidate the cell pellets. After centrifugation, the pellets containing the lipid A covalently attached to the LPS, were washed once more with 3 ml of a single phase Bligh-Dyer mixture. After removing the supernatants from the second extraction, the pellets were resuspended in 3.6 ml of 12.5 mM sodium acetate, pH 4.5, vortexed, and sonicated in a bath sonicator until the suspensions were homogenous. The suspensions were heated at 100 °C for 30 min, cooled, and then converted to two-phase Bligh-Dyer mixtures by the addition of chloroform and water. After thorough mixing, the two phases were separated by

centrifugation. The lower phases were removed and the upper phases were washed once with chloroform. The lower phases from the second extractions were collected, pooled with the first, and dried under a stream of nitrogen. The dried lipids were re-dissolved in chloroform:methanol (4:1, v/v) and spotted onto a TLC plate (10,000 cpm/lane), which was developed in the solvent system chloroform:methanol:pyridine:acetic acid:water (25:10:5:4:3, v/v). After drying, the plate was exposed to a PhosphorImager Screen (GE Healthcare) overnight. Lipids were detected with a Storm 840 PhosphorImager and quantified by scintillation counting. Approximately, 0.25% of the [U-14C] acetate added to the cultures was incorporated into lipid A.

2.2.10 Negative ion electrospray ionization (ESI) of lipid A species

Lipid A species extracted from cells were redissolved in chloroform:methanol (4:1, v/v), subjected to sonic irradiation in a bath sonicator, and subsequently diluted into chloroform:methanol (2:1), containing 1% piperdine. The sample was immediately infused into the ion source at 5-10 μL/min and analyzed by ESI/MS, as described previously (Kanjilal-Kolar et al., 2006, Kanjilal-Kolar & Raetz, 2006). All mass spectra were acquired on a QSTAR XL quadrupole time-of-flight mass spectrometer (ABI/MDS-Sciex, Toronto, Canada) equipped with an electrospray ionization (ESI) source. Spectra were acquired in the negative ion mode and typically were the accumulation of 60 scans

from *m*/*z* 200 to *m*/*z* 2000 atomic mass units. Data acquisition and analysis were performed using Analyst QS software version 1.1.

2.2.11 Growth phenotypes of SR8209 cells expressing RlLpxQ, FnLpxE, and FnLpxF

SR8209 strains expressing pWSK29, pWSK29-LpxE, pWSK29-LpxF, pWSK29-LpxEF, and pWSK29-LpxQEF were grown at 37 ℃ overnight on LB broth containing 100 μg/ml ampicillin. The cultures were used to inoculate 25 mL of prewarmed LB broth (37 ℃) containing 1 mM IPTG and 100 μg/ml ampicillin to A_{600} = 0.02. Whenever the A_{600} reached 0.3-0.4, the cultures were diluted 10-fold into 25 mL of prewarmed LB broth containing 1 mM IPTG and 100 μg/ml ampicillin.

2.2.12 Polymyxin MIC determination

The MIC of polymyxin B sulfate was determined for the MLK1067 and SR8209 strains expressing combinations of FnLpxE, FnLpxF, and RlLpxQ. Briefly, LB supplemented with 100 μg/ml ampicillin and 1 mM IPTG was added to the wells of several 96-well plates (Corning Costar 3596, flat bottomed lid, polystyrene wells). Different concentrations of polymyxin were prepared by making serial dilutions (1:2) of a 50 mg/mL stock into the media. MLK1067 or SR8209 cells expressing pWSK29, pWSK29-LpxE, pWSK29-LpxF, pWSK29-LpxEF, or pWSK29-LpxQEF were prepared by growing the strains overnight in LB broth containing 100 μg/ml ampicillin at 37 °C. The cultures were used to inoculate tubes containing 5 mL of LB broth supplemented with 1

mM IPTG and 100 μg/ml ampicillin to a starting A600 = 0.02. The cultures were grown to an A600 = 0.6 and then diluted 1:100 in LB supplemented with 1 mM IPTG and 100 μg/ml ampicillin. The diluted cultures were further diluted 1:2 into the wells containing media supplemented with polymyxin. The plates were incubated at 37 °C for 20 hours. After the incubation period, 50 μL of a 1 mg/ml [4,5-dimethylthiazol-2-yl]-2,5-diphenyltetrazolium bromide stock solution was added to each well. The plates were incubated for 3 additional hours at 37 °C. Cell viability was assessed colorimetrically. Experiments are the mean of three replicates.

2.2.13 Ca^{2+} sensitivity assay

SR8209 cells harboring pWSK29, pWSK29-LpxE, pWSK29-LpxF, pWSK29-LpxEF, and pWSK29-LpxQEF were grown overnight starting from single colonies in LB broth supplemented with 100 μg/ml ampicillin. The cultures were used to inoculate tubes containing 5 mL of LB broth supplemented with 1 mM IPTG and 100 μg/ml ampicillin to A_{600} = 0.02. The cultures were grown to A_{600} = 0.1 (~10^8 CFU). Six serial dilutions (1:10) of each strain were made in LB broth. Ten μL of each dilution was transferred to individual grids on a 100 X 15 mm square style LB agar plate with 13 mm grids. Strains were plated on agar plates supplemented with 100 μg/ml ampicillin, 1 mM IPTG, and 10 mM $CaCl_2$ or control plates with 100 μg/ml ampicillin and 1 mM IPTG. All strains were plated in duplicate.

Table 1: Bacterial strains and plasmids used in chapter 2

Strain or Plasmid	Genotype or Description	Source or Reference
Strains		
W3110A	Wild type *E. coli*, F-,λ-, aroA::Tn10	(Doerrler et al., 2001)
WBB06	W3110 *mtl*, Δ(*waaC-waaF*)::*tet*6	(Brabetz *et al*., 1997)
MLK1067	W3110 *lpxM::Ωcam*	(Karow & Georgopoulos, 1992)
SR8209	BW25113 *Φ* (p*cpxP-lacZ*) *waaCF* tet *lpxM* <> cam	(Klein *et al*., 2009)
XL1-Blue	*recA1 endA1 gyrA96 thi-1 hsdR17 supE44 relA1 lac*	Stratagene
W3110A/pWSK29	W3110A transformed by pWSK29	this work
W3110A/pWSK29-LpxE	W3110A transformed by pWSK29-LpxE	this work
W3110A/pWSK29-LpxQE	W3110A transformed by pWSK29-LpxQE	this work
WBBO6/pWSK29	WBBO6 transformed by pWSK29	this work
WBBO6/pWSK29-LpxE	WBBO6 transformed by pWSK29-LpxE	this work
WBBO6/pWSK29-LpxQE	WBBO6 transformed by pWSK29-LpxQE	this work
MLK1067/pWSK29	MLK1067 transformed by pWSK29	this work
MLK1067/pWSK29-LpxE	MLK1067 transformed by pWSK29-LpxE	this work
MLK1067/pWSK29-LpxF	MLK1067 transformed by pWSK29-LpxF	this work
MLK1067/pWSK29-LpxQE	MLK1067 transformed by pWSK29-LpxQE	this work
MLK1067/pWSK29-LpxQEF	MLK1067 transformed by pWSK29-LpxQEF	this work
MLK1067pWSK29-LpxEF	MLK1067 transformed by pWSK29-LpxEF	this work
SR8209/ pWSK29	SR8209 transformed by pWSK29	this work
SR8209/ pWSK29-LpxE	SR8209 transformed by pWSK29-LpxE	this work
SR8209/pWSK29-LpxF	SR8209 transformed by pWSK29-LpxF	this work
SR8209/pWSK29-LpxQE	SR8209 transformed by pWSK29-LpxQE	this work
SR8209/pWSK29-LpxQEF	SR8209 transformed by pWSK29-QEF	this work
SR8209/pWSK29-LpxEF	SR8209 transformed by pWSK29-EF	this work
Plasmids		
pQN233	*lpxQ* in pET21a(+)	(Que-Gewirth et al., 2003a)
pWSK29	Low copy vector, Amp^r	(Wang & Kushner, 1991)
pWSK29-LpxE	pWSK29 harboring *FnlpxE*	(Wang et al., 2004)
pWSK29-LpxF	pWSK29 harboring *FnlpxF*	(Wang et al., 2006a)
pWSK29-LpxQE	pWSK29 harboring *RllpxQ and FnlpxE*	this work
pWSK29-LpxQEF	pWSK29 harboring *RllpxQ, FnlpxE, and Fn lpxF*	this work
pWSK29-LPxEF	pWSK29 harboring *FnlpxE* and *Fn lpxF*	this work

Abbreviations: tet-tetracyline, cam-chloramphenicol, amp-ampicillin

Table 2: Oligonucleotide primers used in chapter 2

Name	Sequence
RlegQfor	(5′-CGCGC*TCTAGA*AAGGAGAATTTAAA**ATGACATATGCGCTGTCTTCC**-3′)
RlegQrev	(5′-TTTAAATTCTCCTTCCCGGGCCCGG**TTACCAGTGGAATGAAACGC**-3′)
FnovEfor	(5′-CCGGGCCCGGGAAGGAGAATTTAAA**ATGCTCAAACAGACATTACAA** -3′)
FnovEHind	(5′-CGCGC*AAGCTT***TTAAATAATCTCTCTATTTCT**-3′)
FnovErev	(5′-TTTAAATTCTCCTTCCCGGCCCGGG**TTAAATAATCTCTCTATTTCT**-3′)
FnovFfor	(5′- CCCGGGCCGGGAAGGAGAATTTAAA**TTGGCAAGATTTCATATCAT**A -3′)
FnovFrev	(5′- CGCGC*GGTACC***TTAATATTCTTTTTTACGATA** -3′)
FnovEXba	(5′- CGCGC*TCTAGA*AAGGAGAATTTAAA**ATGCTCAAACAGACATTACA** -3′)

The letters in bold are part of the relevant gene sequence. The letters in italics are recognition sites for restriction enzymes (*XbaI, HindIII,* and *KpnI*). The underlined letters are ribosome binding sites. Translation spacer elements are located between ribosome binding sites and start codons.

2.3 Results

2.3.1 Heterologous co-expression and activity analysis of FnLpxE and RlLpxQ in *E. coli*

Heterologous expression of lipid A modification enzymes in *E. coli* has been demonstrated previously. Wang et al. first reported that expression of the *Francisella novicida* lipid A 1-phosphatase, LpxE (FnLpxE), behind the *lac* promoter on pWSK29 led to robust lipid A 1-dephosphorylation activity in living XL1-Blue cells (Wang et al., 2004). The *in vivo* activity of other heterologously-expressed lipid A modification enzymes, such as the *F. novicida* lipid A 4′-phosphatase, LpxF (FnLpxF), and the *Salmonella typhimurium* 3-O deacylase PagL, has also been demonstrated (Wang et al., 2006a) (Trent et al., 2001b). In this study, we tested whether combinations of modification enzymes could be heterologously co-expressed in order to generate novel lipid A hybrid structures in living *E. coli* cells.

The first combination of lipid A modification enzymes tested was the *Francisella novicida* lipid A 1-phosphatase, FnLpxE, and the *R. leguminosarum* lipid A oxidase, RlLpxQ. In *R. leguminosarum,* RlLpxE and RlLpxQ normally function together to generate some of the unique lipid A species found in that organism (Fig. 12 B and C) (Raetz et al., 2007). LpxQ converts the proximal glucosamine of 1-dephosphorylated lipid A, which is generated by RlLpxE, to an aminogluconate residue (Que-Gewirth et al., 2003a, Que-Gewirth et al., 2003b). We created an inducible expression plasmid to co-

express both genes in *E. coli* by cloning the *RllpxQ* and *FnlpxE* genes behind the *lac* promoter on pWSK29. We used the *FnlpxE* gene because the heterologous expression of many *R. leguminosarum* genes in *E. coli* has yielded low expression levels (Que-Gewirth et al., 2003a, Que-Gewirth et al., 2003b). The RlLpxQ gene was cloned upstream of the *FnlpxE* gene in plasmid pWSK29-LpxQE in order to maximize its expression level. Plasmid pWSK29-LpxQE was transformed into the *E. coli* strain W3110A, and the heptose-deficient strain WBB06 in an effort to generate strains accumulating the structures shown in Fig. 13A.

The *in vitro* activity of recombinantly expressed RlLpxQ and FnLpxE was measured using washed membranes as the enzyme source (Fig. 14). The assay was performed under conditions optimized for LpxQ activity. The product of LpxE, 1-dephospho Kdo_2-lipid IV_A, was formed rapidly in reactions initiated with membranes expressing either pWSK29-LpxE or pWSK29-LpxQE. The membranes expressing pWSK29-LpxQE further metabolized 1-dephopho-Kdo_2-lipid IV_A to a slower migrating product in a time-dependent manner. This slower migrating product is interpreted as the oxidized lipid A product of LpxQ. The faster migrating products indicated by asterisks in Fig. 14 are products generated enzymatically by PagP, a lipid A acyltransferase present in W3110A cells (Bishop *et al.*, 2000).

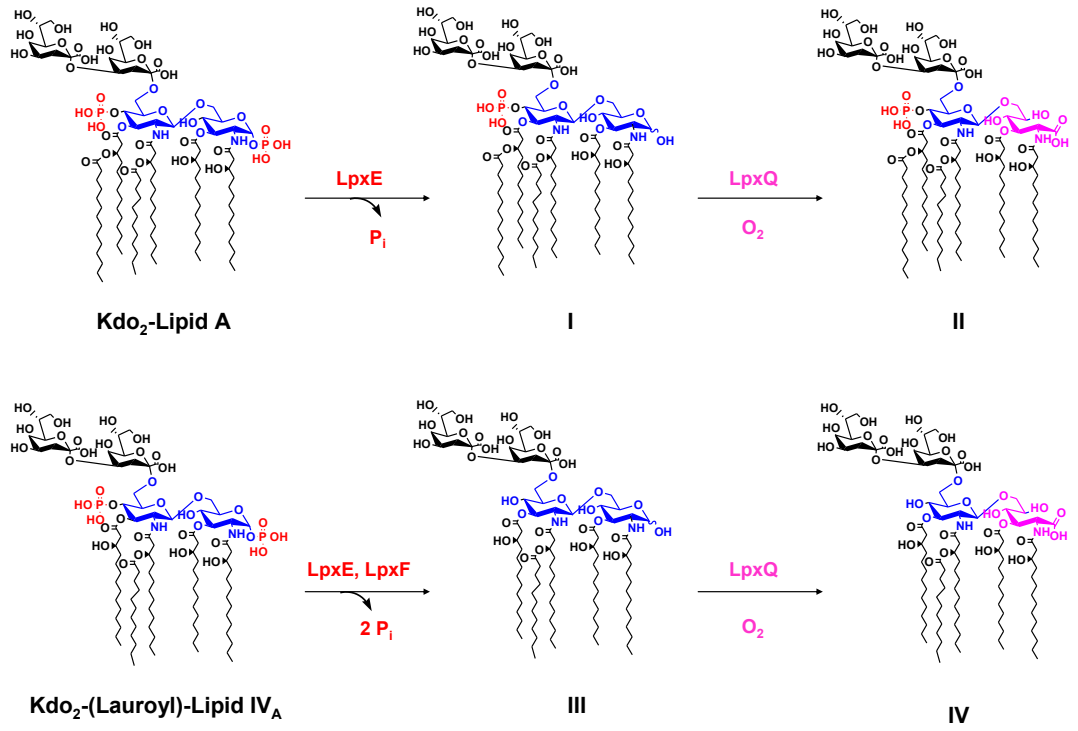

Figure 13: Proposed structures of *E. coli* lipid A hybrids created by heterologous expression of FnLpxE, FnLpxF, and RlLpxQ.

Panel A. Expression of the lipid A 1-phosphatase, LpxE, in *E. coli* strains results in the generation of 1-dephospho Kdo_2-lipid A (Product I) (Karbarz et al., 2003, Wang et al., 2004). Co-expression of LpxE and the lipid A oxidase, LpxQ, together is expected to generate the aminogluconate derivative of *E. coli* lipid A (Product II) (Que-Gewirth et al., 2003a, Que-Gewirth et al., 2003b). **Panel B.** Co-expression of LpxE and the 4′-phosphatase, LpxF, in *msbB* deletion strains of *E. coli* accumulating Kdo_2-(lauroyl)-lipid IV_A is expected to yield a product void of phosphates (product II). The coupled expression of LpxE, LpxF, and LpxQ is expected to generate the oxidized derivative product IV.

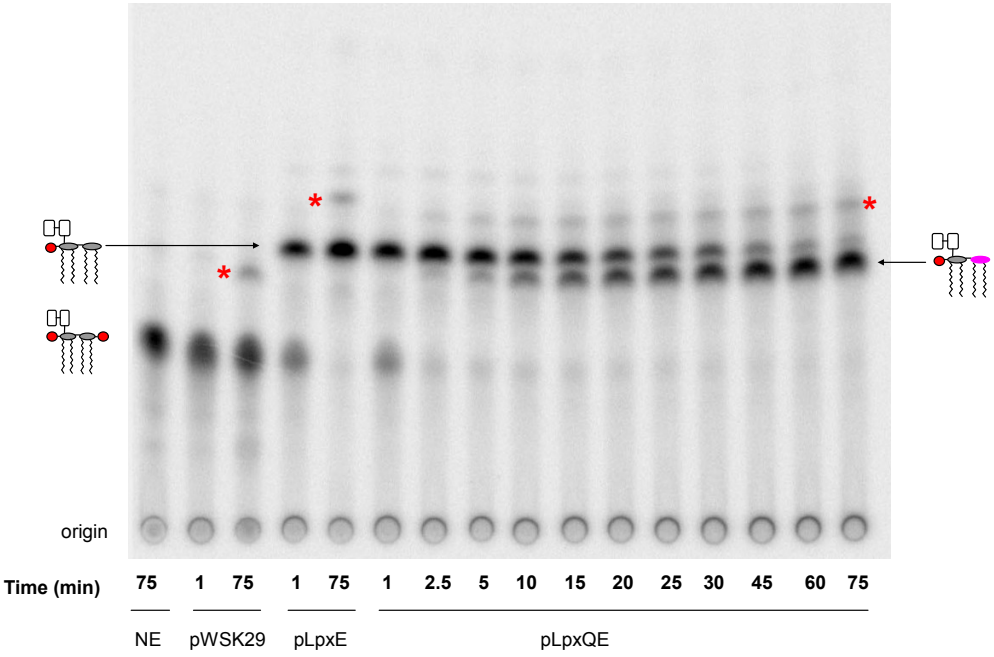

Figure 14: Detection of lipid A phosphatase and oxidase activity in W3110A cells expressing RlLpxQ and FnLpxE.

Membranes of the indicated strains (1.0 mg/mL) were assayed for the indicated times at 30 °C with 10 μM [4′-^{32}P] Kdo_2-lipid IV_A. The products were separated by TLC and analyzed with a PhosphorImager. NE: no enzyme; pWSK29: vector control; pLpxE: W3110A/pWSK29-LpxE membranes; pLpxQE: W3110/pWSK29-LpxQE membranes.

2.3.2 ESI-MS analysis of lipids isolated from W3110A and WBB06 cells expressing LpxE and LpxQ

The negative ion ESI mass spectra of the total lipid A species extracted from the W3110A strains expressing pWSK29, pWSK29-LpxE, and pWSK29-LpxQE is shown in Fig. 15. The predominant lipid A species extracted from the cells expressing the vector control, pWSK29 (Fig. 15A), appears at m/z 1796.24 and corresponds to the $[M-H]^-$ ion of bis-phosphorylated lipid A. A minor amount of 1-dephospho-lipid A (blue arrow) is present and is generated from the acid hydrolysis procedure used to isolate the lipid A. Expression of FnLpxE in W3110A generates massive amounts of 1-dephospho-lipid A (product I in Fig. 13A), consistent with that previously reported (Fig. 15B). The major peak at m/z 1716.28 is interpreted as the $[M-H]^-$ ion of 1-dephospho-lipid A. There is little residual bis-phosphorylated lipid A remaining in this strain. W3110A cells expressing pWSK29-LpxQE (Fig. 15C) accumulate 1-dephospho-lipid A and a new species at m/z 1732.28 (+ 16 amu), which is interpreted as the $[M-H]^-$ ion of oxidized lipid A (product II in Fig. 13A). A portion of the oxidized lipid A was found to be chemically altered by the hydrolysis procedure used in isolating the lipid A from wild-type strains such as W3110A (Fig. 16). This altered species is not formed enzymatically and is interpreted as a β-elimination product of product II (Que-Gewirth et al., 2003b). The formation of product II was dependent on molecular oxygen. Strains expressing

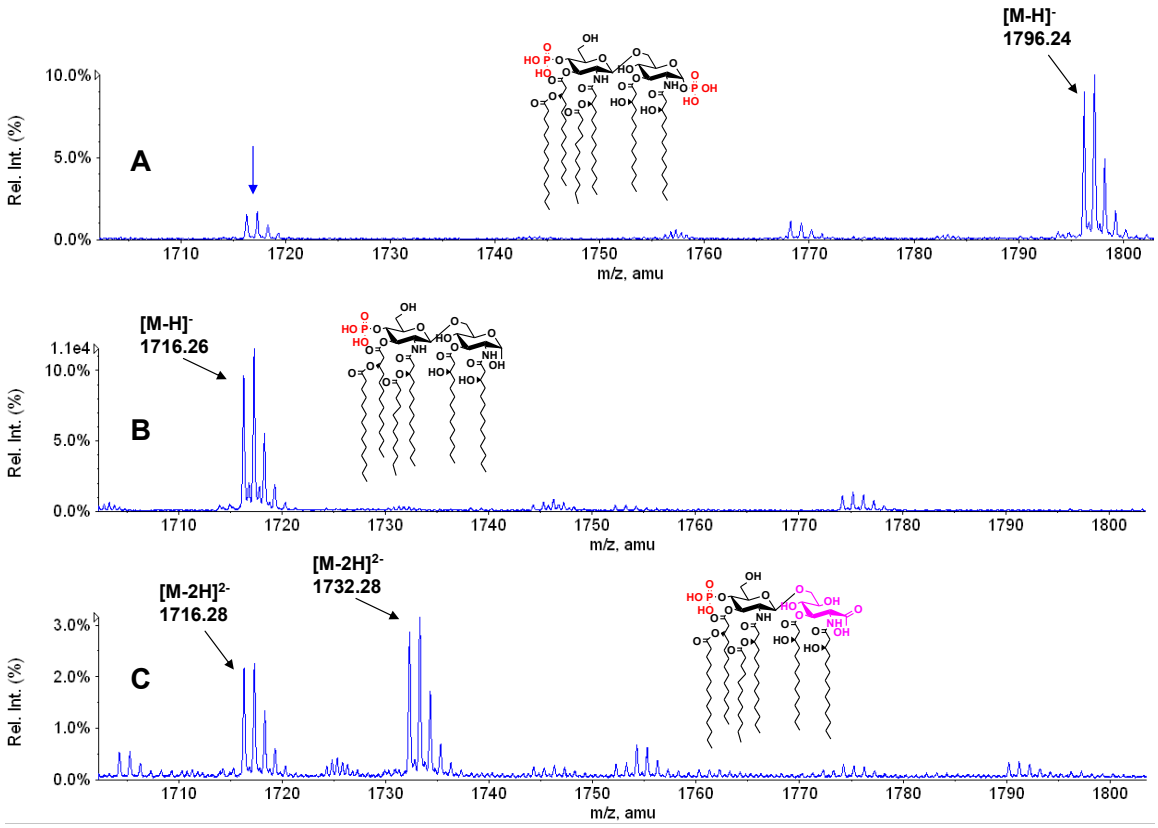

Figure 15: ESI-MS analysis of lipid A extracted from W3110A cells expressing FnLpxE and RlLpxQ.

W3110A cells were grown at 37 °C in the presence of ampicillin and IPTG, and harvested in late log phase. Lipids were extracted as described in materials and methods. **Panel A.** The W3110A cells harboring the control plasmid, pWSK29, accumulate bis-phosphorylated lipid A ([M-H]$^-$ at *m/z* 1796.24). There is a small amount of 1-dephospho lipid A present from the acid hydrolysis procedure used to isolate the lipid A. **Panel B.** W3110A cells expressing FnLpxE accumulate 1-dephospho lipid A ([M-H]$^-$ at *m/z* 1716.26) (Product I in Fig. 13A). There is little detectable wild-type lipid A remaining in this strain. **Panel C.** The W3110A cells expressing FnLpxE and RllpxQ accumulate lipid A species with the expected structures: 1-dephospho lipid A and the oxidized derivative ([M-H]$^-$ at *m/z* at 1733.25) (Product II in Fig. 13A).

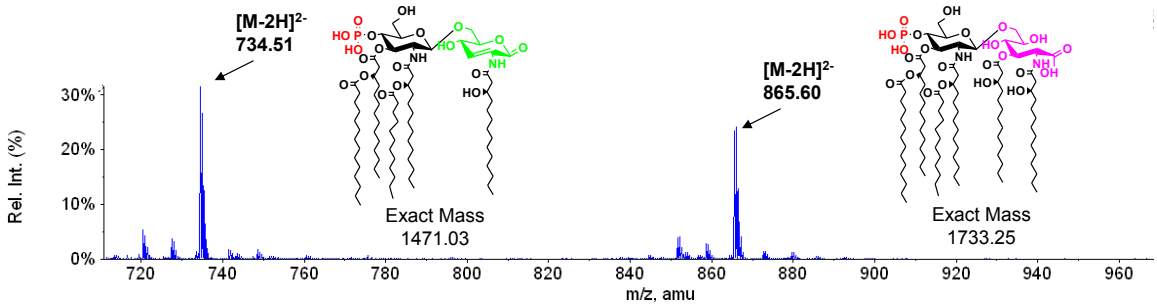

Figure 16: ESI-MS analysis of oxidized lipid A species extracted from W3110A cells.

The W3110A cells expressing pWSK29-LpxQE accumulate oxidized lipid A species and related derivatives. The primary product is 2-amino-2-deoxy-gluconate-lipid A ($[M-2H]^{2-}$ at *m/z* 865.60) (Product II in Fig. 13). A second oxidation product ($[M-2H]^{2-}$ at *m/z* 734.51 is also present. This related derivative is presumably derived from product II during acid hydrolysis, possibly by lactonization of the 2-aminogluconate residue and the subsequent acid-catalyzed elimination of the acyl chain
at position-3.

pWSK29-LpxQE grown anaerobically accumulated only 1-dephospho-lipid A (product I) (data not shown). These results show that FnLpxE and RlLpxQ can function together *in vivo* on lipid A scaffolds that are structurally different from that found in their respective hosts.

WBB06 cells, which are heptose-deficient with deletions spanning the *waaC* and *waaF* genes, were grown expressing pWSK29, pWSK29-LpxE, and pWSK29-LpxQE under identical conditions to that used for the W3110A cells. The negative ion ESI mass spectra are shown in Fig. 17. Under normal conditions WBB06 cells synthesize a truncated LPS consisting mainly of Kdo_2-lipid A. This species, is present in cells expressing pWSK29 (Fig. 17A), can be extracted with phospholipids in a single phase Bligh Dyer extraction procedure. WBB06 cells expressing pWSK29-LpxE generate 1-dephospho Kdo_2-lipid A (Product I in Fig. 13) as their major form of LPS (Fig 18). WBB06 cells expressing pWSK29-LpxQE (Fig. 17B) have only minor amounts of Kdo_2-lipid A remaining. The peak at m/z 1086.17 is consistent with the $[M-2H]^{2-}$ ion of the proposed aminogluconate derivative (Product II in Fig. 13A) and the peak at 1078.37 is consistent with the $[M-2H]^{2-}$ ion of residual 1-dephospho Kdo_2-lipid A. The β-elimination product that accumulates in W3110A cells is not observed in this strain as no acid hydrolysis step was required in isolation of the lipid A. A possible methanolysis

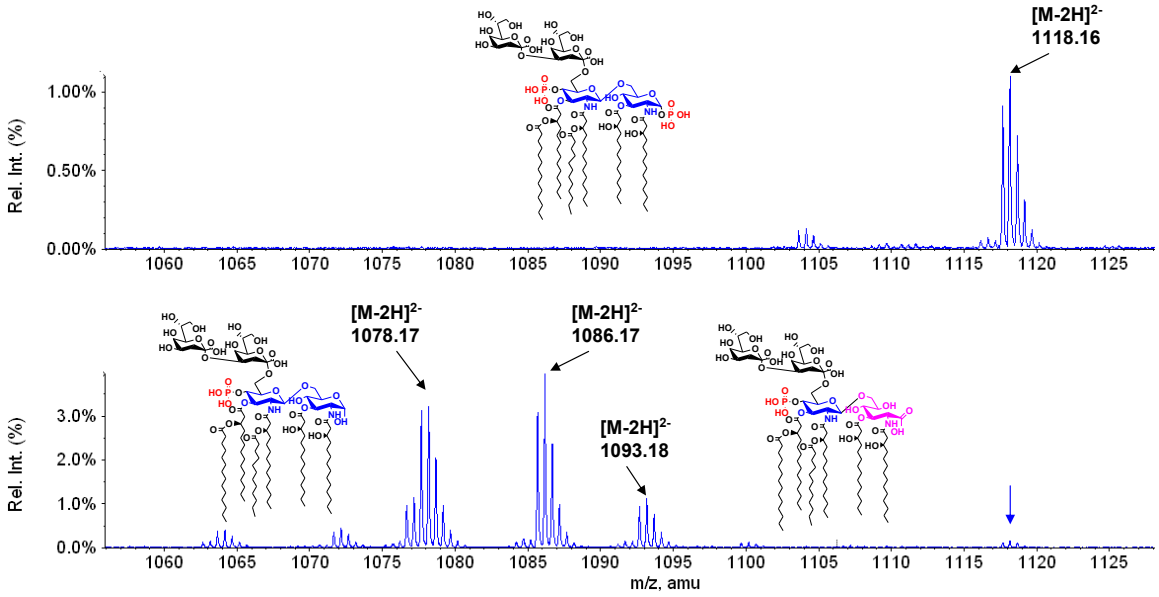

Figure 17: ESI-MS of LPS from heptose deficient *E. coli* cells expressing FnLpxE and RlLpxQ

WBB06 cells were grown at 37 °C in the presence of ampicillin and IPTG, and harvested in late log phase. Lipids were extracted as described in materials and methods. **Panel A.** WBB06 cells harbor deletions in the heptose transferase genes, *waaC* and *waaF (Brabetz et al., 1997)*, and thus accumulate Kdo_2-lipid A ($[M-2H]^{2-}$ at m/z 1118.16) (Product I in Fig. 13A) as their major form of LPS when harboring the control plasmid pWSK29. **Panel B.** WBB06 cells expressing RlLpxQ and FnLpxE accumulate the expected dephosphorylated and oxidized lipid A species (Products I and II in Fig. 13A). The doubly charged peak at *m/z* 1086.17 corresponds to Product II in Fig. 13A and the doubly charged peak at *m/z* 1078.37 corresponds to product I. The peak at *m/z* 1093.18 corresponds to a methanol hydrolysis product of oxidized lipid A. The arrow in the diagram points to residual wild-type lipid A that is not metabolized in this strain.

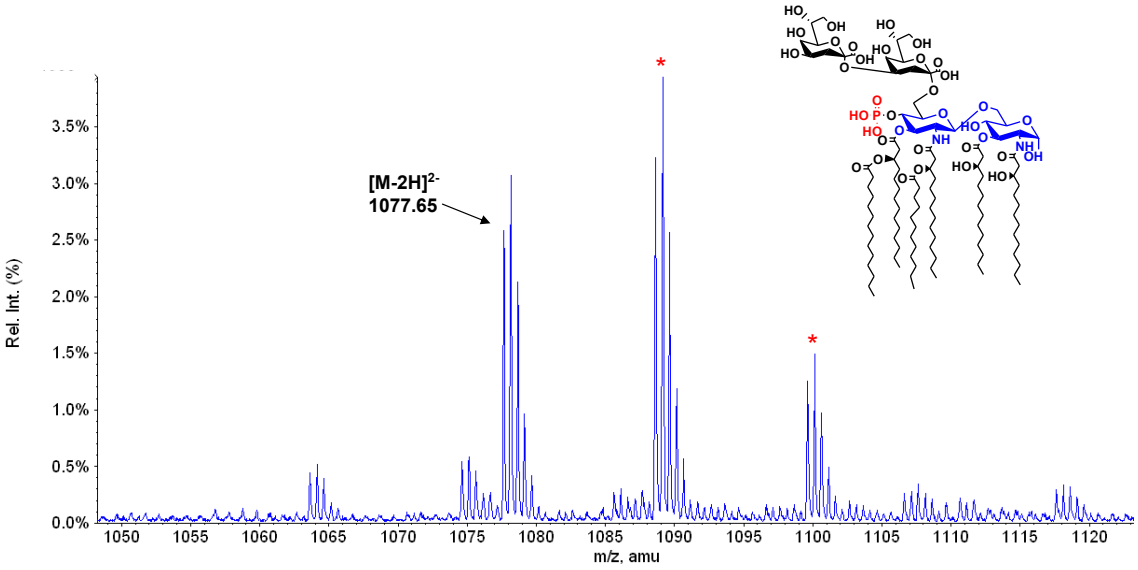

Figure 18: ESI-MS of WBB06 cells expressing LpxE.

WBB06 cells expressing LpxE accumulate 1-dephospho-lipid A species ($[M-2H]^{2-}$ at m/z 1077.65) (Product I in Fig. 13A). Sodium adducts are also present (red asterisks).

product, however, is detected at m/z 1093.18. The aminogluconate moiety of the LpxQ lipid product exists in equilibrium with its corresponding aminogluconolactone form (Que-Gewirth et al., 2003b, Lee et al., 2006). The putative methanolysis product observed in Fig. 17B could be derived from methanol hydrolysis of oxidized lipid A present in the lactone form.

2.3.3 Heterologous co-expression of LpxE, LpxF, and LpxQ in E. coli

We expanded our strategy of altering the lipid A composition of living *E. coli* cells by expressing the 4′-phosphatase, LpxF, in conjunction with LpxE and LpxQ in an attempt to generate the lipid A hybrids shown in Fig. 13B. The proposed lipid A hybrids are similar to the lipid A species found in *Rhizobium* Sin-1, which have been shown to be antagonists of enteric LPS in animal studies (Jeyaretnam et al., 2002, Vandenplas et al., 2002). We utilized *msbB* null strains of *E. coli* to generate the proposed lipid A species because FnLpxF does not dephosphorylate hexaacylated lipid A (Wang et al., 2006a). The plasmids pWSK29, pWSK29-LpxE, pWSK29-LpxF, pWSK29-EF, and pWSK29-QEF were transformed into the *msbB* null strains MLK1067 (Karow & Georgopoulos, 1992), which is derived from W3110, and strain SR8209 (Klein et al., 2009), which lacks both *msbB* and a complete LPS core.

The lipid A species accumulating in the MLK1067 strains expressing LpxE, LpxF, and LpxQ were uniformly labeled with ^{14}C-acetate, isolated, and separated on a TLC

plate (Fig. 19). MLK1067 cells expressing the vector control, pWSK29, accumulated (lauroyl)-lipid IV_A as expected (Fig. 13B). MLK1067 cells expressing either pWSK29-LpxE or pWSK29-LpxF accumulated mono-phosphorylated lipid A species that were more hydrophilic than (lauroyl)-lipid IV_A. The 1-dephospho-(lauroyl)-lipid IV_A species migrated slightly faster than the 4′-dephospho-(lauroyl)-lipid IV_A species. MLK1067 cells expressing pWSK29-LpxEF accumulated a hydrophilic species that ran near the solvent front. This species was interpreted as doubly-dephosphorylated-(lauroyl)-lipid IV_A (product III in Fig. 13B). Expression of pWSK29-LpxQEF in MLK1067 led to the accumulation of several new hydrophilic species. The major lipids accumulating correspond to the doubly dephosphorylated species and its oxidized derivative. The other species present most likely correspond to derivatives of oxidized lipid A formed in the hydrolysis procedure used to isolate the lipid A. The total amount of lipid A in the strains was not greatly affected by the modifications.

2.3.4 ESI-MS analysis of the lipid A species from MLK1067 and SR8209 cells expressing FnLpxE, and FnLpxF, and RlLpxQ

The negative ESI-MS of the MLK1067 strains appears in Fig. 20. The species detected by mass spectrometry correlate with the radiolabeled species in Fig. 19. MLK1067 cells expressing pWSK29 accumulate (lauroyl)-lipid IV_A (Fig. 20A). The expression of either pWSK29-LpxE or pWSK29-LpxF in MLK1067 leads to the

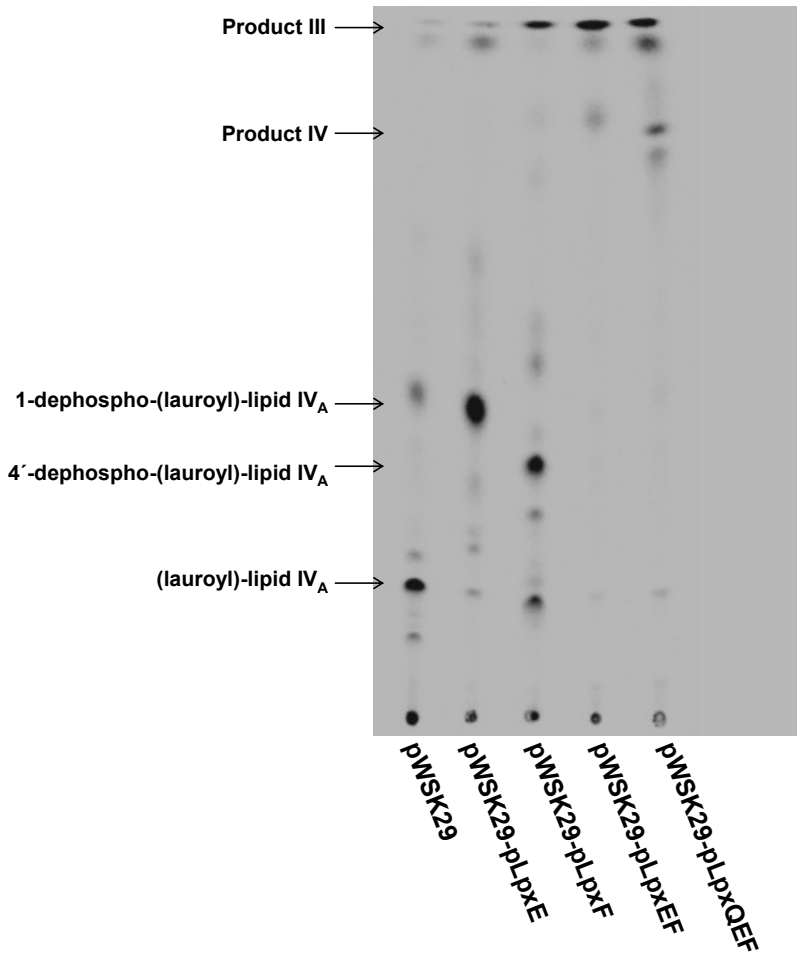

Figure 19: ^{14}C labeling of MLK1067 strains expressing lipid A modification enzymes.

The lipid A species from MLK1067 strains expressing pWSK29, pWSK29-LpxE, pWSK29-LpxF, pWSK29-LpxEF, and pWSK29-LpxQEF were grown on LB broth supplemented with IPTG, ampicillin, and ^{14}C [U-14] acetate. The labeled lipid A species were isolated and separated by TLC as described in materials and methods.

Figure 20: ESI-MS analysis of lipid A extracted from MLK1067 cells expressing FnLpxE, FnLpxF, and RlLpxQ.

MLK1067 cells expressing pWSK29, pWSK29-LpxE, pWSK29-LpxF, pWSK29-LpxEF, and pWSK29-LpxQEF were grown at 37 °C in the presence of ampicillin and IPTG, and harvested in late log phase. Lipids were extracted as described in materials and methods. **Panel A.** MLK1067 strains have deletions in the late acyltransferase gene, lpxM (Karow & Georgopoulos, 1992). MLK1067 cells harboring pWSK29 thus accumulate (lauroyl)-lipid IV_A ($[M-H]^-$ at *m*/*z* 1585.07). A sodium adduct of the species is also present (black asterisk). There is also some 1-dephospho-(lauroyl)-lipid IV_A present, which results from the hydrolysis procedure used to liberate the lipid A (blue asterisk). **Panel B.** Expression of pWSK29-LpxE in MLK1067 leads to the accumulation of 1-dephospho-(lauroyl)-lipid IV_A ($[M-H]^-$ at *m*/*z* 1506.07). **Panel C.** Expression of pWSK29-LpxF in MLK1067 leads to the accumulation of 4′-dephospho-(lauroyl)-lipid IV_A ($[M-H]^-$ at *m*/*z* 1506.07). A small amount of 1,4-di-dephospho-(lauroyl)-lipid IV_A (product IV in Fig. 13) (blue asterisk) was generated in the hydrolysis procedure. **Panel D.** Doubly-dephosphorylated lauroyl)-lipid IV_A ($[M-H]^-$ at *m*/*z* 1426.09) (product III in Fig. 13) accumulates in strains expressing pWSK29-LpxEF. A chloride adduct of the species is also present (red asterisk). **Panel E.** Expression of pWSK29-LpxQEF in MLK1067 generates the dephosphorylated species and its aminogluconate derivative (product IV in Fig. 13) at *m*/*z* 1442.09). A methanolysis product of oxidized lipid A is also present (green asterisk). Chloride adducts of product III (red asterisk), product IV (blue asterisk), and the methanolysis product are also present (orange asterisk).

Figure 20: ESI-MS analysis of lipid A extracted from MLK1067 cells expressing FnLpxE, FnLpxF, and RlLpxQ.

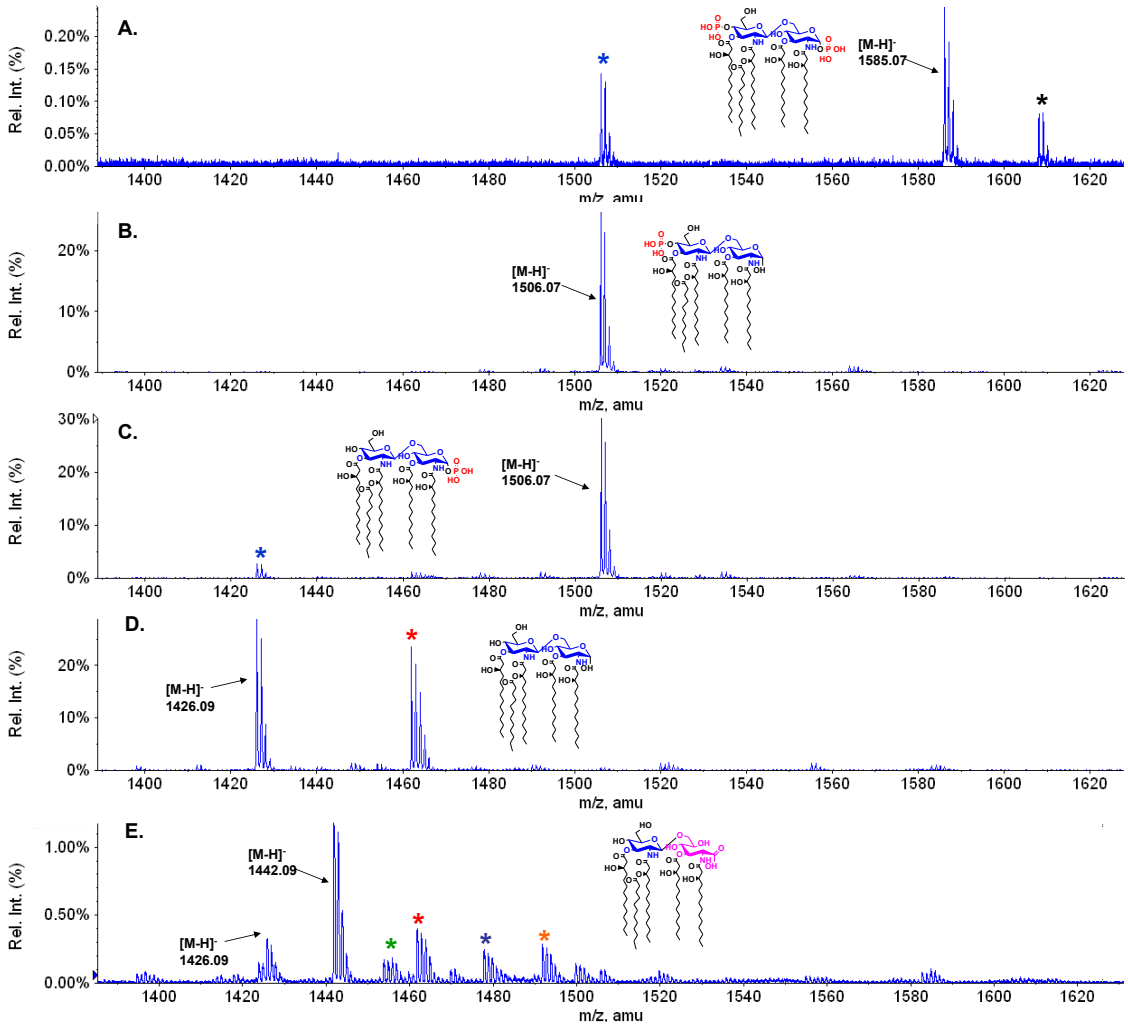

accumulation of mono-phosphorylated lipid A species (Fig. 20B and C). When LpxE and LpxF are co-expressed in this strain, the major lipid that accumulates is doubly-dephosphorylated-(lauroyl)-lipid IV_A (Product III in Fig. 13B) (Fig. 20D). MLK1067 cells expressing pWSK29-LpxQEF have very little residual phosphorylated lipid A and accumulate the expected products: doubly-dephosphorylated-(lauroyl)-lipid IV_A and its oxidized derivative (product IV in Fig. 13) (Fig. 20E). A methanolysis product and a lactone elimination product analogous to that seen in the W3110A strain expressing pWSK-LpxQE are also present in this strain (data not shown).

The ESI-MS of the LPS isolated from SR8209 cells expressing pWSK29, pWSK29-LpxE, pWSK29-LpxF, pWSK29-LpxEF, and pWSK29-LpxQEF is shown in Fig. 21. The doubly charged region of the mass spectrum for each strain is shown. SR8209 cells expressing pWSK29 accumulate Kdo_2-(lauroyl)-lipid IV_A ($[M-2H]^{2-}$ at m/z at 1013.05) as their major form of LPS (Fig. 21A). Expression of either pWSK29-LpxE or pWSK29-LpxF greatly reduces the amount of Kdo_2-(lauroyl)-lipid IV_A (Fig. 21 B and C). A monophosphorylated-Kdo_2-lipid A species accumulates as the major form of LPS in these strains ($[M-2H]^{2-}$ at m/z at 973.08). SR8209 cells expressing pWSK29-EF accumulate 1,4′-di-dephospho-Kdo_2-lipid IV_A (product III in Fig. 13)(Fig. 21D). As seen in Fig. 21E, SR8209 cells expressing pWSK29-LpxQEF accumulate a mixture of 1,4′-di-dephospho-Kdo_2-lipid IV_A and its aminogluconate derivative (product IV in Fig. 13B).

Figure 21: ESI-MS analysis of lipid A extracted from SR8209 cells expressing FnLpxE, FnLpxF, and RlLpxQ.

SR8209 cells were grown at 37 °C in the presence of ampicillin and IPTG, and harvested in late log phase. Lipids were extracted as described in materials and methods. **Panel A.** SR8209 cells harbor deletions in the heptose transferease genes, *waaC* and *waaF* and in the lipid A late acyl transferase gene, LpxM (Klein et al., 2009). SR8209 cells harboring pWSK29 accumulate Kdo_2-(lauroyl)-lipid IV_A ($[M-2H]^{2-}$ at *m*/*z* 1013.05) as their major form of LPS. Sodium and chloride adducts of this species are also present (black and red asterisks, respectively). **Panel B.** SR8209 cells expressing pWSK29-LpxE accumulate 1-dephospho-Kdo_2-(lauroyl)-lipid IV_A ($[M-2H]^{2-}$ at *m*/*z* 973.07). **Panel C.** SR8209 cells expressing pWSK29-LpxF accumulate 4′-dephospho-Kdo_2-(lauroyl)-lipid IV_A ($[M-2H]^{2-}$ at *m*/*z* 973.08). There is some residual wild-type lipid remaining in this strain. **Panel D.** SR8209 cells harboring pSK29-LpxEF accumulate 1,4′-di-dephospho-Kdo_2-(lauroyl)-lipid IV_A ($[M-2H]^{2-}$ at *m*/*z* 933.09) (Product III in Fig. 13B). **Panel E.** SR8209 cells harboring pWSK29-LpxQEF accumulate 1,4′-di-dephospho-Kdo_2-(lauroyl)-lipid IV_A and its oxidized derivative ($[M-2H]^{2-}$ at *m*/*z* 941.11) (Product IV in Fig. 13B). Methanolysis products of the oxidized lipidA species are also present (green asterisk).

Figure 21: ESI-MS analysis of lipid A extracted from SR8209 cells expressing FnLpxE, FnLpxF, and RlLpxQ.

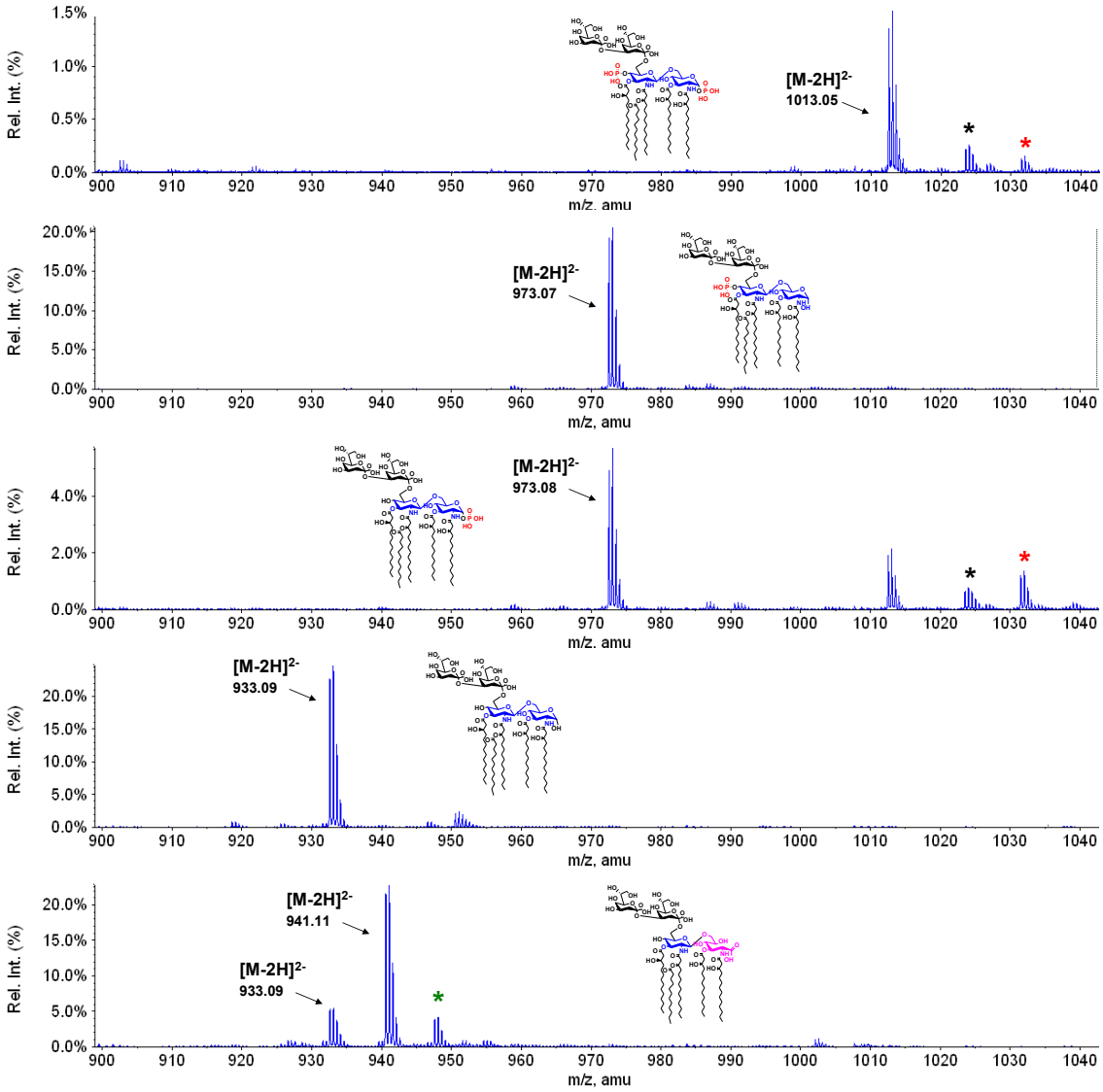

2.3.5 Phenotypes of cells expressing LpxE, LpxF, and LpxQ

The phosphate moieties of lipid A are thought to play a role in maintaining the integrity of the outer membrane of most Gram-negative bacteria. The acidic phosphates are able to bind divalent cations such as Mg^{2+}, thereby cross-linking LPS (Nikaido, 2003). We assessed the importance of these ionic interactions in maintaining outer membrane integrity by examining the growth phenotypes of MLK1067 and SR8209 cells expressing combinations of LpxE, LpxF, and LpxQ.

The outer membrane permeability of MLK1067 cells has been analyzed before. Loss of the 3′-myristoyl chain in this strain does significantly impact resistance to hydrophobic compounds (Vaara & Nurminen, 1999). Expression of the plasmid pWSK29-LpxEF in MLK1067 did not significantly impact the strain's resistance to vancomycin, fusidic acid, or rifamycin SV (Table 3). These results imply that the phosphates of lipid A are not essential for the normal function of the outer membrane permeability barrier. We did not measure the sensitivity of SR8209 expressing pWSK29-LpxEF to these drugs, as it is well established that the outer membrane permeability barrier is impaired in deep rough mutants (Vaara & Nurminen, 1999, Frirdich *et al.*, 2005). SR8209 cells expressing pWSK29-LpxEF and pWSK29-LpxQEF displayed several growth defects. These cells grew slower than cells expressing either

Table 3: MIC values of antibiotics tested with MLK1067 cells expressing pWSK29 and pWSK29-LpxEF

Strain	Antibiotic	MIC*
MLK1067/pWSK29	Rifamycin SV	31.25
	Erythromycin	100
	Vancomycin	500
MLK1067/pWSK29-LpxEF	Rifamycin SV	15.6
	Erythromycin	25
	Vancomycin	500

LpxE or LpxF alone (Fig. 22). Expression of pWSK29-LpxEF was found to be toxic in SR8209. The cells expressing pWSK29-LpxEF failed to grow above A_{600} = 2 in a cumulative growth experiment. SR8209 cells expressing pWSK29-LpxEF and pWSK29-LpxQEF also displayed sensitivity to calcium chloride. Cells expressing these plasmids failed to grow on LB broth plates supplemented with 10 mM $CaCl_2$ (Fig 23). SR8209 cells expressing pWSK29-LpxE displayed sensitivity, but were not as dramatically impaired in growth.

2.3.6 Polymyxin resistance of *E. coli* strains expressing LpxE and LpxF

The phosphate moieties of lipid A are well conserved in enteric LPS and are thus targets of secreted cationic antimicrobial peptides, such as defensins (Zasloff, 2002). *F. novicida* employs lipid A phosphatases to reduce the net negative charge of its LPS, thus altering its susceptibility to cationic antimicrobial peptides. Deletion of LpxF in *F. novicida* results in an extreme hypersensitivity to polymyxin B (Wang et al., 2007). We addressed the effect the phosphatases had in *E. coli* by comparing the MIC values for polymyxin B in the MLK1067 and SR8209 strains expressing pWSK29, pWSK29-LpxE, pWSK29-LpxF, pWSK29-LpxEF, and pWSK29-LpxQEF. Strains expressing pWSK29-LpxEF and pWSK29-LpxQEF were much more resistant to polymyxin compared to the strains expressing the vector control, pWSK29 (Table 4). Removal of the 4′ phosphate impacted polymyxin sensitivity most significantly. The change in MIC values for strains

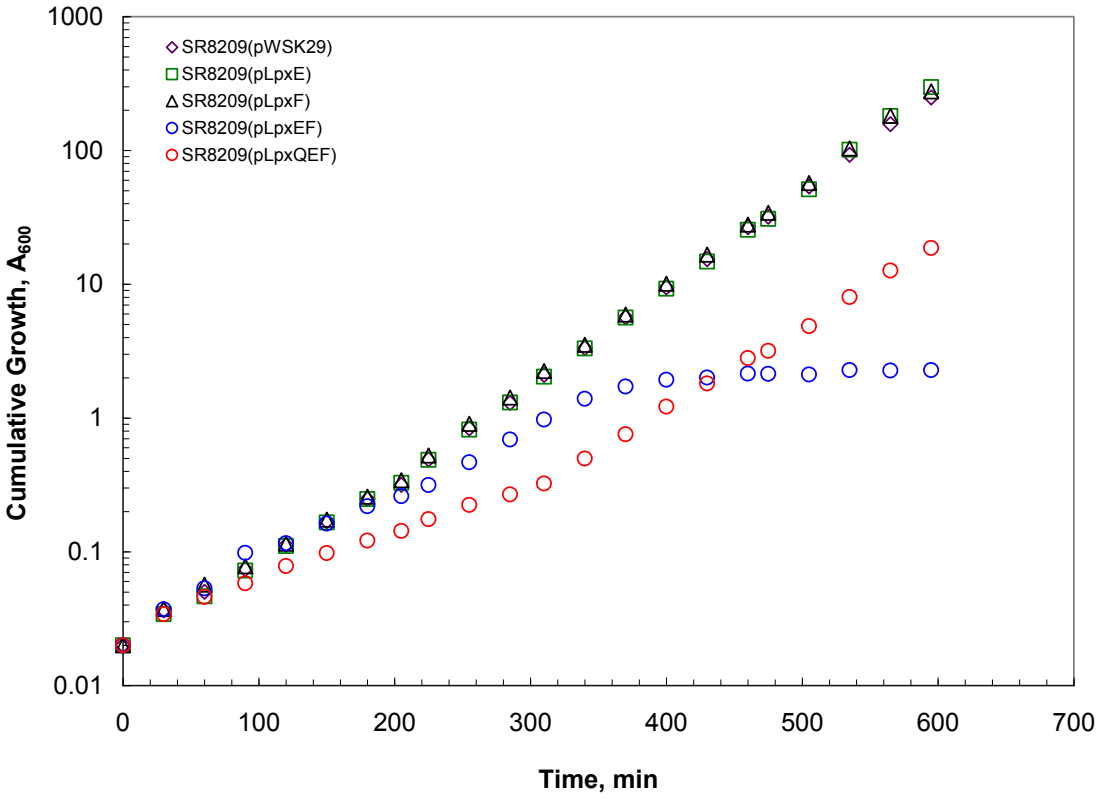

Figure 22: Growth phenotypes of SR8209 cells expressing FnLpxE, FnLpxF, and RlLpxQ.

Cells were grown at 37 °C on LB broth supplemented with 100 μg/ml ampicillin and 1 mM IPTG. The cells were inoculated at an A_{600} = 0.02. The cultures were diluted 10-fold whenever A_{600} reached 0.3-0.4. The cumulative A_{600} was corrected for dilutions.

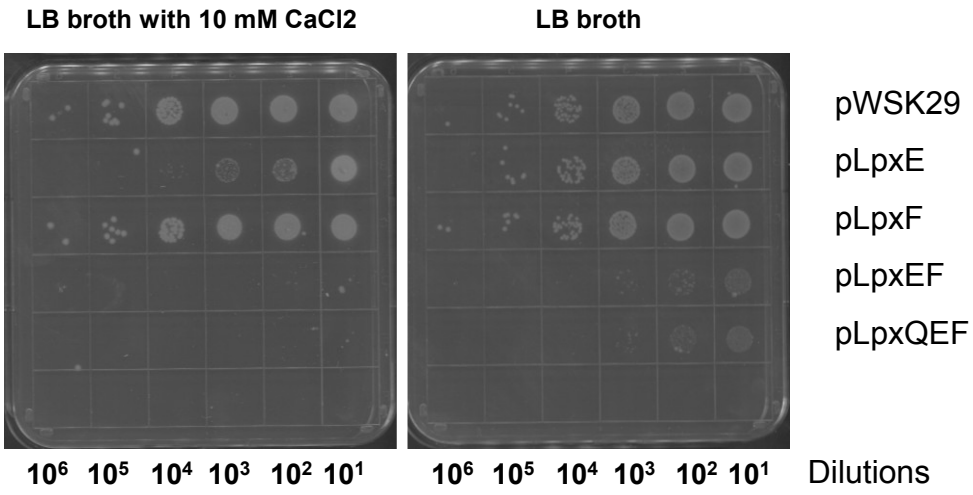

Figure 23: WaaC/WaaF mutants expressing FnLpxE and FnLpxF are sensitive to $CaCl_2$.

Serial dilutions (~10^7 – 10^2 CFU) of SR8209 cells harboring pWSK29, pWSK29-LpxE, pWSK29-LpxF, pWSK29-LpxEF, and pWSK29-LpxQEF were made. Ten μL of each dilution was plated on LB plates supplemented with 100 μg/ml ampicillin, 1 mM IPTG, and 10 mM $CaCl_2$ or control plates with 100 μg/ml ampicillin and 1 mM IPTG.

Table 4: Increased polymyxin resistance of *E. coli* expressing LpxE and LpxF

Strain	Vector	MIC
MLK1067	pWSK29	0.4883
	pWSK29-LpxE	0.970
	pWSK29-LpxF	3.906
	pWSK29-LpxEF	3.906
	pWSK29-LpxQEF	3.906
SR8209	pWSK29	0.244
	pWSK29-LpxE	0.970
	pWSK29-LpxF	15.600
	pWSK29-LpxEF	15.600
	pWSK29-LpxQEF	15.600

expressing pWSK29-LpxEF and pWSK29-LpxQEF is similar to those observed in *pmrA* constitutive strains of *S. typhimurium* (Yethon & Whitfield, 2001). These results support biological studies suggesting a strong binding interaction between lipid A phosphates and polymyxin B (Gunn et al., 1998)

2.4 Discussion

The constitutive lipid A biosynthetic pathway is widely conserved in Gram-negative bacteria. However modifications to lipid A structures can occur (Raetz et al., 2007). The modifications vary from species to species and typically are not required for growth (Raetz et al., 2007). The enzymes responsible for lipid A modifications are often induced under special growth conditions (Gibbons *et al.*, 2005) and can enhance the virulence of pathogens by altering elements of lipid A recognized by TLR-4 receptors (Raetz *et al.*, 2009, Wang et al., 2007). Lipid A modification enzymes can be expressed heterologously in foreign hosts, facilitating the re-engineering of lipid A structures (Raetz et al., 2007, Raetz et al., 2009).

In this chapter, we coupled the over-expression of the *F. novicida* 1-phosphatase, FnLpxE, with the *F. novicida* 4′-phosphatase, FnLpxF, and the *R. leguminosarum* lipid A oxidase, RlLpxQ, to generate novel lipid A hybrids structures in *E. coli* that were completely dephosphorylated and/or partially oxidized, such as those found in *R. leguminosarum* (Fig. 12B and C) and *Rhizobium* Sin-1 (Que et al., 2000a, Que et al., 2000b,

Jeyaretnam et al., 2002). Lipid A hybrids with these structural features are particularly interesting because synthetic lipid A derivatives based on the lipid A structure from *Rhizobium* Sin-1 (Jeyaretnam et al., 2002), have been shown to function as endotoxin antagonist (Vandenplas et al., 2002, Demchenko et al., 2003). The aminogluconate moiety, in particular, is thought to be important for this effect (Santhanam et al., 2004, Lee et al., 2006). When we co-expressed FnLpxE and RlLpxQ together in wild type or heptose-deficient mutants of *E. coli*, greater than 90% of the lipid A was found to be dephosphorylated at the 1-positon, and half of the dephosphorylated product was further converted to the aminogluconate form (Fig. 15). This result demonstrates that lipid A modification enzymes from multiple sources can be expressed heterologously in combination, to facilitate the efficient re-engineering of enteric lipid A.

The interchangeability of lipid A modification enzymes was further demonstrated by coupling the expression of the *F. novicida* 4′-phosphatase, FnLpxF, with FnLpxE and RlLpxQ. The construction of stains accumulating completely dephosphorylated lipid A species and/or partially oxidized derivatives was of special interest because the phosphate moieties of lipid A are thought to be involved in maintaining the stability of the outer membrane (Nikaido, 2003). The acidic phosphate residues of bisphosphorylated lipid A are thought to be involved in binding divalent cations, thereby creating tight lateral interactions in the lipid bilayer (Nikaido, 2003,

Nikaido & Vaara, 1985). Growth in cation poor environments, such as those found in a host during infection, can destabilize this interaction (Gibbons et al., 2005). In *E. coli* and *Salmonella,* the loss in stability can be compensated by the addition of positively charged compounds such as 4-aminoarabinose and phosphoethanolamine to the phosphate moieties (Gunn et al., 1998, Trent *et al.*, 2001a, Lee et al., 2004).

We generated completely dephosphorylated species of lipid A in *E. coli msbB* mutants, which lack a 3′-myristoyl chain, because *F. novicida* LpxF does not utilize hexaacylated lipid A as a substrate (Wang et al., 2006a). Expression of both phosphatases in this background resulted in nearly quantitative dephosphorylation of lipid A (Figs. 19-21). Expression of RlLpxQ with the two phosphatases led to the accumulation of lipid A molecules similar to those found in *R.* Sin-1 (Jeyaretnam et al., 2002) and *R. leguminosarum* (Que et al., 2000a, Que et al., 2000b). The *E. coli msbB* mutant, MLK1067, expressing LpxE and LpxF together was unimpaired in growth and its membrane integrity was not significantly compromised. There were only slight differences in the MIC values of antibiotics such as vancomycin, fusidic acid, erythromycin, and rifamycin SV. These results suggest that the core oligosaccharides and O-chain sugars of LPS are able to maintain membrane stability even when the ionic interactions between neighboring lipid A molecules are disrupted. The phosphate moieties of lipid A are incorporated in the early stages of lipid A biosynthesis and are required for efficient

transport across the inner membrane. Our results, however, show that they are not essential for viability after lipid A transport.

In contrast to the results obtained with MLK1067, we observed growth defects in *msbB* null strains lacking *waaC* and *waaF,* when expressing pWSK29-LpxEF and pWSK29-LpxQEF. These cells accumulated fully dephosphorylated Kdo_2-(lauroyl)-lipid IV_A (Product III in Fig. 13B) and its aminogluconate derivative (Product IV in Fig. 13B) as their major form of LPS. These strains displayed impaired growth in liquid medium and failed to grow in the presence of 10 mM $CaCl_2$. The impairment in growth observed in these cells could be caused by an increase in the permeability of their outer membrane. The phosphate moieties of lipid A normally bind divalent cations such as Mg^{2+} to crosslink LPS monomers. It is possible that the phosphates of lipid A also bind other divalent cations, such as Ca^{2+}, thereby, limiting their influx into cells. The normal intracellular concentration of calcium found in *E. coli* cells is 0.1 μM or less *(Gangola & Rosen, 1987).* Sensitivity to extracellular calcium has also been reported in heptose-deficient strains of *E. coli* lacking EptB, an enzyme responsible for transferring a phosphoethanolamine (pEtN) residue to the outer Kdo of *E. coli.* The pEtN moiety may play a similar role to the lipid A phosphates in rendering the outer membrane less permeable to extracellular metals such as calcium (Reynolds et al., 2005).

Lipid A phosphatases have been described in *R. leguminosarum*, *F. novicida*, *Helicobacter pylori*, and *Porphyromonas gingivalis* (Karbarz et al., 2003, Wang et al., 2006a, Tran *et al.*, 2005, Coats *et al.*, 2009). Chromosomal deletion of the phosphatases in many of these organisms leads to an increase in sensitivity to cationic antimicrobials such as polymyxin B (Tran et al., 2005, Wang et al., 2007). We therefore, expected to see an increase in polymyxin B resistance in *E. coli* strains expressing LpxE and LpxF. There was, indeed, a dramatic shift in the MIC values for polymyxin B sulfate in strains expressing the phosphatases. In the comparison of strains, we found that removal of the 4′-phosphate moiety impacted polymyxin resistance most significantly. The 4′-phosphate, coincidentally, is the site of aminoarabinose addition in polymyxin-resistant strains of *E. coli* and *S. typhimurium (Nummila et al., 1995).* Aminoarabinose modifications to lipid A have been shown to impact resistance to cationic antimicrobials dramatically (Nummila et al., 1995). These results were similar in both MLK1067 and SR8209, which lacks a complete core. The increased polymyxin resistance observed in the strains expressing LpxF alone, however, could be influenced by the increased accessibility of the 4′-phosphate group in the strains lacking the 3′-myristoyl group. In order to determine if this effect is important, mutants of FnLpxF that can metabolize hexaacylated species of lipid A will need to be isolated. Alternatively, LpxF analogs that dephosphorylate hexaacylated lipid A may become available. Such orthologues might

be found in *L. interrogans* or *H. pylori* which synthesize 4′-dephosphorylated hexaacylated lipid A species (Que-Gewirth *et al.*, 2004). Our results support the proposed biological roles of the lipid A phosphatases and are consistent with data demonstrating strong interactions between lipid A phosphates and polymyxin B.

Mutant strains of *E. coli* such as WBB06 and SR8209, which accumulate Kdo_2-lipid A and Kdo_2-(lauroyl)-lipid IV_A as their sole forms of LPS, respectively, are valuable because they can be used as scaffolds for LPS re-engineering. The generation of lipid A hybrids in these backgrounds, such as the ones described in this chapter, may be interesting as potential second generation adjuvants (Baldridge et al., 2004, Stover *et al.*, 2004). Derivatives lacking the 4′-phosphate group, in particular, may function as novel LPS antagonists. Additional lipid A derivatives can be made by expressing lipid A modification enzymes such as the 3-O deacylase, PagL, or the 3′-O deacylase, LpxR, in tandem with LpxE and LpxF. Such lipid A hybrids could be tested as activators of the TLR4-MD2 complex and compete with existing adjuvants such as "monophosphoryl-lipid A" (MPL) (Baldridge et al., 2004). Commercial MPL preparations are usually obtained from *Salmonella* LPS by mild acid hydrolysis and are heterogeneous (Baldridge et al., 2004). Lipid A molecules can be made synthetically (Yoshizaki *et al.*, 2001). However, the preparation of gram quantities is difficult. The novel lipid A hybrids

accumulating in strains expressing lipid A modification enzymes can be isolated and purified using existing methodologies (Raetz *et al.*, 2006).

Lipid A modification enzymes also have the potential of being used in the generation of live bacterial vaccines. Heterologous expression of lipid A modification enzymes such as, LpxE, LpxF, LpxR, and PagL in pathogens such as *Salmonela* or *Yersinia pestis* has the potential of attenuating bacteria by altering lipid A elements recognized by the innate immune response, a property that is beneficial in vaccine development.

In conclusion, we have demonstrated that lipid A modification enzymes can be expressed heterologously in combination to generate novel lipid A hybrid structures in *E. coli*. We demonstrated that one consequence of removing both phosphate moieties is impaired growth, but increased resistance to polymyxin B. Further studies will be done to analyze the integrity of the outer membrane barrier in the strains lacking phosphates and a core. We will assess the permeability barrier of the select stains with other antibiotics and hydrophobic dyes. These results will perhaps give us a better understanding of the function of lipid A. In the future, we will also test the various Kdo_2-lipid A derivates that can be generated by the expression of lipid A modification enzymes as activators of TLR4/MD2.

Chapter 3: Purification and Characterization of the *Rhizobium leguminosarum* Lipid A Oxidase, LpxQ

3.1 Introduction

The bacterial endosymbionts *Rhizobium leguminosarum* and *Rhizobium etli* possess a unique lipid A modification enzyme that oxidizes the proximal glucosamine of lipid A to a 2-amino-2-deoxy-gluconate unit (Fig. 24). The biological function of this modification is unknown. The structural gene encoding the enzyme responsible for this enzymatic modification, *lpxQ*, was previously discovered by expression cloning (Que-Gewirth et al., 2003a). Several homologues of *lpxQ* exist in the α-proteobacteria family of bacteria, but these homologues have not been confirmed as functional lipid A oxidases. A functional orthologue of *lpxQ* is, however, present in the plant pathogen *Agrobacterium tumefaciens* (Que-Gewirth et al., 2003a).

LpxQ was previously shown to be localized to the outer membrane of *R. leguminosarum*. Lipid A oxidation, therefore occurs in the late stages of lipid A assembly (Que-Gewirth et al., 2003a). Outer membrane enzymes such as LpxQ are interesting because very few have been described. All of the known outer membrane enzymes are lipases (Snijder *et al.*, 1999, Nishijima *et al.*, 1977), acyltransferases (Bishop et al., 2000, Hwang *et al.*, 2002), deacylases (Trent et al., 2001a, Rutten et al., 2006, Reynolds *et al.*, 2006), or proteases (Vandeputte-Rutten *et al.*, 2001). LpxQ's function as an oxidase is

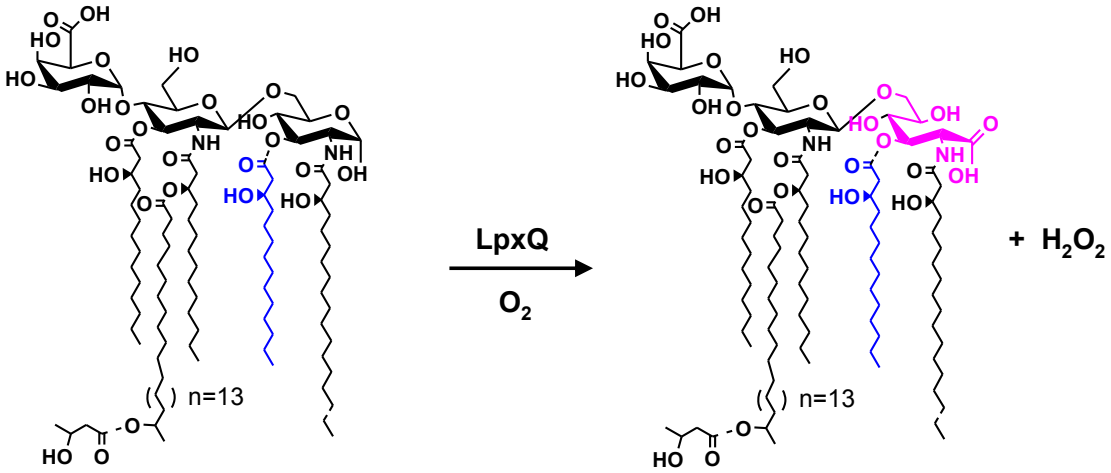

Figure 24: Proposed lipid A oxidation reaction catalyzed by LpxQ

LpxQ converts the proximal dephosphorylated glucosamine residue of *R. leguminosarum* lipid A to a 2-aminogluconate unit. Molecular oxygen is proposed as the electron acceptor in the reaction yielding H_2O_2 as a product.

unique among this class of proteins. Like all outer membrane proteins from Gram-negative bacteria, LpxQ is predicted to adopt a β-barrel structure.

Expression of the *lpxQ* gene in *E. coli* was previously shown to yield a 22 kDa protein localized to the outer membrane (Que-Gewirth et al., 2003a). The recombinantly produced protein was capable of oxidizing a variety of substrates *in vitro.* LpxQ was shown to be active with component B of *Rhizobium leguminosarum* lipid A and with 1-dephospho-lipid IV_A. The products of these reactions were analyzed by mass spectrometry and confirmed to be oxidized (Que-Gewirth et al., 2003a, Que-Gewirth et al., 2003b). The *in vitro* experiment with 1-dephospho lipid IV_A demonstrated that many of the other lipid A modifications found in *R. leguminosarum* and *R. etli*, such as the presence of a 4'-GalA unit in place of the usual phosphate, were not required for LpxQ activity. In support of this, in chapter 2, LpxQ was shown to be capable of oxidizing lipid A in living *E. coli* cells when co-expressed with the lipid A 1-phosphatase, LpxE.

The LpxQ catalyzed oxidation of lipid A was previously shown to be oxygen dependent (Que-Gewirth et al., 2003a, Que-Gewirth et al., 2003b). Oxygen was proposed as an electron acceptor in the reaction, but it was not possible to look for the expected reduction product, H_2O_2, because the membrane source used in the analysis contained catalase. The route of electron transfer in the oxidase reaction also remained unknown. LpxQ does not share significant homology with any other oxidase. Previously it was

shown that the exogenous addition of cofactors such as FAD and PQQ had no effect on activity. The activity of the enzyme, however, was shown to be sensitive to EDTA. The inhibition of activity with EDTA was shown to be reversible with the addition of divalent cations such as $Mg^{2+,}$ Co^{2+}, Ni^{2+}, and Mg^{2+}. The role of divalent cations in the reaction was not determined (Que-Gewirth et al., 2003b).

Two routes of lipid A oxidation have been proposed (Que-Gewirth et al., 2003b). In the lactone pathway, oxidation of the proximal glucosamine of lipid A occurs prior to ring opening, producing a lactone intermediate. This intermediate can be hydrolyzed by water to form the aminogluconate species observed by mass spectrometry. In the other proposed oxidation pathway, the proximal glucosamine ring first opens to its aldehyde configuration. The aldehyde is then hydrated with water from the solvent and oxidized by LpxQ to yield the aminogluconate moiety.

In this chapter, a new purification procedure for the *R. leguminosarum* lipid A oxidase is described. A detailed enzymatic characterization of the novel enzyme, its co-substrates, and products is given herein.

3.2 Materials and Methods

3.2.1 Chemicals and materials

[γ-^{32}P]-ATP was obtained from PerkinElmer Life and Analytical Sciences, Inc. (Waltham, MA). Formic acid, pyridine, and methanol were from Mallinckrodt Baker,

Inc. (Phillipsburg, NJ). The detergent n-dodecyl β-D-maltopyranoside (DDM) was from Anatrace, Inc. (Maummee, OH). Chloroform and silica gel 60 (0.25 mm) thin-layer chromatography (TLC) plates were obtained from EMD Chemicals, Inc. (Gibbstown, NJ). Yeast extract, agar, and tryptone were from Becton, Dickinson, and Co. (Franklin Lakes, NJ). Sodium chloride, and 4-(2-hydroxyethyl)-1-piperazineethanesulfonic acid (HEPES) were from VWR International (West Chester, PA). Bicinchoninic (BCA) protein assay reagents and Triton X-100 were from Thermo Fisher Scientific (Waltham, MA). PCR reagents were purchased from EMD and Stratagene (La Jolla, CA). IPTG, Amplex red (10-acetyl-3,7-dihydroxyphenoxazine), and horseradish peroxidase (HRP) were obtained from Invitrogen (Carlsbad, CA). Diethylaminoethyl (DEAE) cellulose DE52 was from Whatman, Inc. (Florham Park, NJ). The *Non-Interfering* protein assay was from G-Biosciences. All other chemicals were reagent grade and were purchased from either Sigma-Aldrich (St. Louis, MO) or VWR International (West Chester, PA).

3.2.2 Bacterial strains and growth conditions

The bacterial strains and plasmids used and their relevant characteristics are shown in Table 5. *E. coli* strains were grown at 37 °C in LB broth (1% tryptone, 0.5% yeast extract, and 1% sodium chloride) and supplemented with ampicillin (100 μg/mL) as appropriate.

3.2.3 General recombinant DNA techniques

Protocols for handling DNA and preparing *E. coli* for electroporation were performed using standard protocols (Sambrook & Russell, 2001). Transformation-competent cells of *E. coli* were prepared by the method of Inoue et al (Inoue et al., 1990). Plasmids were isolated from cell cultures using the Qiagen Spin Miniprep kit, and DNA fragments were isolated with the Qiaquick Spin kit (Valencia, CA). Pfu Turbo DNA polymerase (Stratagene, La Jolla, CA), T4 DNA ligase (Invitrogen Corp, Carlsbad, CA), restriction endonucleases (New England Biolabs, Ipswich, MA) and shrimp alkaline phosphatase from Affymetrix (Santa Clara, CA) were used according to the manufacturers' instructions. Double stranded DNA sequencing was performed with an ABI Prism 377 instrument at the Duke University DNA Analysis Facility. Primers were purchased from MWG Biotech (Huntsville, AL) and IDT Biosciences (Coralville, IA).

3.2.4 Construction of plasmid pLpxQ-his$_{10}$

The cDNA for *R. leguminosarum* LpxQ (accession number AAO73600) was previously cloned into the vector pET21a(+) vector (EMD Chemicals Inc.). This vector was used as template DNA in a PCR reaction performed with primers LpxQhis6for (5′-CGCGC*CATATG***ACATACGCGCTGCGTTCTTCCG** -3′) and LpxQhis6rev (5′-GCGC*AAGCTT*TCAGTGATGGTGATGGTGATGGCTGCTGCCGCTGCCGCGCGGCAC CAGGCCGCC**CCAGTGGAATGAAACGCCGACGTTGACGGC** -3′). These primers

incorporated a thrombin-cleavable his_6 tag at the C-terminus of the *lpxQ* gene. The coding region of *lpxQ* in the two primers is indicated in bold type, and the restriction enzyme sites are italicized. The PCR product generated with LpxQhis6for and LpxQhis6rev was digested with *Nde*I and *HindIII* and then ligated into pET21a(+), yielding pLpxQ-his_6. pLpxQ-his_6 was transformed into competent *E. coli* XL-1 Blue cells, and its sequence was confirmed by DNA sequencing.

The number of histidine residues coded in plasmid pLpxQ-his_6 was increased from 6 to 10 in a mutagenesis procedure. The insertional mutagenesis procedure was carried out by PCR as recommended by Stratagene. The primers LpxQhis10for (5′-GCAGCCATCACCATCACCATCACCATCACCATCACTGAAAGCTTGCGGCCGCAC TCGAG-3′) and LpxQhis10rev (5′- CTCGAGTGCGGCCGCAAGCTTTCAGTGATGGTG ATGGTGATGGTGATGGTGATGGCTGC -3′) were used to generate plasmid pLpxQ-his_{10}. The resulting plasmid was then transformed into electrocompetent XL-1 Blue cells, and its sequence was confirmed by DNA sequencing. The plasmid was then electroporated into C41(DE3) cells for overexpression.

3.2.5 Expression of LpxQ

C41(DE3) cells expressing pLpxQ-$Chis_{10}$ were grown in a BioFlo 3000 fermentor. First a single colony of *E. coli* containing pLpxQ-his_{10} was inoculated into 5 mL of LB containing ampicillin (100 μg/mL) and grown in a rotary shaker overnight at 37 °C. The

culture was then used to inoculate 200 mL of fresh LB containing ampicillin (100 μg/mL). The culture was grown overnight at 37 °C and was used to inoculate 4 L of media consisting of 2.2% yeast extract, 1.1% tryptone, 1% glycerol, 0.1 M KH_2PO_4, and 2 mM $MgSO_4 \cdot 7H_2O$ in a 6.6 L capacity BioFlo 3000 fermentor vessel (New Brunswick Scientific). Sterilized Antifoam B (Sigma) was added to the fermentor vessel upon inoculation. Cells were grown at 37 °C with agitation at 300 rpm. Cells were oxygenated with house air at 4 L/min. The parameters were maintained during the course of cell growth. When the A_{600} reached 6, the culture was induced with 1 mM isopropyl β-D-thiogalactopyranoside (IPTG) and 25 ml of a 50% glycerol (v/v) solution was added. The cells were grown for three additional hours after induction. The cells were then harvested by centrifugation at 4000 x *g* for 20 min. The cells were washed with 50 mM NaH2PO4, pH 8. The wet cell paste (approximately 80 g) was frozen at –80°C.

3.2.6 Preparation and solubilization of LpxQ membranes

All steps were carried out at 0-4 °C. The frozen wet cell paste was thawed and resuspended in 1 L of 50 mM NaH_2PO_4, pH 8, containing 20% glycerol. The resuspended cells were lysed by three passages through an ice-cold Cell-Cracker (Microfluidics International Corp., Newton MA). Cell debris and unbroken cells were removed by centrifugation at 4000 x *g* for 20 min. Membrane were prepared by ultracentrifugation at 34000 x *g* for 12 h. The membrane pellet was resuspended at 5-10 mg/ml in 50 mM

NaH_2PO_4, pH 8, containing 20% glycerol and stored at -80 °C. The protein concentration was determined by the bicinchoninic acid method using bovine serum albumin as the standard (Smith et al., 1985). The prepared membranes were solubilized by adding appropriate volumes of 10% aqueous Triton X-100 so that the final concentration of Triton X-100 would be 1% and the final protein concentration would be 1 mg/ml. The mixture was incubated for 2 h at 4 °C with gentle mixing and then centrifuged at 34000 x *g* for 12 h at 4 °C to remove any remaining insoluble material.

3.2.7 Purification of LpxQ by Ni-NTA chromatography

Typically, 25 mL of Ni-NTA Superflow™ resin (Qiagen, Valencia, CA) was poured into a gravity-flow column and allowed to settle. The column was washed with water and equilibrated with 5 column volumes of loading/wash buffer (50 mM NaH_2PO_4, pH 8, containing 20 % glycerol, 0.8% Triton X-100, 20 mM imidazole, and 300 mM NaCl). The resin was resuspended in 40 mL of loading buffer and transferred to a 50 mL falcon tube and incubated with rotation at 4 °C for 1 hour. The resin was pelleted by centrifugation at 1000 x *g* for 1 min and resuspended in loading buffer. The solubilized membranes were prepared for loading by adding NaCl and imidazole to a final concentration of 300 mM and 20 mM, respectively. The equilibrated resin was transferred to the prepared load and incubated with rotation for 2 h at 4 °C. The load containing the resin was then applied to the gravity-flow column, and the resin

containing the bound protein was retained. The column was washed with 5 column volumes of the column equilibration buffer. The Triton X-100 was then exchanged for DDM in a series of wash steps. The column was washed with 5 column volumes of buffer containing 50 mM NaH_2PO_4, pH 8, 20 % glycerol, 0.1% DDM, 20 mM imidazole, and 300 mM NaCl and then washed with 5 column volumes containing 50 mM NaH_2PO_4, pH 8, 20 % glycerol, 0.01 % DDM, 20 mM imidazole, and 300 mM NaCl. The detergent-exchanged protein was eluted sequentially with 5 column volumes of similar buffers containing 25, 50, or 500 mM imidazole. The elutions were collected as single column volume fractions. LpxQ was eluted in buffer containing 500 mM imidazole. The fractions containing purified LpxQ were pooled and concentrated about 50-fold with the Centricon Plus-70 Ultracel PL-10 (Millipore Corp., Billerica, MA). LpxQ was typically concentrated to 5-10 mg/ml.

3.2.8 Size-exclusion chromatography

Purified LpxQ was applied to a Superdex 200 10/300 GL column (10 x 300 mm, 24 mL bed volumne; GE Healthcare) using an ÄKTA$_{FPLC}$ controlled by the UNICORN system (GE Healthcare, Waukesha, WI), according to the manufacturer's recommendations. Typically, the flow rate was 0.33 mL/min. The column was pre-equilibrated in 50 mM HEPES, pH 7.5, 0.01 % DDM, 300 mM NaCl, and 20% glycerol.

The concentrated protein was loaded onto the Superdex column after centrifugation at 13000 for 10 min.

3.2.9 SDS-PAGE analysis of LpxQ

Protein samples were visualized by SDS-PAGE using the Mini Protean II electrophoresis system (Bio-Rad.). Samples not subjected to boiling were incubated for 30 min at 40 ^{o}C in membrane protein loading buffer (50 mM Tris, pH 6.8, 12.5 % glycerol, 3% SDS, 50 mM DTT, 0.005% bromophenol blue) (Jagow & Schagger, 1994). Boiled samples were diluted in the same buffer prior to SDS-PAGE. Samples were analyzed using 12% SDS-polyacrylamide gels.

3.2.10 Cross-linking of LpxQ

Chemical cross-linking of LpxQ was performed by adding gluteraldehyde to a final concentration of 0.09% to 10 μg of purified LpxQ. The mixture was incubated at room temperature for 100 min and then analyzed by SDS-PAGE.

3.2.11 Liquid chromatography–mass spectrometry (LC/MS) of the Intact LpxQ protein

Purified LpxQ in 50 mM HEPES, pH 7.5, 0.01 % DDM, 300 mM NaCl, and 20% glycerol was diluted to 1 mg/ml with water and subjected to LC/MS in the positive ion mode as described previously (Six et al., 2008). Briefly, the protein was analyzed on a QSTAR XL quadrupole time-of-flight tandem mass spectrometer (ABI-MDS-Sciex, Foster City, CA) equipped with an electrospray source. The QSTAR was coupled to a

Shimadzu Scientific Instruments (Columbia, MD) LC system which was operated at a flow rate of 200 μL/min with a linear gradient described previously (Six et al., 2008). The solvent used in the gradient were: Solvent A (water:acetontirole (98:2, v/v) with 0.01% acetic acid and solvent B (acetonitrile:water (90:10, v/v) with 0.01% acetic acid. Solvent A was held isocratically for 2 min at 100%. The gradient was linearly increased to 60% B over 18 min and then increased to 100% B over 5 min. A Vydac C4-reverse-phase column (2.1 X 50 mm) was used. MS data acquisition and analysis were performed using the Analyst QS software and BioAnalyst extension software. The de-convoluted mass of the protein was determined from the multiply charged ions using the Bayesian protein reconstruction tool.

3.2.12 Trypsin digestion of purified LpxQ

In-gel digestions of LpxQ were performed with the Trypsin IGD kit (Sigma) and performed according to the manufacturer's recommendations. Briefly, the band of interest was cut with a razor from a SDS-PAGE gel stained with Bio-Safe Coomassie stain (Bio-Rad). The gel piece was placed in a siliconized 1.7 mL tube and destained with 200 μL of destaining solution (200 mM ammonium biocarbonate with 40% acetonitrile). The tube was incubated at 37 ^{o}C during the destaining procedure. The destaining solution was removed and the procedure was repeated again. After removal of the destaining solution, the gel piece was dehyrdrated in a vacuum concentrator. Trypsin

reaction buffer (40 mM ammonium bicarbonate in 9% acetonitrile) was added to gel piece along with 0.4 μg of trypsin. The gel piece was incubated overnight (~16 h) at 37 ^{o}C. The reaction was terminated with the addition of acetic acid to a final concentration of 5% (v/v). The solution containing the tryptic peptides was then analyzed by LC/MS using the LC setup described above for the analysis of intact proteins. A Zorbax SB-C8 reversed-phase column (5 μm, 2.1 × 50 mm) was used for LC/MS analysis of the peptides.

An in-solution digest of LpxQ was performed as follows. Purified LpxQ was diluted three fold into ice-cold acetone. The solution was vortexed and incubated on dry ice for 3 h. The solution was centrifuged at 14,000 *g* for 15 min, and the supernatant was removed. The pellet was washed twice more with ice cold acetone and allowed to air-dry. The pellet was then suspended in 8 M guanidine hydrochloride and placed in a boiling water bath for 10 min. The boiled protein was then diluted 10 fold in 40 mM ammonium bicarbonate/9% acetonitirile. Trypsin was added to the solution at 20 μg/ml. The reaction was incubated for 16 h and the tryptic peptides were analyzed by LC/MS as described above.

3.2.13 Preparation of substrates

The LpxQ substrate, 1-dephospho-Kdo$_2$-lipid IV$_A$, was synthesized *in vitro* from lipid IV$_A$. The lipid IV$_A$ was isolated and purified from strain CMR100 (Reynolds &

Raetz, 2009). This strain has a deletion in its Kdo transferase gene, *kdtA*, and harbors a plasmid overexpressing the ABC transporter, MsbA (Reynolds & Raetz, 2009). Briefly, CMR100 cells were grown at 30 °C in 1 L of LB broth supplemented with 100 μg/ml ampicillin and 1 mM IPTG. The cells were harvested by centrifugation at 4000 x *g* for 20 min when the cells reached an A_{600} of 1.2. The cell pellet was washed with 200 mL of PBS and stored at -80 °C. The cells were later thawed and resuspended in 40 mL of phosphate-buffered saline (PBS) and then converted to a single-phase Bligh-Dyer mixture (chloroform/methanol/PBS, 1:2:0.8 v/v) with the addition of 50 mL of chloroform and 50 mL of methanol. The mixture was incubated for 1 h with mixing and then centrifuged at 4000 x *g* for 20 min. The supernatant was converted to a two-phase Bligh-Dyer mixture (chloroform/methanol/PBS, 2:2:1.8, v/v) with the addition of 25 mL of chloroform and 25 mL of PBS. The phases of the mixture were separated by centrifugation at 4000 x *g* for 20 min. The lower phase containing the lipid IV_A and phospholipids was recovered and dried with a rotary evaporator. The lipid IV_A was purified from the phospholipids over DEAE-cellulose as previously described (Kanipes *et al.*, 2001). The lipid fractions were collected and analyzed by TLC in a chloroform:pyridine:formic acid:water system (50:50:16:5 v/v). The lipids were detected with sulfuric acid charring. The lipid IV_A was retrieved from the DEAE fractions by acidic Bligh-Dyer portioning as described above. The isolated IV_A was converted *in vitro*

to Kdo_2-lipid IV_A using conditions previously reported (Reynolds et al., 2005). The Kdo_2-lipid IV_A was subsequently dephosphorylated at the 1-position with solubilized *R. leguminosarum* LpxE membranes using conditions previously optimized (Kanjilal-Kolar et al., 2006). Solubilized membranes form pLpxE/NovaBlue (DE3) were prepared as previously described, (Karbarz et al., 2009) and used at 0.4 mg/ml. The *in vitro* dephosphorylation reaction was carried out in a buffer consisting of 50 mM MES, pH 6.5, and 0.1% Triton X-100. The reaction was carried out overnight at 30 ^{o}C. The 1-dephospho Kdo_2-lipid IV_A reaction product was extracted by Bligh-Dyer portioning (Bligh & Dyer, 1959), and purified over DEAE-cellulose. The pure 1-dephospho Kdo_2-lipid IV_A was weighed and resuspended to a stock concentration of approximately 1 mM in 25 mM Tris-HCl, pH 7.8, 1 mM EDTA, 1mM EGTA, and 0.1% Triton X-100.

Radiolabeled 1-dephospho Kdo_2-[4′-^{32}P]-lipid IV_A was synthesized as described previously (Kanjilal-Kolar et al., 2006). Briefly, Kdo_2-[4′-^{32}P]lipid IV_A was generated from [γ-^{32}P]ATP and the tetra-acyl disaccharide 1-phosphate acceptor, DSMP (Radika & Raetz, 1988). Membranes overexpressing the *E. coli* 4′-kinase (LpxK) (Garrett et al., 1997), and purified Kdo-transferase (KdtA) and CMP-Kdo synthase (Basu et al., 1999a, Belunis & Raetz, 1992) were used as the enzyme sources. The Kdo_2-[4′-^{32}P]lipid IV_A was desphosphorylated in the same reaction mixture using the conditions described above

for the carrier substrate. The isolation proceeded as described for Kdo_2-[4′-^{32}P]-lipid A (Reynolds et al., 2005).

The substrate 1-dephospho Kdo_2-lipid A was isolated and purified from WBB06 cells expressing pWSK29-LpxE as descried previously (Wang et al., 2004). The pure 1-dephospho Kdo_2-lipid IV_A and 1-dephospho Kdo_2-lipid A were weighed and resuspended to stock concentrations of approximately 1 mM in 25 mM Tris-HCl, pH 7.8, and 0.1% Triton X-100.

The substrate 1-dephospho lipid IV_A was prepared in an *in vitro* reaction starting with lipid IV_A, which was purified as described above. The lipid IV_A was desphosphorylated using purified *R. leguminosarum* LpxE as the enzyme source (Karbarz et al., 2009). Conditions for the desphorphorylation reaction was as described above. The reaction mixture was extracted by the Bligh-Dyer method (Bligh & Dyer, 1959), and the 1-dephospho lipid IV_A was purified over DEAE-cellulose. The purified product was weighed and resuspended to a stock concentration of approximately 1 mM in 25 mM Tris-HCl, pH 7.8, containing 1 mM EDTA, 1mM EGTA, and 0.1% Triton X-100.

The exact concentrations of 1-dephospho-Kdo_2-lipid IV_A and 1-dephospho-Kdo_2-lipid A were determined using the Kdo release assay (Lee & Tsai, 1999). The exact concentration of 1-dephospho-lipid IV_A was determined by phosphate analysis (Chen *et*

al., 1956, Fiske & Subbarow, 1925). The substrates were stored frozen. Prior to use, the lipid substrates were dispersed by sonic irradiation for 1 min in a bath sonicator.

3.2.14 *In vitro* radiochemical activity assay of LpxQ

LpxQ activity was assayed in 10-30 μL reaction mixtures at 30 °C. Standard assay conditions were as follows: the reaction mixtures contained 50 mM MES, pH 6.5, 0.1% Triton X-100, 1 mM MgCl, and 2 μM 1-dephospho Kdo_2-[4′-^{32}P]lipid IV_A (1,000 cpm/nmol). Reactions were initiated with the enzyme source. The reaction mixtures were incubated for the times indicated. Reactions were terminated by spotting 3-μl samples onto a TLC plate, which was developed in the solvent chloroform/methanol/acetic acid/water (25:15:4:4; v/v). After drying and overnight exposure of the plate to a PhosphorImager screen (GE Healthcare), product formation was detected and quantified with a Storm 840 PhosphorImager equipped with ImageQuant software (GE Healthcare).

3.2.15 Assay of LpxQ under anaerobic conditions

The dependency of LpxQ on molecular oxygen was demonstrated by performing assays in an anaerobic chamber (Coy Laboratory Products, Inc, Grass Lake, MI). Reaction tubes containing all assay components except enzyme were equilibrated in the chamber for 30 min. Reactions were initiated with enzyme that was equilibrated in the absence of oxygen.

Assays were performed in the presence of an "oxygen-scrubbing" system in some experiments where indicated. In these experiments, glucose (0.3%, w/v), glucose oxidase (20 μg/mL), and catalase (2 μg/ml) were present in the assay mixture.

Assays performed with the artificial electron acceptor, dichlorophenolindophenol (DCPIP), were performed in the anaerobic chamber. The assays were performed using standard assay conditions with the addition of DCPIP. The concentration of DCPIP was varied from 10 μM – 500 μM.

3.2.16 Detection of hydrogen peroxide

Hydrogen peroxide production was assessed enzymatically with Amplex red (AR, 10-acetyl-3,7-dihyroxyphenoxazine) and horseradish peroxidase (HRP) (Invitrogen). Amplex red is converted to resorufin by HRP in the presence of H_2O_2. Amplex red is colorless whereas resorufin contains a chromophore that can be measured either by absorbance or by fluorescence (Zhou *et al.*, 1997). The reagents were used according to the manufacturer's instructions.

For the end-point assay, 100 μL reactions were prepared. The assays were set up using standard assay conditions; however the reactions contained 10 μM 1-dephospho-Kdo_2-lipid IV_A. Control reactions with H_2O_2 added were also prepared. The reactions were incubated at 30 ^oC until completion. Fifty μL of each reaction was transferred to a single well in a 96 well plate. A solution containing 100 μM AR and 0.2 Units/mL of HRP

was prepared in LpxQ assay buffer. Fifty μL of the prepared solution was added to each sample in the 96 well plate. The samples were incubated at room temperature for 30 minutes, and the amount of H_2O_2 produced was measured with a FluoSTAR Optima microplate reader (BMG Labtech) using excitation at 545 nm and fluorescence detection at 590 nm. The samples were compared with an H_2O_2 standard curve generated under the same conditions.

For some experiments, H_2O_2 was measured in a continuous fashion. The continuous assays were set up using standard conditions but with the inclusion of 50 μM amplex red and 0.1 units/ml HRP. The reactions were initiated by the addition of enzyme, and H_2O_2 was monitored with fluorescence as before. The H_2O_2 concentration was determined using a standard curve generated with H_2O_2 treated in the same manner as the reactions.

3.2.17 Preparation and analysis of the ^{18}O labeled LpxQ reaction product

Fifty μL reaction mixtures were prepared and contained 50 mM MES, pH 6.5, 0.7% n-octyl-β-D-glucoside, 1 mM MgCl, 10 μM 1-dephospho-Kdo_2-lipid IV_A, and 75% ^{18}O-enriched water. The reaction were initiated with purified enzyme. A control reaction was set up with unlabeled water. The reaction mixtures were incubated ~ 16 h at 30 ^{o}C and analyzed by LC/ESI/MS as previously described (Song *et al.*, 2009).

3.2.18 Apparent kinetic parameters and pH dependency of LpxQ

Velocity as a function of 1-dephospho-Kdo_2-lipid IV_A concentration was determined for purified LpxQ using standard assay conditions except that the concentration of 1-dephospho-Kdo_2-lipid IV_A was varied from 0.1 – 80 μM. The velocities were fit a Michaelis-Menton function using Microsoft Excel. Typically, 50- 180 nM of enzyme was used to start the reactions, and time points were taken at 5 min intervals for 30 min.

The pH dependency of LpxQ was determined by assaying LpxQ in a uniform triple buffer system, consisting of 100 mM sodium acetate, 50 mM BisTris, and 50 mM Tris from pH 4.5 to 9, as described previously (Karbarz et al., 2009, McClerren *et al.*, 2005b). Standard assay conditions were used except that the triple buffer system replaced the MES component. Product formation was determined at 10 min.

3.2.19 Effect of detergent on LpxQ activity

LpxQ was assayed under standard assay conditions, except that the concentration of Triton X-100 was varied in the assay from 0.007% to 2 % (v/v) (0.23 mM- 31.1 mM). The 1-dephospho-Kdo_2-lipid IV_A remained fixed at 2 μM. The purified protein was diluted in assay buffer without Triton X-100 to minimize carryover detergent. The 1-dephospho-Kdo_2-lipid IV_A used in this experiment was resuspended in 25 mM Tris-HCl, pH 8.0, containing 1 mM EDTA and 1mM EGTA.

3.2.20 Substrate specificity

The substrate specificity of LpxQ was assessed with 1-dephospho-Kdo_2-lipid IV_A, 1-dephospho-Kdo_2-lipid A, and 1-dephospho-lipid IV_A. Each substrate was assayed at 2 μM. Activity was assessed by monitoring hydrogen peroxide formation with the Amplex Red reagent as described above.

3.2.21 Metal dependency of LpxQ

The metal dependency of LpxQ was determined using standard assay conditions except that the concentration $MgCl_2$ was varied from 0-10 mM.

3.2.22 Inductively coupled plasma emission spectroscopy analysis of LpxQ

Inductively coupled plasma emission spectroscopy (ICP) was performed at the University of Utah. Prior to analysis, LpxQ samples were dialyzed against 0.01 % DDM, 50 mM HEPES, pH 7.5, and 150 mM NaCl. Approximately 0.5 mL of protein solution from the Ni-NTA purification step was dialyzed against 1 L of dialysis buffer. The dialysis procedure was carried out for 24 h at 4 ^{o}C. The dialysis buffer was changed twice during this time. The LpxQ samples and buffer reference samples were analyzed for Cd, Co, Cu, Fe, Mg, Mn, Ni, and Zn. Protein samples were analyzed at 0.33 μM.

3.2.23 Stability experiments with LpxQ

The stability of purified LpxQ was assessed in an assay with Pronase (Roche), a protease with broad specificity. LpxQ samples (1.7 mg/ml) were diluted 2-fold into a)

protein dilution buffer (50 mM HEPES, pH 7.5, 300 mM NaCl, 0.01% DDM) b) 8 M urea, c) 4% SDS, or d) 4% SDS and 8 M urea. The samples containing SDS were placed in a boiling water bath for 10 min. Some samples were incubated with 20 μg of Pronase and incubated for 16 h at 37 ^{o}C. The samples were prepared for SDS-PAGE analysis as described above.

Table 5: Bacterial strains and plasmids used in chapter 3

Strain or Plasmid	Genotype or Description	Source or Reference
C41(DE3)	F *ompT hsds*$_B$ (r_B^- m_B^-)*gal dcm*(DE3) D(srl-recA)306::Tn*10*	Miroux paper
XL1-Blue	*recA1 endA1 gyrA95 thi-1 hsdR17 supE44 relA1 lac* [F′ proAB *lacIqZDM15 Tn*10 (Tet^R)]	Stratagene
CMR100	DY330 (*kdtA::kan*) pWMsbA	(Reynolds & Raetz, 2009)
WBBO6	W3110 *mtl*, Δ(*waaC-waaF*)::*tet*6	(Brabetz et al., 1997)
BLR(DE3)	B strain, DE3 lysogen	EMD
Plasmids		
pQN233	*lpxQ* in pET21a(+)	(Que-Gewirth et al., 2003a)
pQN235	*lpxQ* in pET21b(+) with C-terminal His tag	(Que-Gewirth et al., 2003a)
pET21a(+)	Expression vector containing a T7 promoter, Amp^R	EMD
pLpxQ-his_6	pET21a(+) containing *lpxQ* with C-terminal his_6 tag	This work
pLpxQ-his_{10}	pET21a(+) containing *lpxQ* with C-terminal his_{10} tag	This work

3.3 Results

3.3.1 Overexpression and solubilization of *R. leguminosaraum* LpxQ

LpxQ was previously overexpressed in NovaBlue DE3 cells (Que-Gewirth et al., 2003a). The overexpressed protein in this background was localized to the outer membrane and was catalytically active (Que-Gewirth et al., 2003a). The protein was only moderately overexpressed in this background, and attempts at purification were met with limited success. A new LpxQ overexpression plasmid was constructed by fusing a his_{10} tag to the C-terminus region of LpxQ. The affinity tag was connected to the protein by an 11 residue thrombin-cleavable segment. The plasmid pLpxQ-his_{10} was expressed in C41(DE3), a strain that has been successfully used in the production of many recombinant proteins (Miroux & Walker, 1996). The expression of LpxQ was monitored by SDS-PAGE. A protein with the expected molecular weight of LpxQ was significantly overexpressed in the membrane fraction of C41(DE3) cells after IPTG induction (Fig. 25, lane 2).

Robust LpxQ activity was detected in membranes isolated from C41(DE3) cells expressing pLpxQ-his_{10} using the substrate 1-dephospho-Kdo_2-[4′-^{32}P]lipid-IV_A, a substrate not available previously. A typical activity assay performed with this substrate is shown in Fig. 26. The oxidized product of 1-dephospho-Kdo_2-[4′-^{32}P]lipid-IV_A migrates

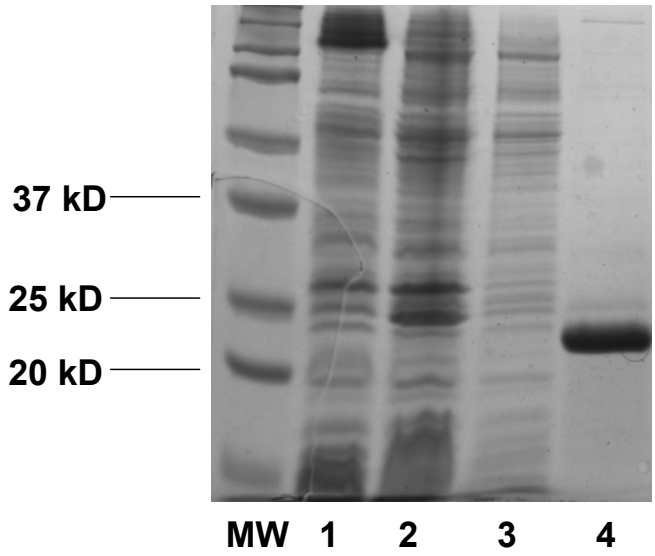

Figure 25: Gel electrophoresis of C-terminally his_{10}-tagged *Rhizobium legmunosarum* LpxQ at various stages of purification

Approximately 10 μg of protein from each step of the purification procedure was loaded onto a 12% SDS-Tris-polyacrylamide gel. Lanes: 1, membranes from C41(DE3)/pet-21a(+) induced with 1 mM IPTG; 2, membranes from C41(DE3)/pLpxQ-his_{10} induced with 1 mM IPTG; 3, Triton-solubilized membranes; 4, LpxQ purified over a Ni-NTA column, pooled, and concentrated. MW denotes the molecular masses of the protein standards. The molecular mass of C-terminally his_{10}-tagged *Rhizobium legmunosarum* LpxQ is 24.3 kDa.

more slowly in the solvent system employed. Product formation under these conditions is linear with time and protein concentration.

Membranes from C41(DE3)/pLpxQ-his$_{10}$ overexpressed LpxQ activity 20-fold relative to *R. leguminosarum* membranes. The membrane-associated activity was typically solubilized at 1 mg/ml with 1% Triton X-100. Typically, 50-70% of the units of activity were solubilized. A significant portion of the overexpressed LpxQ protein band, however, remained insoluble, indicating that much of the protein was present in an inactive form (Fig 25, lane 3). In order to maximize protein expression and to purify milligram quantities of the protein, expression of LpxQ from C41(DE3)/pLpxQhis$_{10}$ was carried out in a 6.6 L capacity fermentor as described in the experimental methods section. The expression of the protein in the fermentor did not change dramatically. A significant percentage of the overexpressed protein still remained insoluble upon solubilization. Growth in the fermentor, however, facilitated the production of large quantities of cells. A single fermentor run typically resulted in ~ 100 grams of wet cell paste.

3.3.2 Purification of His$_{10}$-tagged LpxQ

The His$_{10}$ tag fused to the C-terminus of LpxQ facilitated purification of the protein. The active, solubilized membranes isolated from C41(DE3)/pLpxQ-his$_{10}$ was

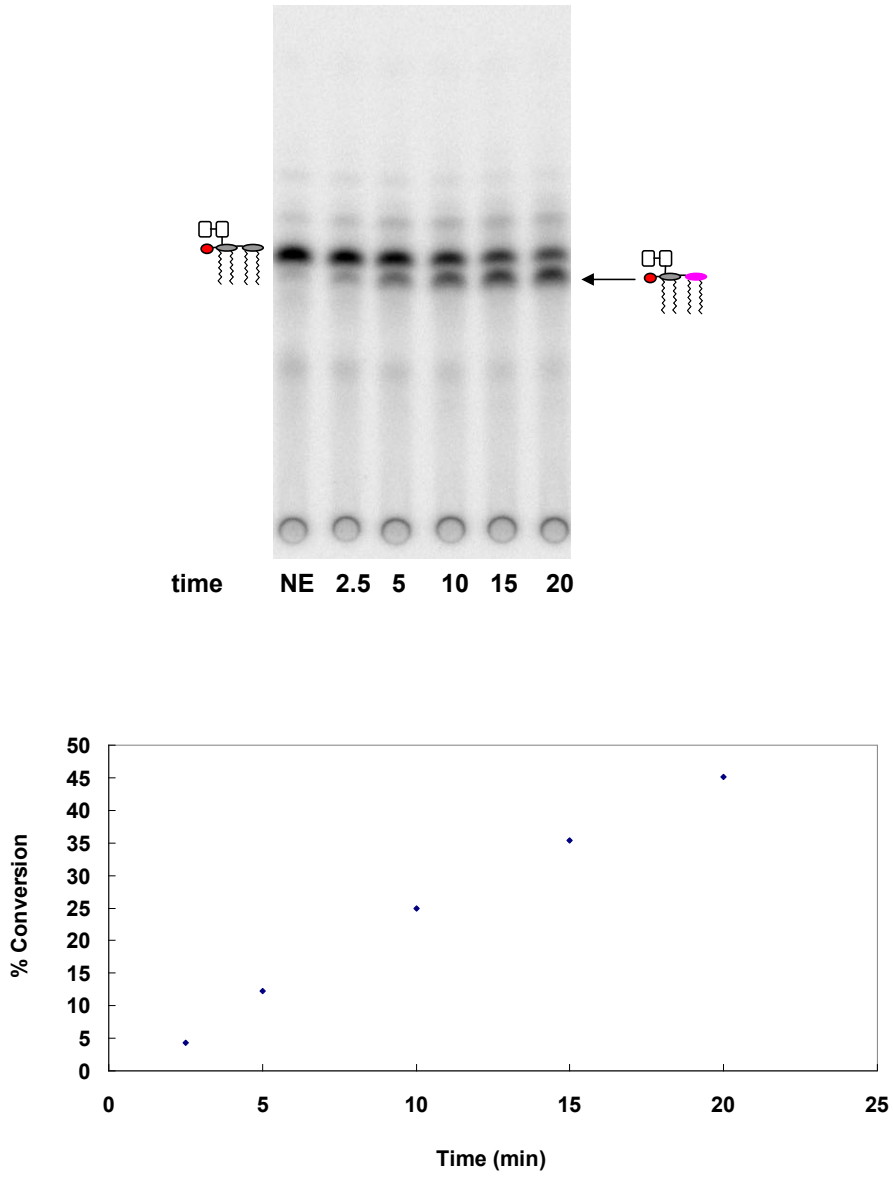

Figure 26: Time dependence of *R. leguminosarum* LpxQ

The oxidation of 1-dephospho-Kdo_2-[4′-^{32}P] lipid IV_A is linear with time and protein concentration. The assay shown here were carried out under standard assay conditions with 2 μM 1-dephospho Kdo_2-lipid IV_A.

applied to a Ni^{2+}-NTA-agarose column as described in the experimental procedures section. A reasonable percentage of the activity was retained and eluted with 500 mM imidazole along with a protein with the expected molecular weight of LpxQ (Fig 25, lane 4). The migration in SDS-PAGE of the purified LpxQ band was found to differ from that of the overexpressed insoluble band in membranes. The purified band ran slightly faster on the gel. The specific activity of the purified enzyme was increased ~25 fold relative to the membrane fraction (Table 6).

3.3.3 LC/ESI/MS of purified intact LpxQ

Purified LpxQ was analyzed by LC/ESIMS as described in the experimental methods section. The protein eluted with DDM on a C4-reverse phase column between 14-16 min. The protein signal, therefore, was significantly suppressed. The deconvoluted mass spectrum shown in Fig. 27 corresponds to a small fraction of the total protein signal that elutes just after DDM (16-16.5 min).

The purified protein was expected to have a mass of 24350 kDa. The first 27 amino acids of the protein are predicted to act as a signal sequence for translocating the protein to the outer membrane. The protein, therefore, is predicted to be cleaved between Ala^{27} and Glu^{28} during protein export. The site of signal processing for LpxQ was previously determined by N-terminal microsequencing and agreed with the predicted sequence. (Que-Gewirth et al., 2003a).

Table 6: Purification of *R. leguminosarum* LpxQ from C41(DE3)/pLpxQ-his$_{10}$.

Step	Protein (mg/ml)	Total Protein (mg/ml)	Specific Activity (nmol/min/mg)	Total Activity (nmol/min)	Purification (Fold)	Yield (%)
Membranes	5.97	2985	0.31	910	1	100
Solubilized Membranes	1.60	1824	0.26	465	0.84	51
Ni-NTA column	9.04	11.75	8.2	96.35	26.5	10.5

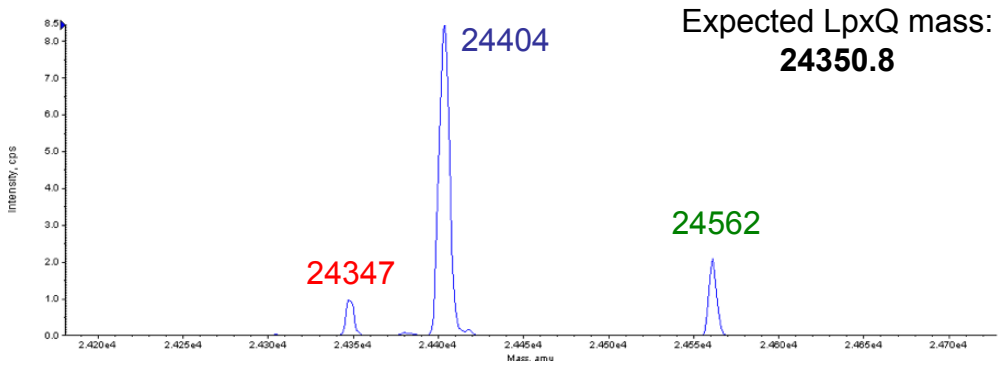

Figure 27: Protein mass spectrum of purified LpxQ

Pure LpxQ was subjected to LC/ESI/MS in the positive ion mode. LpxQ exists as three major species. The most prevalent species (244404) is ~54 units larger than the expected mass (24350.8). The largest species differs by 158 mass units and is derived from miscleavage of the LpxQ signal sequence.

LpxQ was heterogeneous and contained three major species. The most prevalent species detected by mass analysis (24404 kDa) was ~ 54 mass units larger than the predicted size of recombinantly expressed LpxQ. The species at 24347 kDa is within experimental error of the expected mass. The third species was confirmed to be a derivative of LpxQ retaining two additional amino acids at its N-terminus. These amino acids (alanine and serine) are retained in a portion of the species due to mis-cleavage of the signal sequence. In these species, cleavage occurs between Ala^{25} and Ser^{26}. The structural heterogeneity at the N-terminus of the protein could be eliminated by exchanging the native signal sequence of LpxQ with the signal sequence of the protein OmpA (data not shown). The major LpxQ species in Fig. 27 did not change when analyzed in the presence of urea or formic acid, suggesting that the modifications are covalent. Similar modifications were observed in a purified LpxQ homolog from *A. tumefacien*s (data not shown).

3.3.4 Trypsin digest of purified LpxQ

The mass deviations of the intact protein were investigated by proteolytic digestion. In-gel digests were performed on the purified LpxQ band as described in the experimental methods section. The resulting peptide fragments were analyzed by LC/ESI-MS using a C8 reverse-phased column. The majority of the expected tryptic peptides were detected (Table 7). The N-terminal peptide containing the extra amino

Table 7: Results from in-gel tryptic digestion of LpxQ-his$_{10}$

Peptide	Location	Sequence	Detected
1	1-34	EDLQFSIYGGYQTAPHSGVDLSDGTSFTAGWEGK	Yes
2	35-45	SFGSPPYYGAR	Yes
3	46-68	VTWWLENFNKPNWGISLDYTHDK	Yes
4	69-78	VYADDDTLAK	Yes
5	79-100	AGWSHFEFTDGLNLITVNGLYR	
6	101-106	FQDPTR	Yes
7	107	R	Yes
8	108-131	WTPYLGAGIGVNIPHVEVIRPEGK	Yes
9	132-151	TWAYEFGGVTLQAQAGVDFK	Yes
10	152-155	VTER	
11	156-163	WSTFVEYK	Yes
12	164-168	GTYSR	
13	169-180	IDVPIDSGVDLK	Yes
14	191-202	TNIFTNAVNVGVSFHWGGLVPR	Yes
15	203-217	GSGSSHHHHHHHHHH	Yes

Table 8: Fragments of peptide 5 detected from in-solution digest of LpxQ

Sequence	Average Mass
AGWSHFEF	979.44
AGWSHFEFT	1080.48
FTDGLNLITVNG	1262.74
GLNLI	527.69
AGWSHFEF	1036.34
AGWSHFEFTDGLNLITVNGLYR	2509.23

acids due to mis-cleavage of the signal sequence was also detected. The mass of the detected peptides all were within experimental error of their predicted masses (data not shown). Peptide 5 containing residues 79-100 was not detected in several experiments. Therefore, it was thought that the 55 Da shift observed in the mass spectrum of intact LpxQ may be derived from this peptide.

An in-solution digestion procedure was devised to maximize the recovery of the tryptic peptides for mass analysis. Several peptides related to peptide 5 were found in this analysis (Table 8). These peptides were fragments of peptide 5 and were cleaved predominantly between Phe^{8} and Thr^{9}. MS/MS analysis of the peptide fragments revealed that Phe^{8} was the site of covalent modification. Mutation of this residue to an alanine residue eliminated the modification, but had no effect on activity (data not shown).

3.3.5 Size-exclusion chromatography of LpxQ

Purified LpxQ was subjecting to size-exclusion chromatography as described in the experimental methods section (Fig. 28). LpxQ eluted as a uniform symmetric peak at a volume that corresponds to a molecular weight of ~81 kDa. The observed size of LpxQ in the presence of DDM could correspond to one LpxQ monomer (24 kDa) embedded in a large DDM micelle (57 kDa) or a dimer of LpxQ in a minimal amount of DDM.

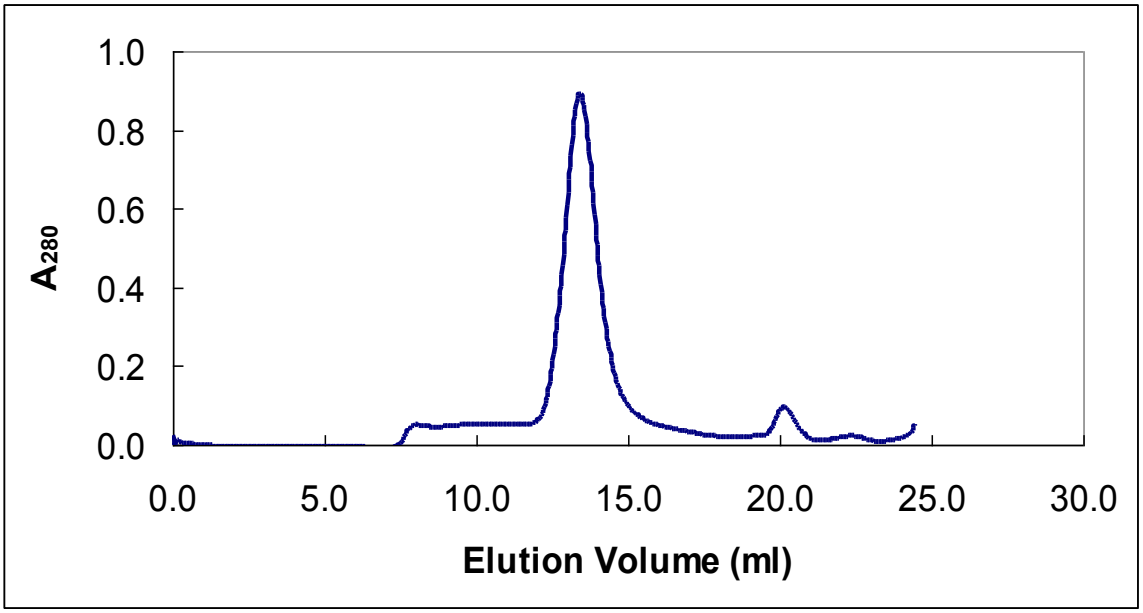

Figure 28: Size exclusion chromatography of *R. leguminosarum* LpxQ.

Purified LpxQ was chromatographed on a 24 mL Superdex 200 column at a flow rate of 0.33 mL/min in 50 mM HEPES, pH 7.5, 20% glycerol, 300 mM NaCl, and 0.01 % DDM. LpxQ eluted at 13.4 mL on the column, corresponding to a size of ~ 80 kDa. The elution profile is consistent with LpxQ existing in solution as a monomer in a large DDM micelle or a dimer of LpxQ in a minimal amount of detergent.

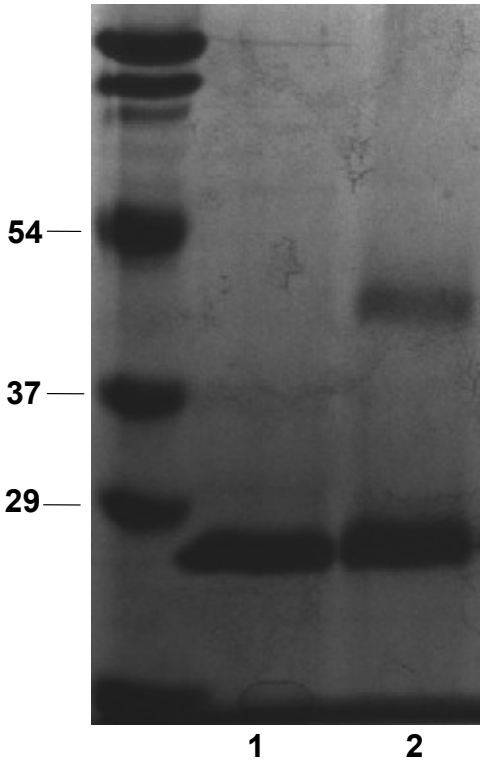

Figure 29:Chemical cross-linking of purified LpxQ

Samples of purified LpxQ were incubated in the presence or absence of 0.09% glutaraldehyde for 100 min at 25 °C. The protein samples were then analyzed by SDS-PAGE electrophoresis. The predicted size of LpxQ is 24.3 kDa. Lane 1) LpxQ. Lane 2) LpxQ treated with 0.09 % gluteraldehyde.

The oligomerization state of purified LpxQ was also probed by chemically cross-linking it with glutaraldehyde. Treatment of LpxQ with glutaraldehyde resulted in the formation of a second species (Fig 29). The second band detected by SDS-PAGE, migrated with the predicted molecular weight of a LpxQ dimer (48 kDa).

3.3.6 LpxQ utilizes molecular oxygen

Previously, the *in vitro* activity of recombinantly expressed LpxQ was shown to be dependent on atmospheric oxygen. Membranes from BLR(DE3)/pQN235 were unable to metabolize ^{14}C-acetate labeled substrates derived from *R. leguminosarum* under anaerobic *conditions* (Que-Gewirth et al., 2003a). The oxygen dependency of LpxQ was confirmed by performing similar assays with the purified protein and 1-dephospho Kdo_2-lipid IV_A (Fig. 30). Identical assays were prepared under aerobic or anaerobic conditions. Under aerobic conditions, the substrate was rapidly converted to the oxidized product. The rate of lipid A oxidation, however, was retarded with the inclusion of an "oxygen-scrubbing" system. Under anaerobic conditions, the substrate was not metabolized. These results strongly support a direct role for oxygen in the LpxQ reaction.

Oxygen's role as a co-substrate in the reaction has previously led to the speculation that it would act as an electron acceptor. To address this possibility, anaerobic assays were performed in an anaerobic chamber with artificial electron

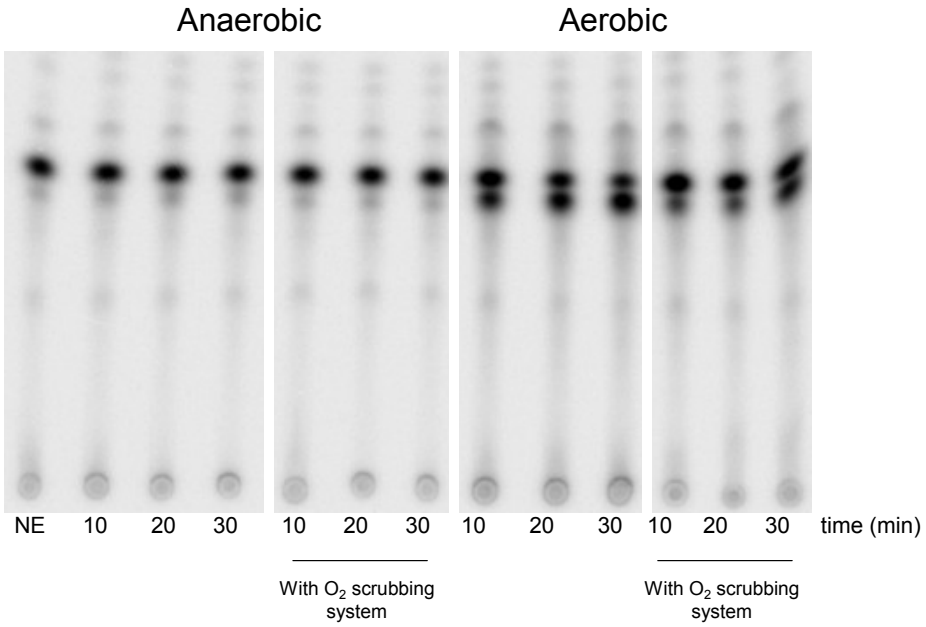

Figure 30: LpxQ activity is dependent upon atmospheric oxygen

The lipid A oxidase assay was performed either in an anaerobic chamber or under ambient atmospheric conditions. In both cases standard assay conditions were employed. An oxygen scrubbing system consisting of 0.3% glucose, 20 μg/mL glucose oxidase, and 2 μg/ml catalase was included in the assay mixture where indicated. The oxidation of 10 μM 1-dephspho-Kdo_2-lipid IV_A was determined after 10, 20, or 30 min at 25 °C using 1.6 μM enzyme. No product formation was observed under anaerobic conditions, and the oxygen scrubbing system retarded the rate of oxidation under aerobic conditions. NE: no enzyme.

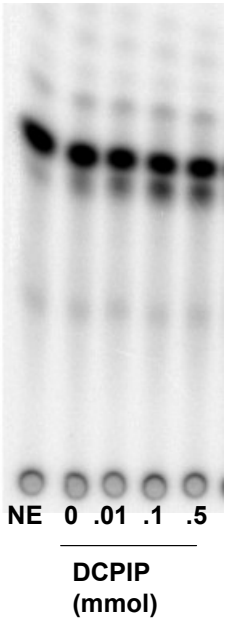

Figure 31: LpxQ can utilize DCPIP as an electron acceptor.

The lipid A oxidase assay was performed in an anaerobic chamber with standard assay conditions. The reactions were supplemented with various concentrations of DCPIP as indicated. Reactions progress was determined after 20 min. NE: no enzyme

acceptors. The artificial electron acceptors P-benzoquinone and DCPIP (2,6-dichlorophenolindophenol) were able to partially rescue LpxQ activity under anaerobic conditions. The assay shown in Fig. 31 was performed in an anaerobic environment in the presence of various concentrations of DCPIP. The results of this assay support the role of oxygen as the electron acceptor in the LpxQ reaction.

3.3.7 LpxQ produces H_2O_2 as a product of lipid A oxidation

The experiments with the artificial electron acceptors were consistent with LpxQ using oxygen as an electron acceptor. The expected product of the LpxQ reaction would therefore be H_2O_2. Attempts to detect H_2O_2 previously with crude membrane preparations were unsuccessful, presumably due to high levels of catalase associated with the enzyme source (Que-Gewirth et al., 2003a, Que-Gewirth et al., 2003b). When purified LpxQ was used as the enzyme source in *in vitro* reactions with 1-dephospho-Kdo_2-lipid-IV_A, H_2O_2 was detected (Fig. 32). The amount of H_2O_2 in *in vitro* reactions was determined at the end point of the LpxQ reaction with a fluorometric assay. In this assay, Amplex Red is added to the LpxQ reaction at the end point, and is oxidized by horseradish peroxidase in the presence of the H_2O_2 produced. As shown in Fig. 32, H_2O_2 was produced in stoichiometric amounts with the oxidized lipid A product. The reactions in Fig. 32 were set up with and without exogenously added H_2O_2. The exogenously added H_2O_2 did not inhibit LpxQ activity, and the H_2O_2 was not degraded.

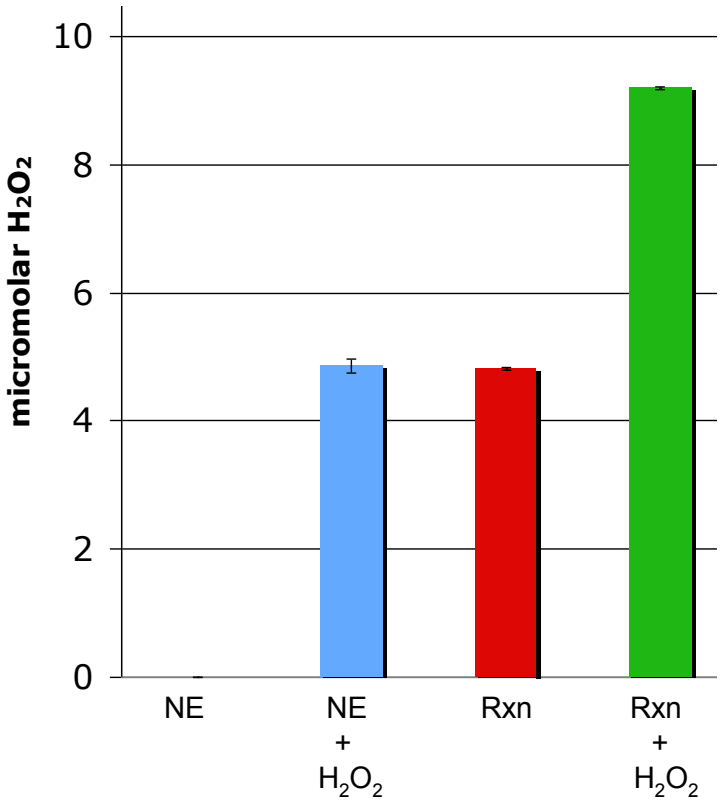

Figure 32: LpxQ produces H_2O_2 as a product of lipid A oxidation.

In vitro reactions were set up with 10 μM 1-dephospho Kdo_2-lipid-IVA. The reactions were carried out to completion and were diluted two-fold into a buffer containing 50 μM amplex red and 0.1 units/ml horseradish peroxidase. The reactions were incubated for 30 min and the fluorescence of each reaction was measured. Control reactions containing H_2O_2 (10 μM) were included as indicated. The amount of H_2O_2 detected is two-fold lower than of that present initially because of the 2-fold dilution involved in the assay. Fluorescence is only detected with the inclusion of exogenous H_2O_2 or from the production of H_2O_2. NE: no enzyme; NE: no enzyme + 10 μM H_2O_2; Rxn: reaction containing oxidized lipid A; Rxn + H_2O_2: reaction containing oxidized lipid A + 10 μM H_2O_2. The amount of H_2O_2 detected in each reaction was one-half of the starting amounts because of the dilution.

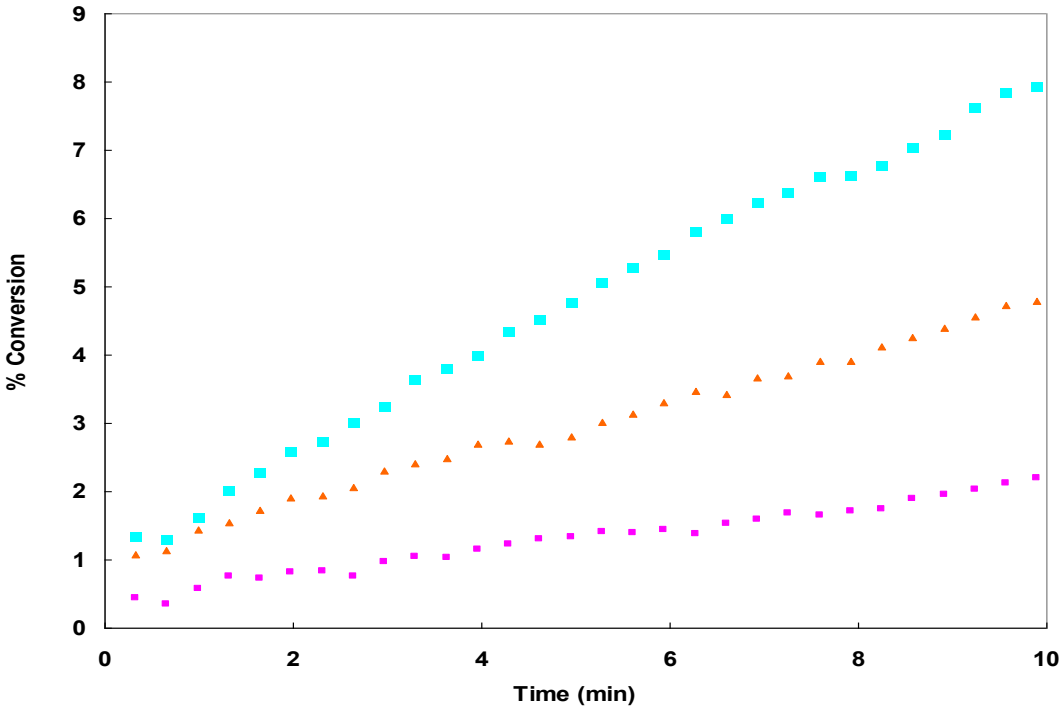

Figure 33: Continuous assay for monitoring lipid A oxidation.

The production of H_2O_2 was monitored continuously with the Amplex Red reagent. Data points were collected in 20 s intervals. The production of H_2O_2 is linear with time and protein concentration. 1-dephospho-Kdo_2-lipid IV_A was assayed at 2 μM with 0.036 μM LpxQ (purple), 0.072 μM LpxQ (orange), and 0.14 μM LpxQ (blue). The concentration of H_2O_2 produced was divided by the concentration of the lipid substrate initially present to determine the fraction of substrate converted to product (% conversion).

These results confirm the role of oxygen as an electron acceptor and show that that the purified enzyme is free of catalase activity.

The spectral properties of the oxidized Amplex Red reaction product, resorufin, were exploited in the development of a continuous assay. The rate of Amplex Red oxidation by HRP and H_2O_2 occurs on a rapid time scale compared to that of H_2O_2 production. Therefore, the rate of H_2O_2 depletion in the coupled assay should be comparable to the rate of lipid A oxidation. LpxQ reactions were set up under normal conditions with the addition of Amplex Red and horseradish peroxidase. The oxidation of 1-dephospho Kdo_2-lipid A was then monitored in real time as a function of H_2O_2 concentration (Fig. 33). The rates of H_2O_2 production were within 2-fold of the rates observed for oxidation of the lipid A substrate observed with the TLC based end-point assays. This discrepancy might be due to inaccuracy in measuring the concentration of the lipid substrate.

3.3.8 Oxygen in the oxidized lipid A product is derived from water

Assays performed in ^{18}O-enriched water demonstrate that the oxygen in the lipid A product of the LpxQ reaction are solvent-derived (Fig. 34). *In-vitro* reactions were prepared in ^{18}O-enriched water or under normal conditions and analyzed by LC/ESI/MS. As shown in panel A, the species corresponding to the 2-aminogluconate product

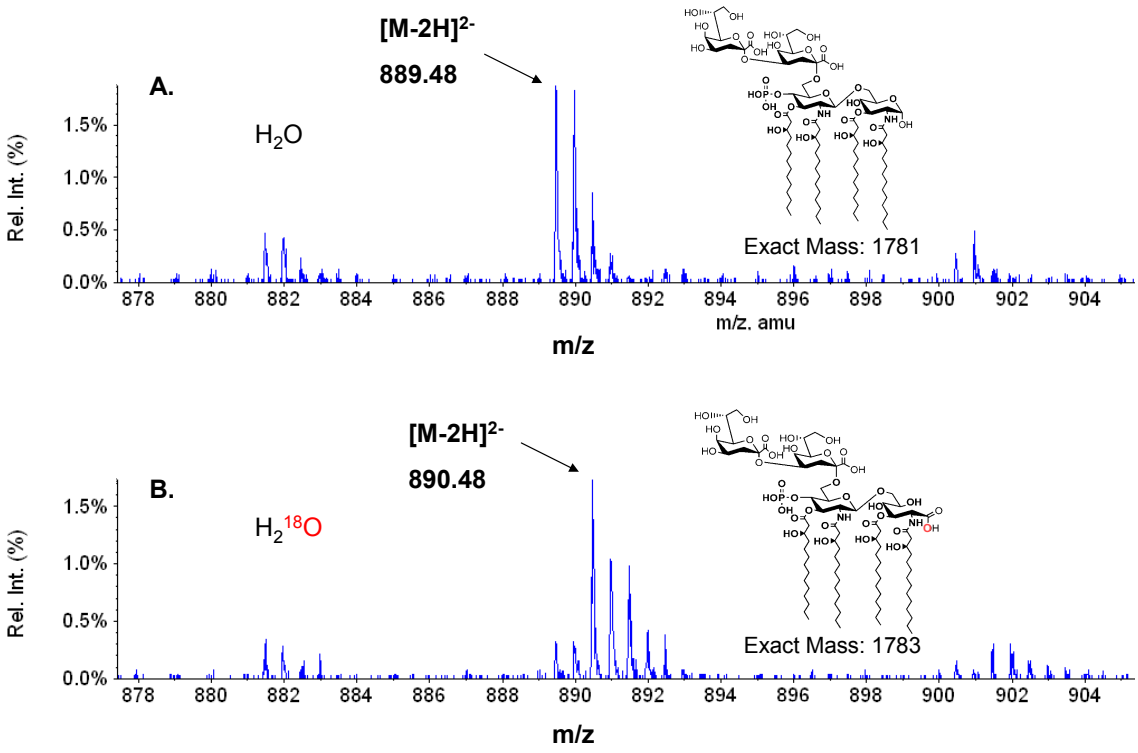

Figure 34: ESI-LC-mass spectrum of oxidized 1-dephospho-Kdo$_2$-lipid IV$_A$ produced *in vitro* in $H_2{}^{16}O$ or $H_2{}^{18}O$-enriched water.

An *in vitro* assay was carried out in $H_2{}^{16}O$ or $H_2{}^{18}O$-enriched water. The products of the two reactions were analyzed by LC/MS/MS. A). LpxQ converts 1-dephospho Kdo$_2$-lipid IV$_A$ to the oxidized derivative ([M-2H]$^{2-}$ at *m*/*z* 889.48). B) In the $H_2{}^{18}O$ water sample, the mass of the oxidized lipid A product ([M-2H]$^{2-}$ at *m*/*z* 890.48) is increased by two daltons.

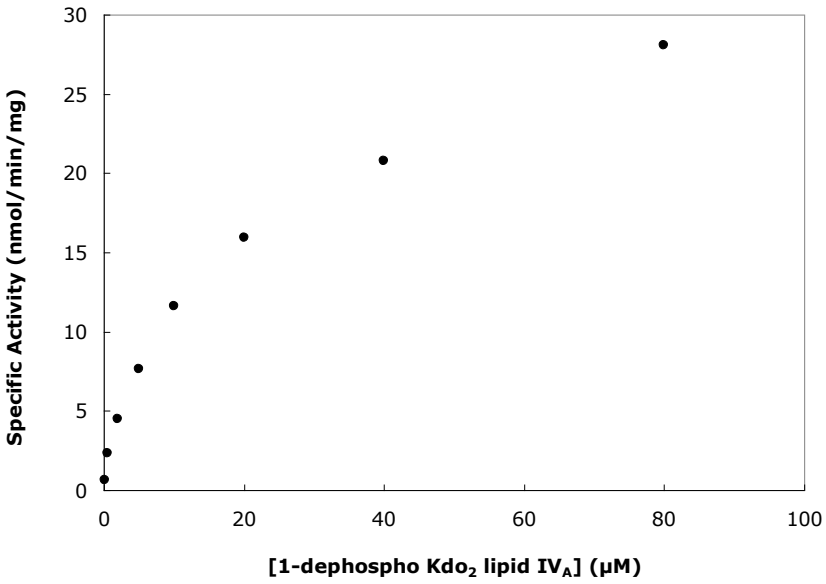

Figure 35: Apparent kinetic parameters of *R. leguminosarum* LpxQ

Purified *R. leguminosarum* LpxQ was assayed under standard conditions, except the concentration of 1-dephospho Kdo_2-lipid IV_A was varied, as indicated. Reaction mixtures were incubated for appropriate times, after which product formation was analyzed by thin layer chromatography and PhosphorImager analysis. The velocities were fit to a standard Michaelis-Menton function using Microsoft Excel. The apparent K_M for 1-dephospho Kdo_2-IV_A is 17.7 μM and the apparent V_{max} is approximately 32.31 nmol/min/mg.

formed in normal water appears as a doubly charged species ($[M-2H]^{2-}$ at m/z 889.48). The product formed in the ^{18}O-enriched water, panel B, also appears as a doubly charged species ($[M-2H]^{2-}$ at m/z 890.48). The difference is mass between the products is consistent with the oxygen in the product in the $H_2{}^{18}O$ reaction being derived from the solvent. These results confirm a role for water in the formation of the 2-aminogluconate moiety of the LpxQ product, but do not however, distinguish between the two routes of lipid A oxidation discussed in the introduction.

3.3.9 Kinetic properties of purified LpxQ and substrate specificity

The kinetic parameters of LpxQ were tested as described in the experimental methods section. The apparent K_M for 1-dephospho-Kdo_2-lipid-IV_A is 17.7 μM and the apparent V_{max} is 32 nmol/min/mg (Fig. 35).

The substrate specificity of LpxQ was investigated under standard assay conditions with 2 μM substrate using the continuous assay described above (Table 9). The Kdo units of lipid A substrates appear to be important for LpxQ activity. LpxQ displayed more than 10 times higher specific activity when assayed with 1-dephospho-Kdo_2-lipid IV_A and 1-dephospho Kdo_2-lipid A compared to 1-dephospho-lipid IV_A. This result is consistent with the localization of LpxQ, which interacts with lipid A in the late stages of lipid A assembly.

Table 9: Relative specific activities of LpxQ with different lipid A substrates.

Substrate	Specific Activity (nmol/min/mg)
1-dephospho Kdo_2-lipid IV_A	4.25
1-dephospho Kdo_2-lipid A	3.26
1-dephospho IV_A	0.30

Relative rates were determined under standard assay conditions with 2 μM substrate as described under *Experimental Procedures* using LpxQ generated after the Ni-NTA step.

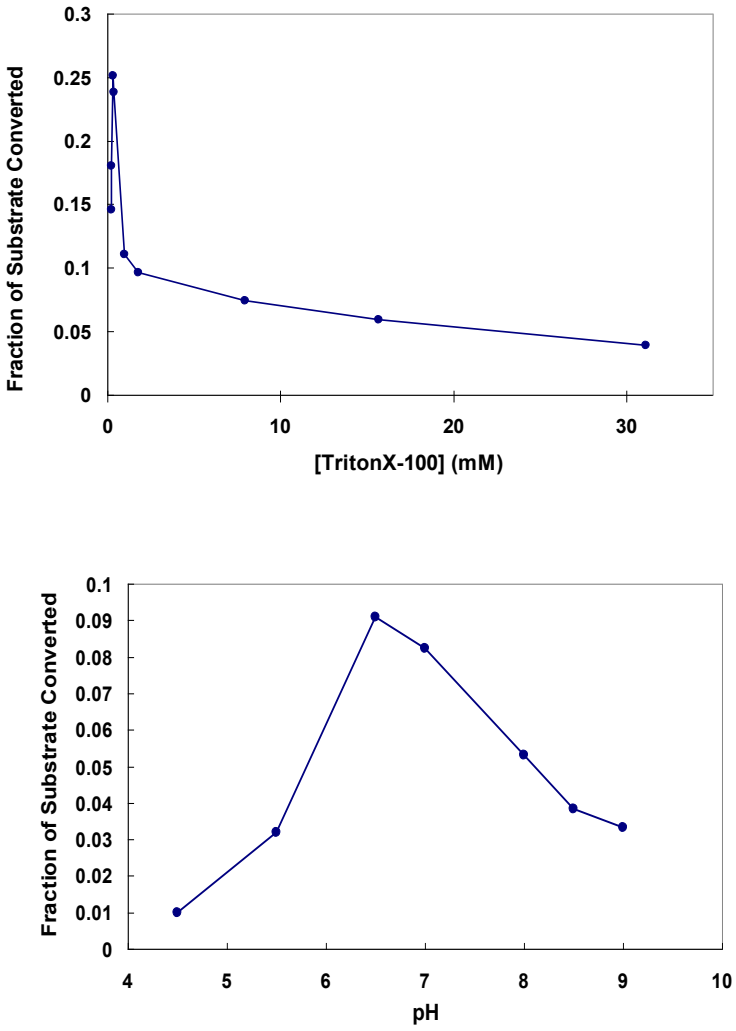

Figure 36: Detergent dependency and pH-rate profile of *R. leguminosarum* LpxQ.

A) The effects of varying Triton X-100 on LpxQ activity were determined. LpxQ was assayed for 10 min at 2 μM 1-dephospho Kdo_2-[4′-^{32}P]-lipid IV_A (1000 cpm/μL) in a total volume of 20 μL at each Triton X-100 concentration. The Triton X-100 concentration (estimated average molecular mass of 647) was varied from 0.23 mM to 31.1 mM, and the fraction of substrate conversion to product was determined. The data points are connected for ease of visualization only. B) *R. leguminosarum* LpxQ was assayed over the indicated pH range under optimized assay conditions with a triple buffer system consisting of 100 mM sodium acetate, 50 mM bis(2-hydroxyethyl)iminotris-(hydroxymethyl) hexane, and 50 mM Tris.

3.3.10 Effects of Triton X-100 and pH on LpxQ activity

The dependency of LpxQ on detergent was investigated. A detergent is necessary in the assay to generate mixed micelles to disperse the substrate. Purified LpxQ was assayed under standard conditions at varying concentrations of Triton X-100 (Fig. 36, panel A). The addition of Triton X-100 in small amounts stimulated activity; however the activity declined as the concentration of detergent increased. The detergent DDM did not substitute for Triton X-100 in the assay (data not shown).

The pH dependency of the LpxQ reaction was measured in a uniform triple buffer system as described in the experimental methods section (Fig 36, panel B). The triple buffer system allowed for a buffer-independent comparison of LpxQ activity in the pH range of 4.5-9. LpxQ activity was optimal near a pH of 6.5.

3.3.11 Metal dependence of LpxQ

LpxQ activity from *R. Leguminosarum* membranes was previously found to be inhibited by the presence of mM amounts of EDTA. The EDTA inhibited reaction, however, could be rescued with the addition of excess Mg^{2+}, Co^{2+}, Ni^{2+}, and Mn^{2+} (Que-Gewirth et al., 2003b). The purified enzyme was also inhibited by EDTA (Fig. 37A). The EDTA-inhibited reaction could be rescued as demonstrated before (data not shown). Other metal chelators such as 2,2′-bipyridyl and o-phenanthroline were tested, but no significant inhibition of LpxQ activity was observed. The purified protein was also

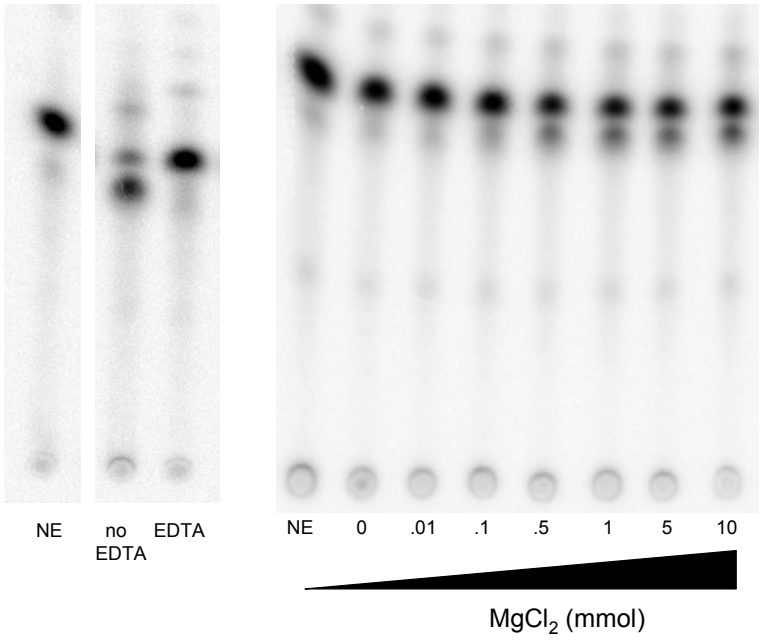

Figure 37: LpxQ is dependent on a divalent cation for activity.

LpxQ activity was measured with 10 μM Kdo_2-lipid IV_A in the absence or presence of the indicated concentrations of $MgCl_2$. Reaction mixtures at 30 °C contained 10 μM 1-dephospho-Kdo_2-[4′^{32}P]lipid IV_A (1000 cpm/μl) 50 mM MES, pH 6.5, 0.05% Triton X-100, enzyme, and $MgCl_2$ at the indicated concentrations in a final volume of 20 μL. Three μL aliquots from each reaction mixture were spotted onto a silica gel 60 plate and developed in chloroform/methanol/water/acetic acid (25:15:4:4, v/v).

Table 10: Inductively coupled plasma-optical emission spectroscopy (ICP-OES) analysis of LpxQ

Metal	Cd	Co	Cu	Fe	Mg	Mn	Ni	Zn
Average concentration of metal (μM)	0.002	0.002	0.367	0.470	.024	0.031	0.474	4.058
Standard Deviation	0.001	0.001	0.006	0.009	0.034	0.0007	0.028	0.0517
Metal to protein ratio	0.001	0.001	0.187	0.230	0.012	0.015	0.275	2.029

stimulated with the addition of $MgCl_2$. The assay in panel B of Fig. 37 shows that LpxQ activity is greatly enhanced with increasing concentrations of the metal. The optimal activity of LpxQ was observed at a $MgCl_2$ concentration of 1 mM. This concentration was maintained in the normal assay conditions. The inclusion of 1 mM $CuCl_2$ was found to be inhibitory (data not shown).

The metal content of purified LpxQ was analyzed by inductively coupled plasma-optical emission spectroscopy (ICP-OES) as described in the experimental methods section. The purified protein co-purified with 2 equivalent zinc ions per monomer of protein (Table 10). In a second experiment, the protein co-purified with 1 equivalent of zinc and 1 equivalent of nickel per monomer of protein (data not shown).

3.3.12 Absorbance properties of purified LpxQ

The UV-Visible spectrum of LpxQ is shown in Fig. 38. The purified protein was yellow. The color corresponded to a peak in the visible spectrum at ~ 440 nm. An additional peak was present at ~ 330 nm. These peaks were present in a ratio of 1:20 and 1:10 with the peak at 280 nm corresponding to the aromatic residues of the protein. The chromophore observed was seen consistently in several preparations. The chromophore was tightly associated with protein and was not liberated in the presence of strong denaturants. The yellow color precipitated with the protein when the protein was precipitated by acetone or TCA precipitation (data not shown).

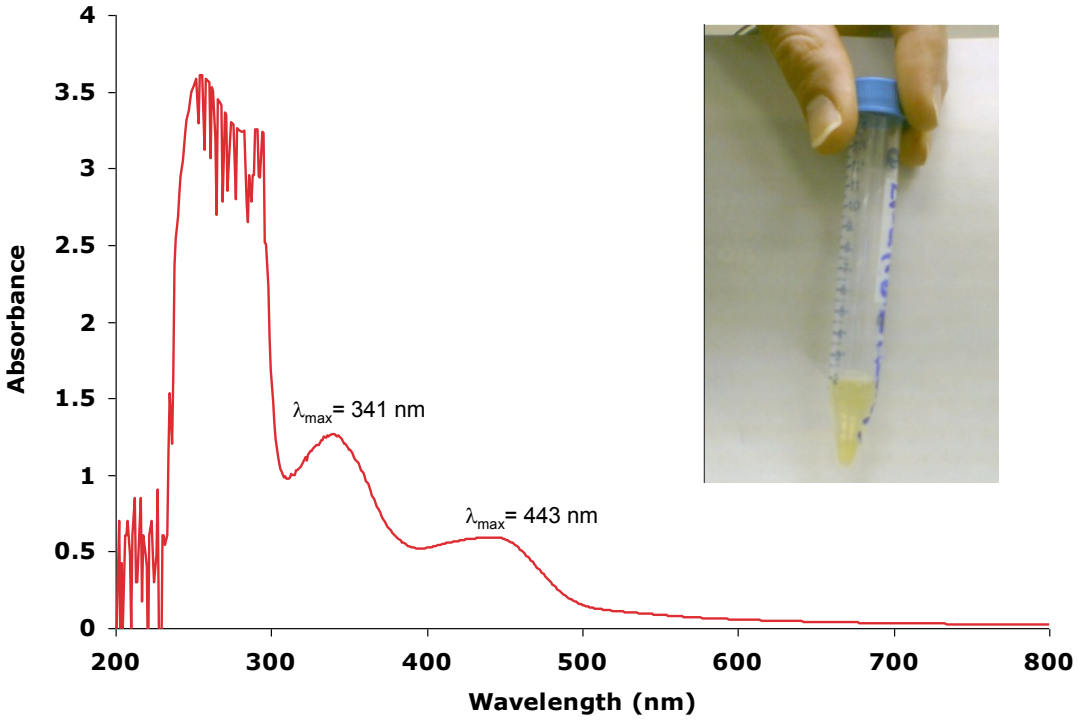

Figure 38: UV-vis scan of purified LpxQ.

Purified LpxQ at 9 mg/ml was scanned from 200 – 800 nm. Absorbance peaks were detected at 280 nm, 340 nm, and 443 nm.

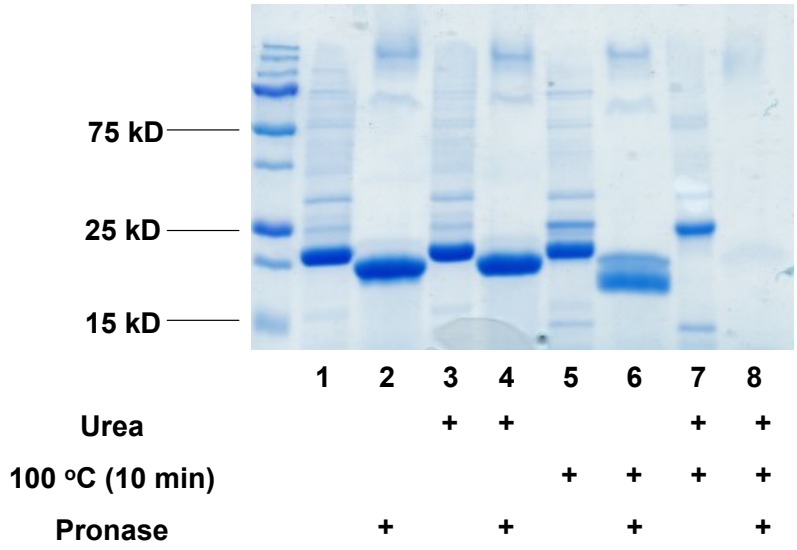

Figure 39: Purified LpxQ is resistant to proteolysis

The stability of LpxQ was assessed with the protease, pronase. Only samples boiled in a strong denaturant can be proteolyzed. Lane 1) LpxQ, 2) LpxQ treated with pronase, 3) LpxQ in 4 M urea, 4) LpxQ in 4 M urea treated with pronase, 5) LpxQ sample boiled in 2 % SDS. 6) LpxQ sample boiled in 2 % SDS and treated with pronase, 7) LpxQ sample boiled in 2 % SDS and 4 M urea, 8) LpxQ sample boiled in 2 % SDS and 4 M urea and treated with pronase.

3.3.13 Stability of LpxQ

Like many other outer membrane proteins, LpxQ displays remarkable stability. The protein is resistant to pronase (Fig. 39). The addition of pronase to purified LpxQ results in proteolytic degradation of minor contaminants present in the preparation, but not LpxQ. The pronase treated LpxQ band migrated faster during SDS-PAGE due to cleavage of the His_{10} tag. Cleavage of the tag was confirmed by western blotting (data not shown). Similar results were obtained when pronase was added in the presence of urea. When LpxQ was boiled in the presence of 2% SDS prior to electrophoresis, a small fraction of the protein band shifted to a higher position on the gel. Treatment of the boiled protein with pronase still resulted in inefficient proteolysis. When the protein was boiled in 2% SDS and urea, the protein band shifted completely to the higher migrating form. The change in migration behavior of boiled LpxQ is consistent with the behavior of other outer membrane proteins with heat treatment (Schnaitman, 1973). Under these conditions, the protein was found to be sensitive to pronase.

3.4 Discussion

LpxQ, the lipid A oxidase, is responsible for oxidizing the proximal glucosamine residue of lipid A to an aminogluconate moiety (Fig 24). LpxQ activity has been confirmed in the endosymbionts *R. leguminosarum* and *R. etli.* Homologues of *lpxQ* are found in several sequenced strains of *Rhizobium* and an orthologue of the gene is present

in the plant pathogen *A. tumefaciens.* Several homologues of *lpxQ* are also found in diverse marine bacteria including: *Oceanicola granulosus, Loktanella vestfoldensis,* and *Sagittula stellata.* The LpxQ primary sequence is distantly related to OmpW, an eight stranded β-barrel protein of unknown function. LpxQ is also predicted to have eight transmembrane stands and most likely adopts the β-barrel structural conformation that is common to most Gram-negative outer membrane proteins.

The structural gene for LpxQ was previously cloned into *E. coli*, and its *in vitro* activity was characterized. The enzyme was shown to be dependent on molecular oxygen and inhibited by EDTA. The role of oxygen and EDTA remained to be elucidated, and there were several unresolved questions concerning the mechanism of LpxQ.

In this chapter, a strategy is described for the purification of poly-histidine tagged LpxQ. A major hurdle to the recombinant expression of LpxQ was the toxicity associated with its expression. The majority of overexpressed protein in strains expressing the LpxQ plasmids was present as inactive material that remained insoluble upon treatment with detergent. The majority of LpxQ activity, however, was solubilized in Triton X-100 and purified to near homogeneity by Ni-NTA affinity chromatography. The purification procedure described here resulted in a ~ 25-fold increase in specific activity. The activity level of LpxQ at various stages of the purification procedure was

assessed with 1-dephospho-Kdo_2-lipid IV_A, a substrate that was not available previously. The TLC-based end point assays demonstrated here with 1-dephospho-Kdo_2-lipid IV_A was an improvement over previous TLC-based assays performed with ^{14}C labeled substrates or 1-dephospho-[4′^{32}P]-lipid IV_A. The separation of the substrates and products in the newly developed assay, however, could be improved further. The purified enzyme was shown to have a preference for substrates containing the Kdo moieties (Table 9), consistent with the enzyme's localization and proposed role in the late stages of lipid A modification (Raetz et al., 2007).

Purified LpxQ was heterogeneous and contained two major covalent modifications. Some of the heterogeneity observed in the purified protein came from mis-cleavage of the LpxQ signal sequence responsible for translocation of the protein. The signal sequence was found to be cleaved between Ala^{27} and Glu^{28} or between Ala^{25} and Ser^{26}. This component of the heterogeneity of the protein could be eliminated by replacing the signal sequence with alternate signal sequences such as that from the *E. coli* outer membrane protein, OmpA (data not shown). Additional heterogeneity was observed in the LpxQ preparation due to an unknown modification. This modification resulted in an increase in mass of ~ 54 Da. The site of the modification at F114 was found by peptide mapping. Mutation of the residue to an alanine reduced the heterogeneity of the protein. The F114A mutation, however, had little effect on LpxQ activity.

The mass-spectrometry based analyses of detergent-solubilized proteins such as LpxQ are significantly hindered by detergents. The spectrum observed in Fig. 27 represents only a small fraction of the total protein signal that is not suppressed by detergent. The available surface-exposed charges in a β-barrel protein like LpxQ are also limited. Various procedures were attempted to remove detergent before the analysis. These procedures involved precipitating the protein and reconstituting it in strong denaturants or acids. The efforts were met with limited success, and the overall analysis did not change. A complicating factor in these approaches was the formation of various adducts with the protein. It is possible that small populations of the protein exist and were not detected.

The oligomerization state of purified LpxQ was probed by size-exclusion chromatography (Fig. 28). When chromatographed in the presence of the detergent, DDM, LpxQ elutes at a size consistent with a monomer in large micelle or perhaps as a dimer in a minimal amount of detergent. The oligomerization state of LpxQ was also probed by chemical cross-linking. A small percentage of LpxQ migrated as a dimer in SDS-PAGE when cross-linked with gluteraldehyde (Fig. 29). The oligomerization state of LpxQ could affect the activity of the enzyme. The oligomerization state of other outer membrane enzymes such as Phospholipase A2 have been shown to be important in regulating activity (Brunie *et al.*, 1985, Jabeen *et al.*, 2005).

The role of oxygen as a co-substrate in the LpxQ reaction was confirmed with the purified protein. LpxQ activity could be reconstituted under anaerobic conditions when artificial electron acceptors were present; thus oxygen's primary role in the reaction was confirmed to be that of an electron acceptor. LpxQ was shown to produce H_2O_2 in stoichiometric amounts with the oxidized lipid A product. The oxygen in the aminogluconate moiety of the lipid A product was also shown to be solvent-derived.

The utilization of oxygen as an electron acceptor facilitated the development of other assays to monitor LpxQ activity. A continuous assay was developed to monitor H_2O_2 as a product of lipid A oxidation over time. The rates of H_2O_2 formation were found to be within 2-fold to that of lipid A oxidation rates determined with the TLC-based end point assays. The continuous assay will be of great value in the future kinetic analysis of LpxQ. A similar continuous assay could be developed under anaerobic conditions with the artificial electron acceptor DCPIP, which has different spectral properties upon reduction.

The kinetic parameters of purified LpxQ were determined primarily with the TLC-based end point assay. Like many other integral membrane enzymes, LpxQ displayed surface dilution kinetics (Fig. 36. panel A). The enzyme was also found to be optimally active in a pH range that agrees with what was previously reported (Fig. 36, panel A) (Que-Gewirth et al., 2003b).

Purified LpxQ contained a chromophore that was detected by UV-visible spectroscopy. The chromophore remained tightly associated with the protein and could not be liberated with strong denaturants or heat treatment. The function or origin of the chromophore remains uncertain. It is possible that the chromophore results from a post-translational modification of the protein. The relationship between the chromophore and the covalent modifications observed by mass spectroscopy has not been established. The chromophore observed could be involved in the transfer of electrons from the lipid A substrate to oxygen. However, at this time, no experimental evidence links the chromophore to LpxQ activity. Attempts to reduce the chromophore with strong reductants and or substrate were not successful (data not shown).

At this time, the method of electron transfer from lipid A substrates to oxygen is not understood. No organic cofactors were found to co-purifiy with LpxQ. The protein was heterogeneous when analyzed by mass spectroscopy (Fig. 27), but the mass shifts observed were too small to account for any large cofactors. An amino acid analysis of the purified protein agreed with expected results (data not shown). The protein did co-purify with divalent cations (Zn and Ni) (Table 10), but the role of these metals is unclear. These divalent cations would not participate directly in electron transfer, but they may play a role in substrate binding or maintenance of tertiary structure. The

purified enzyme was stimulated by the presence of $MgCl_2$ (Fig. 37). The role of this metal in the oxidation of lipid A is also uncertain.

A complicating factor affecting the analysis of purified LpxQ is its remarkable stability. The purified protein resisted degradation in solution when incubated with various proteases (thrombin, pronase, proteinase K, and trypsin). Treatment with the protease, pronase, resulted in cleavage of only the His_{10} tag. The protein became susceptible to proteolytic cleavage only when boiled in the presence of urea. The resulting shift of the protein in SDS-PAGE and protease-sensitivity upon this treatment is consistent with the behavior of other outer membrane proteins (Schnaitman, 1973). The band corresponding to LpxQ boiled in the presence of urea migrates more slowly during SDS-PAGE than untreated LpxQ (Fig. 39). The migration behavior of the heat denatured band in Fig. 39 resembles that of the insoluble protein accumulating in membranes overexpressing LpxQ (Figs. 25), suggesting that the majority of overexpressed enzyme is incorrectly folded.

The purification procedure described here and the development of new assays for LpxQ activity should facilitate future structural and mechanistic studies of LpxQ. Most remaining questions concern the route of electron transfer in the LpxQ-catalyzed reaction. It is conceivable that oxygen could act directly with the lipid A substrate, and the enzyme to reduce oxygen to H_2O_2. In chapter 4, evidence is presented that suggests

LpxQ acts independently of an electron-transferring cofactor. Structural studies will be necessary to elucidate the existence and role of any associated cofactors or novel catalytic sites. As described above, LpxQ displays remarkable stability and should be amendable to X-ray crystallography or NMR studies.

Chapter 4: Isolation and Refolding of Active *Rhizobium leguminosarum* LpxQ from Inclusion Bodies

4.1 Introduction

LpxQ, the lipid A oxidase from *R. leguminosarum* and *R. etli*, is an outer membrane enzyme that oxidizes the proximal glucosamine unit of lipid A that has been dephosphorylated at the 1-position. The enzyme utilizes oxygen as a cosubstrate and generates H_2O_2. A purification procedure for a C-terminally His_{10}-tagged version of LpxQ was described in chapter 3. The purified protein exhibited two physical properties that are common among outer membrane proteins from Gram-negative bacteria: significant stability and heat modifiability. These properties arise from the β-barrel structural conformation that these proteins adopt.

The β-barrel proteins are cylindrical-shaped proteins composed of transmembrane β-strands. The β-strands are arranged in an anti-parallel fashion and are stabilized by hydrogen bonding. The first transmembrane strand is hydrogen bonded to the last forming the closed barrel arrangement. The hydrophobic residues of these proteins are usually oriented toward the outside surface of the barrel and face the lipid bilayer, whereas the hydrophilic residues typically face the interior. The strands that connect consecutive ß-strands on the extracellular surface are known as loops, and the strands that make these connections on the periplasmic side are known as turns. The β-

barrel protein fold is found in the outer membrane proteins of chloroplasts, mitochondria, and Gram-negative bacteria.

Outer membrane proteins are targeted to the outer membrane via a signal peptide. The signal peptide is required for translocation across the inner membrane and is cleaved by a signal peptidase in the periplasm. The mechanism of how the proteins are folded *in vivo* after this cleavage event is not well understood, but the process is thought to involve chaperones and other protein folding partners. If the outer membrane proteins are expressed recombinantly without their signal sequence, they accumulate as insoluble aggregates in the cytosolic compartment of cells. The insoluble inclusion bodies accumulate in large quantity and are easy to purify. The successful refolding of native functional proteins from inclusion bodies has been demonstrated for many outer membrane proteins, including the enzymes PagP, PagL and LpxR of the lipid A system.

Several methods have been described for the proper refolding of outer membrane proteins (Fig. 40). These procedures usually involve solubilizing the inclusion body proteins in a strong denaturant such as urea or guanidinium hydrochloride. The denaturant is then removed by dilution or dialysis into a solvent containing detergents, phospholipids, or other synthetic membrane components. Alternatively, the denaturant can be removed by immobilizing the denatured protein on a column. The protein can

then be refolded by passage of refolding buffers. The composition of the refolding buffers in these procedures have significant effects on the refolding process; thus the optimal conditions for refolding must be determined empirically. Some variables of importance are the method of dilution, dialysis (single step vs. multi-step), time, temperature, and protein concentration. A refolding procedure is generally considered successful when ~ 30% of the unfolded protein is refolded into the native state.

The outer membrane lipid A modification enzymes PagP, PagL, and LpxR have all been refolded *in vitro*, and their 3-dimensional structures have been determined. PagP and PagL each have 8 transmembrane strands and LpxR has 12 transmembrane strands. Based on its amino acid sequence and size, LpxQ is predicted to have 8 transmembrane strands. A refolding procedure has not been described yet for LpxQ. In this chapter procedures are described for the successful refolding of LpxQ from inclusion bodies. LpxQ is shown to refold into an active form based on an SDS-PAGE migration assay and by a functional activity assay. The *in vitro* refolding procedure demonstrated here has implications regarding the mechanism and cofactor requirements of LpxQ.

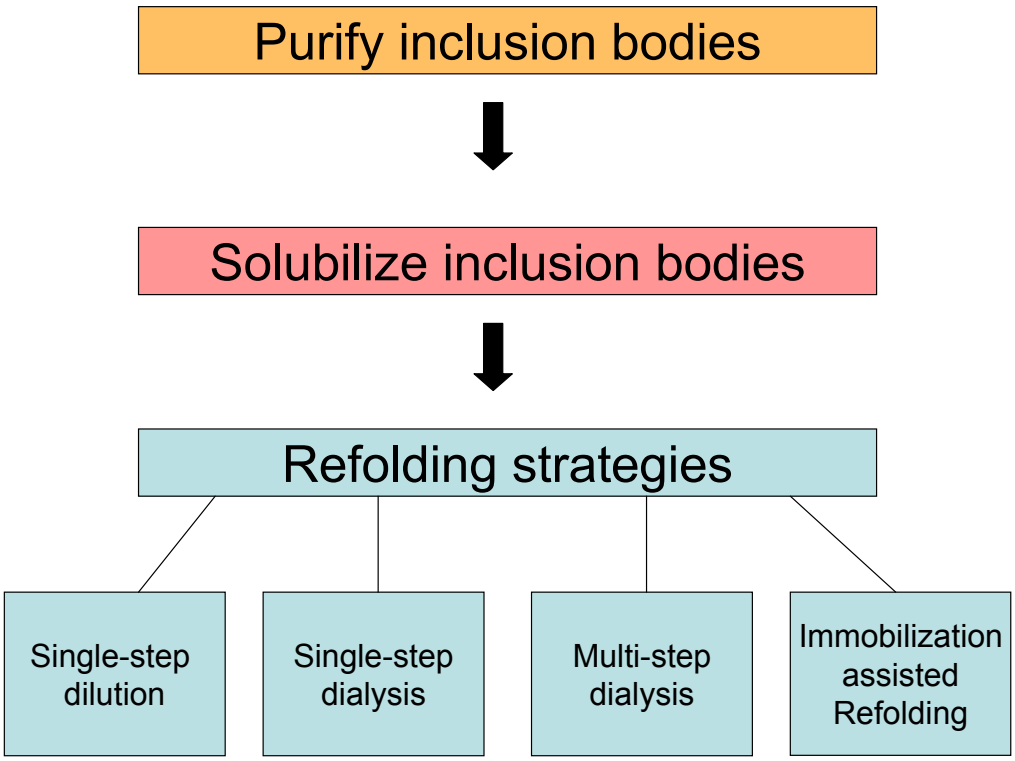

Figure 40: Protein refolding strategies.

Several strategies have been developed for refolding LpxQ. Inclusion bodies are isolated as aggregates and solubilized in strong denaturants such as guanidine hydrochloride or urea. The solubilized protein from the inclusion bodies can be refolded by decreasing the concentration of denaturant by dialysis, dilution, or by buffer exchange on a column.

4.2 Materials and Methods

4.2.1 Chemicals and materials

[γ-^{32}P]-ATP was obtained from PerkinElmer Life and Analytical Sciences, Inc. (Waltham, MA). Methanol was from Mallinckrodt Baker, Inc. (Phillipsburg, NJ). Chloroform and silica gel 60 (0.25 mm) thin-layer chromatography (TLC) plates were obtained from EMD chemicals, Inc. (Gibbstown, NJ). Yeast extract, agar, and tryptone were from Becton, Dickinson, and Co. (Frankln Lakes, NJ). Sodium chloride, and 4-(2-hydroxyethyl)-1-piperazineethanesulfonic acid (HEPES) wee from VWR International (West Chester, PA). Bicinchoninic (BCA) protein assay reagents and Triton X-100 were from Thermo Fisher Scientific (Waltham, MA). PCR reagents were purchased from EMD and Stratagene (La Jolla, CA). IPTG was obtained from Invitrogen (Carlsbad, CA). All other chemicals were reagent grade and were purchased from either Sigma-Aldrich (St. Louis, MO) or VWR International (West Chester, PA).

4.2.2 Bacterial strains and growth conditions

The bacterial strains and plasmids used and their relevant characteristics are shown in Table 11. *E. coli* strains were grown at 37 °C in LB broth (1% tryptone, 0.5% yeast extract, and 1% sodium chloride) and supplemented with ampicillin (100 μg/mL) as appropriate.

4.2.3 General recombinant DNA techniques

Protocols for handling DNA and preparing *E. coli* for electroporation were performed using standard protocols (Sambrook & Russell, 2001). Transformation-competent cells of *E. coli* were prepared by the method of Inoue et al (Inoue et al., 1990). Plasmids were isolated from cell cultures using the Qiagen Spin Miniprep kit, and DNA fragments were isolated with the Qiaquick Spin Kits (Valencia, CA). Pfu Turbo DNA polymerase (Stratagene, La Jolla, CA)), T4 DNA ligase (Invitrogen Corp, Carlsbad, CA), restriction endonucleases (New England Biolabs, Ipswich, MA) and shrimp alkaline phosphatase from Affymetrix (Santa Clara, CA) were used according to the manufacturers' instructions. Double stranded DNA sequencing was performed with an ABI Prism 377 instrument at the Duke University DNA Analysis Facility. Primers were purchased from IDT Biosciences (Coralville, IA).

4.2.4 Construction of plasmid pLpxQIB-his$_{10}$

The first 28 amino acids of LpxQ, which normally encode a signal sequence for the export of LpxQ to the outer membrane, were deleted and replaced with a single methionine residue in a site-directed mutagenesis reaction. The deletion procedure was carried out by PCR as recommended by Stratagene. Plasmid pLpxQ-his$_{10}$ was used as the template DNA. The primers LpxQIBfor (5′-CTTTAAGAAGGAGATATACAT**ATGGAAGACCTGCAATTCTCCATCT**-3′) and LpxQIBrev (5′-AGATGGAGAATTGCA

GGTCTTCCATATGTATATCTCCTTCTTAAAG-3′) were used to generate plasmid pLpxQIB-his$_{10}$. The sequence in bold type in the primer LpxQIBfor corresponds to the *N*-terminal coding region of LpxQ. The plasmid pLpxQIB-his$_{10}$ was first transformed into competent *E. coli* XL-1 Blue cells, and its sequence was confirmed by DNA sequencing. The plasmid was then transformed into electrocompetent C41(DE3) cells.

4.2.5 Isolation and purification of LpxQ inclusion bodies

A single colony of C41(DE3)/pLpxQIB-his$_{10}$ was inoculated into 5 mL of LB medium, supplemented with ampicillin (100 μg/mL), and grown in a rotary shaker overnight at 37 °C. This culture was used to inoculate 1 L of fresh LB broth containing ampicillin (100 μg/mL). The culture was inoculated at an A_{600} of 0.01 and grown with shaking at 225 rpm at 37 °C. When the A_{600} reached 0.5, the cells were induced with 1 mM isopropyl β-D-thiogalactopyranoside (IPTG) and grown for 3 additional h. The cells were then harvested at 4 °C by centrifugation at 4000 x *g* for 20 min. The cell pellet was then washed with 40 mL of 50 mM HEPES, pH 7.5 and stored at -80 °C.

The frozen cell pellet was thawed and resuspended in 25 ml of 50 mM HEPES, pH 7.5. The resuspended cells were lysed by passage through a chilled French pressure cell at 18,000 p.s.i. The cellular debris, unbroken cells, and inclusion bodies were collected by centrifugation at 9000 x *g* for 20 min. The precipitated material was homogenized in 25 mL of 50 mM HEPES, pH 7.5, containing 1 mM EDTA and 2% Triton

X-100, and incubated at room temperature for 1 h with intermittent inversion on a rotating apparatus. The homogenized suspension was then centrifuged at 31000 x *g* for 15 min at 4 °C. The precipitate containing the inclusion bodies was then washed by homogenization in 25 mL of 50 mM HEPES, pH 7.5, containing 1 mM EDTA, and incubated at 4 °C for 1 hr. The suspension was then centrifuged at 31000 x *g* for 15 min at 4 °C. The precipitate was washed by homogenization in 25 mL of 2 M guanidine hydrochloride, 50 mM HEPES, pH 7.5, supplemented with 1 mM EDTA and 10% glycerol. After incubation with intermittent rotation for 1 h, the suspension was centrifuged at 31000 x g for 15 min at 4 °C. The precipitate was resuspended in 25 ml of 4 M guanidine hydrochloride, 50 mM HEPES, pH 7.5, containing 1 mM EDTA and 10 % (v/v) glycerol. After incubation for 1 h at 4 °C, the suspension was centrifuged at 31000 x g for 15 min. The supernatant from this step contained the purified and solubilized LpxQ inclusion bodies at a concentration of 5-10 mg/ml. The protein concentration of the inclusion bodies was determined by the bicinchoninic acid method, using bovine serum albumin as the standard (Smith et al., 1985).

4.2.6 Liquid chromatography – mass spectrometry (LC/MS) of the intact protein

Purified, solubilized LpxQ inclusion bodies were subjected to LC/MS in the positive mode as described in Chapter 3. The purified inclusion bodies were diluted to 1 mg/ml in 4 M guanidine hydrochloride prior to sample analysis.

4.2.7 Multiple-step dialysis refolding

The isolated inclusion bodies were refolding using a multi-step dialysis procedure. The isolated inclusion bodies were diluted to 1 mg/ml in a buffer consisting of 4 M guanidine hydrochloride, 50 mM HEPES, pH 7.5, 1 mM EDTA, 10 % glycerol, 1 mM $MgCl_2$, and 0.5% Triton. Two ml of the protein solution was dialyzed against 500 mL of a buffer consisting of 2 M guanidine hydrochloride, 1 mM $MgCl_2$, 0.5 % Triton X-100, 50 mM HEPES, pH 7.5, and 10 % (v/v) glycerol. This dialysis step and all subsequent steps were carried out at 4 ^{o}C in a Slide-a-Lyzer dialysis cassette with a 10 KDa molecular weight cutoff Thermo Fisher Scientific (Waltham, MA) After 1 h, the dialysis cassette was transferred to 500 mL of the same buffer containing 1 M guanidine hydrochloride. Dialysis was carried out for 1 h, and the dialysis cassette was transferred to 500 mL of the same buffer containing 0.5 M guanidine hydrochloride. After dialysis for 1 hour, the cassette was transferred to 500 mL of the same buffer lacking guanidine hydrochloride. The protein was dialyzed for 1 hour in this buffer. The dialysis buffer was changed and the protein was dialyzed for 1 additional hour. The dialysis buffer was changed twice more after 1 h and 4 h. The cassette was dialyzed in the final buffer for 16 h. The soluble material was collected by centrifugation at 4000 x *g* for 20 min. The refolding procedure described above was also performed at room temperature where noted.

4.2.8 SDS-PAGE analysis of LpxQ

Protein samples were visualized by SDS-PAGE as described in Chapter 3. Briefly, samples were diluted in a 4X stock solution consisting of 200 mM Tris, pH 6.8, 50 % glycerol, 12% SDS, 200 mM DTT, 0.02% bromophenol blue and incubated for 30 min at 40 ^{o}C prior to SDS-PAGE (Jagow & Schagger, 1994).

4.2.9 Preparation of substrates

Preparation of the radiolabeled substrate, 1-dephospho-Kdo_2-[4′-^{32}P]lipid IV_A, and the corresponding cold carrier substrate are described in Chapter 3.

4.2.10 In vitro radiochemical activity assay of LpxQ

LpxQ activity was assayed in 10-30 μL reaction mixtures at 30 ^{o}C. Standard assay conditions were as follows: the reaction mixtures contained 50 mM MES, pH 6.5, 0.1% Triton X-100, 1 mM MgCl, and 2 μM 1-dephospho-Kdo_2-[4′-^{32}P]lipid IV_A (1,000 cpm/nmol). Reactions were initiated with the enzyme source. The reaction mixtures were incubated for the times indicated. Reactions were terminated by spotting 3-μl samples onto a TLC plate, which was developed in the solvent chloroform/methanol/acetic acid/water (25:15:4:4; v/v). After drying and overnight exposure of the plate to a PhosphorImager screen (GE Healthcare), product formation was detected and quantified with a Storm 840 PhosphorImager equipped with ImageQuant software (GE Healthcare).

4.2.11 Protein folding by rapid dilution

Critical parameters for efficient protein refolding were investigated using the QuickFold Protein Refolding Kit (Athena Enzyme Systems). A rapid dilution strategy to refold the protein was developed using the identified parameters. Purified inclusion bodies were diluted to 1 mg/mL in 4 M guanidine hydrochloride, 50 mM HEPES, pH 7.5, 1 mM EDTA, and 10% glycerol. Fifty μL of each solution was then transferred to 950 μL of the refolding buffers supplied with the kit and immediately vortexed. The solutions were then incubated at room temperature for 1 h and then incubated at 4 °C for 16 h. The solutions were centrifuged at 10,000 x *g* for 10 min. The supernatant containing the refolded inclusion bodies was transferred to a new tube. Refolding was then assessed by SDS-PAGE electrophoresis and by activity assays.

4.2.12 Proteinase K digestion of refolded LpxQ inclusion bodies

Proteinase K (Sigma) was added to samples of refolded LpxQ inclusion bodies at a final concentration of 0.02 mg/mL. The reactions were incubated at 0 °C for 1 h. The samples were then analyzed by SDS-PAGE.

Table 11: Bacterial strains and plasmids used in chapter 4

Strain or Plasmid	Genotype or Description	Source or reference
Strains		
C41(DE3)	F *ompT hsds*$_B$ ($r_B^- m_B^-$)*gal dcm*(DE3) D(srl-recA)306::Tn*10*	(Miroux & Walker, 1996)
XL1-Blue	*recA1 endA1 gyrA95 thi-1 hsdR17 supE44 relA1 lac* [F′ proAB *lacIqZDM15 Tn*10 (Tet^R)]	Stratagene
Plasmids		
pET21a(+)	Expression vector containing a T7 promoter, Amp^R	Novagen
pLpxQ-his$_{10}$	pET21a(+) containing *lpxQ*	Chapter 3
pLpxQIB-his$_{10}$	pET21a(+) containing *lpxQ* without signal sequence	This work

Abbreviations: Amp: ampicillin

4.3 Results

4.3.1 Expression and Isolation of LpxQ Inclusion bodies

The purification procedure for LpxQ described in chapter 3 yielded protein with no detectable organic cofactor(s). To address the issue of whether a cofactor was required for LpxQ activity, an attempt was made to isolate and refold LpxQ from inactive inclusion bodies. The signal sequence of the His_{10}-tagged protein described in chapter 3 was replaced with a single methionine residue. Expression of the LpxQ inclusion bodies in strain C41(DE3) was considerably less toxic compared to that observed for the enzyme with its signal sequence. The milky, white inclusion bodies were collected in the insoluble fraction after lysing the cells. The LpxQ inclusion bodies made up ~ 90% of the insoluble material (Fig. 41, lane 2). The inclusion bodies were washed in a series of steps with 2% Triton X-100 and 2 M guanidine hydrochloride to remove contaminating proteins (Fig. 41, lanes 3-7). The washed inclusion bodies were solubilized with 4 M guanidine hydrochloride (Fig, 41, lane 8). Approximately 50 mg of the inclusion body LpxQ protein were produced per L of culture. There was no color associated with the solubilized inclusion bodies.

The mass of the purified LpxQ from the inclusion bodies was determined by LC/ESI/MS. As shown in Fig. 42, the LpxQ from the isolated inclusion bodies was

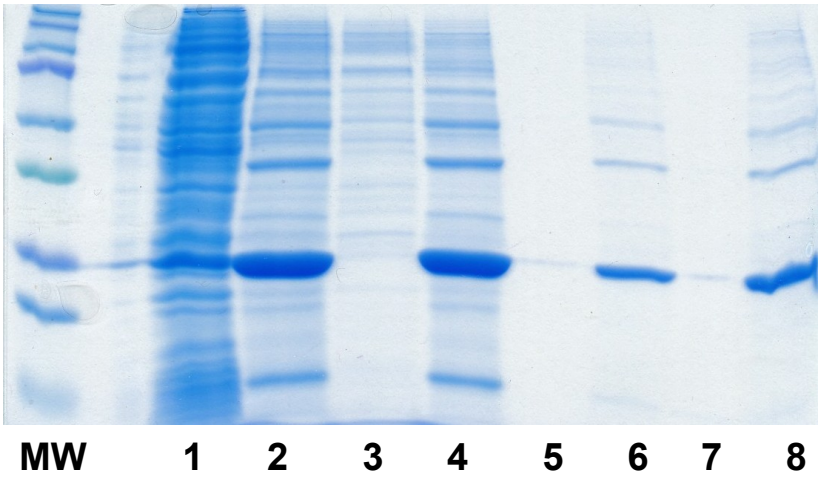

Figure 41: Isolation of LpxQ-containing inclusion bodies

LpxQ inclusion bodies were isolated from C41(DE3) cells expressing pLpxQIB-his10.Cells were resuspended in 50 mM Hepes, pH 7.5 and lysed by French press. The insoluble cell lysate was washed in a buffer containing 2.0% Triton X-100 and 1 mM EDTA. The insoluble inclusion bodies were then washed in a buffer lacking Triton X-100. The washed inclusion bodies were solubilized in 4 M guanidine HCl, 1 mM EDTA, 50 mM Hepes, pH 7.5,, and 10% glycerol. Lane 1) Soluble cell lysate; 2) Insoluble cell lysate; 3) 2.0% Triton X-100 wash (soluble portion); 4) 2.0% Triton X-100 wash (insoluble protion); 5 Detergent-free buffer wash (soluble portion); 6) detergent-free buffer wash (insoluble portion); 7) 2M guanidine HCl wash (soluble portion); 8) 4 M guanidine HCl wash (soluble protion)

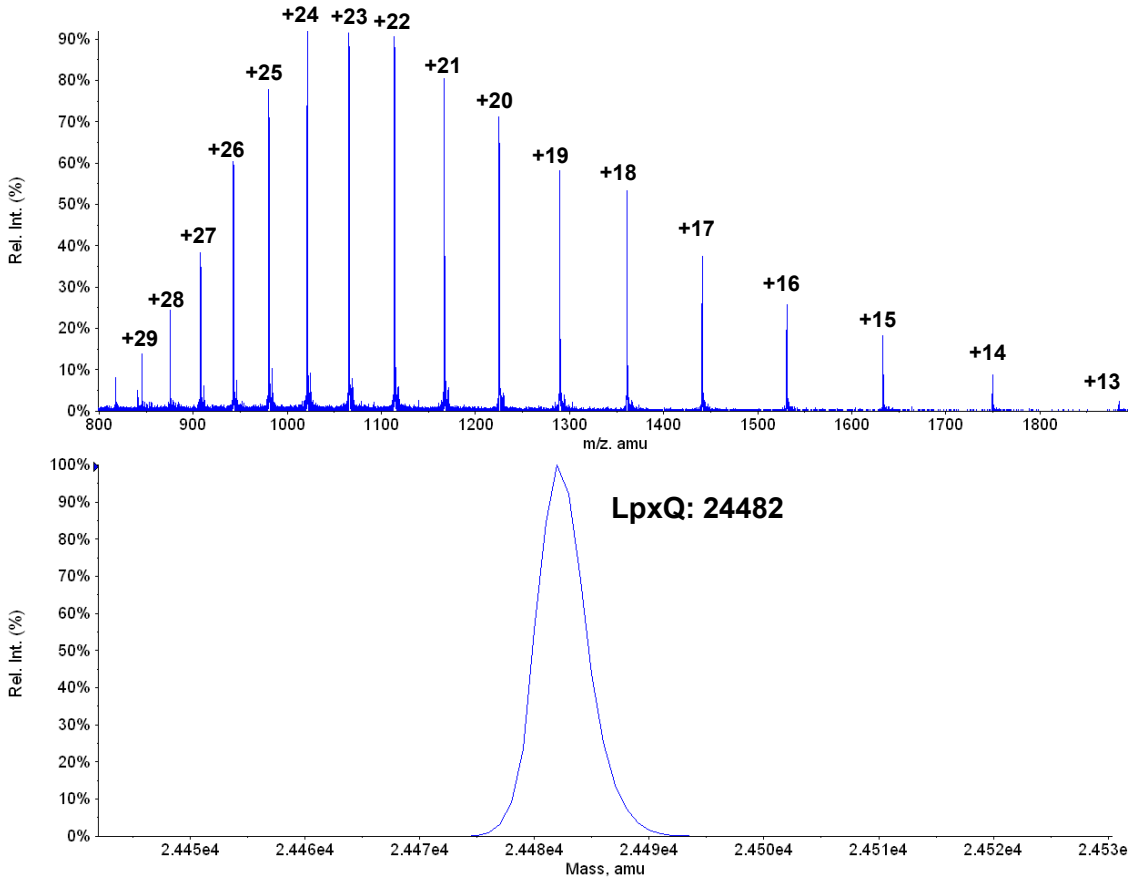

Figure 42: LC/ESI/MS of purified LpxQ inclusion bodies

Isolated LpxQ from inclusion bodies were subjected to LC/ESI/MS in the positive ion mode. A) LpxQ elutes between 17 and 20 min. The peaks for the *m*/*z* range of 800-1900 amu are shown, corresponding to various charge states (H^+) of LpxQ ranging from +13 to +28. B) The deconvoluted mass of unfolded LpxQ from inclusion bodies is 24482 Da, consistent with the predicted size of LpxQ inclusion bodies (24481.8 Da). The protein identification program parameters were limited to proteins in the molecular mass range of 12-30 kDa using the *m*/*z* range of 800-2000.

homogeneous. The purified LpxQ from the inclusion bodies ionized with high efficiency because the solubilization buffer lacked detergent.

4.3.2 LpxQ from inclusion bodies can be refolded

The purified LpxQ from inclusion bodies was refolded in a multi-step dialysis procedure. The refolding buffer solutions all contained 0.5% Triton X-100, which was necessary for refolding to occur. The refolding of LpxQ was monitored by SDS-PAGE electrophoresis. The unfolded LpxQ from the inclusion bodies (Fig. 43, lane 2) had a lower electrophoretic mobility than the purified, correctly folded protein (Fig. 43, lane 1). The migration behavior of the unfolded inclusion body LpxQ was similar to that observed with heat denatured LpxQ (as described in chapter 3). The protein recovered from the multi-step dialysis refolding procedure ran as a mixture of these two species (lane 3). In addition, an additional protein band appeared upon refolding. This band, marked by an asterisk in Fig. 43, corresponds to a dimer of LpxQ. These results show that LpxQ's migration behavior changes in SDS-PAGE upon refolding, consistent with the behavior of other outer membrane proteins that have been refolded *in vitro* (Schnaitman, 1973, Bishop et al., 2000, Kleinschmidt, 2003).

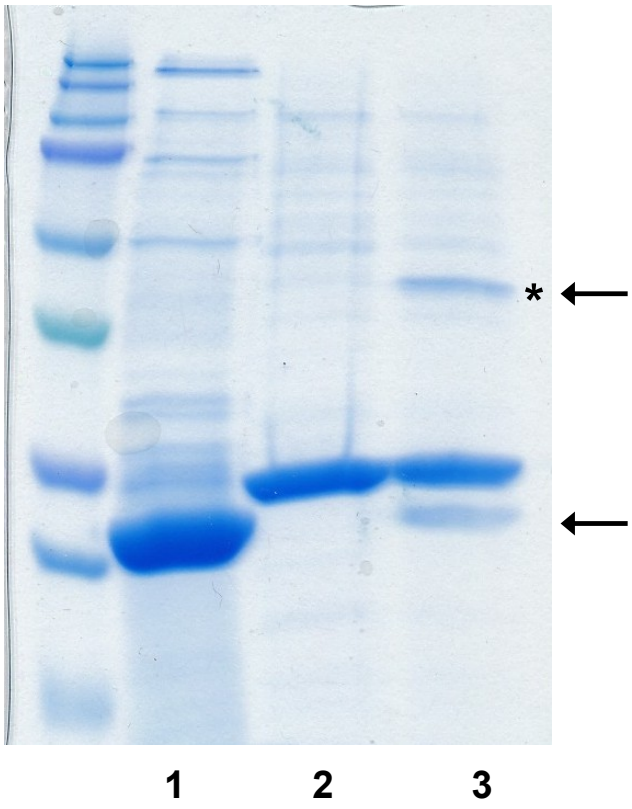

Figure 43: Gel shift assay for protein refolding.

This experiment is from multi-step dialysis procedure. Refolding of LpxQ is assessed by a change in electrophoretic mobility. Lane 1) purified LpxQ from C41(DE3)/pLpxQ-his$_{10}$. Lane 2) isolated LpxQ inclusion bodies. Lane 3) refolded LpxQ. The bands in lane 3 marked by an arrows indicate refolded LpxQ species. The asterisk corresponds to a dimer of LpxQ.

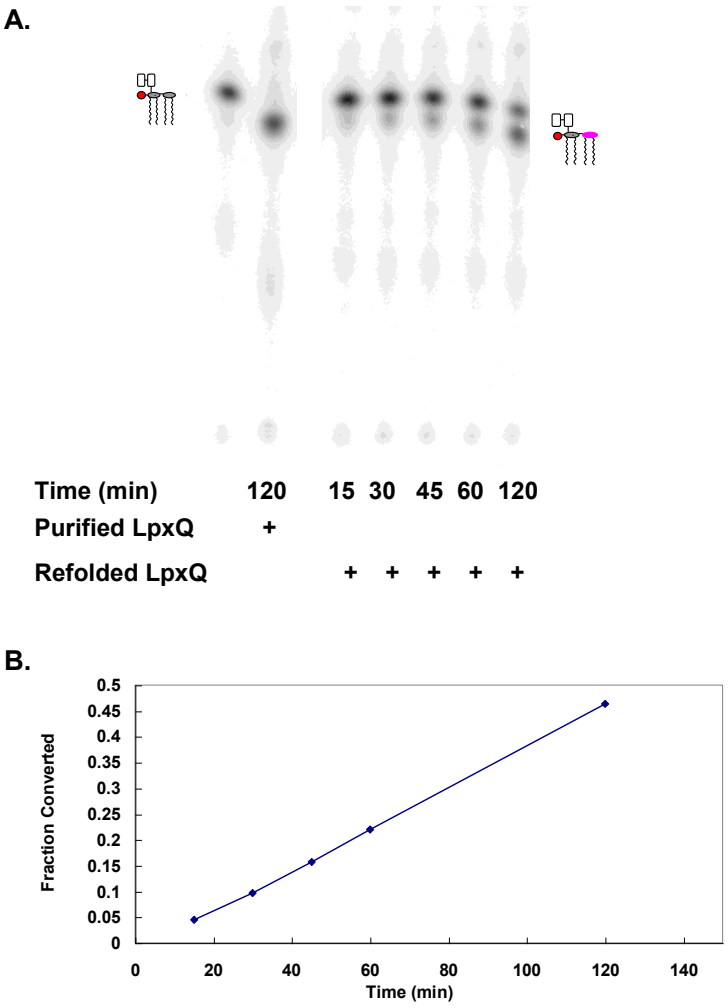

Figure 44: *In vitro* assay of refolded LpxQ isolated from inclusion bodies

Reaction mixtures at 30 °C contained 2 μM 1-dephospho-Kdo_2-lipid IV_A, (1000 cpm/μL), 1-dephospho-Kdo_2-[4′^{32}P]lipid IV_A, 50 mM MES, pH 6.5, 1 mM $MgCl_2$, 0.05% Triton X-100, and enzyme as indicated in a final volume of 50 μL. At the indicated times, 3 μL portions were withdrawn and spotted onto a silica gel 60 plate and developed in chloroform/methanol/water/acetic acid (25:15:4:4, v/v). **A.** Image of a time course with refolded LpxQ inclusion bodies at 2 μM. Purified LpxQ from C41(DE3)/pLpxQ-his_{10} was used as a positive control. B. Refolded LpxQ activity is linear with time.

4.3.3 Refolded LpxQ from inclusion bodies are catalytically active

Refolded LpxQ was assayed with the substrate 1-dephospho-Kdo_2-lipid IV_A (Fig. 44). The activity of the refolded protein was linear with time and protein concentration. The specific activity of the refolded material was 10-fold lower than that of the protein isolated from membranes (chapter 3). The difference in the activity of the two proteins could be related to the mixed population of correctly folded and misfolded proteins in the refolded LpxQ sample observed by SDS-PAGE (Fig. 43).

Activity was measured from each step of the multi-step dialysis procedure. As shown in Fig. 45, the solubilized inclusion bodies lacked activity prior to the refolding procedure. As the denaturant concentration was reduced in successive steps, LpxQ became active. There was no significant change in the activity once the denaturant was completely removed.

4.3.4 Influence of additives on LpxQ refolding

The optimal conditions for refolding the LpxQ from the inclusion bodies were explored using the QuickFold Protein Refolding Kit (Athena Enzyme Systems). This screen is based on the "rapid dilution" of unfolded inclusion bodies into buffers containing various components that assist with protein folding. The results of the screen are shown in Table 12. Refolding of LpxQ was assessed both by the gel electrophoresis

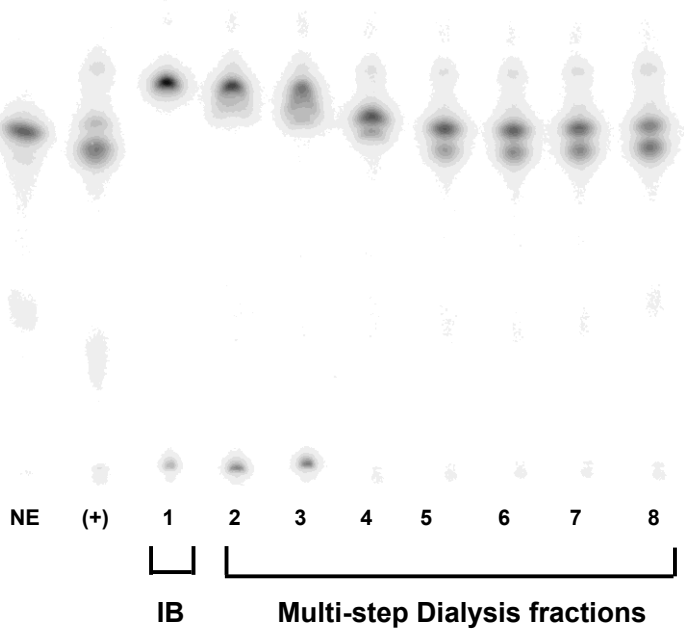

Figure 45: Activity analysis of fractions from the multi-step dialysis procedure.

Reaction mixtures at 30 °C contained 2 μM 1-dephospho-Kdo_2-lipid IV_A, 1000 cpm/μL 1-dephospho-Kdo_2-[4′^{32}P]lipid IV_A, 50 mM MES, pH 6.5, 1 mM $MgCl_2$, 0.05% triton X-100 in a final volume of 20 μL. The reactions were started with the addition of enzyme. After 1 h, 3 μL aliquots were spotted onto a silica gel 60 plate which was developed in chloroform/methanol/water/acetic acid (25:15:4:4, v/v). Purified LpxQ from C41(DE3)/pLpxQ-his_{10} was used as a positive control. The inclusion bodies were assayed prior to folding and at each step of the multi-step dialysis procedure. All reactions corresponding to the mult-step dialysis procedure are indicated. The enzyme source from each refolding step was diluted 10 fold into the assay. NE: no enzyme; (+): purifed LpxQ from C41(DE3)/pLpxQ-his_{10}; 1: unfolded LpxQ inclusion bodies; 2: dialysate from 2 M guanidine hydrochloride dialysis step; 3: dialysate from 1 M guanidine hydrochloride dialysis step; 4: dialysate from 0.5 M guanidine hydrochloride dialysis step; 5: dialysate from 0 M guanidine dialysis step a; 6: dialysate from 0 M guanidine hydrochloride step b; 7 dialysate from 0 M guanidine hydrochloride step c; 8: dialysate from 0 M guanidine hydrochloride step d.

Table 12: Results of rapid dilution screen for optimizing LpxQ refolding conditions

Component	1	2	3	4	5	6	7	8	9	10	11	12	13	14	15
50 mM MES pH 6.0	X	X	X	X	X	X	X								
50 mM Tris-HCl pH 8.5								X	X	X	X	X	X	X	X
9.6 mM NaCl/ 0.4 M mM KCl	X	X	X					X	X	X	X				
240 mM NaCl/ 10 mM KCl				X	X	X	X					X	X	X	X
2 mM MgCl2/ 2mM CaCl2	X	X		X			X	X		X				X	X
1 mM EDTA			X		X	X			X		X	X	X		
0.5 M Arginine		X		X		X			X	X			X	X	
0.4 M Sucrose			X		X	X		X		X				X	X
0.75 M Guanidine HCl	X		X		X		X		X	X			X	X	
0.5% Triton X-100	X		X	X		X		X			X		X	X	
0.05% PEG 3550		X	X			X	X	X	X			X		X	
1 mM DTT	X		X		X		X		X		X		X		X
1 mM GSH/GSSH		X		X		X		X		X		X		X	
Gel Shift by gel	✓		✓	✓		✓		✓			✓		✓	✓	
Active	✓		✓	✓		✓									

mobility assay described above and by functional activity assays. Some of the conditions produced refolded proteins that displayed a change in mobility in SDS-PAGE, but no lipid A oxidase activity. This result could be due to the protein refolding into an inactive form. Alternatively, components in the refolding buffers could be inhibitory in the activity analysis. The components that had the most significant impact on refolding were Triton X-100, NaCl, and arginine. The detergent was critical for refolding to occur. The protein displayed a change in mobility in SDS-PAGE only when Triton X-100 was present. In later screens, it was shown that other detergents such as DDM could substitute for Triton in the refolding buffers (data not shown). The presence of either divalent cations or EDTA did not have much impact on folding.

4.3.5 Refolded LpxQ is protease resistant

The multi-step dialysis refolding procedure as well as the quick-dilution refolding procedure described above both produced a mixture of "refolded LpxQ" and incorrectly folded LpxQ (Fig 43). The two species could not be separated by Ni-NTA chromatography or by size exclusion chromatography (data not shown). A significant population of the unfolded protein, however, did precipitate when the procedures were performed at room temperature. The SDS-PAGE analysis of a multi-step dialysis

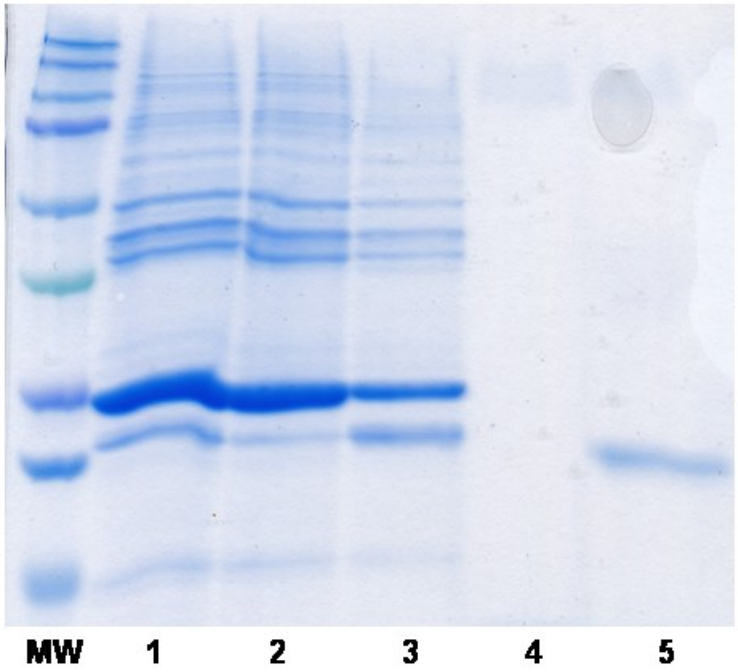

Figure 46: Refolded LpxQ is proteinase K resistant.

LpxQ was refolded from inclusion bodies at room temperature using the multi-step dialysis procedure described in the experimental procedures section. The dialysate from the last step of the refolding procedure was centrifuged at 4000 x g. The soluble portion was then digested with proteinase K. Lane 1) Refolded LpxQ reaction mixture (pre-centrifugation); Lane 2) Refolded LpxQ reaction mixture (post-centrifugation precipitate); Lane 3) Refolded LpxQ reaction mixture (post-spin soluble portion); Lane 4) Proteinase K; Lane 5) Refolded LpxQ reaction mixture (post-spin soluble portion) treated with Proteinase K.

procedure performed at room temperature is shown in Fig. 46. In lane 1, the total protein recovered from the procedure is shown. A large percentage of the unfolded protein precipitated after centrifugation (Fig. 46, lane 2). The soluble portion still contained a mixed population of protein species (Fig. 5, lane 3), but the ratio of folded protein to unfolded protein was dramatically improved. The addition of proteinase K to the refolded mixture resulted in complete degradation of the unfolded sample (Fig. 46, lane 5). This result shows that refolded LpxQ, like the native protein isolated form membranes, is resistant to proteolysis. The addition of proteinase K did not inhibit LpxQ activity (data not shown).

4.4 Discussion

The expression of many integral membrane proteins is toxic to hosts such as *E. coli*. The outer membrane protein (OMP) class of membrane proteins from Gram-negative bacteria, however, can be overexpressed in an aggregated form known as inclusion bodies and refolded into a native state *in vitro*. This alternative approach of producing outer membrane proteins typically yields relatively pure protein in large quantities. A variety of refolding strategies have been developed in the last decade. These strategies have been applied to many OMPs including enzymes that catalyze reactions involving lipid A. The three-dimensional structures of refolded PagP, PagL, and LpxR have all been reported. (Ahn *et al.*, 2004, Rutten et al., 2006, Rutten *et al.*, 2009).

A refolding strategy has not been described for the lipid A oxidase, LpxQ. LpxQ is unique among the outer membrane enzymes that operate on lipid A. PagP, PagL, and LpxR catalyze reactions involving the addition or removal of acyl chains. LpxQ, on the other hand, catalyzes a reaction involving the transfer of electrons from lipid A to oxygen. Refolding strategies were initially avoided because it was thought that a cofactor would be involved in mediating the electron-transfer event. In chapter 3, a purification procedure was described for recombinantly expressed LpxQ. In the purified preparation of LpxQ, no cofactor could be detected. Therefore, it was proposed that LpxQ could be mediating the electron transfer event in the absence of a cofactor. This proposal was evaluated by expressing the protein as inclusion bodies, refolding it *in vitro*, and assessing its activity. In this chapter, several lines of evidence support the view that refolded LpxQ is active in the absence of cofactors.

The production of the inclusion bodies in *E. coli* was noticeably less toxic than production of the recombinant LpxQ protein with its signal sequence. The isolated LpxQ from the inclusion bodies was relatively pure and homogenous in mass. Several protein refolding methods were attempted with the LpxQ inclusion bodies, but the greatest success came with a multi-step dialysis procedure and a rapid dilution procedure. The protein did refold in an on-column refolding procedure, but the efficiency of the procedure was low (data not shown).

Refolding was judged by two criteria: the ability of the protein to display a gel-shift behavior in SDS-PAGE and by catalytic activity. The optimal conditions for refolding were found by screening conditions with various additives such as salt, arginine, $MgCl_2$, EDTA, and reducing agents. A detergent was required for proper refolding under all conditions tested. Most experiments were carried out with the detergent, Triton X-100. However, other detergents such as DDM were able to substitute. Arginine was identified as the second most important factor in refolding LpxQ. This additive is commonly found in protein refolding conditions and is thought to be important in suppressing protein aggregation. The protein was able to refold in the presence of EDTA. This observation further complicates the role of metal(s) in the LpxQ reaction. The purified protein isolated from membranes was shown to purify with two equivalents of zinc or 1 equivalent of zinc and 1 equivalent of nickel, and required magnesium to be supplemented in the assay for full stimulation of its activity. Further work needs to be done to determine the importance of these metals. These issues will be addressed by analyzing the metal content of the refolded enzyme and by analyzing its dependency on divalent cations in the *in vitro* assay.

One obstacle associated with the refolded protein is the accumulation of a mixed population of folded and unfolded species (Fig. 43). The soluble "unfolded" species did not precipitate readily unless the refolding procedure was carried out at room

temperature (Fig. 46) or if the protein was folded at higher protein concentrations (data not shown). The presence of the unfolded protein in the refolded fractions could be a cause of the lower specific activity observed in the refolded protein preps. The reason why a portion of the unfolded protein remains soluble is unclear. However, the unfolded protein could be degraded by proteolysis. The susceptibility of the unfolded protein to the protease proteinase K was consistent with that observed with heat denatured LpxQ (chapter 3). The resistance of refolded LpxQ to the protease is perhaps the most compelling evidence that LpxQ has adopted the stable β-barrel fold it is expected to have in nature.

The refolded protein will need to be analyzed further to confirm the absence of cofactors. It is conceivable that a small population of LpxQ is modified in the refolding procedure in order to generate active enzyme. Such a modification would have to be catalyzed in the test tube and would potentially involve a self-processing event. The cofactor itself would need to be generated from LpxQ, itself. There are precedents for such reactions. For example, green fluorescent protein (GFP) from the jellyfish *Aequorea victoria*, for example, generates its chromophore by undergoing a autocatalytic reaction. The chromophore is formed from post-translational modifications that occur in the presence of oxygen. Three consecutive residues in the protein, serine, tyrosine, and glycine, react to form the five membered chromophore ring in an intermolecular

reaction. Interestingly, the chromophore in GFP has been shown to form both *in vivo* and *in vitro*. If LpxQ undergoes similar events, it has not been detected thus far. The yellow chromophore that was observed with the purified protein from membranes has not been observed with the refolded protein preparations. In addition, no significant change in the mass of the protein has been observed in the refolded protein, but as discussed in chapter 3, the detergent present in the refolded protein mixture could suppress minor, modified species. Current efforts are underway to isolate larger quantities of refolded LpxQ to address this issue. In addition refolding will be attempted under anaerobic conditions.

The biological function of LpxQ is unknown. The role of the lipid A modification it processes in *Rhizobium* has not been determined from nodulation studies. The protein, however is unique in that it is the only described outer membrane oxidase in Gram-negative bacteria. The mechanism of the protein may be unique as well. At the present time, it is believed that LpxQ facilitates the electron transfer event in the absence of a cofactor by directly interacting with dioxygen. If this is the case, LpxQ would be associated with the rare family of cofactor-free oxidases and oxygenases (Fetzner, 2002). Enzymes in this family include 1*H*-3-hydroxy-4-oxoquinoline 2,4 dioxygenase (Fischer & Fetzner, 2000), ActVA-Orf6 monooxygenase (Sciara *et al.*, 2003), pqqC (Magnusson *et al.*,

2004), and urate oxidase (Kahn & Tipton, 1998). Site-directed mutagenesis of LpxQ and structural studies will be needed to further elucidate the mechanism by which LpxQ oxidizes lipid A.

Chapter 5: Altered Lipid A Structures and Polymyxin Sensitivity of *Rhizobium etli* Mutants Lacking the LpxE and LpxF Phosphatases

5.1 Introduction

Gram-negative bacteria have an asymmetric outer membrane composed of an inner leaflet of glycerophospholipids and an outer leaflet of lipopolysaccharide (LPS) (Raetz & Whitfield, 2002). LPS functions as a protective barrier and consists of three domains: (1) the lipid A moiety, (2) a nonrepeating core oligosaccharide, and (3) a distal *O*-antigen polysaccharide (Raetz & Whitfield, 2002, Nikaido, 2003). The lipid A component of LPS is a relatively conserved structural feature of Gram-negative bacteria and serves as the membrane anchor for LPS (Raetz & Whitfield, 2002). It is required for growth in almost all Gram-negative bacteria (Raetz & Whitfield, 2002) and is the "endotoxin" component of LPS associated with the complications of severe Gram-negative sepsis (Russell, 2006). Lipid A is a potent stimulator of inflammation and of innate immunity in animals via the Toll-like receptor-4/MD-2 (TLR4/MD-2) complex (Park et al., 2009).

In most enteric Gram-negative bacteria, the lipid A moiety of LPS is a hexa-acylated disaccharide of glucosamine that is phosphorylated at positions 1 and 4′ (Fig. 47) (Raetz & Whitfield, 2002). Pharmacological studies have shown that both phosphate groups, the glucosamine disaccharide, and the proper arrangement of the

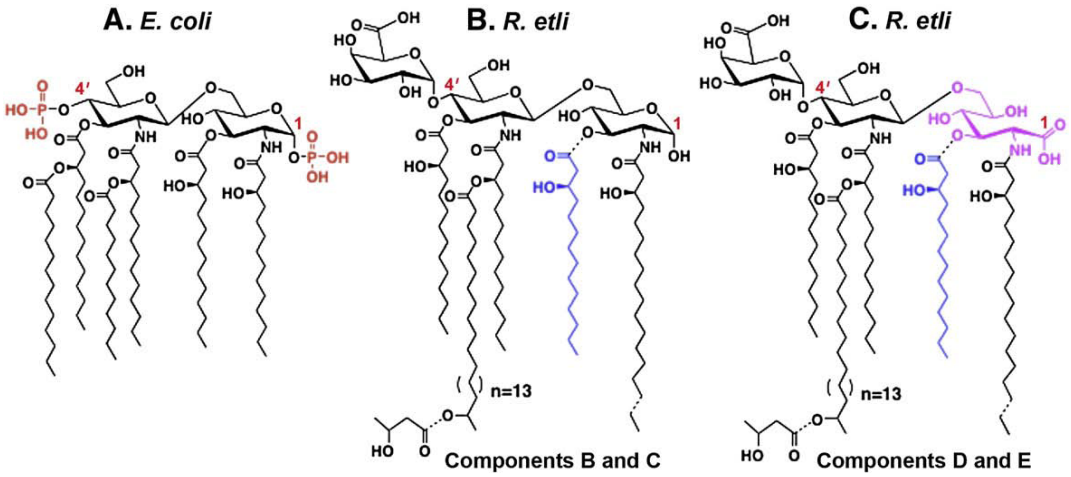

Figure 47: Structures of the major lipid A species present in *E. coli* and *R. etli*

A. The predominant lipid A moiety of *E. coli* LPS consists of a hexa-acylated disaccharide of glucosamine, substituted with monophosphate groups (red) at the 1- and 4′-positions. There is very little acyl chain heterogeneity (Raetz et al., 2007). **B. and C.** The major lipid A species in *R. etli* and *R. leguminosarum* lack phosphate substituents and are more heterogeneous with respect to fatty acyl chain length (Que et al., 2000a, Que et al., 2000b). Components B and C are constructed around the typical glucosamine disaccharide found in the lipid A of other Gram-negative organisms. Components D and E feature an aminogluconate unit (magenta) in place of the proximal glucosamine residue, derived by the LpxQ-catalyzed oxidation of B and C, respectively (Que-Gewirth et al., 2003a, Que-Gewirth et al., 2003b). All *R. etli* lipid A species contain a galacturonic acid moiety at position-4′ in place of the more typical monophosphate group, and they also contain an unusual C28 secondary acyl chain that may be further derivatized at the 27-OH moiety with a β-hydroxybutyrate group (Bhat et al., 1994). Components C and E differ from B and D by the absence of a hydroxyacyl chain at position 3 (blue), which is removed by the deacylase PagL (Basu et al., 1999a). Dashed bonds highlight the most prominent microheterogeneity of *R. etli* lipid A with respect to its acyl chains and the presence of the β-hydroxybutyrate substituent. Microheterogeneity arising from minor branched-chain or even chain fatty acids is not indicated but is apparent in the mass spectra shown below.

fatty acyl chains are important for full activation of TLR4/MD-2 (Rietschel et al., 1994). Monophosphorylated lipid A analogues, lacking the 1-phosphate group, retain some of the immune-stimulatory properties of *Escherichia coli* lipid A but show greatly reduced toxicity in animals (Qureshi *et al.*, 1982a, Baldridge et al., 2004). Monophosphorylated lipid A preparations are therefore being developed as adjuvants in human vaccines (Baldridge et al., 2004).

Many animal pathogens adapt strategies for modifying their lipid A structure to evade detection and early clearance by the innate immune system (Raetz et al., 2007). These lipid A modifications include dephosphorylation, changes in acylation status, or attachment of amino-sugars to neutralize the negative charges of the phosphate moieties (Raetz et al., 2007). The lipid A components of *Francisella novicida* and *Francisella tularensis*, the causative agents of tularemia in mice and humans, respectively, illustrate some of these principles. *Francisella* lipid A molecules lack the 4′-phosphate group and the 3′-hydroxyacyl chain (Vinogradov *et al.*, 2002, Wang et al., 2006b, Wang et al., 2007), both of which are removed during the later stages of lipid A assembly (Raetz et al., 2009).

Modifications to lipid A are not unique to pathogenic bacteria. For instance, some of the lipid A modifications seen in *F. tularensis* also occur in *Rhizobium etli*, a plant endosymbiont that participates in a nitrogen-fixing symbiosis with leguminous plants

(Raetz et al., 2007, Bhat et al., 1994). *R. etli* lives intracellularly within nodules that form on roots. The lipid A of *R. etli*, which consists of a mixture of related components (Fig. 47 B and C) (Que et al., 2000a, Que et al., 2000b), lacks both the 1- and 4′-phosphate groups present in the lipid A of enteric bacteria (Bhat et al., 1994). The 4′-phosphate moiety is replaced with a galacturonosyl residue, whereas the 1-dephosphorylated proximal glucosamine residue is present either in the hemiacetal form (Fig. 47B) or as an oxidized 2-amino-2-deoxy-gluconate unit (Fig. 47C) (Bhat et al., 1994), (Que et al., 2000a, Que et al., 2000b). *R. etli* lipid A also differs from that of *E. coli* with respect to its acylation status (Fig. 47). *R. etli* lipid A lacks the secondary laurate and myristate chains found in *E. coli*, but instead is acylated with a secondary 27-hydroxyoctacosanoate chain (27OHC28:0) at the 2′-position (Bhat et al., 1994, Que et al., 2000a, Que et al., 2000b, Bhat et al., 1991b). This residue may be esterified with a β-hydroxybutyrate moiety (Figs. 47B and C) (Bhat et al., 1994, Que et al., 2000a, Que et al., 2000b). Differences in fatty acyl chain length, especially at the 2 position, further contribute to *R. etli* lipid A micro-heterogeneity (not shown in Fig. 47).

Lipid A biosynthesis in *R. etli* diverges from that of *E. coli* after the formation of the tetra-acylated intermediate Kdo_2-lipid IV_A, as shown schematically in Fig. 48 (Raetz et al., 2007). *R. etli* utilizes similar enzymes as found in *E. coli* to convert UDP-GlcNAc

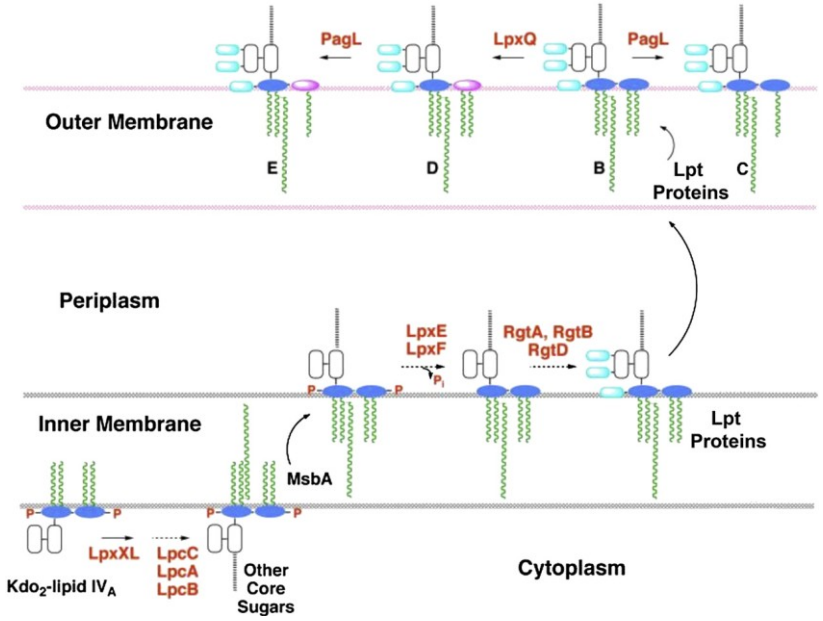

Figure 48: Topography of LPS assembly and lipid A modifications in *R. etli*.

With the exception of the UDP-diacylglucosamine hydrolase LpxH, which is replaced by LpxI (L. E. Metzler and C. R. H. Raetz, in preparation), the constitutive enzymes that generate the phosphorylated intermediate Kdo_2-lipid IV_A in *E. coli* are also present in *R. etli* (Price et al., 1994). The assembly of *R. etli* lipid A diverges after Kdo_2-lipid IV_A formation, starting with the addition of the 27-hydroxyoctacosanoate chain (27OHC28:0), catalyzed by LpxXL (Basu et al., 2002). After completion of core glycosylation and transport to the outer surface of the inner membrane by MsbA, LpxF and LpxE remove the phosphate moieties at the 4′- and 1-positions, respectively (Karbarz et al., 2003, Wang et al., 2004, Wang et al., 2006a). Next, RgtD is thought to utilize dodecaprenyl phosphate-galacturonic acid to incorporate the 4′-galacturonic acid residue, and RgtA/RbtB similarly modify the outer Kdo unit (Kanjilal-Kolar et al., 2006, Kanjilal-Kolar & Raetz, 2006). After completion of *O*-antigen assembly (not shown) and transport to the outer membrane by the Lpt proteins (Ruiz et al., 2009), the ester-linked hydroxyacyl chain at position 3 may be removed by the deacylase PagL (Basu et al., 1999a, Rutten et al., 2006), and the proximal glucosamine may be converted to the aminogluconate unit by the oxidase LpxQ (Que-Gewirth et al., 2003a, Que-Gewirth et al., 2003b). The orientation of the LpxQ active site within the outer membrane is not established unequivocally. The color scheme is as follows: glucosamine, *blue*; Kdo, *white*; galacturonic acid, *cyan*; aminogluconate, *magenta*; phosphate groups, *red*; fatty acyl chains, *green*.

into Kdo_2-lipid IV_A, which is then processed differently by enzymes unique to *R. etli* (Fig. 48) (Price et al., 1994). The enzyme LpxXL incorporates the sole secondary acylchain (27OHC28:0), which is supplied by the unique acyl carrier protein, AcpXL (Brozek et al., 1996a, Brozek et al., 1996b, Basu et al., 2002). After formation of the acyloxyacyl chain and addition of other core sugars (Brozek et al., 1996b, Kadrmas *et al.*, 1998), lipid A molecules are flipped to the outer leaflet of the inner membrane by the ABC transporter MsbA (Fig. 48) (Raetz et al., 2007), where the lipid A phosphatases LpxE (Karbarz et al., 2003, Wang et al., 2004) and LpxF (Price et al., 1995, Wang et al., 2006a) dephosphorylate them. After removal of the 4′-phosphate moiety, the enzyme RgtD is proposed to glycosylate the 4′-position with a galacturonic acid residue, using dodecaprenyl-phosphate galacturonic acid as its donor substrate (Kanjilal-Kolar et al., 2006, Kanjilal-Kolar & Raetz, 2006). After removal of the 1-phosphate moiety on the outer surface of the inner membrane and transport to the outer membrane, the lipid A oxidase LpxQ oxidizes the proximal glucosamine residue to the 2-aminogluconate unit (Fig. 47 and Fig. 48) in an oxygen-dependent reaction (Que-Gewirth et al., 2003a, Que-Gewirth et al., 2003b). In parallel, the ester-linked hydroxyacyl chain at position 3 may be removed by the outer membrane deacylase PagL (Basu et al., 1999a, Rutten et al., 2006) (Fig. 48). The functional significance of these lipid A modifications in *R. etli* is unknown.

A previously reported 4′-phosphatase *lpxF* mutant of *F. novicida* is very sensitive to polymyxin and is highly attenuated in a mouse infection model (Wang et al., 2007). In the present study we address the functional roles of the two lipid A phosphatases of *R. etli* encoded by *lpxE* and *lpxF* (Karbarz et al., 2003, Wang et al., 2004, Wang et al., 2006a, Karbarz et al., 2009) by constructing mutants with deletions in one or both of these genes. The recently completed genome sequence of *R. etli* revealed only two plausible candidate genes encoding these phosphatases (Gonzalez *et al.*, 2006). Deletion mutants of the individual phosphatases and a double-knockout mutant were constructed by replacing these genes with spectinomycin and/or gentamicin cassettes. The biochemical and physiological properties of these mutant strains are reported in this chapter.

5.2 Materials and Methods

5.2.1 Materials

[γ-^{32}P] ATP was obtained from PerkinElmer Life And Analytical Sciences, Inc. (Waltham, MA). [^{14}C]-acetate (sodium salt) was obtained from GE Healthcare (Chalfont St. Giles, UK). Acetic acid, ammonium acetate, chloroform, formic acid, and glass-backed 0.25-mm Silica Gel-60 thin-layer chromatography (TLC) plates were from EMD Chemicals, Inc. (Gibbstown, NJ). Pyridine and methanol were from Mallinckrodt Baker, Inc. (Phillipsburg, NJ). Yeast extract, agar, and tryptone were from Becton, Dickinson, and Company (Franklin Lakes, NJ). Sodium chloride was from VWR International (West

Chester, PA). Bicinchoninic acid (BCA) protein assay reagents and Triton X-100 were from Thermo Fisher Scientific (Waltham, MA). Diethylaminoethyl (DEAE) cellulose DE52 was from Whatman, Inc. (Florham Park, NJ). GenomicPrep Cells and Tissue DNA Isolation kit was from GE Healthcare (Chalfont St. Giles, UK). All other chemicals were reagent grade and were purchased from either Sigma-Aldrich (St. Louis, MO) or VWR International (West Chester, PA).

5.2.2 Bacterial strains, growth conditions, and molecular biology protocols

The bacterial strains and plasmids used and their relevant characteristics are shown in Table 13. *R. etli* strains were grown at 29–30 °C on complex tryptone yeast extract medium (TY) supplemented with 4.5–10 mM $CaCl_2$ (Johnston & Beringer, 1975). *Rhizobium* stains were grown in media supplemented with the following concentrations of antibiotics where appropriate: neomycin (200 μg/mL), gentamicin (35 μg/mL), nalidixic acid (20 μg/mL), streptomycin (200 μg/mL), and spectinomycin (200 μg/mL). *E. coli* strains were cultured on LB broth at 37 °C (Miller, 1972). Growth media were supplemented with the following concentrations of antibiotics where appropriate: kanamycin (50 μg/mL), gentamicin (10 μg/mL), carbenicillin (100 μg/mL), or spectinomycin (200 μg/mL). Derivatives of the suicide plasmid pK18*mobsac*B (Table 13) were mobilized into *R. etli* strains by triparental mating using the mobilizing plasmid pRK2013, as described previously (Ruvkun & Ausubel, 1981). Recombinant DNA

techniques were performed according to standard protocols (Sambrook & Russell, 2001) using *E. coli* DH5α as a host strain (Hanahan, 1983). The XL-PCR kit (Applied Biosystems) was used for amplifying DNA sequences from *R. etli* genomic DNA.

5.2.3 Exchange of the rhizobial *lpxE* and *lpxF* genes with a spectinomycin resistance cassette

The oligonucleotide primers o1phosph_A (5′-ACG TTC TAG ATG GAT GCC GGT TTC GTC ACC GAC G-3′) and o1phosph_B (5′-ACG TCC CGG GCG CCA GCG CCT ATC AAG GGA AGC-3′) were used to amplify about 1 kb of genomic DNA upstream of the putative *lpxE* gene from *R. etli* CE3. The primers o4phosph_A (5′-ACG TTC TAG AGC ACG AGG CGG CCT TCG GCA TCG-3′) and o4phosph_B (5′-ACG TCC CGG GCA AGC AGT GCC CAC CAC GTC CAG-3′) were used to amplify about 1 kb of genomic DNA upstream of the putative *lpxF* gene. These primers introduced *Xba*I and *Sma*I sites (underlined) into the PCR products. After digestion with the respective enzymes, the PCR products were cloned as *Xba*I/*Sma*I fragments into pUC18, to yield plasmids pCCS72a and pCCS73a. Similarly, the primers o1phosph_C (5′-ACG TCC CGG GCG CCG GAT GGC TGG CCA CTC GC-3′) and o1phosph_D (5′-ACG TGA ATT CTC GGT GCC ACC ATG GGC CAG G-3′) were used to amplify 1 kb of genomic DNA downstream of the *lpxE* gene. The primers o4phosph_C (5′-ACG TCC CGG GTC TTC GCA GCG CTG CTG GCG TTA ACT G-3′), and o4phosph_D (5′-ACG TGA ATT CCT GCA TGC GTC TCC AGG AAA CCG-3′) were used to amplify about 1 kb of genomic

DNA downstream of the *lpxF* gene. The primers introduced *Sma*I and *Eco*RI sites (underlined) into the PCR products. After digestion with the respective enzymes, the *Sma*I/*Eco*RI-digested PCR products were cloned into pCCS72a and pCCS73a to yield plasmids pCCS72b and pCCS73b. Subsequently, the spectinomycin resistance cassette from the plasmid pHY109 was subcloned as a *Sma*I fragment between the flanking sequences in pCCS72b and pCCS73b to generate plasmids pCCS74a and pCCS75a. The whole cassettes containing the flanking regions and the spectinomycin resistance cassette were then subcloned as *Xba*I/*Eco*RI-fragments into the suicide vector pK18*mobsacB* (Table 13) to yield plasmids pCCS74b and pCCS75b. Using pRK2013 as a helper plasmid, pCCS74b and pCCS75b were introduced by triparental mating into wild-type *R. etli* CE3. Transconjugants were selected on TY medium containing neomycin and spectinomycin to select for single recombinants in a first step. The single recombinants were grown under nonselective conditions in complex medium for 1 day before being plated on TY medium containing spectinomycin and 10% sucrose (wt./vol.) to select for the loss of the vector backbone of pK18*mobsacB* from the bacterial genome. Several candidates grew after 5 days. Southern blot analysis confirmed that the putative mutant strains were double recombinants in which the *lpxE* gene or *lpxF* genes were replaced with a spectinomycin cassette (data not shown).

5.2.4 Construction of a *R. etli* double mutant deficient in the *lpxE* and *lpxF* genes

The suicide plasmid pCCS74b (Table 13), which was used in the construction of the *lpxE* mutant, was digested with *Sma*I to liberate its spectinomycin resistance cassette. Plasmid pACΩ-Gm (Table 13) was digested with *Sma*I to release a gentamicin cassette, which was subsequently ligated into the *SmaI*-digested pCCS74b plasmid to yield plasmid pCCS76. The suicide plasmid pCCS76 was then conjugated into CS506 in order to construct the double mutant. Conjugation and subsequent selection were performed as described above for the single mutants. Double mutants were confirmed by Southern blot analysis (data not shown), and the mutant CS513 was selected for a detailed analysis. In this strain, the *lpxF* gene is substituted with a spectinomycin resistance cassette and the *lpxE* gene is substituted with a gentamicin resistance cassette.

5.2.5 Lipid A extraction

Lipid A from *R. etli* was isolated as described previously (Que et al., 2000a, Que et al., 2000b); however, the conditions used for hydrolysis differed. Previous hydrolysis conditions utilized 12.5 mM sodium acetate at pH 4.5 with 1% SDS (Que et al., 2000a, Que et al., 2000b). To simplify the analysis of the lipid A species, 1% acetic acid was used for hydrolysis in the absence of SDS. Under these hydrolysis conditions, the labile glycosidic linkage between the Kdo moiety and lipid A is cleaved selectively. One liter of TY broth, supplemented with 10 mM $CaCl_2$ and antibiotics, was inoculated with 4 mL

of a fresh culture of bacteria. The flasks were shaken (225 rpm) at 30 °C overnight until the A_{600} reached 1.2. The cells were harvested by centrifugation at 5000 × g for 20 min at 4 °C. The cells were resuspended, washed once with 250 mL chilled phosphate-buffered saline (PBS) (Dulbecco & Vogt, 1954), and centrifuged once more. The washed cell pellets were frozen at −80 °C. Thawed cell pellets were resuspended in 48 mL PBS. The glycerophospholipids were extracted by adding 60 mL of chloroform and 120 mL of methanol to convert the cell suspension into a single-phase Bligh–Dyer mixture (chloroform/methanol/PBS, 1:2:0.8, vol./vol./vol.) (Bligh & Dyer, 1959). The cells were extracted for 1 h and were centrifuged at 4000 × *g* for 20 min. The insoluble material was recovered and washed once more with 60 mL of a fresh, single-phase Bligh–Dyer mixture. The insoluble material was again recovered by centrifugation. The washed pellet was then suspended in 54 mL of 1% acetic acid and subjected to probe sonic irradiation. The suspension was boiled for 30 min and cooled to room temperature. The suspension was then converted to a two-phase Bligh–Dyer mixture (chloroform/methanol/1% acetic acid, 2:2:1.8, vol./vol./vol.) (Bligh & Dyer, 1959) by adding 60 mL of chloroform and 60 mL of methanol. The phases were mixed thoroughly and separated by centrifugation at 4000 × *g* for 20 min. The lower phase was retrieved, while the upper phase was washed once with 60 mL preequilibrated lower phase and centrifuged again. The second lower phase was retrieved, pooled with the first lower

phase, and dried with a rotary evaporator. The remaining phospholipids were removed from the dried, crude lipid A by DEAE-cellulose column chromatography as described previously (Que et al., 2000a). After TLC in a chloroform/methanol/water/ammonium hydroxide system (40:25:4:2, vol./vol./vol./vol.), the lipids were visualized by sulfuric acid charring.

5.2.6 Negative ion electrospray ionization mass spectrometry (ESI/MS) of Lipid A species

Lipid A species recovered from the cells were redissolved in chloroform/methanol (4:1, vol./vol.), subjected to sonic irradiation in a bath sonicator, and subsequently diluted into chloroform/methanol (2:1, vol./vol.). The samples were supplemented with 1% piperdine and immediately infused into the ion source at 5–10 μL/min and analyzed by ESI/MS, as described previously (Kanjilal-Kolar et al., 2006, Kanjilal-Kolar & Raetz, 2006). All mass spectra were acquired on a QSTAR XL quadrupole time-of-flight mass spectrometer (ABI/MDS-Sciex, Toronto, Canada). Spectra were acquired in the negative ion mode from 200 to 2400 amu. Some spectra were the accumulation of 60 scans. Data acquisition and analysis were performed using Analyst QS software version 1.1.

5.2.7 Preparation of membranes and substrates

All enzyme preparations were carried out at 0–4 °C. The bicinchoninic acid method (Smith et al., 1985) was used to determine protein concentrations, using bovine

serum albumin as a standard. Cell-free extracts and washed membranes were prepared as described previously (Basu et al., 2002) and stored in aliquots at −80 °C. The preparation of carrier Kdo_2-lipid IV_A (Six et al., 2008) and Kdo_2-[4′-^{32}P]-lipid IV_A was described previously (Reynolds et al., 2005). The substrates were stored as aqueous dispersions in 25 mM Tris–HCl, pH 7.8, containing 1 mM EDTA, 1 mM EGTA, and 0.1% Triton X-100. Before use, the lipid substrates were subjected to sonic irradiation for 1 min in a bath sonicator.

5.2.8 *In vitro* assay of 4′-Phosphatase activity

LpxF activity was determined as described (Basu *et al.*, 1999b). Standard assay conditions for detecting 4′-phosphatase activity were as follows: the reaction mixture (10–20 μL) contained 50 mM MES, pH 6.5, 0.1% Triton X-100, 2 mM dithiothreitol, 2 mM EDTA, 10 mM potassium phosphate, and 5 μM Kdo_2-[4′-^{32}P]lipid IV_A (1000 cpm/nmol). Reactions were initiated with the enzyme source. The reaction mixtures were incubated at 30 °C for the indicated times. Reactions were terminated by spotting 3-μL samples onto a TLC plate, which was developed in the solvent chloroform/pyridine/88% formic acid/water (30:70:16:10, vol./vol./vol./vol.). After drying and overnight exposure of the plate to a PhosphorImager screen (GE Healthcare), product formation was detected and quantified with a Storm 840 PhosphorImager equipped with ImageQuant software (GE Healthcare).

5.2.9 Assay of polymyxin sensitivity

The outer membrane integrity of wild-type *R. etli* and each of the phosphatase mutant strains was evaluated by examining sensitivity to the cationic antibacterial peptide polymyxin B sulfate (Sigma). A disk diffusion test was performed by placing sterile 6-mm filter paper disks onto a lawn of cells that had been freshly plated on TY agar using a sterile cotton swab from a culture at A_{600} of $\sim$ 0.2. Polymyxin (1 μL of a 2, 10, or 20 mg/mL stock solution) was then applied to the disks. After 40 h of growth at 30 °C, the diameters of the zones of clearing were measured, providing an assessment of the relative polymyxin sensitivity.

5.2.10 *In vivo* labeling of *R. etli* strains with [^{14}C]-acetate and quantitative analysis of lipid extracts

The lipid compositions of *R. etli* wild-type CE3 and the three mutant strains CS501, CS506 and CS513 were determined after labeling with [1-^{14}C]-acetate. Cultures (1 mL) in TY medium, supplemented with 4.5 mM $CaCl_2$, were inoculated from overnight cultures grown in the same medium. Each culture was radiolabeled with 1 μCi [1-^{14}C]-acetate (GE Healthcare; 60 mCi/mmol) and then incubated for 8 h. The cells were harvested by centrifugation, washed with 500 μl of water, and resuspended in 100 μl of water. The lipids were extracted according to the method of Bligh and Dyer (Bligh & Dyer, 1959). The chloroform phase was used for lipid analysis on TLC plates,

and after two-dimensional separation, the individual lipids were quantified using a Storm 820 PhosphorImager (GE Healthcare).

5.2.11 Plant test for symbiotic phenotype characterization

Phaseolus vulgaris cv. Negro Jamapa seeds were surface-sterilized with 1.2% sodium hypochlorite and germinated on 1% (wt./vol.) water agar as described previously (Vinuesa *et al.*, 1999). Seedlings were transferred to 250-mL flasks filled with vermiculite and nitrogen-free nutrient solution (Fahraeus, 1957), and inoculated with about 10^5 CFU of bacteria per plant. Plants were grown in a controlled growth chamber at 28 °C with a 15-h a day/9-h night cycle and harvested 21 days after inoculation. Nitrogenase activity of nodulated roots was determined by the acetylene reduction assay as described previously (Martinez *et al.*, 1985). Nitrogen fixation activity per plant was normalized with respect to the nodule fresh weight per plant.

Table 13: Bacteria strains and plasmids used in chapter 5

Strain or Plasmid	Genotype or Description	Source or reference
Strains		
R. etli CE3	Spontaneous Sm^r derivative of wild-type strain CFN42, NaI^r	(Noel *et al.*, 1984)
CS501	*LpxE* mutant, spectinomycin-resistant	this work
CS506	*LpxF* mutant, spectinomycin-resistant	this work
CS513	*LpxE*/*LpxF* mutant, derived from CS506, gentamicin-resistant	this work
E. coli		
DH5α	*recA*1 ϕ80 *lacZ*Δ*M15*	(Hanahan, 1983)
Plasmids		
pRK2013	helper plasmid, kanamycin/neomycin-resistant	(Figurski & Helinski, 1979)
pK18*mobsac*B	suicide vector, kanamycin/neomycin-resistant	(Schafer *et al.*, 1994)
pUC18	cloning vector, carbenicillin-resistant	(Yanisch-Perron *et al.*, 1985)
pHY109	spectinomycin resistance-conferring Ω interposon cloned in the *Eco*RI restriction sites of plasmid pCHO341	(Osteras *et al.*, 1998)
pACΩ-Gm	broad host range vector containing gentamicin resistance cassette	(Schweizer, 1993)
pCCS72a	pUC18 derivative containing 1 kb of sequence upstream of *lpxE* as a *Sma*I/*Eco*RI fragment	this work
pCCS73a	pUC18 derivative containing 1 kb of sequence upstream of *lpxF* as a *Xba*I/*Sma*I fragment	this work
pCCS72b	pUC18 derivative containing 1 kb of sequence upstream and downstream of LpxE as *Xba*I/*Sma*I and *Sma*I/*Eco*RI fragments	this work
pCCS73b	pUC18 derivative containing 1 kb of sequence upstream and downstream of LpxF as *Xba*I/*Sma*I and *Sma*I/*Eco*RI fragments	this work
pCCS74a	pUC18 derivative containing spectinomycin cassette flanked by upstream and downstream regions of LpxE	this work
pCCS75a	pUC18 derivative containing spectinomycin cassette flanked by upstream and downstream regions of LpxF	this work
pCCS74b	suicide plasmid for construction of *lpxE* mutant by substitution with a spectinomycin resistance cassette	this work
pCCS75b	suicide plasmid for construction of *lpxF* mutant by substitution with a spectinomycin resistance cassette	this work
pCCS76	suicide plasmid for construction of *lpxElpxF* double mutant by substitution of the *lpxF* gene with a gentamicin cassette	this work

Abbreviations: Sm-streptomycin sulfate, NaI-nalidixic acid.

5.3 Results

5.3.1. Candidate genes encoding the *R. etli* lipid A 1- and 4′-phosphatases

Using the sequence of the protein encoded by the *lpxE* gene from *R. leguminosarum* 3841 (Karbarz et al., 2003) and the sequence of the protein encoded by the *lpxF* gene from *F. novicida* (Wang et al., 2006a), the genome of *R. etli* CFN42 (Gonzalez et al., 2006) was searched for the corresponding candidates. The 232-amino acid protein encoded by ABC92837 is 92% identical to *R. leguminosarum* LpxE, and the 257-amino acid protein encoded by ABC90258 is 30% identical to *F. novicida* LpxF. Both genes are located on the *R. etli* chromosome (Gonzalez et al., 2006), and both proteins are predicted to contain six transmembrane helices. The LpxE protein of *R. etli* most closely matches homologues from *R. leguminosarum*, *Agrobacterium tumefaciens*, *Sinorhizobium meliloti*, *Mesorhizobium loti*, and *F. tularensis* subsp. *novicida* (Fig. 49), all of which are α-proteobacteria with the exception of *Francisella*. The putative LpxF protein from *R. etli* most closely matches homologues from the α-proteobacteria *R. leguminosarum*, *Rhodospirillum rubrum*, *Rhodopseudomonas palustris*, *Xanthobacter autotrophicus*, and *Bradyrhizobium* sp. BTAi1, the β-proteobacteria *Dechloromonas aromatica*, and the γ-proteobacteria *F. tularensis* (Fig. 50). Both LpxE and LpxF contain variations of the lipid phosphate phosphatase sequence motif described by Stukey and Carman (Stukey & Carman, 1997).

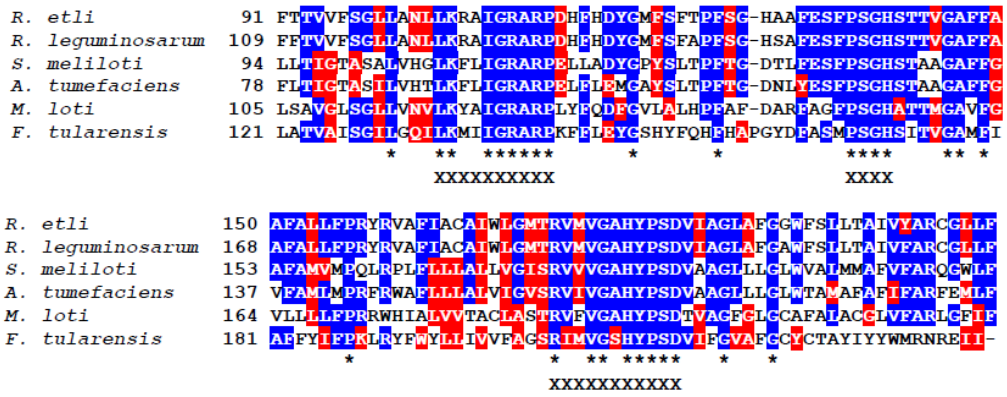

Figure 49: Alignment of LpxE sequences.

Comparison of *Rhizobium etli* lipid A 1-phosphatase (LpxE) with LpxE sequences from *Rhizobium leguminosarum* and *Francisella tularensis* and LpxE-like sequences from *Sinorhizobium meliloti*, *Agrobacterium tumefaciens* and *Mesorhizobium loti*. Identical residues are marked in black and similar residues are shaded in gray. Asterisks indicate amino acid residues conserved in all sequences. The Xs indicate sequence motifs that have been described as part of a conserved phosphatase sequence motif (Stukey & Carman, 1997). Accession numbers are as follows: *Rhizobium etli* CFN 42 LpxE, ABC92837; *Rhizobium leguminosarum* str. 3841 LpxE; *Sinorhizobium meliloti* 1021 ORF, CAC47890; *Agrobacterium tumefaciens* str. C58 ORF, AAK88333; *Mesorhizobium loti* MAFF303099 ORF, BAB47690; *Francisella tularensis* subsp. *novicida* LpxE, AAU11503.

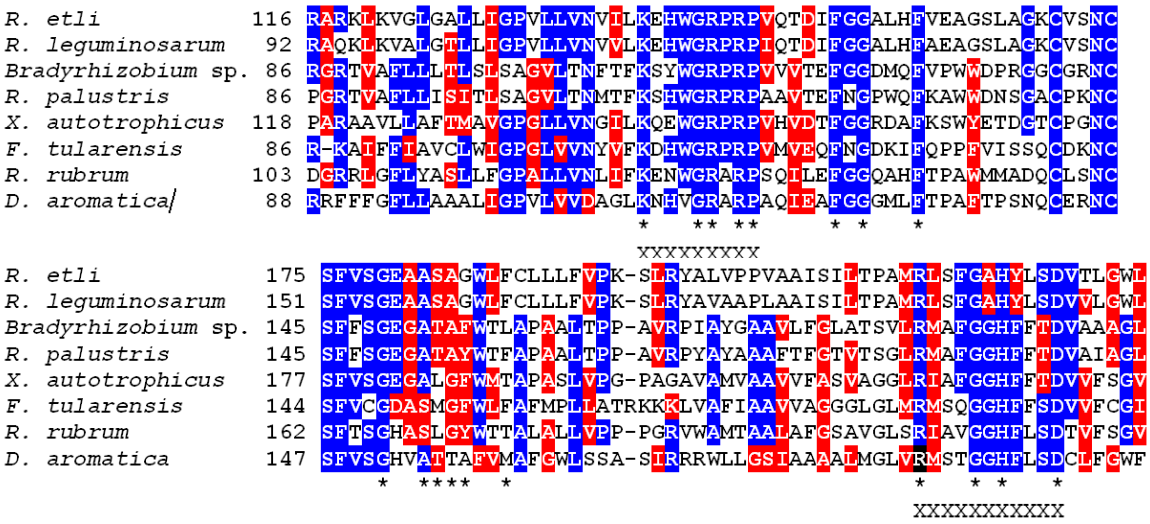

Figure 50: Alignment of LpxF sequences.

Comparison of *Rhizobium etli* lipid A 4′-phosphatase (LpxF) with LpxF sequences from *Rhizobium leguminosarum* and *Francisella tularensis* and LpxF-like sequences from *Bradyrhizobium* sp., *Rhodopseudomonas palustris*, *Xanthobacter autotrophicus*, *Francisella tularensis*, *Rhodospirillum rubrum* and *Dechloromonas aromatica*. Identical residues are marked in black, similar residues are shaded in gray. Asterisks indicate amino acid residues conserved in all sequences. The Xs indicate sequences that have been described as part of a conserved phosphatase sequence motif (Stukey & Carman, 1997). Accession numbers are as follows: *Rhizobium etli* CFN 42 LpxF, ABC90258; *Rhizobium leguminosarum* str. 3841 LpxF, ABC96320; *Bradyrhizobium* sp. BTAi1, EAP31306; *Rhodopseudomonas palustris* CGA009 ORF, CAE25837; *Xanthobacter autotrophicus* Py2 ORF, EAS13873; *Francisella tularensis* subsp. *novicida* LpxF, ABC96319; *Rhodospirillum rubrum* ATCC 11170 ORF, ABC23868; *Dechloromonas aromatica* RCB ORF, AAZ48208.

5.3.2. Lipid A from wild-type *R. etli* and the phosphatase knockout strains

Deletion mutants of the *lpxE* and *lpxF* genes were isolated in *R. etli* as described in Section 2. The single mutants were expected to accumulate the structures shown in Fig. 51A and B. The double knockout of the two phosphatases was expected to accumulate lipid A species with the two phosphate groups retained at the 1 and 4′ positions, similar to the lipid A molecules found in *S. meliloti* (Fig. 51C) (Gudlavalleti & Forsberg, 2003).

Lipid A from each of the *R. etli* strains was obtained by hydrolyzing delipidated cell pellets in 1% acetic acid. The lipid A components released in this manner from the wild-type migrated as multiple bands, designated A, B, C, D, and E (Fig. 52), when analyzed by TLC (Que et al., 2000a, Que et al., 2000b). The previously determined structures of B, C, D, and E (Que et al., 2000b) are shown in Fig. 47 B and C. Component A (Fig. 52) is an artifact arising from component D by β-elimination during the hydrolysis process (Fig. 53) (Que et al., 2000a, Que et al., 2000b). The TLC patterns of the lipid A species from the *lpxF* and *lpxE* mutants were distinctly different from that of the wild-type (Fig. 52). The *lpxF* deletion strain CS506 contained lipid A species A′, B′, C′, D′, and E′ (Fig. 52), which migrated more slowly during TLC, consistent with the presumed retention of the 4′-phosphate group (Fig. 51A). The lipid A species from the *lpxE* mutant also migrated more slowly than those of the wild-type but

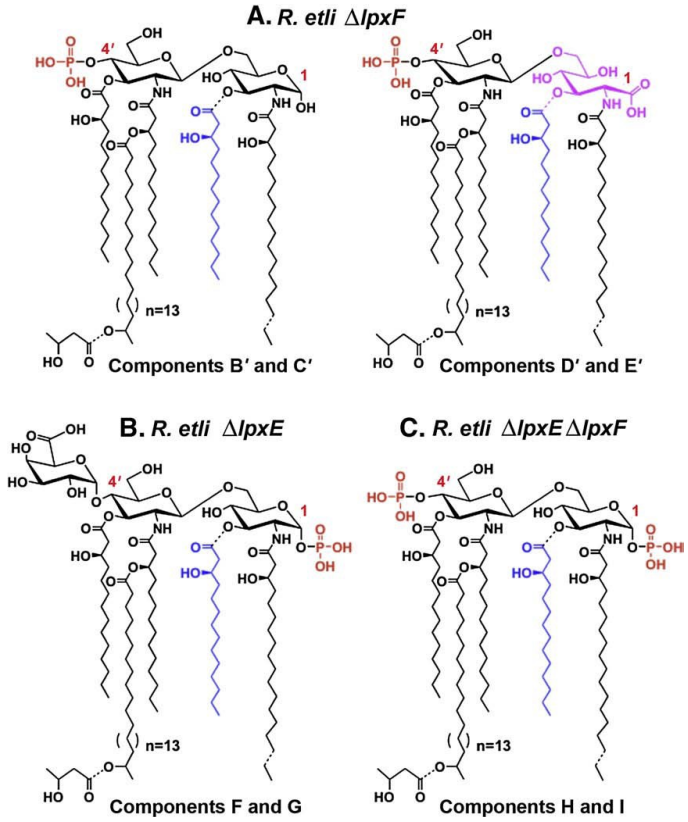

Figure 51: Predicted structures of the major lipid A species in *lpxF*, *lpxE*, and *lpxE*/*lpxF* deletion mutants of *R. etli*.

A. The proposed major lipid A species (B′, C′, D′, and E′) of the *R. etli* LpxF mutant should resemble that of the wild-type, except that the 4′-galacturonic acid unit would be replaced with a monophosphate group (red). Components D′ and E′ feature an aminogluconate unit (magenta) in place of the proximal glucosamine residue found in components B′ and C′. Components C′ and E′ differ from B′ and D′ by the absence of a hydroxyacyl chain at position 3 (blue). **B.** The proposed major lipid A species (F and G) of the *R. etli* LpxE mutant should be less heterogeneous than wild-type, because the proximal glucosamine unit cannot be oxidized by LpxQ. Component G differs from F by the absence of a hydroxyacyl chain at position 3 (blue). **C.** The proposed major lipid A species (H and I) of the double mutant should retain phosphate groups (red) at both the 1- and 4′-positions, resembling the lipid A of *S. meliloti* (Gudlavalleti & Forsberg, 2003). Component I differs from H by the absence of a hydroxyacyl chain at position 3 (blue). The exact masses predicted for these predominant lipid A molecular species are shown in Table 14.

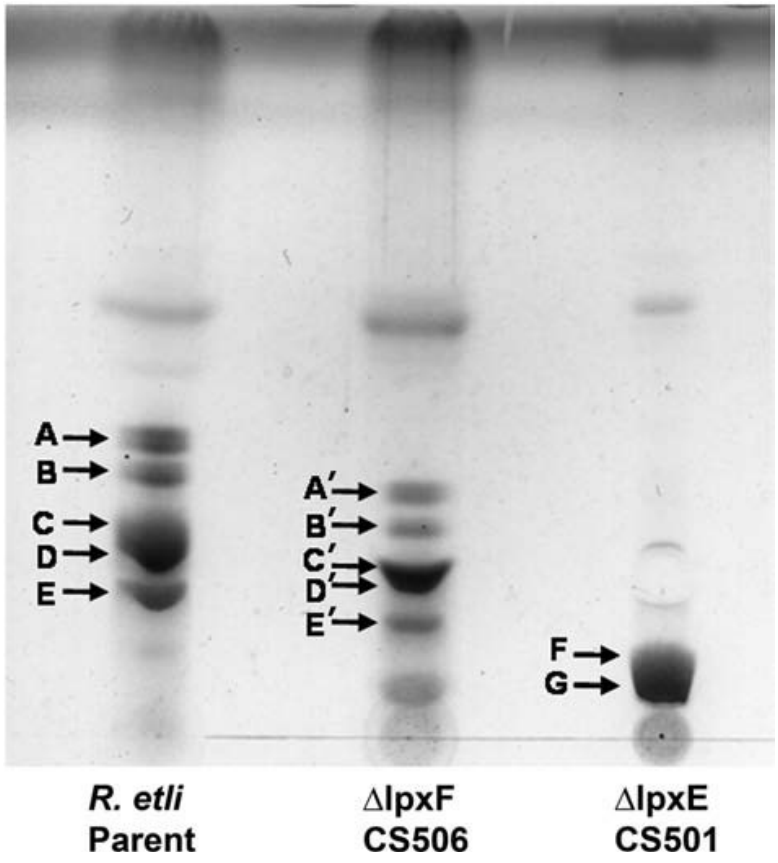

Figure 52: TLC analysis of lipid A species released by acetic acid hydrolysis from wild-type and phosphatase mutants

Approximately 5 μg of the lipid A molecules released from wild-type *R. etli* or the single phosphatase mutants by hydrolysis in 1% acetic acid were spotted onto a silica gel 60 TLC plate, which was developed in the solvent system $CHCl_3$/MeOH/H_2O/NH_4OH (40:25:4:2, vol./vol./vol./vol.). The lipids were detected after chromatography by spraying with 10% sulfuric acid in ethanol and charring on a hot plate. The tentative assignments of the lipid species are based on their relative migrations in this experiment, which were previously validated for the wild-type (Que et al., 2000a, Que et al., 2000b).

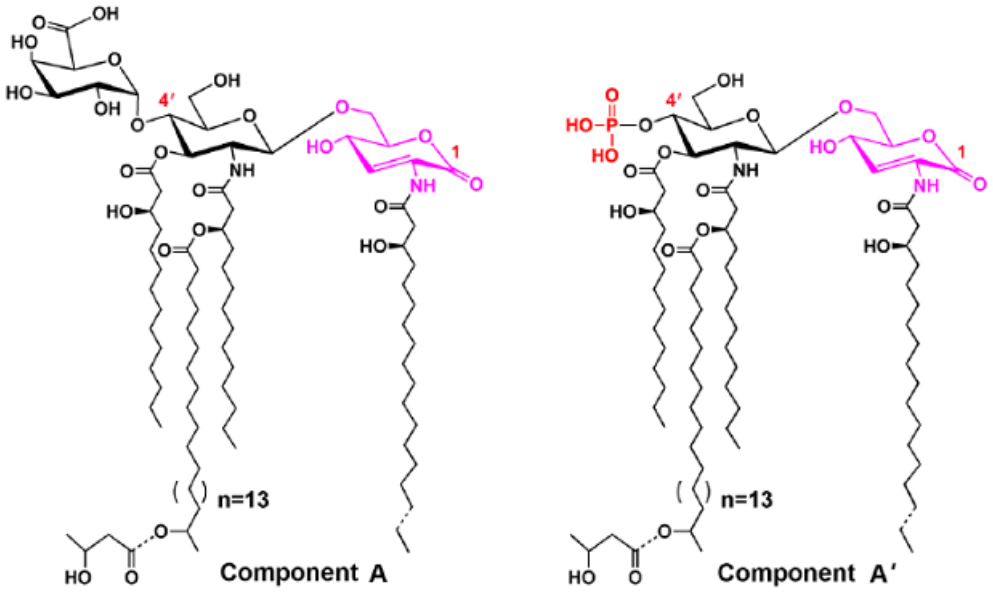

Figure 53: Lipid A hydrolysis artifact.

A. Component A from *R. etli* is most likely a hydrolysis artifact derived from component D (Que et al., 2000a, Que et al., 2000b). Component A is most likely created by the lactonization of the 2-aminogluconate residue and the subsequent acid-catalyzed elimination of the acyl chain at the 3 position. **B.** A similar component is observed in the 4′-phosphatase knockout strain. The exact masses of the most abundant species are shown.

consisted of only two major components, designated F and G (Fig. 52). The retention of the phosphate group at the 1-position of these lipid A molecules prevents their oxidation by LpxQ (Fig. 48) (Que-Gewirth et al., 2003a, Que-Gewirth et al., 2003b), thereby reducing their overall microheterogeneity (Fig 51B). The lipid A species of the *lpxE/lpxF* double mutant migrated even more slowly compared to the others and likewise showed less microheterogeneity (see below).

5.3.3. ESI/MS analysis of the lipid A species

The negative ion ESI mass spectra of the total lipid A species extracted from the wild-type and the single phosphatase mutants are shown in Fig. 54. The predicted masses of the major molecular species are listed in Table 14. In Fig. 54A, which shows the spectrum of wild-type R. etli lipid A, there are several clusters of ions that are consistent with previous assignments (Que et al., 2000a, Que et al., 2000b). In the region between m/z 1850 and 2050, the most intense ion is observed at m/z 2000.49, which is interpreted as the $[M-H]^-$ ion of component D (Fig. 47C). The $[M-H]^-$ ion of component B, which is the biosynthetic precursor of D (Fig. 47B), is seen at m/z 1984.48. The $[M-H]^-$ ions of the deacylated versions of components B and D (designated C and E in Fig. 47) are seen at m/z 1758.28 and 1774.29, respectively (Fig. 54A). The intense peak at m/z 1738.26 corresponds to component A (Fig. 53), which arises from D during acid hydrolysis (Que et al., 2000a, Que et al., 2000b). There is significant additional

microheterogeneity in all these lipid A species because of acyl chain length differences and/or the presence of a β-hydroxybutyryl moiety at the 27:OH position of the 2′-acyloxyacyl chain (difference of 86 amu) (Bhat et al., 1994, Que et al., 2000a, Que et al., 2000b). These additional differences are annotated in the legend to Fig. 54.

The singly charged lipid A species from the *lpxF* 4′-phosphatase mutant CS506 are shown in Fig. 54B. The overall pattern of peaks in this mutant resembles that of the wild-type (Fig. 52 and Fig. 54A); however, all of the ions are shifted to *m*/*z* values that are 96 amu smaller than wild-type (Fig. 54B versus Fig. 54A). This change in mass results from the replacement of the galacturonic acid residue at the 4′-position with a phosphate moiety. No residual wild-type lipid A species are detected. The major peak at *m*/*z* 1904.40 is interpreted as the $[M - H]^-$ ion of component D′ (Fig. 51 and Fig. 52). The $[M - H]^-$ ion of component B′, the biosynthetic precursor of the D′, is observed at *m*/*z* 1888.28. The 3-*O*-deacylated versions of these species and the elimination product, A′, appear in the clusters of ions below *m*/*z* 1700. Additional lipid A microheterogeneity due to acyl chain length differences and partial substitution with the β-hydroxybutyryl moiety is annotated in the legend to Fig. 54.

The singly charged lipid A species obtained from the *lpxE* 1-phosphatase mutant CS501 are shown in Fig. 54C. As in the *lpxF* mutant, no peaks corresponding to residual wild-type lipid A molecules are detected. Two new major lipid A species are present in

this strain (Fig. 52). The peaks at m/z 2064.43 and m/z 1838.24 are interpreted as the [M − H]− ions of components F and G, respectively (Fig. 51 and Fig. 52). There are no aminogluconate-containing lipid A derivatives in this strain because the presence of the 1-phosphate group prevents oxidation by LpxQ (Fig. 51B). The peaks are therefore all shifted to correspondingly higher *m*/*z* values. Additional lipid A microheterogeneity arising from acyl chain differences and the β-hydroxybutyryl moiety is annotated in the legend to Fig. 54.

5.3.4. ESI/MS of the lipid A species from the double lpxE/lpxF mutant

The lipid A molecules of the *lpxE*/*lpxF* double mutant contain two phosphate moieties. Therefore, the predominant lipid A ions seen in the negative mode are doubly charged, as shown in Fig. 55. The $[M - 2H]^{2-}$ ions of components H and I (Fig. 51C and Table 14) are observed at *m*/*z* 983.64 and 870.56, respectively (Fig. 55). These species resemble those of the *lpxE* single mutant in that they lack the components harboring the aminogluconate modification in the proximal unit. Their masses are shifted to lower values compared to wild-type because of the replacement of the 4′-galacturonic acid residue with a phosphate moiety. The additional microheterogeneity arising from acyl chain differences and partial substitution with the β-hydroxybutyryl moiety is indicated in the legend to Fig. 55.

Figure 54: ESI/MS analysis of lipid A species released by acetic acid hydrolysis from wild-type and single phosphatase mutants.

The lipid A released from the wild-type or the phosphatase deletion mutants by 1% acetic acid hydrolysis was analyzed by negative ion ESI/MS. **A.** The peaks in the singly charged region corresponding to the four major components of wild-type *R. etli* lipid A (B, C, D, and E), shown in Figs. 47B and C, are labeled and color-coded. Component A (Fig. 53) is an elimination artifact derived from D during hydrolysis (Que et al., 2000a, Que et al., 2000b). There is additional microheterogeneity (see below) with regard to acyl chain length or the presence of the β-hydroxybutyrate substituent for each component, in agreement with previous studies (Bhat et al., 1994). **B.** The spectrum in the singly charged region of the lipid A from the LpxF 4′-phosphatase mutant shows the same relative pattern of peaks as the wild-type, but each component (B′, C′, D′, and E′) is shifted by 96 amu because of the replacement of the 4′-galacturonic acid moiety with a phosphate group (Fig. 51A). **C.** The spectrum in the singly charged region of the lipid A species from the LpxE 1-phosphatase mutant (Fig. 51B) shows peaks at increased *m*/*z* values because of the retention of the phosphate group at the 1-position. There are also fewer lipid A components in this mutant because oxidation of the proximal glucosamine unit by LpxQ cannot occur. The hydrolysis artifacts (A and A′), seen in wild-type *R. etli* and mutant CS506, respectively, are therefore not present in this strain. Additional microheterogeneity in fatty acid chain length (14 or 28 amu) and partial substitution with β-hydroxybutyrate (86 amu) is observed in the lipid A species of all these strains. Each major lipid A species and some of its corresponding acyl chain variants are grouped by color. Symbols indicate the following amu shifts: for Panels A and B: + = (−28), ⁎ = (−86), • = (−86 and −28); for Panel C: + = (−28), ⁎ = (−86), • = (−86 and −28), ⋆ = (+ 28), ⁝ = (+ 14), α = (−86 and + 28), ¢ = (−14), π = (−86 and + 14), ∂ = (−86 and + 14 and + 28), λ = (−86 and −14).

Figure 54: ESI/MS analysis of lipid A species released by acetic acid hydrolysis from wild-type and single phosphatase mutants.

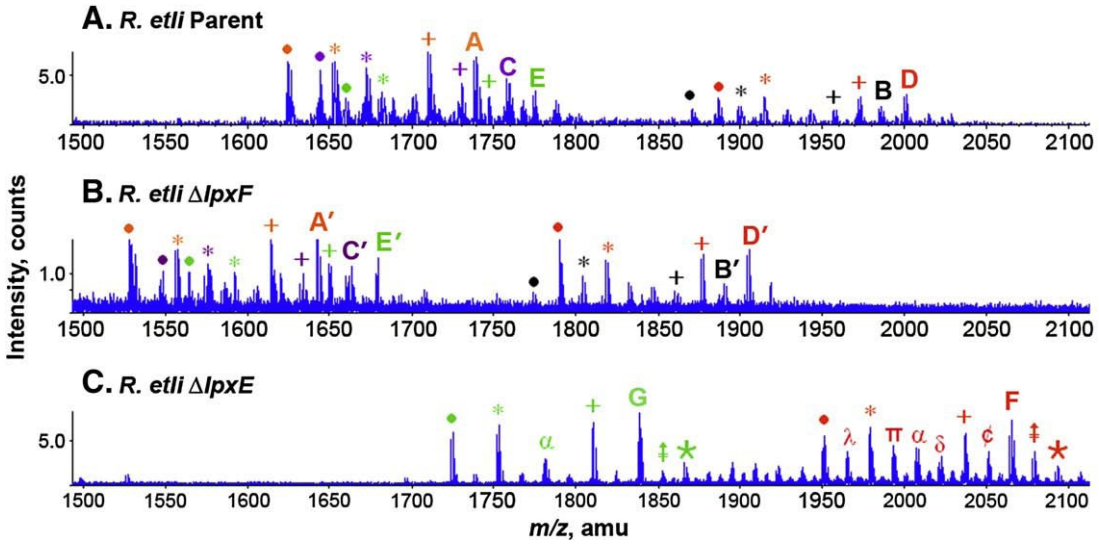

Table 14: Masses of lipid A components from *R. etli* wild-type and phosphatase knockout strains

Strain						
R etli	Component	**B**	**C**	**D**	**E**	**A**
	Molecular formula	$C_{110}H_{204}N_2O_{27}$	$C_{96}H_{178}N_2O_{25}$	$C_{110}H_{204}N_2O_{28}$	$C_{96}H_{178}N_2O_{26}$	$C_{96}H_{174}N_2O_{24}$
	Exact Mass	1985.47	1759.27	2001.46	1775.27	1739.25
	Observed m/z $[M-H]^-$	1984.48	1758.28	2000.49	1774.29	1738.26
CS506	Component	**B'**	**C'**	**D'**	**E'**	**A'**
	Molecular formula	$C_{104}H_{197}N_2O_{24}P$	$C_{90}H_{171}N_2O_{22}P$	$C_{104}H_{197}N_2O_{25}P$	$C_{90}H_{171}N_2O_{23}P$	$C_{90}H_{167}N_2O_{21}P$
	Exact Mass	1889.4	1663.21	1905.39	1679.2	1643.18
	Observed m/z $[M-H]^-$	1888.28	1662.20	1904.40	1678.21	1642.18
CS501	Component	**F**	**G**			
	Molecular formula	$C_{110}H_{205}N_2O_{30}P$	$C_{96}H_{179}N_2O_{28}P$			
	Exact Mass	2065.43	1839.24			
	Observed m/z $[M-H]^-$	2064.43	1838.24			
CS513	Component	**H**	**I**			
	Molecular formula	$C_{104}H_{198}N_2O_{27}P_2$	$C_{90}H_{172}N_2O_{25}P_2$			
	Exact Mass	1969.37	1743.17			
	Observed m/z $[M-2H]^{2-}$	983.64	870.56			

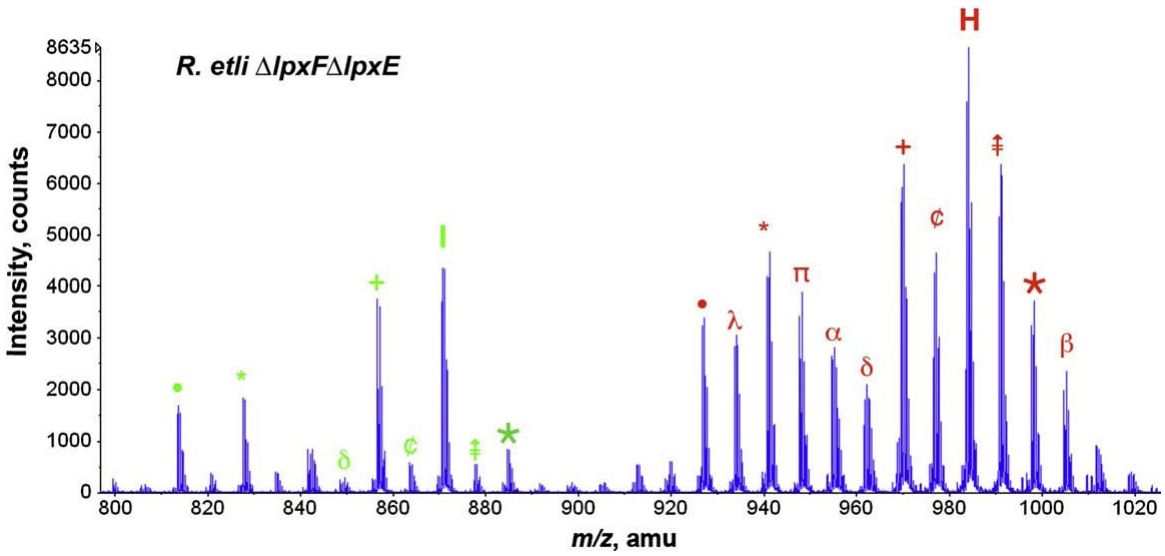

Figure 55: ESI/MS analysis of lipid A species released by acetic acid hydrolysis from the double phosphatase mutant

The spectrum in the negative ion mode was the accumulation of 60 scans from 200 to 2400 amu. Only the doubly charged ions of the spectrum are shown, because the peaks of the singly charged species are very small. The two major lipid A components of this mutant (H and I) lack the galacturonic modification at the 4′-position, which is replaced by a phosphate group, and do not contain the aminogluconate unit (Fig. 51C). Heterogeneity in fatty acid chain length (14 or 28 amu) and partial substitution with β-hydroxybutyrate (86 amu) is observed. The major lipid A species and their corresponding acyl chain variants are grouped by color. Symbols indicate the following amu shifts: + = (−28), ⁎ = (−86), • = (−86 and −28), ★ = (+ 28), ‡ = (+ 14), β = (+ 28 and + 14), ¢ = (−14), π = (−86 and + 14), α = (−86 and + 28), ð = (−86 and + 14 and + 28), λ = (−86 and −14).

5.3.5. Determination of lipid A phosphatase activity in wild-type *R. etli* and the *lpxF* mutant

The *in vitro* LpxF activity of the wild-type and the two single mutants was measured using washed membranes as the enzyme source. In this assay system, the substrate Kdo_2-[4′-^{32}P]-lipid IV_A is dephosphorylated and free inorganic phosphate is released as $^{32}P_i$. As shown in Fig. 56, the robust 4′-phosphatase activity that is characteristic of wild-type *R. etli* membranes (Price et al., 1995) is absent in the *lpxF* mutant CS506 but is present in the *lpxE* mutant CS501.

The 1-phosphatase activity encoded by *R. etli lpxE* cannot be assayed in crude membranes preparations, and therefore, its absence in *lpxE* mutant membranes could not be demonstrated (not shown). However, in *R. leguminosarum* and *F. novicida* membranes, LpxE activity is easily detected with Kdo_2-[4′-^{32}P]-lipid IV_A as the substrate under otherwise similar conditions (Karbarz et al., 2003, Wang et al., 2004). It may be that *R. etli* extracts contain an inhibitor of LpxE activity that interferes with the assay.

5.3.6. Polymyxin sensitivity of *R. etli* strains

Polymyxin-resistant strains of *E. coli* and *Salmonella typhimurium* survive by modifying their lipid A phosphate groups with 4-amino-4-deoxy-l-arabinose and phosphoethanolamine (Raetz et al., 2007). The reduction of the net negative charge on lipid A helps reduce the binding of polymyxin and other cationic antimicrobial peptides. *R. etli* removes the phosphate groups from its lipid A during biosynthesis (Fig. 48), and

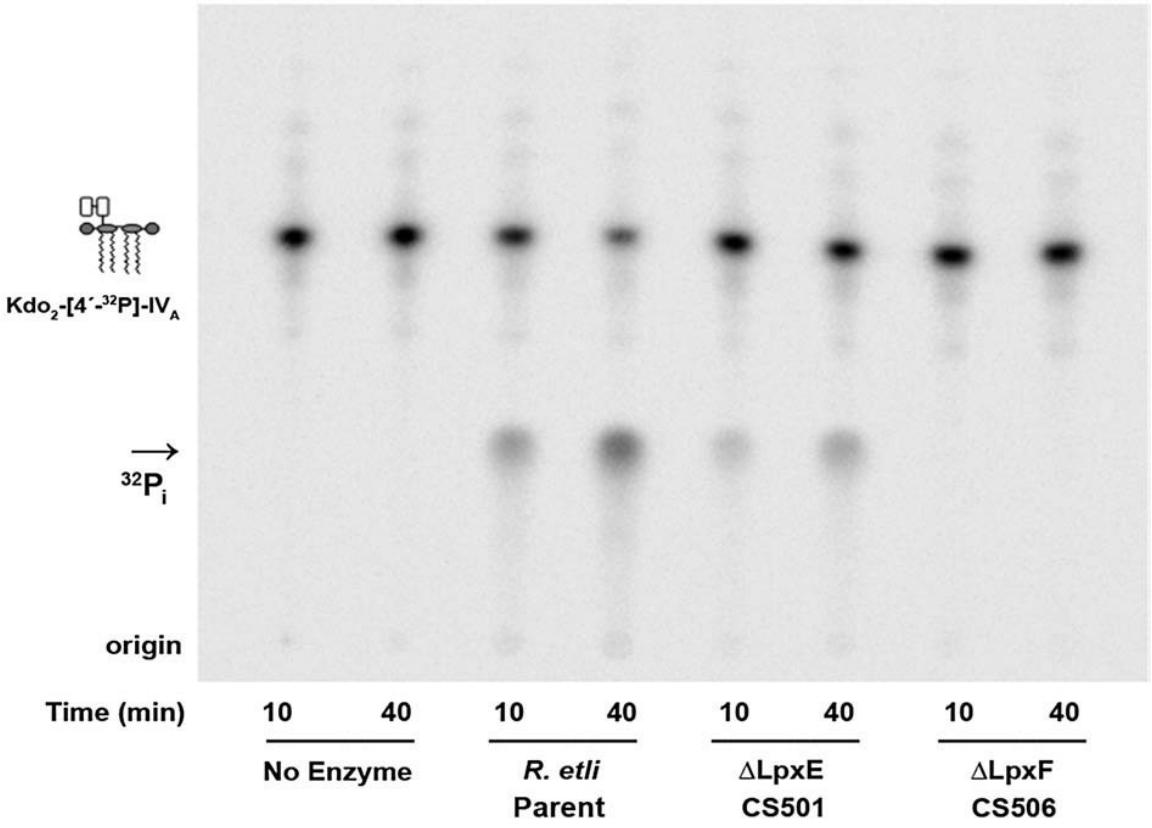

Figure 56: Absence of 4′-phosphatase activity in membranes *R. etli* deletion mutant CS506

Membranes of the indicated strains (0.25 mg/mL) were assayed for 4′-phosphatase activity at 30 °C with 5 μM [4′-^{32}P]Kdo_2-lipid IV_A. The products were separated by TLC using the solvent chloroform/pyridine/88% formic acid/water (30:70:16:10, vol./vol./vol./vol.), followed by detection with a PhosphorImager. No enzyme; parent, *R. etli* CE3 wild-type; CS501, *R. etli* Δ*lpxE*; CS506, *R. etli* Δ*lpxF*.

replaces them with galacturonic acid and aminogluconate residues (Fig. 47 and Fig. 48). The substitution of phosphate groups with these moieties would also reduce the net negative charge of lipid A. To determine if retention of one or both phosphate groups leads to polymyxin hypersensitivity, disk diffusion assays with polymyxin B were performed. Both the *lpxE* and *lpxF* single mutants showed increased sensitivity to polymyxin B compared to wild-type (Table 15), and the double mutant showed the greatest sensitivity.

5.3.7. Membrane lipid composition of *R. etli* strains

The *R. etli* lipid A phosphatases LpxE and LpxF contain sequence motifs that are present in many other lipid phosphate phosphatases (Stukey & Carman, 1997), suggesting a conserved structure and mechanism of action. However, some LpxE orthologues, such as that found in *A. tumefaciens*, do not show lipid A 1-phosphatase activity. Instead, the putative *A. tumefaciens* LpxE orthologue dephosphorylates phosphatidylglycerol phosphate (Gonzalez et al., 2006). The overall membrane lipid composition of the *R. etli* wild-type and the phosphatase knockouts was therefore examined to exclude the possibility of other alterations in lipid composition. The strains were grown in TY medium, and their membrane lipids were labeled with [14C]-acetate. The lipids were extracted, separated by TLC and quantified by PhosphorImager analysis (Table 16). No significant differences were observed between the wild type and the

mutants. The major membrane lipids in each of these strains were phosphatidylcholine, phosphatidylethanolamine, phosphatidyldimethylethanolamine, phosphatidylglycerol, cardiolipin, sulfolipid, and ornithine lipid, consistent with published data (Geiger *et al.*, 1999).

5.3.8. Symbiotic phenotypes of the *R. etli* phosphatase mutants

P. vulgaris roots were inoculated with *R. etli*, the *lpxE* mutant CS501, the *lpxF* mutant CS506, and the double mutant CS513. Eight plants were inoculated in each of four independent experiments, which are highlighted by the differential shading of the columns. One independent experiment therefore consists of 40 plants (8 control plants that were not inoculated, 8 plants inoculated with wild type CE3, 8 plants inoculated with CS501, 8 plants inoculated with CS506, and 8 plants inoculated with CS513). Three weeks after the inoculation, all four strains had induced the formation of nodules that were similar in appearance. Acetylene reduction assays were performed to determine if any of the strains were defective in nitrogen fixation. No significant differences were observed when nitrogen fixing activities per gram of nodule fresh weight were compared (Fig. 57). To exclude the possibility that the lack of a symbiotic phenotype was caused by contaminating wild-type cells, bacteria were reisolated from the nodules and their genomic DNA probed by Southern blotting to confirm their identity (data not shown).

Table 15: Increased polymyxin sensitivity of *R. etli* CE3 mutants lacking the lipid A phosphatases

	Zone of clearing diameter (mm)[a]		
	Amount of polymyxin added per disk		
Strain	(2 μg)	(10 μg)	(20 μg)
R. etli CE3	8	10	12
CS501 (Δ*lpxE*)	9	12	14
CS506 (Δ*lpxF*)	10	14	15
CS513 (Δ*lpxE*/Δ*lpxF)*	15	17	18

[a]The diameter of the disk is 6 mm, and the diameter of the zone of clearing shown above includes the disk diameter. The precision of the measurement of the diameter is ± 0.5 mm.

Table 16: Membrane lipid composition of *R. etli* CE3 strains

Component	*R. etli* CE3	CS501	CS503	CS513
		Δ*lpxE*	Δ*lpxF*	Δ*lpxE*/ Δ*lpxF*
PE	36.8 ± 1.4	40.9 ± 2.7	38.4 ± 0.3	41.9 ± 1.7
PC	34.5 ± 3.9	33.9 ± 5.5	35.8 ± 1.1	30.2 ± 1.2
OL	5.5 ± 1.2	5.1 ± 0.8	4.5 ± 0.4	4.7 ± 0.8
PG	14.5 ± 1.3	11.2 ± 0.9	13.8 ± 1.7	14.3 ± 2.1
CL	5.3 ± 2.4	5.9 ± 2.0	4.2 ± 0.4	5.9 ± 1.7
SL	1.8 ± 0.8	1.0 ± 0.5	0.8 ± 0.3	1.0 ± 0.6
DMPE	1.9 ± 0.6	2.1 ± 0.7	1.7 ± 0.1	2.1 ± 0.9

The data in this table was collectd by C. Sohlenkamp.

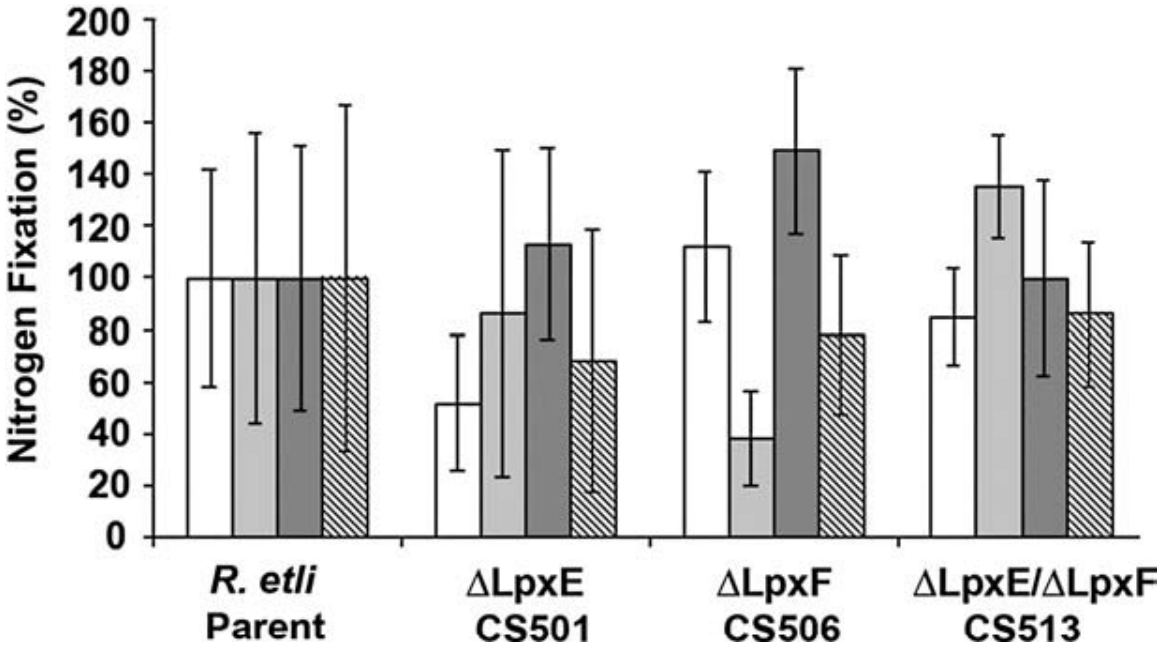

Figure 57: Nitrogen fixation in nodules of wild-type and mutant *R. etli*

Nitrogen fixation activity was determined using an acetylene reduction assay. Every strain was analyzed in four independent experiments, each comprised of 8 plants, as highlighted by the differential shading of the four columns. Columns show the relative nitrogen fixation activity and error bars indicate the standard deviations within each of the four independent experiments. Nitrogen fixation activity is expressed as the amount of ethylene formed per weight of fresh nodule, normalized to the nitrogen fixation activity of the wild-type CE3. Parent, *R. etli* CE3 wild-type; CS501,*R. etli* lipid A 1-phosphatase Δ*lpxE* mutant; CS506, *R. etli* lipid A 4′-phosphatase Δ*lpxF* mutant; CS513, *R. etli* mutant deficient in Δ*lpxF* and **Δ***lpxE*. This data was collected by C. Sohlenkamp.

5.4 Discussion

Lipid A, the hydrophobic moiety of LPS, is recognized by Toll-like receptor 4 (TLR-4) in animals, triggering the innate immune response (Park et al., 2009, Beutler et al., 2006, Akira *et al.*, 2006). The constitutive lipid A biosynthetic pathway is largely conserved in Gram-negative bacteria (Raetz et al., 2007), but species-specific modifications of lipid A may play a role in helping pathogens evade the innate immune response (Raetz et al., 2007). For example, *Escherichia coli* and *S. enterica* sv. *typhimurium* modify their lipid A with 4-aminoarabinose and phosphoethanolamine moieties in response to changes in environmental conditions found within their respective hosts, conferring resistance to cationic antimicrobial peptides (Raetz et al., 2007). These covalent modifications are controlled by the two component regulatory systems PhoP/Q and PmrA/B, which are induced by low Mg^{2+} and low pH, respectively (Gibbons et al., 2005).

Rhizobia form chronic infections on plant root hair cells during symbiosis, and like animal pathogens must survive within host-membrane-derived intracellular compartments during this process. The bacteria adapt to dramatic changes in acidity, osmolarity, and oxygen tension in these compartments. Most of the unusual covalent modifications characteristic of *R. etli* lipid A are observed in free-living bacteria (Que et al., 2000a, Que et al., 2000b) but it was, nevertheless, proposed that some of these lipid A

modifications might play a role in the bacteria–plant symbiosis. Dephosphorylation of *R. etli* lipid A was of special interest because pharmacological studies have indicated that the presence of both phosphate groups on lipid A are important for its cytokine-inducing activities in animal systems (Rietschel et al., 1994). Furthermore, a recently isolated 4′-phosphatase mutant of the animal pathogen *F. novicida*, was shown to display dramatically attenuated virulence in mice (Wang et al., 2007). The *F. novicida* 4′-phosphatase mutant was viable but severely limited in its ability to kill mice compared to wild-type strains because of its hypersensitivity to cationic antimicrobial peptides (Wang et al., 2007).

We have now constructed and characterized a 1-phosphatase (*lpxE*) mutant, a 4′-phosphatase (*lpxF*) mutant, and a 1-/4′-phosphatase (*lpxE*/*lpxF*) double mutant of *R. etli*. The candidate phosphatase genes were found by searching the recently completed *R. etli* genome (Gonzalez et al., 2006) with the LpxE sequence from *R. leguminosarum* (Karbarz et al., 2003) and the LpxF sequence from the *F. novicida* (Wang et al., 2006a). LpxE and LpxF both reside in the inner membrane with active sites that face the periplasm (Wang et al., 2004, Wang et al., 2006a), and both have absolute specificity in selecting the site of dephosphorylation on lipid A (Wang et al., 2004, Wang et al., 2006a, Karbarz et al., 2009, Basu et al., 1999b). LpxE and LpxF do not share significant similarity in their primary amino acid sequences (Wang et al., 2004, Wang et al., 2006a), but both contain variations

of the phosphatase sequence motif described by Stukey and Carman (Stukey & Carman, 1997).

We have demonstrated that the LpxE and LpxF mutant strains accumulate lipid A species retaining one or both phosphate moieties, as predicted by the pathway shown in Fig. 48 and Fig. 51. The retention of the phosphate groups at the 4′-position blocks the incorporation of a galacturonic acid residue (Fig. 51 and Fig. 54), and the presence of a phosphate group at the 1-position prevents the oxidation of the proximal glucosamine residue to 2-aminogluconate (Fig. 51 and Fig. 54). The results indicate that the two lipid A phosphatases work independently of each other, have no established order for operation, and are solely responsible for the lipid A dephosphorylaion seen in *R. etli* (Que et al., 2000a, Que et al., 2000b).

The free-living *R. etli* phosphatase mutants had no changes in growth rate, and the membrane lipid composition remained unchanged (Table 16), indicating that these phosphatases do not have any significant activity directed towards other lipid substrates. Both phosphatase mutants, however, showed an increase in sensitivity to the cationic antimicrobial drug, polymyxin, consistent with the increase in net negative charge provided by the retention of the phosphate groups. The *lpxE*/*lpxF* double mutant, which accumulates bisphosphorylated lipid A species similar to that found in *S. meliloti*

(Gudlavalleti & Forsberg, 2003) (Fig. 51 and Fig. 55), displayed the greatest sensitivity to polymyxin (Table 15).

Despite having dramatically altered lipid A structures, all the mutants were found to form normal nodules and were equally competent in nitrogen fixation when compared to the wild-type strain (Fig. 57). This implies that dephosphorylation of lipid A, as well as modification with galacturonic acid and aminogluconate residues, is not essential for establishing an effective symbiosis. However, subtle alterations in the time course of nodule formation cannot yet be excluded. These modifications may also play other roles for the bacteria in their native environment. The removal of the phosphate groups from the lipid A molecules may be important in the rhizosphere, which is much more diverse than the controlled sterile environment used in our study (Fig. 57). One likely advantage of *R. etli* dephosphoryating its lipid A may be resistance to cationic antimicrobial peptides, like polymyxin (Table 15). Dephosphorylation of lipid A could protect *R. etli* in the rhizosphere from diverse cationic antimicrobial compounds. Plants have been shown to produce defense compounds of this kind (Campbell *et al.*, 2002, Epand & Vogel, 1999). The further modifications to the lipid A disaccharide backbone of lipid A molecules in *R. etli* after dephosphorylation could play a role in maintaining membrane stability in the absence of phosphate groups. These modifications might also function to conserve phosphorus in low-phosphate environments.

To date, the only characterized lipid A mutants of a *Rhizobium* species are ones that affect lipid A acylation (Sharypova et al., 2003, Vedam *et al.*, 2003). Mutants that harbor a disruption in the gene encoding the acyl carrier protein that carries the (27OHC28:0) moiety (AcpXL) have been constructed in both *R. leguminosarum* and *S. meliloti* (Sharypova et al., 2003, Vedam et al., 2003). These mutants are of interest because the (27OHC28:0) moiety is found in nearly all members of the Rhizobiaceae family (Bhat *et al.*, 1991a). The *acpXL* mutants lacked the modification with the (27OHC28:0) moiety but were shown to contain a small amount of C18:0 at the 2′-secondary position (Vedam et al., 2003). Both mutants displayed sensitivity to detergents, acidic conditions, and changes in osmolarity, and both also displayed slow nodulation kinetics compared to wild-type cells. However, the nodules displayed a normal morphology and fixed nitrogen, but differed slightly in bacteroid development (Vedam et al., 2003). In *S. meliloti*, *lpxXL* and *acpXL/lpxXL* mutants were also described (Ferguson *et al.*, 2005). These mutants lacked secondary acyl chains, but were found to form nitrogen fixing nodules in a delayed manner. Hence, it was originally reported that the 28 carbon fatty acyl chain is beneficial, but not critical for symbiosis to occur. A recent report claims that a *R. leguminosarum acpXL* mutant supposedly regains the ability to acylate the lipid A of bacteroids with the 27-hydroxyoctacosanoic acid moiety in the nodule environment by an uncharacterized mechanism (Vedam et al., 2006), the details of which require further

investigation. Although improbable, it likewise remains possible that the host plant has mechanisms for removing the lipid A phosphate groups that are present in the phosphatase mutant strains in the *in planta* environment. An analysis of the lipid A from the mutant bacteroids will be necessary to clarify this issue.

Little is known about the response of plants to lipid A-like molecules (Zeidler et al., 2004); however, plants do have systems of immunity (Jones & Dangl, 2006). Recognition of conserved microbial molecules like lipid A, could result in the activation of various antimicrobial effectors that ward off attacks by plant pathogens. It is not known which molecular features of lipid A are ultimately responsible for these effects. Defining how the plant perceives lipid A and other microbial molecules might aid in our understanding of how symbiotic bacteria evade these plant-associated immune responses.

In summary, the galacturonate and aminogluconate modifications of lipid A seen in *R. etli* appear not to be required for nodulation. We conclude that these modifications most likely play a role in stabilizing the outer membrane of the bacteria and might also be involved in protecting the symbiont from the immune response of the host plant during pathogenic infections. We speculate that the dephosphorylation of lipid A molecules in *R. etli* might allow the plant to discriminate between plant pathogens and symbiotic bacteria and assist the bacteroids in evading the immune response of plants

during pathogenic infections. Future work will address the roles that the lipid A components from symbiotic bacteria and plant pathogens play in eliciting or suppressing plant defenses.

5.5 Statement of collaborative work

The data and text presented in this chapter has been published by Ingram, B.O., Sohlenkamp C., Geiger, O., and Raetz, C.R.H. It appears in *BBA-Mol Cell Biol L.* as "Altered lipid A structures and polymyxin hypersensitivity of *Rhizobium etli* mutants lacking the LpxE and LpxF phosphatases.Article *in press.*

Some of the data in this chapter was collected in collaboration. C. Sohlenkamp generated the knockout strains, conducted the nodulation studies (Fig. 57), and quantified the phospholipids (Table 16).

Chapter 6: Identification and Characterization of the *Rhizobium etli* PagL gene

6.1 Introduction

The bacterial endosymbionts *R. etli* and *R. leguminosarum* are heterogeneous in their lipid A composition. These bacteria contain both tetraacylated and pentaacylated species. The tetraacylated species arise from a membrane-bound deacylase (Fig. 58) (Basu et al., 1999a). The activity of this enzyme was previously characterized from *R. leguminosarum* membranes. The *R. leguminosarum* enzyme was shown to be capable of removing the 3-O acyl chain of lipid A precursors including lipid IV_A and Kdo_2-lipid IV_A. The activity of the enzyme was also shown to be dependent on the presence of both detergent and divalent cations. (Basu et al., 1999a). The identification of the gene responsible for the enzymatic activity has not been determined.

A 3-*O*-deacylase activity similar to that described in *R. leguminosarum* has been described in *S. typhimurium* and *P. aeruginosa* (Trent et al., 2001a, Geurtsen *et al.*, 2005, Rutten et al., 2006). The protein responsible for this activity, in these organisms, PagL, is found in many other Gram-negative bacteria. An intriguing feature of the PagL homologs is their low primary sequence conservation (Geurtsen et al., 2005). In distant related homologs, only the active site residues are completely conserved. In this chapter, homologs of PagL are described in *R. etli* and *S. meliloti*. We show that the two homologs

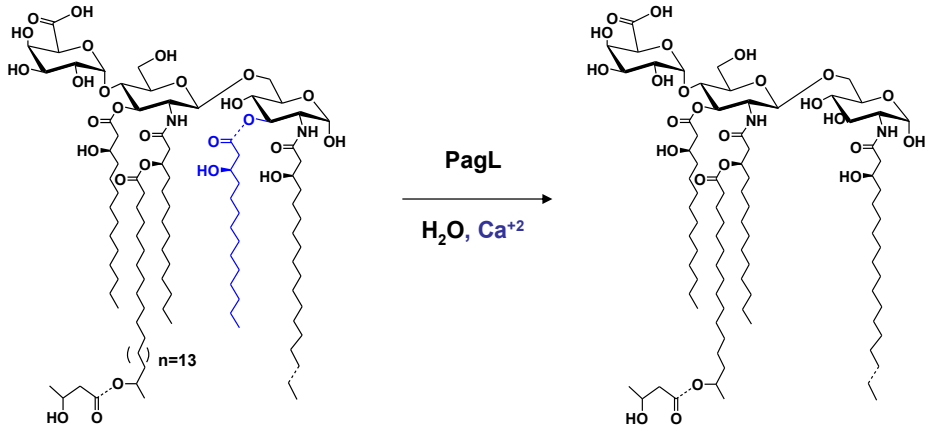

Figure 58: Proposed reaction catalyzed by *R. etli* PagL.

The *R. etli pagL* homolog is proposed to catalyze the removal of the 3-*O* acyl chain from *R. etli* lipid A. The enzyme requires divalent cations, such as Ca^{2+} for activity *in vitro (Basu et al., 1999a)*.

are functional deacylases. The *R. etli* protein is shown to have the same properties as the protein characterized from *R. leguminosarum* membranes.

The biological role of the PagL-catalyzed modification is unknown in many of the organisms it is found in. Given its presence in both pathogenic and non-pathogenic bacteria, it is believed not to be important in pathogenesis. Recently it was reported, that *R. etli* bacteroids isolated from nodules were exclusively tetraacylated (D'Haeze et al., 2007). This result suggested a key role for the lipid A deacylation modification in the nodule environment. In an effort to determine the importance of PagL activity, we constructed a *R. etli PagL* mutant. The biological properties of the mutant are described herein.

6.2 Materials and Methods

6.2.1 Materials

[γ-^{32}P] ATP was obtained from PerkinElmer Life And Analytical Sciences, Inc. (Waltham, MA). Acetic acid, ammonium acetate, chloroform, formic acid, and glass-backed 0.25-mm Silica Gel-60 thin layer chromatography (TLC) plates were from EMD Chemicals, Inc. (Gibbstown, NJ). Pyridine and methanol were from Mallinckrodt Baker, Inc. (Phillipsburg, NJ). Yeast extract, agar, and tryptone were from Becton, Dickinson, and Company (Franklin Lakes, NJ). Sodium chloride and 4-(2-hydroxyethyl)-1-piperazineethanesulfonic acid (HEPES) were from VWR International (West Chester,

PA). Bicinchoninic (BCA) protein assay reagents and Triton X-100 were from Thermo Fisher Scientific (Waltham, MA). Diethylaminoethyl (DEAE) cellulose DE52 was from Whatman, Inc. (Florham Park, NJ). PCR reagents were purchased from EMD and Stratagene (La Jolla, CA). IPTG was from Invitrogen (Carlsbad, CA).All other chemicals were reagent grade and were purchased from either Sigma-Aldrich (St. Louis, MO) or VWR International (West Chester, PA).

6.2.2 Bacterial strains, growth conditions and molecular biology protocols

The bacterial strains and plasmids used and their relevant characteristics are shown in Table 17. *R. etli* strains were grown at 30 °C on complex tryptone yeast extract medium (TY) supplemented with 10 mM $CaCl_2$ (Beringer, 1974). *Rhizobium* stains were grown in media supplemented with the following concentrations of antibiotics where appropriate: neomycin (200 μg/mL), nalidixic acid (20 μg/mL) (streptomycin (200 μg/mL), and spectinomycin (200 μg/mL). *E coli* strains were cultured on LB broth at 37 °C. Growth media were supplemented with the following concentrations of antibiotics where appropriate: kanamycin (50 μg/mL), carbenicillin (100 μg/mL), spectinomycin (200 μg/mL), or ampicillin (100 μg/mL). Derivatives of the suicide plasmid pK18*mobsac*B (Table 17) were mobilized into *R. etli* strains by triparental mating using the mobilizing plasmid pRK2013, as described previously (Ruvkun & Ausubel, 1981). Recombinant DNA techniques were performed according to standard protocols (Sambrook & Russell,

2001) using *E. coli* DH5α as a host strain (Hanahan, 1983). The XL-PCR kit (Applied Biosystems) was used for amplifying DNA sequences from *R. etli* genomic DNA.

6.2.3 Construction of plasmids RePagL and SmPagL

The primers RePagLfor (5′-CGCGC*CATATG***AGGGTCGAGTTCGGAAAG ATCG**-3′) and RePagLrev (5′-GCGCG*AAGCTT***TCAGAACTTGTAGCCGATCTGG ATGCCG** -3′) were used to amplify the *R. etli pagL* gene from genomic DNA. The primers SmPagLfor (5′- CGCGC*CATATG***AGAGATTTCCGCTCGGTTGCAGG**-3′) and SmPagLrev (5′- CGCG*AAGCTT***TTAGAACGTGTAGCCGAGCATCAACC**-3′) were used to amplify the *S. meliloti pagL* gene from genomic DNA. The coding region of PagL in the two primers is indicated in bold type, and the restriction enzyme sites are italicized. Both of the PCR products were digested with *Nde*I and *HindIII* and ligated into pET23a(+) (EMD Chemicals Inc.), yielding plasmids RlPagL and SmPagL. The plasmids were transformed into competent *E. coli* DH5α cells and their sequence was confirmed by DNA sequencing. The plasmids were then transformed into BLR(DE3) cells.

6.2.4 Exchange of the *R. etli pagL* gene with a spectinomycin resistance cassette

A pagL deletion mutant in *R. etli* was constructed using the same procedures used in chapter 5 for generating the single phosphatase knockout strains. PCR and molecular cloning methods were utilized to generate a plasmid containing a

spectinomycin cassette flanked by the upstream and downstream regions of R. etli *pagL*. The cassette and flanking regions were subcloned from the plasmid into the suicide vector pK18*mobsacB* and introduced by triparental mating into wild-type *R. etli* CE3 using pRK2013 as a helper plasmid. The selection procedure described in chapter 5 was used for selecting recombinants. Southern Blot analysis was used to confirm deletion of the PagL gene.

6.2.5 Expression of PagL

Single colonies of BLR(DE3)/RePagL and BLR(DE3)/SmPagL were used to inoculate 5 mL of LB supplemented with 100 μg/mL ampicillin. The cultures were grown overnight at 37 °C with shaking at 225 rpm and used to inoculate 200 mL of LB broth supplemented with ampicillin (100 μg/mL) to a starting A_{600} ~ 0.01. The cells were grown with shaking at 37 °C until the A_{600} reached 0.6, at which time 1 mM IPTG was added. The cells were grown for 3 additional hours and harvested by centrifugation at 4000 x g for 20 min at 4 °C. The cells were washed with 50 mM HEPES, pH 7.5. The washed cell pellet was stored frozen at -80 °C.

6.2.6 Preparation of *R. etli* and *E. coli* membranes

All enzyme preparations were carried out at 0-4 °C. The bicinchoninic acid method (Smith et al., 1985) was used to determined protein concentrations, using bovine

serum albumin as a standard. Washed membranes were prepared as described previously (Basu et al., 2002) and stored in aliquots at -80 °C.

6.2.7 Preparation of substrates

The preparation of carrier lipid IV_A was described in chapter 3. [4′-^{32}P]-lipid IV_A was prepared as described previously (Basu et al., 1999a). The substrates were stored frozen as aqueous dispersions in 25 mM Tris-HCl, pH 7.8, containing 1 mM EDTA, 1mM EGTA, and 0.1% Triton X-100.

6.2.8 Lipid A extraction

Lipid A from the *R. etli* strains was isolated from delipidated cell pellets with 1% acetic acid as described in chapter 5. The lipid A was analyzed by TLC as described in chapter 5.

6.2.9 Negative Ion Electrospray Ionization (ESI) of Lipid A Species

Lipid A species extracted from cells were analyzed by ESI-MS as described in chapter 5.

6.2.10 In vitro assay of 3-*O* deacylase activity

The 3-*O* deacylase activity of *R. etli* membranes was determined as previously described (Basu et al., 1999a). Standard assay conditions were as follows: the reaction mixture (10-20 μl) contained 50 mM MES, pH 6.25, 1.0% Triton X-100, 2 mM dithiothreitol, 2 mM EDTA, 20 mM $CaCl_2$, and 10 μM [4′-^{32}P]lipid IV_A (1,000 cpm/nmol).

The E. *coli* membranes expressing RePagL and SmPagL were assayed under different conditions where noted. In these instances, the 3-*O* deacylase activity was assayed in a buffer containing 50 mM HEPES, pH 8, 0.1% Triton, 0.5 M NaCl., and 10 μM [4′-^{32}P]lipid IV_A (1,000 cpm/nmol). $CaCl_2$ was added to this assay buffer at various concentrations where indicated. Reactions were initiated with the enzyme source. The reaction mixtures were incubated at 30 °C for the indicated times. The reactions were terminated by spotting 3-μL samples onto a TLC plate, which was developed in the solvent chloroform/pyridine/88% formic acid/water (30:70:16:10, v/v). After drying and overnight exposure of the plate to a PhosphorImager screen (GE Healthcare), product formation was detected and quantified with a Storm 840 PhosphorImager equipped with ImageQuant software (GE Healthcare).

6.2.11 Plant test for symbiotic phenotype characterization

The symbiotic phenotype characterization was carried out as described in chapter 5. Plants were grown in a controlled growth chamber at 28 °C with a 15 h day/ 9 h night cycle. The nodules were analyzed 10, 12, 14, 16, and 19 d after inoculation. Nitrogenase activity of nodulated roots was determined by the acetylene reduction assay as described previously (Martinez et al., 1985).

Table 17: Bacteria strains and plasmids used in chapter 6

Strain or Plasmid	Genotype or Description	Source or reference
Strains		
R. etli CE3	Spontaneous Sm^r derivative of wild-type strain CFN42, NaI^r	(Noel et al., 1984)
CS4	*pagL* mutant, spectinomycin-resistant	this work
CS10	*pagL* mutant, spectinomycin-resistant	this work
E. coli		
DH5α	*recA*1 ϕ80 *lacZΔM15*	(Hanahan, 1983)
BLR(DE3)	B strain, DE3 lysogen	EMD
W3110	Wild type, F^-, λ^-	*E. coli* genetic stock center (Yale)
Plasmids		
pET23(a)+	T7*lac* expression vector, Amp^r	EMD
RePagL	*R. etli pagL* in pET23a(+)	this work
SmPagL	*S. meliloti pagL* in pET23a(+)	this work
pRK2013	helper plasmid, kanamycin/neomycin-resistant	(Figurski & Helinski, 1979)
pK18*mobsac*B	suicide vector, kanamycin/neomycin-resistant	(Schafer et al., 1994)

Abbreviations: Sm-streptomycin sulfate, NaI-nalidixic acid, Amp-ampicillin

6.3 Results

6.3.1 Identification of PagL homologs in *R. etli* and *S. meliloti*

The amino acid sequence of the *Pseudomonas aeruginosa* PagL gene (accession number NP_253350) (Geurtsen et al., 2005, Rutten et al., 2006) was used as a probe to identify putative PagL homologs in members of the *Rhizobiaceae* family. Homologs were found in *Agrobacterium tumefaciens*, *Agrobacterium vitis* S4, *Rhizobium. etli*, *R. leguminosarum* bv. *trifolii*, *Rhizobium* sp. NGR234, *Sinorhizobium medicae* WSM4 1, and *S. meliloti* 1021 in the NCBI data base (http://www.ncbi.nlm.nih.gov/sutils/genom_table.cgi). A focus was placed on the *R. etli* homolog because 3-*O* deacylase activity in *R. etli* accounts for some of the heterogeneity found in that organism (Basu et al., 1999a, Que et al., 2000a, Que et al., 2000b). The *S. meliloti* gene was also of interest, because *S. meliloti* extracts are reported to lack 3-*O*-deacylase activity.

The 192-amino acid PagL homolog from *R. etli* (accession number ABC91065) and the 196-amino acid PagL homolog from *S. meliloti* (accession number NP_385884) were 34% identical on the amino acid level to *P. aeruginosa* PagL. The sequence alignment of the proteins with the *P. aeruginosa* gene is shown in Fig. 59. The two *Rhizobium* homologs were predicted to have signal peptide sequences, consistent with the proposed outer membrane localization of PagL (Trent et al., 2001a, Rutten et al., 2006). The homologs also contain histidine, serine, asparagine, and phenylalanine

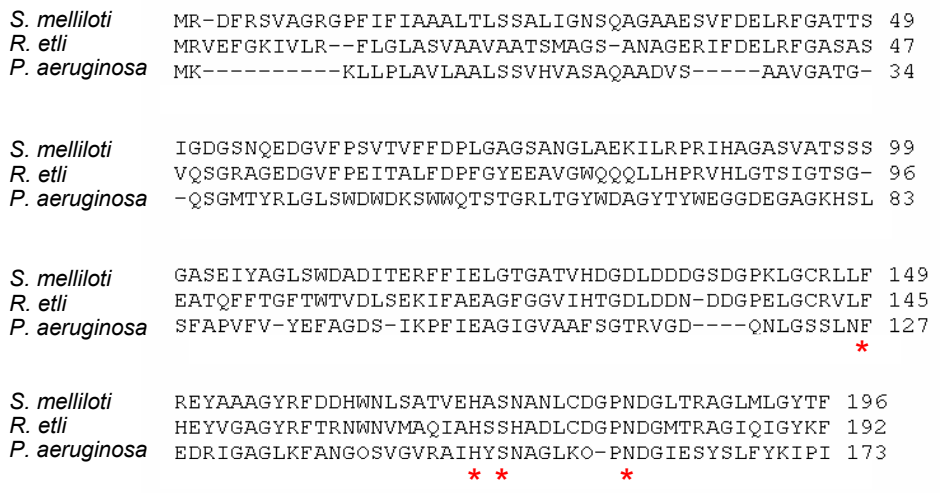

Figure 59: Multiple sequence alignment of the PagL proteins from *S. meliloti*, *R. etli*, and *P. aeruginosa*.

The sequences were aligned using ClustalW2 (http://www.ebi.ac.uk/Tools/clustalw2/index.html). The active site residues are indicated by red asterisks. The GenBankTM protein accession numbers for the genes are as follows: *S. meliloti*, NP_385884; *R.* etli, ABC91065; *P. aeruginosa* NP_253350.

residues which are involved in making up the active site, oxyanion hole, and substrate-binding pocket of *P. aeruginosa* PagL (Geurtsen et al., 2005, Rutten et al., 2006).

6.3.2 *In vitro* activity and catalytic properties of heterologously expressed RePagL and SmPagL

The *R. etli* and *S. meliloti* homologs were cloned from genomic DNA and overexpressed heterologously in *E. coli* as described in materials and methods. The membranes from these over-expressing strains were assayed in parallel with membranes from *R. etli* CE3 and *E. coli* W3110. In this assay system, the substrate [4′-^{32}P]-lipid IV_A is deacylated and the more hydrophilic product migrates more slowly. As shown in Fig 60, membranes overexpressing the PagL homologues generated a product with the same mobility as that generated from *R. etli*. This activity was absent in the *E. coli* W3110 membranes and from *E. coli* cells expressing the vector control.

The PagL homologs were assayed using the conditions previously optimized for measuring 3-*O*-deacylase activity in *R. leguminosarum* membranes (Basu et al., 1999a). These assay conditions included 20 mM calcium, as it was found that the activity in *R. leguminosarum* membranes was inhibited by EDTA and stimulated by calcium (Basu et al., 1999a). A metal requirement, however, has not been reported for other PagL homologs such as that from *S. typhimurium* or *P. aeruginosa* (Trent et al., 2001a, Rutten et al., 2006). When the overexpressed *R. etli* and *S. meliloti* PagL homologs were assayed

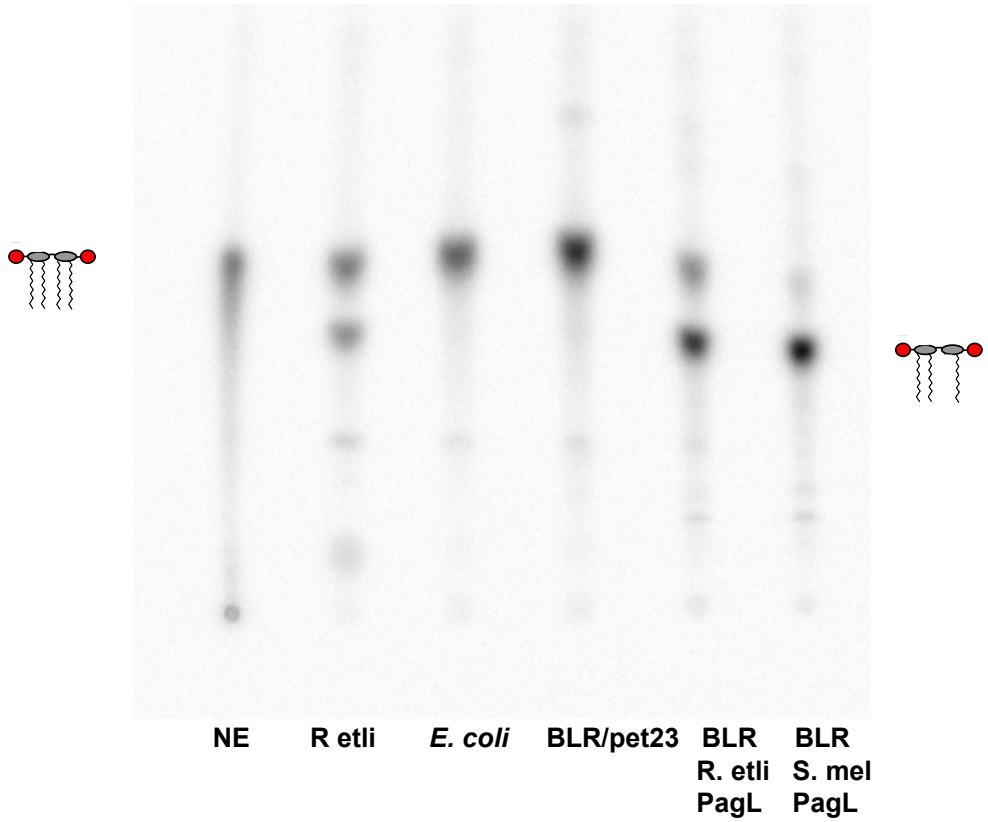

Figure 60: 3-*O* deacylation of [4′-^{32}P]lipid IV$_A$ by membranes of *R. etli* and *E. coli* membranes expressing *R. etli* PagL and *S. meliloti*. PagL.

Membranes of the indicated strains were assayed for 3-*O* deacylase activity. The assay was carried out in 50 mM MES, pH 6.25, 1.0% Triton X-100, 2 mM dithiothreitol, 2 mM EDTA, 20 mM $CaCl_2$, and 10 μM [4′-^{32}P]lipid IV$_A$ (1,000 cpm/nmol), and the membranes were used at 1 mg/ml. After incubation for 1 h at 30 °C, the products were separated by thin layer chromatography and detected with a PhosphorImager. NE: no enzyme; *R. etli*: *R. etli* membranes; *E. coli*: W3110 membranes; BLR/pet23: BLR(DE3)/pET23(a)+ membranes; BLR-R.etli PagL: BLR(DE3)/RePagL membranes; BLR-S.mel PagL: BLR(DE3)/SmPagL membranes.

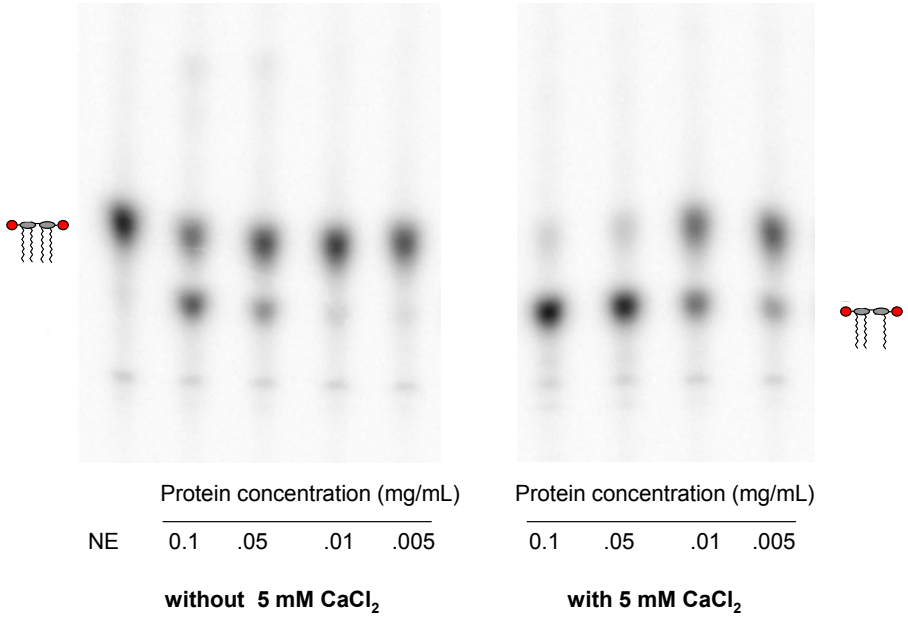

Figure 61: Calcium dependency of *R. etli* PagL

E. coli cells expressing RePagL were assayed in 50 mM HEPES, pH 8, 0.1% Triton, 0.5 M NaCl., and 10 μM [4′-^{32}P]lipid IV_A (1,000 cpm/nmol). The assay was performed with and without 5 mM $CaCl_2$. The membranes were used at the indicated concentrations. Reaction mixtures were incubated for 1 h at 30 °C, after which product formation was analyzed by thin layer chromatography and PhosphorImager analysis.

using the conditions reported for measuring *S. typhimurium* PagL activity (Trent et al., 2001b), the specific activities were significantly higher. Both proteins however, were still stimulated by the addition of calcium. Fig. 61 shows an assay performed using the conditions optimized for *S. typhimurium* PagL. The assay was performed by varying the concentration of protein in the absence or presence of 5 mM calcium. There is a significant increase in the activity of the *R. etli* PagL homolog when calcium is included.

6.3.3 Determination of lipid A phosphatase activity in R. etli and knockout strains

A deletion mutant of the *pagL* gene was constructed in *R. etli* as described in the materials and methods section. The *in vitro* 3-*O*-deacylase activity of the mutant and the parental wild-type strain was measured using washed membranes as the enzyme source. As shown in Fig. 62, the 3-*O*-deacylase activity that is characteristic of wild-type *R. etli* cells is absent in the *pagL* mutants (CS4 and CS10). The *E. coli* membranes over-expressing the two PagL homologues were included as positive controls.

6.3.4 Lipid A isolation from the R.etli wild-type and PagL knockout strain

The lipid A components released from the wild-type cells migrated as multiple species, when analyzed by TLC (Fig. 63) (Que et al., 2000a, Que et al., 2000b). The structures of the major lipid A components (A, B, C, D, and E) (Fig. 47) were described in chapter 5. The TLC pattern of the lipid A species from the *pagL* mutant differs from the wild-type in that it is less heterogeneous. The mutant only contained 3 major lipid A

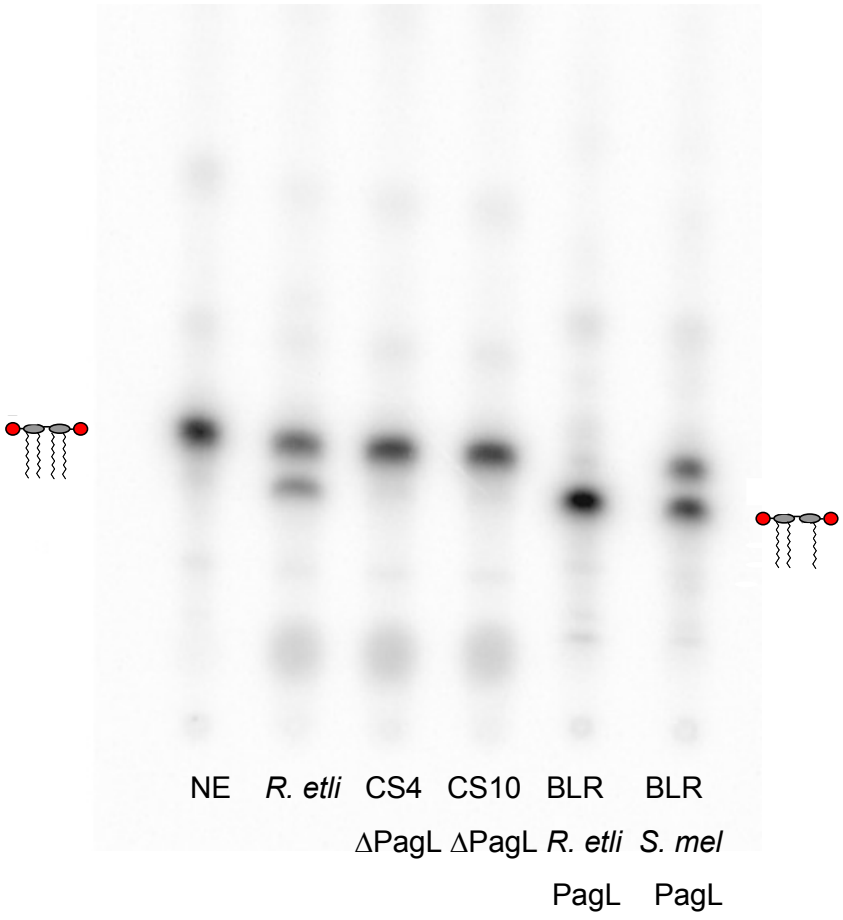

Figure 62: Absence of 3-O deacylase activity in PagL deletion strains CS4 and CS10

Membranes of the indicated strains (1.0 mg/mL) were assayed for 3-*O* deacylase activity at 30 °C with 10 μM [4′-^{32}P]-lipid IV_A. The products were separated by TLC followed by detection with a Phosphorimager. NE: No enzyme; *R. etli*: *R. etli* wild-type; CS4: *R. etli ΔpagL*; CS10: *R. etli ΔpagL*; BLR *R. etli* PagL: BLR(DE3)/RePagL membranes; BLR *S. mel* PagL: BLR(DE3)/SmPagL membranes.

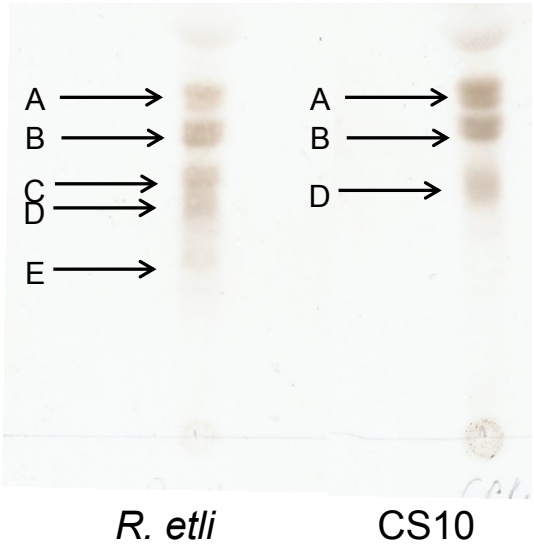

Figure 63: TLC analysis of lipid A species released by acetic acid hydrolysis from wild-type and pagL mutants

Approximately 5 μg of the lipid A released from wild-type *R. etli* cells or the *pagL* mutant, CS10, was spotted onto a TLC plate, which was developed in the solvent system $CHCl_3$/MeOH/H_2O/NH_4OH (40:25:4:2, v/v). The lipids were detected after chromatography by spraying with 10% sulfuric acid in ethanol and charring on a hot plate.

species (components A, B, and D) and lacked the normal 3-*O*-deacylated species (components C and E) (Fig. 47).

6.3.5 ESI-MS analysis of lipid A species from wild-type and *pagL* mutant

The negative ion ESI mass spectra of the unfractionated lipid A species extracted from the *R. etli* and *pagL* mutant are shown in Fig. 64. In panel A, there are 2 major lipid A species (components C and A) (Fig. 47) between *m/z* 1600 and 1800. Component C is the 3-*O*-deacylated species derived from component B, and component A is the proposed hydrolysis product derived from component D. The m/z of these ions are 1758.28 and 1738.26, respectively. There is significant microheterogeneity in the lipid A species because of acyl chain differences, as noted previously and in chapter 5 (Que et al., 2000a, Que et al., 2000b). In panel B of Fig. 64, the same cluster of ions between m/z 1600 and 1800 is shown for the *pagL* mutant. Component A is seen, but the deacylated component C is absent consistent with the TLC analysis (Fig. 63)

6.3.6 Symbiotic phenotype of R. etli strains

Phaseolus vulgaris roots were inoculated with the *R. etli* wild-type strain and the *pagL* mutant strain, CS4. The roots of the plant were analyzed 7, 10, 12, 14, 16, and 19 d after inoculation (Fig. 65). Both strains caused the formation of root nodules on the plant. The total number of nodules per plant was similar between the two plants, however, the *pagL* mutant developed red nitrogen-fixing nodules at a slower rate compared to the

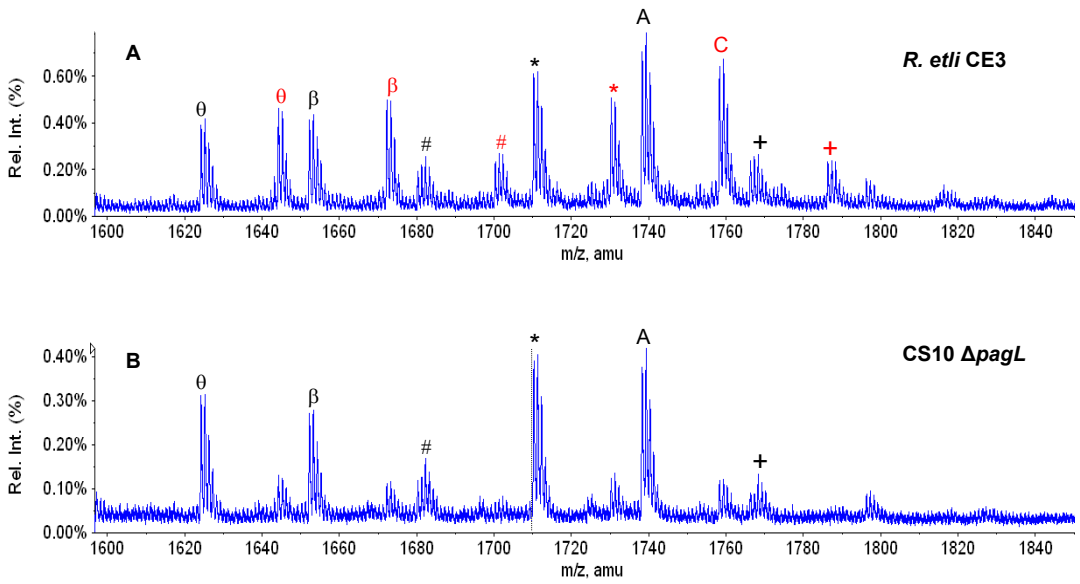

Figure 64: ESI/MS of lipid A components from *R. etli* and the PagL knockout strains CS10.

The lipid A from the wild-type and PagL deletion strain was extracted as described and analyzed by negative ion ESI/MS. Panel A. In the spectrum of the wild-type strain, the cluster of ions shown between 1620 amu and 1800 amu corresponds to the deacylated lipid A species found in wild-type *R. etli* lipid A (components C). Component A, which is derived from component D is also in this region. There is significant heterogeneity with regard to acyl chain length for the components shown. Panel B. In the spectrum of the PagL mutant (CS10), the cluster of ions shown between 1620 amu and 1800 corresponds to the lipid A hydrolysis product which is derived from component D. The deacylated species present in the wild type (component C) strain is absent. Heterogeneity in fatty acid chain length (14 or 28 atomic mass units) and partial substitution with β-hydroxybutyrate (86 atomic mass units) is observed in both strains. Each major lipid A species and its corresponding acyl chain variants are grouped by color. Symbols indicate the following amu shifts: + = (+28) ∗ = (-28) # = (-86 + 28) β = (-86) θ = (-86 + -28).

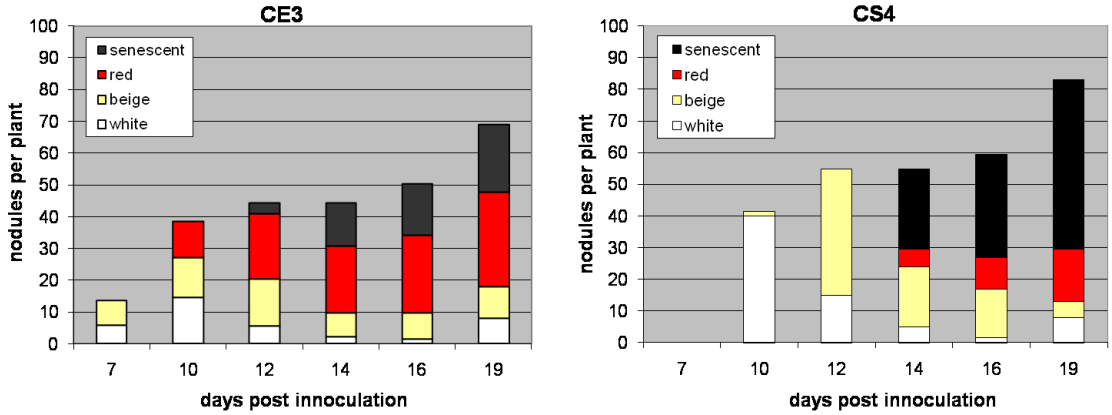

Figure 65: Analysis of nodules on *P. vulgaris* plants inoculated with *R. etli* and PagL knockout strains.

The nodules on *P. vulgaris* plants were analyzed at the indicated days after inoculation. The number of nodules and their color are indicated. The nodule normally start out as white, then transition to beige, then red, and turn brown to black in senescence. Nitrogen fixation activity is highest when the nodules are red. This data was collected by C. Sohlenkamp.

wild-type, suggesting that the kinetics of nodulation between the strains differed. Acetylene reduction assays performed 21d after inoculation, nonetheless, revealed no major difference in nitrogen fixing activities of the wild-type and mutant strain (data not shown).

6.4 Discussion

Lipid A in *R. leguminosarum* and *R. etli* is composed of tetraacylated and pentaacylated species (Que et al., 2000a, Que et al., 2000b). The tetraacylated species were proposed to be derived from a membrane-bound deacylase specific for the 3-*O* acyl chain of lipid A (Basu et al., 1999a). An enzyme possessing similar activities was discovered in *S. typhimurium*. (Trent et al., 2001b) The gene encoding the enzyme in *S. typhimurium* was shown to be a PhoP/PhoQ-activated gene (Trent et al., 2001b). The lipase was thus named PagL. The PagL gene was subsequently found in many other Gram-negative bacteria including *P. aeruginosa*, *P. syringae*, *Burkholderia fungorum*, *Bordetella* spp. *B. pertussis*, *B. bronchiseptica* (Geurtsen et al., 2005). There was low sequence homology among the PagL homologs. The low sequence homology, however, facilitated identification of the active site residues of the PagL family of proteins (Geurtsen et al., 2005). The x-ray crystal structure of PagL from *P. aeruginosa* was recently solved confirming the role of many of these identified residues (Rutten et al., 2006).

Using the *P. aeruginosa* PagL protein sequence as a probe, homologs of the protein were found in *Rhizobium* species including *R. etli* and *S. meliloti*. The active site residues of the proteins were conserved with that of the other described PagL genes (Geurtsen et al., 2005). To address if the putative *R. etli* PagL homolog was responsible for the deacylase activity previously described in that organism, the gene was cloned and expressed recombinantly in *E. coli* and deleted in *R. etli*.

The activity of the overexpressed *R. etli* and *S. meliloti* PagL homologs was localized to the membrane fractions of *E. coli*. Both overexpressed proteins displayed activity under conditions described previously for analyzing *R. leguminosarum* deacylase activity (Basu et al., 1999a). The PagL homologs, however, displayed a significant increase in activity when assayed using the conditions optimized for the *S. typhimurium* PagL protein (Trent et al., 2001b). The assay conditions for the *R. leguminosarum* deacylase activity were previously optimized using crude *R. leguminosarum* membranes (Basu et al., 1999a). The *R. leguminosarum* membranes may contain inhibitors or other components that impact the activity of the deacylase. The conditions previously described for assaying *R. leguminosarum* activity however included calcium chloride, as the activity was shown to be metal dependent (Basu et al., 1999a). Consistent with this observation, the activity of the recombinantly expressed *R. etli* PagL protein was found to be dependent on the presence of divalent cations. There was a significant increase in

activity of the protein when assayed in the presence of calcium chloride. This property is different among the other described PagL proteins. Both the *S. typhimurium* and *P. aeruginosa* PagL proteins are active even in the presence of EDTA (Trent et al., 2001a, Rutten et al., 2006). This difference could reflect differences in mechanism or regulation of the proteins.

A deletion mutant of the putative *pagL* gene was made in *R. etli*. The mutant lacked *in vitro* deacylase activity and its lipid A was primarily pentaacylated. The *R. etli* PagL homolog, therefore, was confirmed to be the deacylase responsible for generating the tetraacylated species found in *R. etli* and *R. leguminosarum*.

PagL now appears to be widespread among Gram-negative bacteria (Geurtsen et al., 2005). It is present in both pathogenic and non-pathogenic bacteria. It is an outer membrane enzyme that appears to be up-regulated in response to environmental stimuli (Bishop, 2008). In *S. typhimurium*, PagL is activated by the two-component regulatory system PhoP/PhoQ. (Trent et al., 2001b) The PagL gene in organisms such as *S. meliloti* could be regulated by similar systems. Here, we show that the PagL homolog found in *S. meliloti* is a 3-*O*-deacylase. Free-living *S. meliloti* are normally not deacylated (Gudlavalleti & Forsberg, 2003). 3-*O*-deacylation of lipid A in *S. meliloti* could be important under some conditions.

The role of the deacylase, like the other lipid A modifications in *R. etli* and *R. leguminosarum* is unclear. Free-living *R. etli* and *R. leguminosarum* are primarily both pentaacylated and tetraacylated suggesting that PagL is constitutively active (Que et al., 2000a, Que et al., 2000b). Interestingly, the lipid A isolated from *R. etli* bacteroids is reported to consist mainly of tetraacylated species, suggesting that PagL is up-regulated in the nodule environment (D'Haeze et al., 2007). To address if PagL activity was important for nodulation, the symbiotic phenotype of the PagL mutant was analyzed. The PagL mutant was able to form nitrogen-fixing nodules, but nodule development differed slightly. The mutant displayed slower nodulation kinetics. A similar phenotype has been described for *R. leguminosarum* mutants deficient in other lipid A modification enzymes.

In conclusion, we have shown that *R. etli* possesses a PagL homolog that is responsible for generating the tetraacylated species of lipid A. The *R. etli* homolog shares distant homology with other PagL homologs. It is, however, unique among the described PagL proteins in its requirement for divalent cations. Despite the apparent up-regulation of PagL in bacterial nodules, the modification catalyzed by PagL does not appear to required for nitrogen-fixation. The 3-O deacylation reaction, like the lipid A phosphatase reactions, could play a role in protecting bacterial symbionts from the

immune response of plants during pathogenic infections. Future work will address the roles of lipid A modifications in such processes.

6.5 Statement of collaborative work

Some of the data in this chapter was collected in collaboration. Christian Sohlenkamp generated the knockout strain and conducted the nodulation studies (Fig. 65).

Chapter 7: Summary, Discussion, and Future Directions

Lipid A in Rhizobium

The lipid A moiety of LPS from *R. leguminosarum* and *R. etli* is structurally unique when compared to the lipid A of common *Enterobacteriaceae* such as *E. coli* (Raetz et al., 2007). The lipid A in these nitrogen-fixing bacterial endosymbionts lacks phosphate residues and contains only one secondary acyl chain. A galacturonic acid moiety replaces the 4′-position phosphate and the proximal glucosamine residue exists in the hemiacetal form or as an aminogluconate moiety. There is additional heterogeneity in regards to acyl chain number and length (Que et al., 2000a, Que et al., 2000b).

Lipid A biosynthesis in *R. leguminosarum* and *R. etli* has now been extensively investigated. The unique structural features of these bacteria arise from modification enzymes that process Kdo_2-lipid-IV_A, a lipid A biosynthetic intermediate that is common in almost all Gram-negative bacteria. These enzymes include a lipid A 1-phosphatase (LpxE) (Karbarz et al., 2003), a lipid A 4′-phosphatase (LpxF) (Wang et al., 2006a), a 3-O-deacylase (PagL) (Basu et al., 1999a), a long chain acyltransferase (LpxXL) (Basu et al., 2002), a lipid A oxidase (LpxQ) (Que-Gewirth et al., 2003a, Que-Gewirth et al., 2003b), and a sugar-nucleotide dependent core glycosyltransferase (RgtD) (Kanjilal-Kolar et al.,

2006). In this dissertation, we investigated the mechanisms and/or biological roles of four of these enzymes.

Heterologous expression of lipid A modification enzymes

In chapter 2, we showed that the lipid A modification enzymes from *R. etli* can be expressed heterologously in combination in *E. coli* to generate novel lipid A hybrids *in vivo*. The expression of the lipid A modifications enzymes in *E. coli* allowed us to verify the activities that had been previously ascribed to them and allowed us to assess the substrate requirements of the modification enzymes. We also showed that LpxQ could function *in vivo* in foreign host as long as 1-dephosphorylated lipid A was available. We discovered that *E. coli* accumulating di-dephosphorylated lipid A was viable but had growth defects in the absence of inner core sugars.

We also examined the polymyxin resistance of *E. coli* cells expressing the R. *leguminosarum* and *R. etli* enzymes. Heterologous expression of LpxE and LpxF in *E. coli* resulted in an increase in resistance to polymyxin, a cationic antimicrobial peptide. The level of resistance seen with the expression of the phosphatases is similar to that observed in polymyxin-resistant strains of *E. coli*. Based on the data in chapter 2 as well as in many other works (Karbarz et al., 2003, Wang et al., 2006a), it seems that a major function of the lipid A phosphatases, LpxE and LpxF, is to assist bacteria in evading cationic antimicrobials. This function makes sense in terms of aiding pathogens in

evading the immune response of hosts, but the function of the phosphatases in *R. etli* and *R. leguminosarum* is less clear. The expression of other lipid A modification enzymes in *E. coli* should give insights into the unique role lipid A modifications play in various biological processes.

Purification of the lipid A oxidase

In chapter 3, we described a purification procedure for the lipid A oxidase, LpxQ. Because LpxQ expresses poorly in *E. coli*, a large-scale purification procedure was developed. The activity of LpxQ was monitored using a new, improved *in vitro* assay. The purification of LpxQ and its enzymatic characterization allowed us to confirm that the protein is an oxidase. Oxygen was confirmed to be an electron acceptor in the reaction, as H_2O_2 was found to be produced in stoichiometric amounts with oxidized lipid A. We utilized this property in developing a new fluorometric assay for monitoring lipid A oxidation.

A great amount of time and effort went into looking for an electron-transferring cofactor associated with LpxQ. The purified protein was heterogeneous in mass and co-purified with a yellow chromophore. We were however, unable to find an association between these properties and enzymatic activity. We found that some of the heterogeneity in term of mass arose from miscleavage of LpxQ's signal sequence. The recombinant protein also contained a modification of ~55 mass units. This modification,

however, did not affect the activity of the enzyme. The protein did co-purify with metals, but not redox-active metals. These results all reflected the possibility that LpxQ might function in the absence of an exogenous cofactor. To address this issue, we attempted to refold LpxQ from inclusion bodies. In chapter 4, we demonstrated that LpxQ can be refolded. The refolded protein was shown to possess the stability and activity of the enzyme produced *in vivo.* Interestingly, the yellow chromophore and mass deviations were not observed with the refolded protein.

Based on these findings, our current hypothesis is that LpxQ functions *in vivo* without an electron-transferring cofactor. In the absence of a cofactor, LpxQ could oxidize lipid A by a mechanism involving direct electron transfer to oxygen. There are very few enzymes that participate in this kind of electron transfer. The best example is urate oxidase which oxidizes uric acid to 5-hydroxyisourate (Kahn & Tipton, 1998). Interestingly, urate oxidase is involved in metabolic processes that are upregulated during plant nodulation.

The *Rhizobium etli* lipid A 3-*O*-deacylase, PagL

The 3-*O*-deacylase protein encoding the 3-*O*-deacylase was found by looking for PagL homologs in *R. etli*. Using the *P. aeruginosa pagL* gene as a probe, we found homologs in many members of the *Rhizobium* family including *R. etli* and *S. meliloti.* In

chapter 6, we showed that both genes encoded functional 3-O-deacylases when expressed heterologously in *E. coli*.

The activity of the *S. meliloti* homolog is intriguing as 3-*O*-deacylase activity is normally absent in *S. meliloti (Basu et al., 1999a)*. This suggests that the activity of the *S. meliloti* PagL could be up-regulated under certain conditions, perhaps in the nodule environment. In support of this, lipid A isolated from *R. etli* bacteroids is reported to be exclusively tetraacylated (D'Haeze et al., 2007). The regulation of lipid A modifications in *R. etli* and *R. leguminosarum* has not been addressed. Several of the modifications appear to be constitutively expressed under free-living growth conditions. It would be of interest to determine what mechanisms influence the expression of the modification enzymes. In enteric bacteria, lipid A modifications are commonly regulated by two component regulatory systems (Raetz et al., 2007). At the present time, no two-component regulatory system in *R. etli* or *R. leguminosarum* is known to be involved in lipid A modification.

Role of lipid A modifications in bacterial-plant symbiosis

In chapters 5 and 6, we investigated the relationship between lipid A modifications and bacteria-plant symbiosis. It has long been speculated that the lipid A modifications could play a role in this process. In this work we describe the construction of *R. etli* strains lacking the lipid A phosphates, LpxE and LpxF, and the 3-O-deacylase,

PagL. We show that the loss of modifications derived from these enzymes do not significantly impact the symbiotic relationship between *R. etli* and its host plant, *P. vulgaris*. The results presented here along with other reports suggest that lipid A modifications are not required for bacterial-plant symbiosis. The lipid A modifications may play a role in protecting the endosymbionts from the immune response of plants during infection. Future studies should address the role of lipid A in eliciting such immune responses.

Although the function of lipid A modifications in *Rhizobium* have not been elucidated, the modification enzymes may have applications in vaccine development and the production of therapeutic drugs to treat Gram-negative sepsis.

References

Aderem, A. & R. J. Ulevitch, (2000) Toll-like receptors in the induction of the innate immune response. Nature **406**: 782-787.

Ahn, V. E., E. I. Lo, C. K. Engel, L. Chen, P. M. Hwang, L. E. Kay, R. E. Bishop & G. G. Prive, (2004) A hydrocarbon ruler measures palmitate in the enzymatic acylation of endotoxin. EMBO J **23**: 2931-2941.

Akira, S., S. Uematsu & O. Takeuchi, (2006) Pathogen recognition and innate immunity. Cell **124**: 783-801.

Anderson, K. V., G. Jurgens & C. Nusslein-Volhard, (1985) Establishment of dorsal-ventral polarity in the Drosophila embryo: genetic studies on the role of the Toll gene product. Cell **42**: 779-789.

Anderson, M. S., H. G. Bull, S. M. Galloway, T. M. Kelly, S. Mohan, K. Radika & C. R. H. Raetz, (1993) UDP-N-acetylglucosamine acyltransferase of Escherichia coli. The first step of endotoxin biosynthesis is thermodynamically unfavorable. J Biol Chem **268**: 19858-19865.

Anderson, M. S. & C. R. H. Raetz, (1987) Biosynthesis of lipid A precursors in Escherichia coli. A cytoplasmic acyltransferase that converts UDP-N-acetylglucosamine to UDP-3-O-(R-3-hydroxymyristoyl)-N-acetylglucosamine. J Biol Chem **262**: 5159-5169.

Anderson, M. S., A. D. Robertson, I. Macher & C. R. H. Raetz, (1988) Biosynthesis of lipid A in Escherichia coli: identification of UDP-3-O-[(R)-3-hydroxymyristoyl]-alpha-D-glucosamine as a precursor of UDP-N2,O3-bis[(R)-3-hydroxymyristoyl]-alpha-D-glucosamine. Biochemistry **27**: 1908-1917.

Babinski, K. J., S. J. Kanjilal & C. R. H. Raetz, (2002a) Accumulation of the lipid A precursor UDP-2,3-diacylglucosamine in an Escherichia coli mutant lacking the lpxH gene. J Biol Chem **277**: 25947-25956.

Babinski, K. J., A. A. Ribeiro & C. R. H. Raetz, (2002b) The Escherichia coli gene encoding the UDP-2,3-diacylglucosamine pyrophosphatase of lipid A biosynthesis. J Biol Chem **277**: 25937-25946.

Baldridge, J. R. & R. T. Crane, (1999) Monophosphoryl lipid A (MPL) formulations for the next generation of vaccines. Methods **19**: 103-107.

Baldridge, J. R., P. McGowan, J. T. Evans, C. Cluff, S. Mossman, D. Johnson & D. Persing, (2004) Taking a Toll on human disease: Toll-like receptor 4 agonists as vaccine adjuvants and monotherapeutic agents. Expert Opin Biol Ther **4**: 1129-1138.

Barb, A. W., L. Jiang, C. R. Raetz & P. Zhou, (2007) Structure of the deacetylase LpxC bound to the antibiotic CHIR-090: Time-dependent inhibition and specificity in ligand binding. Proc Natl Acad Sci U S A **104**: 18433-18438.

Barb, A. W., T. M. Leavy, L. I. Robins, Z. Guan, D. A. Six, P. Zhou, M. J. Hangauer, C. R. Bertozzi & C. R. Raetz, (2009) Uridine-based inhibitors as new leads for antibiotics targeting Escherichia coli LpxC. Biochemistry **48**: 3068-3077.

Bartling, C. M. & C. R. Raetz, (2009) Crystal structure and acyl chain selectivity of Escherichia coli LpxD, the N-acyltransferase of lipid A biosynthesis. Biochemistry **48**: 8672-8683.

Basu, S. S., M. J. Karbarz & C. R. H. Raetz, (2002) Expression cloning and characterization of the C28 acyltransferase of lipid A biosynthesis in Rhizobium leguminosarum. J Biol Chem **277**: 28959-28971.

Basu, S. S., K. A. White, N. L. Que & C. R. H. Raetz, (1999a) A deacylase in Rhizobium leguminosarum membranes that cleaves the 3-O-linked beta-hydroxymyristoyl moiety of lipid A precursors. J Biol Chem **274**: 11150-11158.

Basu, S. S., J. D. York & C. R. H. Raetz, (1999b) A phosphotransferase that generates phosphatidylinositol 4-phosphate (PtdIns-4-P) from phosphatidylinositol and lipid A in Rhizobium leguminosarum. A membrane-bound enzyme linking lipid a and ptdins-4-p biosynthesis. J Biol Chem **274**: 11139-11149.

Belunis, C. J., K. E. Mdluli, C. R. H. Raetz & F. E. Nano, (1992) A novel 3-deoxy-D-manno-octulosonic acid transferase from Chlamydia trachomatis required for expression of the genus-specific epitope. J Biol Chem **267**: 18702-18707.

Belunis, C. J. & C. R. Raetz, (1992) Biosynthesis of endotoxins. Purification and catalytic properties of 3-deoxy-D-manno-octulosonic acid transferase from Escherichia coli. J Biol Chem **267**: 9988-9997.

Beringer, J. E., (1974) R factor transfer in Rhizobium leguminosarum. J Gen Microbiol **84**: 188-198.

Beutler, B. & A. Cerami, (1988) Tumor necrosis, cachexia, shock, and inflammation: a common mediator. Annu Rev Biochem **57**: 505-518.

Beutler, B., Z. Jiang, P. Georgel, K. Crozat, B. Croker, S. Rutschmann, X. Du & K. Hoebe, (2006) Genetic analysis of host resistance: Toll-like receptor signaling and immunity at large. Annu Rev Immunol **24**: 353-389.

Bhat, U. R. & R. W. Carlson, (1992) Chemical characterization of pH-dependent structural epitopes of lipopolysaccharides from Rhizobium leguminosarum biovar phaseoli. J Bacteriol **174**: 2230-2235.

Bhat, U. R., R. W. Carlson, M. Busch & H. Mayer, (1991a) Distribution and phylogenetic significance of 27-hydroxy-octacosanoic acid in lipopolysaccharides from bacteria belonging to the alpha-2 subgroup of Proteobacteria. Int J Syst Bacteriol **41**: 213-217.

Bhat, U. R., L. S. Forsberg & R. W. Carlson, (1994) Structure of lipid A component of Rhizobium leguminosarum bv. phaseoli lipopolysaccharide. Unique nonphosphorylated lipid A containing 2-amino-2-deoxygluconate, galacturonate, and glucosamine. J Biol Chem **269**: 14402-14410.

Bhat, U. R., H. Mayer, A. Yokota, R. I. Hollingsworth & R. W. Carlson, (1991b) Occurrence of lipid A variants with 27-hydroxyoctacosanoic acid in lipopolysaccharides from members of the family Rhizobiaceae. J Bacteriol **173**: 2155-2159.

Bishop, R. E., (2008) Structural biology of membrane-intrinsic beta-barrel enzymes: sentinels of the bacterial outer membrane. Biochim Biophys Acta **1778**: 1881-1896.

Bishop, R. E., H. S. Gibbons, T. Guina, M. S. Trent, S. I. Miller & C. R. H. Raetz, (2000) Transfer of palmitate from phospholipids to lipid A in outer membranes of gram-negative bacteria. EMBO J **19**: 5071-5080.

Bligh, E. G. & W. J. Dyer, (1959) A rapid method of total lipid extraction and purification. Can J Biochem Physiol **37**: 911-917.

Bos, M. P., B. Tefsen, J. Geurtsen & J. Tommassen, (2004) Identification of an outer membrane protein required for the transport of lipopolysaccharide to the bacterial cell surface. Proc Natl Acad Sci U S A **101**: 9417-9422.

Brabetz, W., S. Muller-Loennies, O. Holst & H. Brade, (1997) Deletion of the heptosyltransferase genes rfaC and rfaF in Escherichia coli K-12 results in an Re-type lipopolysaccharide with a high degree of 2-aminoethanol phosphate substitution. Eur J Biochem **247**: 716-724.

Brade, H., (1999) Endotoxin in health and disease, p. xviii, 950 p. Marcel Dekker, New York.

Braun, M. & T. J. Silhavy, (2002) Imp/OstA is required for cell envelope biogenesis in Escherichia coli. Mol Microbiol **45**: 1289-1302.

Broughton, W. J., S. Jabbouri & X. Perret, (2000) Keys to symbiotic harmony. J Bacteriol **182**: 5641-5652.

Brozek, K. A., R. W. Carlson & C. R. Raetz, (1996a) A special acyl carrier protein for transferring long hydroxylated fatty acids to lipid A in Rhizobium. J Biol Chem **271**: 32126-32136.

Brozek, K. A., K. Hosaka, A. D. Robertson & C. R. H. Raetz, (1989) Biosynthesis of lipopolysaccharide in Escherichia coli. Cytoplasmic enzymes that attach 3-deoxy-D-manno-octulosonic acid to lipid A. J Biol Chem **264**: 6956-6966.

Brozek, K. A., J. L. Kadrmas & C. R. Raetz, (1996b) Lipopolysaccharide biosynthesis in Rhizobium leguminosarum. Novel enzymes that process precursors containing 3-deoxy-D-manno-octulosonic acid. J Biol Chem **271**: 32112-32118.

Brozek, K. A. & C. R. H. Raetz, (1990) Biosynthesis of lipid A in Escherichia coli. Acyl carrier protein-dependent incorporation of laurate and myristate. J Biol Chem **265**: 15410-15417.

Brunie, S., J. Bolin, D. Gewirth & P. B. Sigler, (1985) The refined crystal structure of dimeric phospholipase A2 at 2.5 A. Access to a shielded catalytic center. J Biol Chem **260**: 9742-9749.

Bryant, C. E., D. R. Spring, M. Gangloff & N. J. Gay, (2010) The molecular basis of the host response to lipopolysaccharide. Nat Rev Microbiol **8**: 8-14.

Buchanan, B. B., W. Gruissem & R. L. Jones, (2000) Biochemistry & molecular biology of plants, p. xxxix, 1367 p. American Society of Plant Physiologists, Rockville, Md.

Buetow, L., T. K. Smith, A. Dawson, S. Fyffe & W. N. Hunter, (2007) Structure and reactivity of LpxD, the N-acyltransferase of lipid A biosynthesis. Proc Natl Acad Sci U S A **104**: 4321-4326.

Campbell, G. R., B. L. Reuhs & G. C. Walker, (2002) Chronic intracellular infection of alfalfa nodules by Sinorhizobium meliloti requires correct lipopolysaccharide core. Proc Natl Acad Sci U S A **99**: 3938-3943.

Carlson, R. W., L. S. Forsberg, N. P. Price, U. R. Bhat, T. M. Kelly & C. R. H. Raetz, (1995) The structure and biosynthesis of Rhizobium leguminosarum lipid A. Prog Clin Biol Res **392**: 25-31.

Chen, P. S., T. Y. Toribara & H. Warner, (1956) Microdetermination of Phosphorus. Analytical Chemistry **28**: 1756-1758.

Clements, J. M., F. Coignard, I. Johnson, S. Chandler, S. Palan, A. Waller, J. Wijkmans & M. G. Hunter, (2002) Antibacterial activities and characterization of novel inhibitors of LpxC. Antimicrob Agents Chemother **46**: 1793-1799.

Clementz, T., J. J. Bednarski & C. R. Raetz, (1996) Function of the htrB high temperature requirement gene of Escherchia coli in the acylation of lipid A: HtrB catalyzed incorporation of laurate. J Biol Chem **271**: 12095-12102.

Clementz, T. & C. R. H. Raetz, (1991) A gene coding for 3-deoxy-D-manno-octulosonic-acid transferase in Escherichia coli. Identification, mapping, cloning, and sequencing. J Biol Chem **266**: 9687-9696.

Clementz, T., Z. Zhou & C. R. Raetz, (1997) Function of the Escherichia coli msbB gene, a multicopy suppressor of htrB knockouts, in the acylation of lipid A. Acylation by MsbB follows laurate incorporation by HtrB. J Biol Chem **272**: 10353-10360.

Coats, S. R., J. W. Jones, C. T. Do, P. H. Braham, B. W. Bainbridge, T. T. To, D. R. Goodlett, R. K. Ernst & R. P. Darveau, (2009) Human Toll-like receptor 4 responses to P. gingivalis are regulated by lipid A 1- and 4'-phosphatase activities. Cell Microbiol **11**: 1587-1599.

Coggins, B. E., X. Li, A. L. McClerren, O. Hindsgaul, C. R. H. Raetz & P. Zhou, (2003) Structure of the LpxC deacetylase with a bound substrate-analog inhibitor. Nat Struct Biol **10**: 645-651.

Coggins, B. E., A. L. McClerren, L. Jiang, X. Li, J. Rudolph, O. Hindsgaul, C. R. H. Raetz & P. Zhou, (2005) Refined solution structure of the LpxC-TU-514 complex and pKa analysis of an active site histidine: insights into the mechanism and inhibitor design. Biochemistry **44**: 1114-1126.

Coico, R., (2005) Gram staining. Curr Protoc Microbiol **Appendix 3**: Appendix 3C.

Coleman, J. & C. R. Raetz, (1988) First committed step of lipid A biosynthesis in Escherichia coli: sequence of the lpxA gene. J Bacteriol **170**: 1268-1274.

Cullimore, J. V., R. Ranjeva & J. J. Bono, (2001) Perception of lipo-chitooligosaccharidic Nod factors in legumes. Trends Plant Sci **6**: 24-30.

Cuny, G. D., (2009) A new class of UDP-3-O-(R-3-hydroxymyristol)-N-acetylglucosamine deacetylase (LpxC) inhibitors for the treatment of Gram-negative infections: PCT application WO 2008027466. Expert Opin Ther Pat **19**: 893-899.

D'Haeze, W. & M. Holsters, (2002) Nod factor structures, responses, and perception during initiation of nodule development. Glycobiology **12**: 79R-105R.

D'Haeze, W., C. Leoff, G. Freshour, K. D. Noel & R. W. Carlson, (2007) Rhizobium etli CE3 bacteroid lipopolysaccharides are structurally similar but not identical to those produced by cultured CE3 bacteria. J Biol Chem **282**: 17101-17113.

de Maagd, R. A., A. S. Rao, I. H. Mulders, L. Goosen-de Roo, M. C. van Loosdrecht, C. A. Wijffelman & B. J. Lugtenberg, (1989) Isolation and characterization of mutants of Rhizobium leguminosarum bv. viciae 248 with altered lipopolysaccharides: possible role of surface charge or hydrophobicity in bacterial release from the infection thread. J Bacteriol **171**: 1143-1150.

Demchenko, A. V., M. A. Wolfert, B. Santhanam, J. N. Moore & G. J. Boons, (2003) Synthesis and biological evaluation of Rhizobium sin-1 lipid A derivatives. J Am Chem Soc **125**: 6103-6112.

Denarie, J., F. Debelle & J. C. Prome, (1996) Rhizobium lipo-chitooligosaccharide nodulation factors: signaling molecules mediating recognition and morphogenesis. Annu Rev Biochem **65**: 503-535.

Doerrler, W. T., M. C. Reedy & C. R. H. Raetz, (2001) An Escherichia coli mutant defective in lipid export. J Biol Chem **276**: 11461-11464.

Duelli, D. M., A. Tobin, J. M. Box, V. S. Kolli, R. W. Carlson & K. D. Noel, (2001) Genetic locus required for antigenic maturation of Rhizobium etli CE3 lipopolysaccharide. J Bacteriol **183**: 6054-6064.

Dulbecco, R. & M. Vogt, (1954) Plaque formation and isolation of pure lines with poliomyelitis viruses. J Exp Med **99**: 167-182.

Epand, R. M. & H. J. Vogel, (1999) Diversity of antimicrobial peptides and their mechanisms of action. Biochim Biophys Acta **1462**: 11-28.

Fahraeus, G., (1957) The infection of clover root hairs by nodule bacteria studied by a simple glass slide technique. J Gen Microbiol **16**: 374-381.

Ferguson, G. P., A. Datta, R. W. Carlson & G. C. Walker, (2005) Importance of unusually modified lipid A in Sinorhizobium stress resistance and legume symbiosis. Mol Microbiol **56**: 68-80.

Fetzner, S., (2002) Oxygenases without requirement for cofactors or metal ions. Appl Microbiol Biotechnol **60**: 243-257.

Figurski, D. H. & D. R. Helinski, (1979) Replication of an origin-containing derivative of plasmid RK2 dependent on a plasmid function provided in trans. Proc Natl Acad Sci U S A **76**: 1648-1652.

Fischer, F. & S. Fetzner, (2000) Site-directed mutagenesis of potential catalytic residues in 1H-3-hydroxy-4-oxoquinoline 2,4-dioxygenase, and hypothesis on the catalytic mechanism of 2,4-dioxygenolytic ring cleavage. FEMS Microbiol Lett **190**: 21-27.

Fiske, C. H. & Y. Subbarow, (1925) The colorimetric determination of phosphorus. Journal of Biological Chemistry **66**: 375-400.

Forsberg, L. S. & R. W. Carlson, (1998) The structures of the lipopolysaccharides from Rhizobium etli strains CE358 and CE359. The complete structure of the core region of R. etli lipopolysaccharides. J Biol Chem **273**: 2747-2757.

Frirdich, E., C. Bouwman, E. Vinogradov & C. Whitfield, (2005) The role of galacturonic acid in outer membrane stability in Klebsiella pneumoniae. J Biol Chem **280**: 27604-27612.

Gangloff, M. & N. J. Gay, (2004) MD-2: the Toll 'gatekeeper' in endotoxin signalling. Trends Biochem Sci **29**: 294-300.

Gangola, P. & B. P. Rosen, (1987) Maintenance of intracellular calcium in Escherichia coli. J Biol Chem **262**: 12570-12574.

Garrett, T. A., J. L. Kadrmas & C. R. H. Raetz, (1997) Identification of the gene encoding the Escherichia coli lipid A 4'-kinase. Facile phosphorylation of endotoxin analogs with recombinant LpxK. J Biol Chem **272**: 21855-21864.

Garrett, T. A., N. L. Que & C. R. H. Raetz, (1998) Accumulation of a lipid A precursor lacking the 4'-phosphate following inactivation of the Escherichia coli lpxK gene. J Biol Chem **273**: 12457-12465.

Gay, N. J., M. Gangloff & A. N. Weber, (2006) Toll-like receptors as molecular switches. Nat Rev Immunol **6**: 693-698.

Geiger, O., V. Rohrs, B. Weissenmayer, T. M. Finan & J. E. Thomas-Oates, (1999) The regulator gene phoB mediates phosphate stress-controlled synthesis of the membrane lipid diacylglyceryl-N,N,N-trimethylhomoserine in Rhizobium (Sinorhizobium) meliloti. Mol Microbiol **32**: 63-73.

Geiger, O., H. P. Spaink & E. P. Kennedy, (1991) Isolation of the Rhizobium leguminosarum NodF nodulation protein: NodF carries a 4'-phosphopantetheine prosthetic group. J Bacteriol **173**: 2872-2878.

Geurtsen, J., L. Steeghs, J. T. Hove, P. van der Ley & J. Tommassen, (2005) Dissemination of lipid A deacylases (pagL) among gram-negative bacteria: identification of active-site histidine and serine residues. J Biol Chem **280**: 8248-8259.

Gibbons, H. S., S. R. Kalb, R. J. Cotter & C. R. H. Raetz, (2005) Role of Mg2+ and pH in the modification of Salmonella lipid A after endocytosis by macrophage tumour cells. Mol Microbiol **55**: 425-440.

Golenbock, D. T., R. Y. Hampton, N. Qureshi, K. Takayama & C. R. H. Raetz, (1991) Lipid A-like molecules that antagonize the effects of endotoxins on human monocytes. J Biol Chem **266**: 19490-19498.

Gonzalez, V., R. I. Santamaria, P. Bustos, I. Hernandez-Gonzalez, A. Medrano-Soto, G. Moreno-Hagelsieb, S. C. Janga, M. A. Ramirez, V. Jimenez-Jacinto, J. Collado-Vides & G. Davila, (2006) The partitioned Rhizobium etli genome: genetic and metabolic redundancy in seven interacting replicons. Proc Natl Acad Sci U S A **103**: 3834-3839.

Gronow, S., G. Xia & H. Brade, (2010) Glycosyltransferases involved in the biosynthesis of the inner core region of different lipopolysaccharides. Eur J Cell Biol **89**: 3-10.

Gudlavalleti, S. K. & L. S. Forsberg, (2003) Structural characterization of the lipid A component of Sinorhizobium sp. NGR234 rough and smooth form lipopolysaccharide. Demonstration that the distal amide-linked acyloxyacyl residue containing the long chain fatty acid is conserved in rhizobium and Sinorhizobium sp. J Biol Chem **278**: 3957-3968.

Gunn, J. S., K. B. Lim, J. Krueger, K. Kim, L. Guo, M. Hackett & S. I. Miller, (1998) PmrA-PmrB-regulated genes necessary for 4-aminoarabinose lipid A modification and polymyxin resistance. Mol Microbiol **27**: 1171-1182.

Hanahan, D., (1983) Studies on transformation of Escherichia coli with plasmids. J Mol Biol **166**: 557-580.

Hashimoto, C., K. L. Hudson & K. V. Anderson, (1988) The Toll gene of Drosophila, required for dorsal-ventral embryonic polarity, appears to encode a transmembrane protein. Cell **52**: 269-279.

Heine, H. & A. J. Ulmer, (2005) Recognition of bacterial products by toll-like receptors. Chem Immunol Allergy **86**: 99-119.

Helander, I. M., I. Kilpelainen & M. Vaara, (1994) Increased substitution of phosphate groups in lipopolysaccharides and lipid A of the polymyxin-resistant pmrA

mutants of Salmonella typhimurium: a 31P-NMR study. Mol Microbiol **11**: 481-487.

Hernick, M., S. G. Gattis, J. E. Penner-Hahn & C. A. Fierke, (2010) Activation of Escherichia coli UDP-3-O-[(R)-3-hydroxymyristoyl]-N-acetylglucosamine deacetylase by Fe2+ yields a more efficient enzyme with altered ligand affinity. Biochemistry **49**: 2246-2255.

Hoshino, K., O. Takeuchi, T. Kawai, H. Sanjo, T. Ogawa, Y. Takeda, K. Takeda & S. Akira, (1999) Cutting edge: Toll-like receptor 4 (TLR4)-deficient mice are hyporesponsive to lipopolysaccharide: evidence for TLR4 as the Lps gene product. J Immunol **162**: 3749-3752.

Hwang, P. M., W. Y. Choy, E. I. Lo, L. Chen, J. D. Forman-Kay, C. R. H. Raetz, G. G. Prive, R. E. Bishop & L. E. Kay, (2002) Solution structure and dynamics of the outer membrane enzyme PagP by NMR. Proc Natl Acad Sci U S A **99**: 13560-13565.

Ingram, B. O., C. Sohlenkamp, O. Geiger & C. R. Raetz, (2010) Altered lipid A structures and polymyxin hypersensitivity of Rhizobium etli mutants lacking the LpxE and LpxF phosphatases. Biochim Biophys Acta. **1801**: 593-604

Inoue, H., H. Nojima & H. Okayama, (1990) High efficiency transformation of Escherichia coli with plasmids. Gene **96**: 23-28.

Jabeen, T., S. Sharma, N. Singh, R. K. Singh, P. Kaur, M. Perbandt, C. Betzel, A. Srinivasan & T. P. Singh, (2005) Crystal structure of a calcium-induced dimer of two isoforms of cobra phospholipase A2 at 1.6 A resolution. Proteins **59**: 856-863.

Jackman, J. E., C. A. Fierke, L. N. Tumey, M. Pirrung, T. Uchiyama, S. H. Tahir, O. Hindsgaul & C. R. H. Raetz, (2000) Antibacterial agents that target lipid A biosynthesis in gram-negative bacteria. Inhibition of diverse UDP-3-O-(r-3-hydroxymyristoyl)-n-acetylglucosamine deacetylases by substrate analogs containing zinc binding motifs. J Biol Chem **275**: 11002-11009.

Jackman, J. E., C. R. H. Raetz & C. A. Fierke, (1999) UDP-3-O-(R-3-hydroxymyristoyl)-N-acetylglucosamine deacetylase of Escherichia coli is a zinc metalloenzyme. Biochemistry **38**: 1902-1911.

Jackman, J. E., C. R. H. Raetz & C. A. Fierke, (2001) Site-directed mutagenesis of the bacterial metalloamidase UDP-(3-O-acyl)-N-acetylglucosamine deacetylase (LpxC). Identification of the zinc binding site. Biochemistry **40**: 514-523.

Jagow, G. v. & H. Schagger, (1994) A practical guide to membrane protein purification, p. xvii, 166 p. Academic Press, San Diego.

Janeway, C. A., Jr. & R. Medzhitov, (2002) Innate immune recognition. Annu Rev Immunol **20**: 197-216.

Jeyaretnam, B., J. Glushka, V. S. Kolli & R. W. Carlson, (2002) Characterization of a novel lipid-A from Rhizobium species Sin-1. A unique lipid-A structure that is devoid of phosphate and has a glycosyl backbone consisting of glucosamine and 2-aminogluconic acid. J Biol Chem **277**: 41802-41810.

Jin, M. S., S. E. Kim, J. Y. Heo, M. E. Lee, H. M. Kim, S. G. Paik, H. Lee & J. O. Lee, (2007) Crystal structure of the TLR1-TLR2 heterodimer induced by binding of a tri-acylated lipopeptide. Cell **130**: 1071-1082.

Johnston, A. W. & J. E. Beringer, (1975) Identification of the rhizobium strains in pea root nodules using genetic markers. J Gen Microbiol **87**: 343-350.

Jones, J. D. & J. L. Dangl, (2006) The plant immune system. Nature **444**: 323-329.

Kadrmas, J. L., D. Allaway, R. E. Studholme, J. T. Sullivan, C. W. Ronson, P. S. Poole & C. R. H. Raetz, (1998) Cloning and overexpression of glycosyltransferases that generate the lipopolysaccharide core of Rhizobium leguminosarum. J Biol Chem **273**: 26432-26440.

Kadrmas, J. L., K. A. Brozek & C. R. Raetz, (1996) Lipopolysaccharide core glycosylation in Rhizobium leguminosarum. An unusual mannosyl transferase resembling the heptosyl transferase I of Escherichia coli. J Biol Chem **271**: 32119-32125.

Kadrmas, J. L. & C. R. H. Raetz, (1998) Enzymatic synthesis of lipopolysaccharide in Escherichia coli. Purification and properties of heptosyltransferase i. J Biol Chem **273**: 2799-2807.

Kahn, K. & P. A. Tipton, (1998) Spectroscopic characterization of intermediates in the urate oxidase reaction. Biochemistry **37**: 11651-11659.

Kanipes, M. I., S. Lin, R. J. Cotter & C. R. H. Raetz, (2001) Ca2+-induced phosphoethanolamine transfer to the outer 3-deoxy-D-manno-octulosonic acid moiety of Escherichia coli lipopolysaccharide. A novel membrane enzyme dependent upon phosphatidylethanolamine. J Biol Chem **276**: 1156-1163.

Kanjilal-Kolar, S., S. S. Basu, M. I. Kanipes, Z. Guan, T. A. Garrett & C. R. H. Raetz, (2006) Expression cloning of three Rhizobium leguminosarum lipopolysaccharide core galacturonosyltransferases. J Biol Chem **281**: 12865-12878.

Kanjilal-Kolar, S. & C. R. Raetz, (2006) Dodecaprenyl phosphate-galacturonic acid as a donor substrate for lipopolysaccharide core glycosylation in Rhizobium leguminosarum. J Biol Chem **281**: 12879-12887.

Kannenberg, E. L. & N. J. Brewin, (1989) Expression of a cell surface antigen from Rhizobium leguminosarum 3841 is regulated by oxygen and pH. J Bacteriol **171**: 4543-4548.

Kannenberg, E. L. & N. J. Brewin, (1994) Host-plant invasion by Rhizobium: the role of cell-surface components. Trends Microbiol **2**: 277-283.

Kannenberg, E. L. & R. W. Carlson, (2001) Lipid A and O-chain modifications cause Rhizobium lipopolysaccharides to become hydrophobic during bacteroid development. Mol Microbiol **39**: 379-391.

Kannenberg, E. L., E. A. Rathbun & N. J. Brewin, (1992) Molecular dissection of structure and function in the lipopolysaccharide of Rhizobium leguminosarum strain 3841 using monoclonal antibodies and genetic analysis. Mol Microbiol **6**: 2477-2487.

Karbarz, M. J., S. R. Kalb, R. J. Cotter & C. R. H. Raetz, (2003) Expression cloning and biochemical characterization of a Rhizobium leguminosarum lipid A 1-phosphatase. J Biol Chem **278**: 39269-39279.

Karbarz, M. J., D. A. Six & C. R. Raetz, (2009) Purification and characterization of the lipid A 1-phosphatase LpxE of Rhizobium leguminosarum. J Biol Chem **284**: 414-425.

Karow, M. & C. Georgopoulos, (1992) Isolation and characterization of the Escherichia coli msbB gene, a multicopy suppressor of null mutations in the high-temperature requirement gene htrB. J Bacteriol **174**: 702-710.

Kelly, T. M., S. A. Stachula, C. R. H. Raetz & M. S. Anderson, (1993) The firA gene of Escherichia coli encodes UDP-3-O-(R-3-hydroxymyristoyl)-glucosamine N-acyltransferase. The third step of endotoxin biosynthesis. J Biol Chem **268**: 19866-19874.

Kim, H. M., B. S. Park, J. I. Kim, S. E. Kim, J. Lee, S. C. Oh, P. Enkhbayar, N. Matsushima, H. Lee, O. J. Yoo & J. O. Lee, (2007) Crystal structure of the TLR4-MD-2 complex with bound endotoxin antagonist Eritoran. Cell **130**: 906-917.

Klein, G., B. Lindner, W. Brabetz, H. Brade & S. Raina, (2009) Escherichia coli K-12 Suppressor-free Mutants Lacking Early Glycosyltransferases and Late Acyltransferases: minimal lipopolysaccharide structure and induction of envelope stress response. J Biol Chem **284**: 15369-15389.

Kleinschmidt, J. H., (2003) Membrane protein folding on the example of outer membrane protein A of Escherichia coli. Cell Mol Life Sci **60**: 1547-1558.

Kline, T., N. H. Andersen, E. A. Harwood, J. Bowman, A. Malanda, S. Endsley, A. L. Erwin, M. Doyle, S. Fong, A. L. Harris, B. Mendelsohn, K. Mdluli, C. R. H. Raetz, C. K. Stover, P. R. Witte, A. Yabannavar & S. Zhu, (2002) Potent, novel in vitro inhibitors of the Pseudomonas aeruginosa deacetylase LpxC. J Med Chem **45**: 3112-3129.

Kundi, M., (2007) New hepatitis B vaccine formulated with an improved adjuvant system. Expert Rev Vaccines **6**: 133-140.

Lee, B. I. & S. W. Suh, (2003) Crystal structure of UDP-N-acetylglucosamine acyltransferase from Helicobacter pylori. Proteins **53**: 772-774.

Lee, C. H. & C. M. Tsai, (1999) Quantification of bacterial lipopolysaccharides by the purpald assay: measuring formaldehyde generated from 2-keto-3-deoxyoctonate and heptose at the inner core by periodate oxidation. Anal Biochem **267**: 161-168.

Lee, H., F. F. Hsu, J. Turk & E. A. Groisman, (2004) The PmrA-regulated pmrC gene mediates phosphoethanolamine modification of lipid A and polymyxin resistance in Salmonella enterica. J Bacteriol **186**: 4124-4133.

Lee, H. S., M. A. Wolfert, Y. Zhang & G. J. Boons, (2006) The 2-aminogluconate isomer of rhizobium sin-1 lipid A can antagonize TNF-alpha production induced by enteric LPS. Chembiochem **7**: 140-148.

Lemaitre, B., J. M. Reichhart & J. A. Hoffmann, (1997) Drosophila host defense: differential induction of antimicrobial peptide genes after infection by various classes of microorganisms. Proc Natl Acad Sci U S A **94**: 14614-14619.

Ma, B., C. M. Reynolds & C. R. Raetz, (2008) Periplasmic orientation of nascent lipid A in the inner membrane of an Escherichia coli LptA mutant. Proc Natl Acad Sci U S A **105**: 13823-13828.

Magnusson, O. T., H. Toyama, M. Saeki, A. Rojas, J. C. Reed, R. C. Liddington, J. P. Klinman & R. Schwarzenbacher, (2004) Quinone biogenesis: Structure and mechanism of PqqC, the final catalyst in the production of pyrroloquinoline quinone. Proc Natl Acad Sci U S A **101**: 7913-7918.

Martinez, E., M. A. Pardo, R. Palacios & M. A. Cevallos, (1985) Reiteration of nitrogen fixation gene sequences and specificity of Rhizobium in nodulation and nitrogen fixation in Phaseolus vulgaris. J. Gen. Microbiol. **131**: 1779-1786.

Matsushima, N., T. Tanaka, P. Enkhbayar, T. Mikami, M. Taga, K. Yamada & Y. Kuroki, (2007) Comparative sequence analysis of leucine-rich repeats (LRRs) within vertebrate toll-like receptors. BMC Genomics **8**: 124.

McClerren, A. L., S. Endsley, J. L. Bowman, N. H. Andersen, Z. Guan, J. Rudolph & C. R. H. Raetz, (2005a) A slow, tight-binding inhibitor of the zinc-dependent deacetylase LpxC of lipid A biosynthesis with antibiotic activity comparable to ciprofloxacin. Biochemistry **44**: 16574-16583.

McClerren, A. L., P. Zhou, Z. Guan, C. R. H. Raetz & J. Rudolph, (2005b) Kinetic analysis of the zinc-dependent deacetylase in the lipid A biosynthetic pathway. Biochemistry **44**: 1106-1113.

Medzhitov, R. & C. Janeway, Jr., (2000a) Innate immune recognition: mechanisms and pathways. Immunol Rev **173**: 89-97.

Medzhitov, R. & C. Janeway, Jr., (2000b) Innate immunity. N Engl J Med **343**: 338-344.

Meredith, T. C., P. Aggarwal, U. Mamat, B. Lindner & R. W. Woodard, (2006) Redefining the requisite lipopolysaccharide structure in Escherichia coli. ACS Chem Biol **1**: 33-42.

Metzger, L. E. t. & C. R. Raetz, (2009) Purification and characterization of the lipid A disaccharide synthase (LpxB) from Escherichia coli, a peripheral membrane protein. Biochemistry **48**: 11559-11571.

Miller, J. H., (1972) Experiments in molecular genetics, p. xvi, 466 p. Cold Spring Harbor Laboratory, [Cold Spring Harbor, N.Y.].

Miller, S. I., R. K. Ernst & M. W. Bader, (2005) LPS, TLR4 and infectious disease diversity. Nat Rev Microbiol **3**: 36-46.

Miroux, B. & J. E. Walker, (1996) Over-production of proteins in Escherichia coli: mutant hosts that allow synthesis of some membrane proteins and globular proteins at high levels. J Mol Biol **260**: 289-298.

Miyake, K., (2006) Roles for accessory molecules in microbial recognition by Toll-like receptors. J Endotoxin Res **12**: 195-204.

Mochalkin, I., J. D. Knafels & S. Lightle, (2008) Crystal structure of LpxC from Pseudomonas aeruginosa complexed with the potent BB-78485 inhibitor. Protein Sci **17**: 450-457.

Mullarkey, M., J. R. Rose, J. Bristol, T. Kawata, A. Kimura, S. Kobayashi, M. Przetak, J. Chow, F. Gusovsky, W. J. Christ & D. P. Rossignol, (2003) Inhibition of endotoxin response by e5564, a novel Toll-like receptor 4-directed endotoxin antagonist. J Pharmacol Exp Ther **304**: 1093-1102.

Nikaido, H., (1996) Escherichia coli and Salmonella: Cellular and Molecular Biology, p. 29-46. ASM Press, Washington, D.C.

Nikaido, H., (2003) Molecular basis of bacterial outer membrane permeability revisited. Microbiol Mol Biol Rev **67**: 593-656.

Nikaido, H. & M. Vaara, (1985) Molecular basis of bacterial outer membrane permeability. Microbiol Rev **49**: 1-32.

Nishijima, M., S. Nakaike, Y. Tamori & S. Nojima, (1977) Detergent-resistant phospholipase A of Escherichia coli K-12. Purification and properties. Eur J Biochem **73**: 115-124.

Noel, K. D., A. Sanchez, L. Fernandez, J. Leemans & M. A. Cevallos, (1984) Rhizobium phaseoli symbiotic mutants with transposon Tn5 insertions. J Bacteriol **158**: 148-155.

Noel, K. D., K. A. Vandenbosch & B. Kulpaca, (1986) Mutations in Rhizobium phaseoli that lead to arrested development of infection threads. J Bacteriol **168**: 1392-1401.

Nummila, K., I. Kilpelainen, U. Zahringer, M. Vaara & I. M. Helander, (1995) Lipopolysaccharides of polymyxin B-resistant mutants of Escherichia coli are extensively substituted by 2-aminoethyl pyrophosphate and contain aminoarabinose in lipid A. Mol Microbiol **16**: 271-278.

O'Neill, L. A. & A. G. Bowie, (2007) The family of five: TIR-domain-containing adaptors in Toll-like receptor signalling. Nat Rev Immunol **7**: 353-364.

Odegaard, T. J., I. A. Kaltashov, R. J. Cotter, L. Steeghs, P. van der Ley, S. Khan, D. J. Maskell & C. R. H. Raetz, (1997) Shortened hydroxyacyl chains on lipid A of Escherichia coli cells expressing a foreign UDP-N-acetylglucosamine O-acyltransferase. J Biol Chem **272**: 19688-19696.

Onishi, H. R., B. A. Pelak, L. S. Gerckens, L. L. Silver, F. M. Kahan, M. H. Chen, A. A. Patchett, S. M. Galloway, S. A. Hyland, M. S. Anderson & C. R. Raetz, (1996) Antibacterial agents that inhibit lipid A biosynthesis. Science **274**: 980-982.

Osteras, M., E. Boncompagni, N. Vincent, M. C. Poggi & D. Le Rudulier, (1998) Presence of a gene encoding choline sulfatase in Sinorhizobium meliloti bet operon: choline-O-sulfate is metabolized into glycine betaine. Proc Natl Acad Sci U S A **95**: 11394-11399.

Park, B. S., D. H. Song, H. M. Kim, B. S. Choi, H. Lee & J. O. Lee, (2009) The structural basis of lipopolysaccharide recognition by the TLR4-MD-2 complex. Nature **458**: 1191-1195.

Parrillo, J., (1993) Pathogenic mechanisms of septic shock. N Engl J Med **328**: 1427-1428.

Perera, P. Y., T. Y. Chan, D. C. Morrison & S. N. Vogel, (1992) Detection and analysis of the 80-kd lipopolysaccharide receptor in macrophages derived from Lpsn and Lpsd mice. J Leukoc Biol **51**: 501-506.

Perotto, S., Brewin, N.J., and Kannenberg, E.L., (1994) Cytological evidence for a host defense response that reduces cell and tissue invasion in pea nodules by lipopolysaccharide-defective mutants of Rhizobium legumonsarum strain-3841. Mol. Plant Microbe Interact **7**: 99-112.

Perret, X., C. Staehelin & W. J. Broughton, (2000) Molecular basis of symbiotic promiscuity. Microbiol Mol Biol Rev **64**: 180-201.

Persing, D. H., R. N. Coler, M. J. Lacy, D. A. Johnson, J. R. Baldridge, R. M. Hershberg & S. G. Reed, (2002) Taking toll: lipid A mimetics as adjuvants and immunomodulators. Trends Microbiol. **10**: S32-37.

Pirrung, M. C., L. N. Tumey, A. L. McClerren & C. R. H. Raetz, (2003) High-throughput catch-and-release synthesis of oxazoline hydroxamates. Structure-activity relationships in novel inhibitors of Escherichia coli LpxC: in vitro enzyme inhibition and antibacterial properties. J Am Chem Soc **125**: 1575-1586.

Polissi, A. & C. Georgopoulos, (1996) Mutational analysis and properties of the msbA gene of Escherichia coli, coding for an essential ABC family transporter. Mol Microbiol **20**: 1221-1233.

Poltorak, A., X. He, I. Smirnova, M. Y. Liu, C. Van Huffel, X. Du, D. Birdwell, E. Alejos, M. Silva, C. Galanos, M. Freudenberg, P. Ricciardi-Castagnoli, B. Layton & B. Beutler, (1998) Defective LPS signaling in C3H/HeJ and C57BL/10ScCr mice: mutations in Tlr4 gene. Science **282**: 2085-2088.

Poltorak, A., P. Ricciardi-Castagnoli, S. Citterio & B. Beutler, (2000) Physical contact between lipopolysaccharide and toll-like receptor 4 revealed by genetic complementation. Proc Natl Acad Sci U S A **97**: 2163-2167.

Poole, P. S., N. A. Schofield, C. J. Reid, E. M. Drew & D. L. Walshaw, (1994) Identification of chromosomal genes located downstream of dctD that affect the requirement for calcium and the lipopolysaccharide layer of Rhizobium leguminosarum. Microbiology **140 (Pt 10)**: 2797-2809.

Price, N. P., B. Jeyaretnam, R. W. Carlson, J. L. Kadrmas, C. R. H. Raetz & K. A. Brozek, (1995) Lipid A biosynthesis in Rhizobium leguminosarum: role of a 2-keto-3-deoxyoctulosonate-activated 4' phosphatase. Proc Natl Acad Sci U S A **92**: 7352-7356.

Price, N. P., T. M. Kelly, C. R. H. Raetz & R. W. Carlson, (1994) Biosynthesis of a structurally novel lipid A in Rhizobium leguminosarum: identification and characterization of six metabolic steps leading from UDP-GlcNAc to 3-deoxy-D-manno-2-octulosonic acid2-lipid IV_A. J Bacteriol **176**: 4646-4655.

Priefer, U. B., (1989) Genes involved in lipopolysaccharide production and symbiosis are clustered on the chromosome of Rhizobium leguminosarum biovar viciae VF39. J Bacteriol **171**: 6161-6168.

Que-Gewirth, N. L., M. J. Karbarz, S. R. Kalb, R. J. Cotter & C. R. H. Raetz, (2003a) Origin of the 2-amino-2-deoxy-gluconate unit in Rhizobium leguminosarum lipid A. Expression cloning of the outer membrane oxidase LpxQ. J Biol Chem **278**: 12120-12129.

Que-Gewirth, N. L., S. Lin, R. J. Cotter & C. R. H. Raetz, (2003b) An outer membrane enzyme that generates the 2-amino-2-deoxy-gluconate moiety of Rhizobium leguminosarum lipid A. J Biol Chem **278**: 12109-12119.

Que-Gewirth, N. L., A. A. Ribeiro, S. R. Kalb, R. J. Cotter, D. M. Bulach, B. Adler, I. S. Girons, C. Werts & C. R. H. Raetz, (2004) A methylated phosphate group and four amide-linked acyl chains in leptospira interrogans lipid A. The membrane anchor of an unusual lipopolysaccharide that activates TLR2. J Biol Chem **279**: 25420-25429.

Que, N. L., S. Lin, R. J. Cotter & C. R. H. Raetz, (2000a) Purification and mass spectrometry of six lipid A species from the bacterial endosymbiont Rhizobium etli. Demonstration of a conserved distal unit and a variable proximal portion. J Biol Chem **275**: 28006-28016.

Que, N. L., A. A. Ribeiro & C. R. H. Raetz, (2000b) Two-dimensional NMR spectroscopy and structures of six lipid A species from Rhizobium etli CE3. Detection of an acyloxyacyl residue in each component and origin of the aminogluconate moiety. J Biol Chem **275**: 28017-28027.

Qureshi, N., K. Takayama & E. Ribi, (1982) Purification and structural determination of non-toxic lipid A obtained from the lipopolysaccharide of Salmonella typhimurium. J. Biol. Chem. **257**: 11808-11815.

Qureshi, S. T., (1999) Endotoxin-tolerant mice have mutations in toll-like receptor 4 (Tlr4) (vol 189, pg 615, 1999). Journal of Experimental Medicine **189**: 1519-1519.

Radika, K. & C. R. H. Raetz, (1988) Purification and properties of lipid A disaccharide synthase of Escherichia coli. J Biol Chem **263**: 14859-14867.

Raetz, C. R. & S. L. Roderick, (1995) A left-handed parallel beta helix in the structure of UDP-N-acetylglucosamine acyltransferase. Science **270**: 997-1000.

Raetz, C. R. H., (1996a). In: Escherichia coli and Salmonella: Cellular and Molecular Biology. F. C. Neidhardt (ed). Washington D.C.: ASM Press, pp. 1035-1063.

Raetz, C. R. H., T. A. Garrett, C. M. Reynolds, W. A. Shaw, J. D. Moore, D. C. Smith, Jr., A. A. Ribeiro, R. C. Murphy, R. J. Ulevitch, C. Fearns, D. Reichart, C. K. Glass, C. Benner, S. Subramaniam, R. Harkewicz, R. C. Bowers-Gentry, M. W. Buczynski, J. A. Cooper, R. A. Deems & E. A. Dennis, (2006) Kdo_2-Lipid A of Escherichia coli, a defined endotoxin that activates macrophages via TLR-4. J Lipid Res **47**: 1097-1111.

Raetz, C. R. H., Z. Guan, B. O. Ingram, D. A. Six, F. Song, X. Wang & J. Zhao, (2009) Discovery of new biosynthetic pathways: the lipid A story. J Lipid Res **50 Suppl**: S103-108.

Raetz, C. R. H., C. M. Reynolds, M. S. Trent & R. E. Bishop, (2007) Lipid A modification systems in gram-negative bacteria. Annu Rev Biochem **76**: 295-329.

Raetz, C. R. H. & C. Whitfield, (2002) Lipopolysaccharide endotoxins. Annu Rev Biochem **71**: 635-700.

Ray, B. L., G. Painter & C. R. H. Raetz, (1984) The biosynthesis of gram-negative endotoxin. Formation of lipid A disaccharides from monosaccharide precursors in extracts of Escherichia coli. J Biol Chem **259**: 4852-4859.

Ray, B. L. & C. R. H. Raetz, (1987) The biosynthesis of gram-negative endotoxin. A novel kinase in Escherichia coli membranes that incorporates the 4'-phosphate of lipid A. J Biol Chem **262**: 1122-1128.

Reyes, C. L. & G. Chang, (2005) Structure of the ABC transporter MsbA in complex with ADP.vanadate and lipopolysaccharide. Science **308**: 1028-1031.

Reynolds, C. M., S. R. Kalb, R. J. Cotter & C. R. H. Raetz, (2005) A phosphoethanolamine transferase specific for the outer 3-deoxy-D-manno-octulosonic acid residue of

Escherichia coli lipopolysaccharide. Identification of the eptB gene and Ca2+ hypersensitivity of an eptB deletion mutant. J Biol Chem **280**: 21202-21211.

Reynolds, C. M. & C. R. Raetz, (2009) Replacement of lipopolysaccharide with free lipid A molecules in Escherichia coli mutants lacking all core sugars. Biochemistry **48**: 9627-9640.

Reynolds, C. M., A. A. Ribeiro, S. C. McGrath, R. J. Cotter, C. R. Raetz & M. S. Trent, (2006) An outer membrane enzyme encoded by Salmonella typhimurium lpxR that removes the 3'-acyloxyacyl moiety of lipid A. J Biol Chem **281**: 21974-21987.

Rietschel, E. T., T. Kirikae, F. U. Schade, U. Mamat, G. Schmidt, H. Loppnow, A. J. Ulmer, U. Zähringer, U. Seydel, F. Di Padova, M. Schreier & H. Brade, (1994) Bacterial endotoxin: molecular relationships of structure to activity and function. FASEB Journal **8**: 217-225.

Robins, L. I., A. H. Williams & C. R. Raetz, (2009) Structural basis for the sugar nucleotide and acyl-chain selectivity of Leptospira interrogans LpxA. Biochemistry **48**: 6191-6201.

Rock, F. L., G. Hardiman, J. C. Timans, R. A. Kastelein & J. F. Bazan, (1998) A family of human receptors structurally related to Drosophila Toll. Proc Natl Acad Sci U S A **95**: 588-593.

Ruiz, N., L. S. Gronenberg, D. Kahne & T. J. Silhavy, (2008) Identification of two inner-membrane proteins required for the transport of lipopolysaccharide to the outer membrane of Escherichia coli. Proc Natl Acad Sci U S A **105**: 5537-5542.

Ruiz, N., D. Kahne & T. J. Silhavy, (2009) Transport of lipopolysaccharide across the cell envelope: the long road of discovery. Nat Rev Microbiol **7**: 677-683.

Russell, J. A., (2006) Management of sepsis. N Engl J Med **355**: 1699-1713.

Rutten, L., J. Geurtsen, W. Lambert, J. J. Smolenaers, A. M. Bonvin, A. de Haan, P. van der Ley, M. R. Egmond, P. Gros & J. Tommassen, (2006) Crystal structure and catalytic mechanism of the LPS 3-O-deacylase PagL from Pseudomonas aeruginosa. Proc Natl Acad Sci U S A **103**: 7071-7076.

Rutten, L., J. P. Mannie, C. M. Stead, C. R. Raetz, C. M. Reynolds, A. M. Bonvin, J. P. Tommassen, M. R. Egmond, M. S. Trent & P. Gros, (2009) Active-site architecture

and catalytic mechanism of the lipid A deacylase LpxR of Salmonella typhimurium. Proc Natl Acad Sci U S A **106**: 1960-1964.

Ruvkun, G. B. & F. M. Ausubel, (1981) A general method for site-directed mutagenesis in prokaryotes. Nature **289**: 85-88.

Sambrook, J. & D. R. Russell, (2001) Molecular Cloning: a Laboratory Manual. Cold Spring Harbor Press, Cold Spring Harbor, NY.

Santhanam, B., M. A. Wolfert, J. N. Moore & G. J. Boons, (2004) Synthesis and biological evaluation of a lipid A derivative that contains an aminogluconate moiety. Chemistry **10**: 4798-4807.

Schafer, A., A. Tauch, W. Jager, J. Kalinowski, G. Thierbach & A. Puhler, (1994) Small mobilizable multi-purpose cloning vectors derived from the Escherichia coli plasmids pK18 and pK19: selection of defined deletions in the chromosome of Corynebacterium glutamicum. Gene **145**: 69-73.

Schnaitman, C. A., (1973) Outer membrane proteins of Escherichia coli. II. Heterogeneity of major outer membrane polypeptides. Arch Biochem Biophys **157**: 553-560.

Schweizer, H. D., (1993) Small broad-host-range gentamycin resistance gene cassettes for site-specific insertion and deletion mutagenesis. Biotechniques **15**: 831-834.

Sciara, G., S. G. Kendrew, A. E. Miele, N. G. Marsh, L. Federici, F. Malatesta, G. Schimperna, C. Savino & B. Vallone, (2003) The structure of ActVA-Orf6, a novel type of monooxygenase involved in actinorhodin biosynthesis. EMBO J **22**: 205-215.

Segovia, L., J. P. Young & E. Martinez-Romero, (1993) Reclassification of American Rhizobium leguminosarum biovar phaseoli type I strains as Rhizobium etli sp. nov. Int J Syst Bacteriol **43**: 374-377.

Sharypova, L. A., K. Niehaus, H. Scheidle, O. Holst & A. Becker, (2003) Sinorhizobium meliloti acpXL mutant lacks the C28 hydroxylated fatty acid moiety of lipid A and does not express a slow migrating form of lipopolysaccharide. J Biol Chem **278**: 12946-12954.

Six, D. A., S. M. Carty, Z. Guan & C. R. H. Raetz, (2008) Purification and mutagenesis of LpxL, the lauroyltransferase of Escherichia coli lipid A biosynthesis. Biochemistry **47**: 8623-8637.

Smith, P. K., R. I. Krohn, G. T. Hermanson, A. K. Mallia, F. H. Gartner, M. D. Provenzano, E. K. Fujimoto, N. M. Goeke, B. J. Olson & D. C. Klenk, (1985) Measurement of protein using bicinchoninic acid. Anal Biochem **150**: 76-85.

Snijder, H. J., I. Ubarretxena-Belandia, M. Blaauw, K. H. Kalk, H. M. Verheij, M. R. Egmond, N. Dekker & B. W. Dijkstra, (1999) Structural evidence for dimerization-regulated activation of an integral membrane phospholipase. Nature **401**: 717-721.

Song, F., Z. Guan & C. R. Raetz, (2009) Biosynthesis of Undecaprenyl Phosphate-Galactosamine and Undecaprenyl Phosphate-Glucose in Francisella novicida (dagger). Biochemistry.

Spaink, H. P., (2002) Plant-microbe interactions: a receptor in symbiotic dialogue. Nature **417**: 910-911.

Spaink, H. P., A. Kondorosi & P. J. J. Hooykaas, (1998) The rhizobiaceae : molecular biology of model plant-associated bacteria, p. xiii, 566 p. Kluwer Academic, Dordrecht ; Boston.

Sperandeo, P., R. Cescutti, R. Villa, C. Di Benedetto, D. Candia, G. Deho & A. Polissi, (2007) Characterization of lptA and lptB, two essential genes implicated in lipopolysaccharide transport to the outer membrane of Escherichia coli. J Bacteriol **189**: 244-253.

Sperandeo, P., F. K. Lau, A. Carpentieri, C. De Castro, A. Molinaro, G. Deho, T. J. Silhavy & A. Polissi, (2008) Functional analysis of the protein machinery required for transport of lipopolysaccharide to the outer membrane of Escherichia coli. J Bacteriol **190**: 4460-4469.

Sperandeo, P., C. Pozzi, G. Deho & A. Polissi, (2006) Non-essential KDO biosynthesis and new essential cell envelope biogenesis genes in the Escherichia coli yrbG-yhbG locus. Res Microbiol **157**: 547-558.

Stevenson, G., B. Neal, D. Liu, M. Hobbs, N. H. Packer, M. Batley, J. W. Redmond, L. Lindquist & P. Reeves, (1994) Structure of the O antigen of Escherichia coli K-12 and the sequence of its rfb gene cluster. J Bacteriol **176**: 4144-4156.

Stover, A. G., J. Da Silva Correia, J. T. Evans, C. W. Cluff, M. W. Elliott, E. W. Jeffery, D. A. Johnson, M. J. Lacy, J. R. Baldridge, P. Probst, R. J. Ulevitch, D. H. Persing & R. M. Hershberg, (2004) Structure-activity relationship of synthetic toll-like receptor 4 agonists. J Biol Chem **279**: 4440-4449.

Stukey, J. & G. M. Carman, (1997) Identification of a novel phosphatase sequence motif. Protein Sci **6**: 469-472.

Swoboda, J. G., J. Campbell, T. C. Meredith & S. Walker, (2010) Wall teichoic acid function, biosynthesis, and inhibition. Chembiochem **11**: 35-45.

Tran, A. X., M. E. Lester, C. M. Stead, C. R. H. Raetz, D. J. Maskell, S. C. McGrath, R. J. Cotter & M. S. Trent, (2005) Resistance to the antimicrobial peptide polymyxin requires myristoylation of Escherichia coli and Salmonella typhimurium lipid A. J Biol Chem **280**: 28186-28194.

Trent, M. S., W. Pabich, C. R. Raetz & S. I. Miller, (2001) A PhoP/PhoQ-induced Lipase (PagL) that catalyzes 3-O-deacylation of lipid A precursors in membranes of Salmonella typhimurium. J Biol Chem **276**: 9083-9092.

Triplett, E. W., (2000) Prokaryotic nitrogen fixation : a model system for the analysis of a biological process, p. xix, 800 p. Horizon Scientific, Wymondham.

Ulevitch, R. J. & P. S. Tobias, (1999) Recognition of gram-negative bacteria and endotoxin by the innate immune system. Curr Opin Immunol **11**: 19-22.

Vaara, M., (1992) Agents that increase the permeability of the outer membrane. Microbiol Rev **56**: 395-411.

Vaara, M. & M. Nurminen, (1999) Outer membrane permeability barrier in Escherichia coli mutants that are defective in the late acyltransferases of lipid A biosynthesis. Antimicrob Agents Chemother **43**: 1459-1462.

Vandenbosch, K. A., D. J. Bradley, J. P. Knox, S. Perotto, G. W. Butcher & N. J. Brewin, (1989) Common components of the infection thread matrix and the intercellular

space identified by immunocytochemical analysis of pea nodules and uninfected roots. EMBO J **8**: 335-341.

Vandenplas, M. L., R. W. Carlson, B. S. Jeyaretnam, B. McNeill, M. H. Barton, N. Norton, T. F. Murray & J. N. Moore, (2002) Rhizobium sin-1 lipopolysaccharide (LPS) prevents enteric LPS-induced cytokine production. J Biol Chem **277**: 41811-41816.

Vandeputte-Rutten, L., R. A. Kramer, J. Kroon, N. Dekker, M. R. Egmond & P. Gros, (2001) Crystal structure of the outer membrane protease OmpT from Escherichia coli suggests a novel catalytic site. Embo J **20**: 5033-5039.

Vedam, V., J. G. Haynes, E. L. Kannenberg, R. W. Carlson & D. J. Sherrier, (2004) A Rhizobium leguminosarum lipopolysaccharide lipid-A mutant induces nitrogen-fixing nodules with delayed and defective bacteroid formation. Mol Plant Microbe Interact **17**: 283-291.

Vedam, V., E. Kannenberg, A. Datta, D. Brown, J. G. Haynes-Gann, D. J. Sherrier & R. W. Carlson, (2006) The pea nodule environment restores the ability of a Rhizobium leguminosarum lipopolysaccharide acpXL mutant to add 27-hydroxyoctacosanoic acid to its lipid A. J Bacteriol **188**: 2126-2133.

Vedam, V., E. L. Kannenberg, J. G. Haynes, D. J. Sherrier, A. Datta & R. W. Carlson, (2003) A Rhizobium leguminosarum AcpXL mutant produces lipopolysaccharide lacking 27-hydroxyoctacosanoic acid. J Bacteriol **185**: 1841-1850.

Vinogradov, E., M. B. Perry & J. W. Conlan, (2002) Structural analysis of Francisella tularensis lipopolysaccharide. Eur. J. Biochem. **269**: 6112-6118.

Vinuesa, P., B. L. Reuhs, C. Breton & D. Werner, (1999) Identification of a plasmid-borne locus in Rhizobium etli KIM5s involved in lipopolysaccharide O-chain biosynthesis and nodulation of Phaseolus vulgaris. J Bacteriol **181**: 5606-5614.

Vollmer, W., D. Blanot & M. A. de Pedro, (2008) Peptidoglycan structure and architecture. FEMS Microbiol Rev **32**: 149-167.

Vorachek-Warren, M. K., S. Ramirez, R. J. Cotter & C. R. H. Raetz, (2002) A triple mutant of Escherichia coli lacking secondary acyl chains on lipid A. J Biol Chem **277**: 14194-14205.

Wang, R. F. & S. R. Kushner, (1991) Construction of versatile low-copy-number vectors for cloning, sequencing and gene expression in Escherichia coli. Gene **100**: 195-199.

Wang, X., M. J. Karbarz, S. C. McGrath, R. J. Cotter & C. R. H. Raetz, (2004) MsbA transporter-dependent lipid A 1-dephosphorylation on the periplasmic surface of the inner membrane: topography of francisella novicida LpxE expressed in Escherichia coli. J Biol Chem **279**: 49470-49478.

Wang, X., S. C. McGrath, R. J. Cotter & C. R. H. Raetz, (2006a) Expression cloning and periplasmic orientation of the Francisella novicida lipid A 4'-phosphatase LpxF. J Biol Chem **281**: 9321-9330.

Wang, X., A. A. Ribeiro, Z. Guan, S. N. Abraham & C. R. H. Raetz, (2007) Attenuated virulence of a Francisella mutant lacking the lipid A 4'-phosphatase. Proc Natl Acad Sci U S A **104**: 4136-4141.

Wang, X., A. A. Ribeiro, Z. Guan, S. C. McGrath, R. J. Cotter & C. R. H. Raetz, (2006b) Structure and biosynthesis of free lipid A molecules that replace lipopolysaccharide in Francisella tularensis subsp. novicida. Biochemistry **45**: 14427-14440.

White, K. A., I. A. Kaltashov, R. J. Cotter & C. R. H. Raetz, (1997) A mono-functional 3-deoxy-D-manno-octulosonic acid (Kdo) transferase and a Kdo kinase in extracts of Haemophilus influenzae. J Biol Chem **272**: 16555-16563.

Williams, A. H., R. M. Immormino, D. T. Gewirth & C. R. H. Raetz, (2006) Structure of UDP-N-acetylglucosamine acyltransferase with a bound antibacterial pentadecapeptide. Proc Natl Acad Sci U S A **103**: 10877-10882.

Williams, A. H. & C. R. Raetz, (2007) Structural basis for the acyl chain selectivity and mechanism of UDP-N-acetylglucosamine acyltransferase. Proc Natl Acad Sci U S A **104**: 13543-13550.

Wu, T., A. C. McCandlish, L. S. Gronenberg, S. S. Chng, T. J. Silhavy & D. Kahne, (2006) Identification of a protein complex that assembles lipopolysaccharide in the outer membrane of Escherichia coli. Proc Natl Acad Sci U S A **103**: 11754-11759.

Yanisch-Perron, C., J. Vieira & J. Messing, (1985) Improved M13 phage cloning vectors and host strains: nucleotide sequences of the M13mp18 and pUC19 vectors. Gene **33**: 103-119.

Yethon, J. A. & C. Whitfield, (2001) Purification and characterization of WaaP from Escherichia coli, a lipopolysaccharide kinase essential for outer membrane stability. J Biol Chem **276**: 5498-5504.

Yoshizaki, H., N. Fukuda, K. Sato, M. Oikawa, K. Fukase, Y. Suda & S. Kusumoto, (2001) First Total Synthesis of the Re-Type Lipopolysaccharide Angew Chem Int Ed Engl **40**: 1475-1480.

Young, K., L. L. Silver, D. Bramhill, P. Cameron, S. S. Eveland, C. R. H. Raetz, S. A. Hyland & M. S. Anderson, (1995) The envA permeability/cell division gene of Escherichia coli encodes the second enzyme of lipid A biosynthesis. UDP-3-O-(R-3-hydroxymyristoyl)-N-acetylglucosamine deacetylase. J Biol Chem **270**: 30384-30391.

Zasloff, M., (2002) Antimicrobial peptides of multicellular organisms. Nature **415**: 389-395.

Zeidler, D., U. Zahringer, I. Gerber, I. Dubery, T. Hartung, W. Bors, P. Hutzler & J. Durner, (2004) Innate immunity in Arabidopsis thaliana: lipopolysaccharides activate nitric oxide synthase (NOS) and induce defense genes. Proc Natl Acad Sci U S A **101**: 15811-15816.

Zhou, M., Z. Diwu, N. Panchuk-Voloshina & R. P. Haugland, (1997) A stable nonfluorescent derivative of resorufin for the fluorometric determination of trace hydrogen peroxide: applications in detecting the activity of phagocyte NADPH oxidase and other oxidases. Anal Biochem **253**: 162-168.

Zhou, Z., K. A. White, A. Polissi, C. Georgopoulos & C. R. H. Raetz, (1998) Function of Escherichia coli MsbA, an essential ABC family transporter, in lipid A and phospholipid biosynthesis. J Biol Chem 273: 12466-12475.

Biography

Brian O'Neal Ingram was born May 18, 1981 in Martinsville, Virginia. He graduated from Laurel Park High School in 1999. In the fall of that year, he enrolled at Radford University. During his undergraduate studies, he pariticpated in NSF-REU research programs at the Univeristy of Kansas and the University of Pennsylvania during the summers of 2002 and 2003. In 2004, Brian graduated *magna cum laude* from Radford University with a B.S. degree in Chemistry and a minor in Biology. He enrolled in the Biochemistry department at Duke University in the fall of 2004 and joined the Raetz lab in the spring of 2005. The following is a list of his publications.

Publications

Gokulrangan, G., Unruh, J.R., Holub, D.F., Ingram, B., Johnson, C.K., Wilson, G.S. "DNA aptamer-based bioanalysis of IGE by fluorescence anisotropy" *Anal. Chem*. 2005, 77, 1963-1970.

Raetz C.R.H., Guan Z., Ingram B.O., Six D.A., Song F,, Wang X., Zhao J. "Discovery of new biosynthetic pathways: the lipid A story" *J Lipid Res*. 2009, 50, S103-8.

Ingram, B.O., Sohlenkamp C., Geiger, O., Raetz, C.R.H. "Altered lipid A structures and polymyxin hypersensitivity of *Rhizobium etli* mutants lacking the LpxE and LpxF phosphatases. *BBA-Mol Cell Biol L. In press*

Ingram, B.O., Raetz C.R.H. "Purification and characterization of the *R. leguminosarum* lipid A oxidase, LpxQ. (manuscript in preparation).

Ingram, B.O., Masoudi A., Raetz, C.R.H. "Heterologous expression of lipid A modifying enzymes in *Eschericia coli* facilitates the re-engineering of LPS. (manuscript in preparation).